

**Geotechnical Factors Affecting the Application of  
Pre-split Blasting to Rock Slopes**

**Paul Worsey**

**Department of Mining Engineering, University of  
Newcastle-upon-Tyne  
August 1981**

NEWCASTLE UPON TYNE UNIVERSITY LIBRARY
ACCESSION No. 81-00083
LOCATION Thesis L2430

ABSTRACT

Previous approaches to pre-split blasting have tended to concentrate on the mathematical theory of dynamic stress wave interaction, whilst recognising some interaction with quasi-static stresses induced by expanding gases in the borehole. However the decoupling introduced during pre-splitting is specifically designed to reduce dynamic effects and to emphasize quasi-static effects, and it can be argued that the process has more in common with hydrofracture than with conventional use of explosives.

Investigation of the mechanics involved during the fracturing process around both single and multiple line charges in model testing in polyester resin proved the quasi-static gas component of energy release to be the predominant mechanism controlling fracture growth around blast holes and in the formation of pre-split fractures.

Both field and test observations indicate that the predominant geotechnical factor affecting the relative success of pre-splitting is the orientation of major

discontinuities and or sets in relation to the pre-split line. Decreasing discontinuity intersection angle is shown to progressively increase overbreak from ninety degrees to twenty degrees, below which a dramatic increase in overbreak is observed with a failure of the pre-split in the final face. Discontinuity frequency is shown to have no major discernable effect on the success of pre-splitting.

The effects of further varying geotechnical factors on the success of pre-split blasting are discussed, including anisotropy, grain size, texture, weathering, ground water, stability and geostatic stress fields.

**CONTENTS**

1 INTRODUCTION . . . . . 1

2 SUMMARY OF PREVIOUS WORK . . . . . 4

    2.1 Origin of Pre-split Blasting . . . . . 4

    2.2 Practical Field Use . . . . . 6

    2.3 Role of Pre-split Blasting . . . . . 7

    2.4 Theoretical and Small Scale Modelling . . . . . 8

    2.5 Analytical Assessments of the Geotechnical Factors  
        Effecting Pre-splitting in the Field . . . . . 13

3 THEORY OF PRE-SPLITTING . . . . . 15

    3.1 Components of Explosive Energy Release . . . . . 15

    3.2 Rock Fracturing by the Dynamic Component of Energy  
        Release . . . . . 16

        3.2.1 Factors Affecting the Dynamic Component Magnitude  
            . . . . . 17

        3.2.2 Dynamic Component in Rock . . . . . 21

        3.2.3 Dynamic Fracturing . . . . . 22

    3.3 Rock Fracturing by the Quasi-static Gas Component of  
        Energy Release . . . . . 28

        3.3.1 Calculation of the Quasi-static Component . . . 28

        3.3.2 Mechanisms of Quasi-static Fracturing . . . . . 30

3.4	Theory of Mechanisms of Fracture Between Multiple Holes	38
3.4.1	Dynamic Approach to Pre-split Blasting	38
3.4.2	Quasi-static Gas Pressure Approach	43
3.4.3	Combination Approach to the Mechanics of Pre-splitting	46
3.5	The Role of the Pre-split Plane in Blast Damage Prevention	49
3.5.1	Dynamic Reflection Theory	51
3.5.2	Venting of Bulk Gases Theory	52
4	TESTING OF THEORY BY MODEL BLASTING	56
4.1	Aims	56
4.2	Separation of Dynamic and Quasi-Static Effects	56
4.3	Material Used in Testing	59
4.4	Machining of Blocks	59
4.5	Explosives Used in Testing	60
4.6	Method	61
4.6.1	Constraints	65
4.6.2	General Assembly	68
4.7	Measurement of Blast Damage and Fracturing	72
4.7.1	Determination of Blast Damage Zone	72
4.7.2	Need for Measurement and the Qualification of the Use of the Blast Damage Zone	74
4.8	Results	78
4.8.1	Series (a) Experiments	78

4.8.2	Series (b) Experiments . . . . .	85
4.8.3	Series (c) Experiments . . . . .	92
4.8.4	Series (d) Experiments . . . . .	96
4.8.5	Series (e) Experiments . . . . .	102
4.8.6	Combination of Results from Series (a), (b) and (c) . . . . .	102
4.9	Conclusions . . . . .	108
4.9.1	. . . . .	108
4.9.2	. . . . .	110
4.9.3	. . . . .	110
4.9.4	. . . . .	110
4.9.5	. . . . .	111
4.9.6	. . . . .	111
4.9.7	Formation of a Pre-split . . . . .	112
5	NON-GEOTECHNICAL FACTORS AFFECTING THE SUCCESS OF PRE-SPLITTING . . . . .	114
5.1	Explosive and Borehole Parameters . . . . .	114
5.1.1	Foreword . . . . .	114
5.1.2	Borehole Separation . . . . .	115
5.1.3	Borehole Size . . . . .	116
5.1.4	Explosive Type . . . . .	117
5.1.5	Charge Density . . . . .	124
5.1.6	Decoupling . . . . .	125
5.2	Charging . . . . .	128
5.2.1	Type of Explosive Train Used . . . . .	129

5.2.2	Detonation . . . . .	132
5.2.3	Base Charges . . . . .	136
5.2.4	Stemming . . . . .	138
5.3	Drilling Accuracy . . . . .	139
5.3.1	Borehole Layout (Marking Out) . . . . .	139
5.3.2	Drilling Platform Rigidity . . . . .	140
5.3.3	Drill Alignment and Face Height . . . . .	142
5.3.4	Borehole Wander . . . . .	149
5.3.5	Measurement of the Effect of Drilling Inaccuracies on a Pre-split . . . . .	154
5.4	Proximity of Bulk Charge . . . . .	159
6	THE EFFECT OF SINGLE DISCONTINUITIES (EXPERIMENTAL) . . .	163
6.1	Theory . . . . .	163
6.2	Affect on the Success of a Pre-split . . . . .	174
6.3	Experimentation in Resin . . . . .	175
6.3.1	Method . . . . .	177
6.3.2	Results . . . . .	178
6.4	Experimentation in Rock . . . . .	193
6.4.1	Method . . . . .	195
6.4.2	Results . . . . .	198
6.5	Experimentation in Concrete . . . . .	210
6.5.1	Method . . . . .	211
6.5.2	Results . . . . .	213
6.6	Conclusions . . . . .	219

7	EFFECT OF SINGLE DISCONTINUITIES - FIELD OBSERVATIONS . . . . .	222
7.1	Borehole Fracturing to Jointing . . . . .	222
7.1.1	Field Data Recorded . . . . .	222
7.1.2	Results . . . . .	224
7.1.3	Summary of Results . . . . .	227
7.2	Effect of Joint Intersection of Boreholes . . . . .	228
7.3	Effect of the Continuity of Discontinuities . . . . .	230
7.4	Large Scale Discontinuities Acting as Pre-splits . . . . .	235
7.5	Conclusions . . . . .	237
8	THE EFFECT OF MULTIPLE DISCONTINUITIES AND THEIR FREQUENCY . . . . .	238
8.1	Theory . . . . .	238
8.2	Method . . . . .	240
8.3	Results . . . . .	242
8.4	Field Observations . . . . .	247
8.4.1	Measurements . . . . .	247
8.4.2	Discussion of Results . . . . .	248
8.5	Conclusions . . . . .	250
9	ROCK STRENGTH . . . . .	252
9.1	Important Considerations . . . . .	252
9.2	Laboratory Testing . . . . .	253
9.2.1	Materials . . . . .	254
9.2.2	Experimental Method . . . . .	255
9.2.3	Results . . . . .	256

9.3	Effect of Pre-splitting on Insitu Strength . . . . .	263
9.3.1	Method . . . . .	263
9.3.2	Results . . . . .	264
9.4	Field Data . . . . .	266
9.4.1	Method . . . . .	266
9.4.2	Results . . . . .	267
9.4.3	Discussion of Results . . . . .	268
9.5	Conclusions . . . . .	272
10	WEATHERING . . . . .	274
10.1	Weathering Processes in Relation to the Rock Mass	274
10.2	Effect of Weathering and Recommendations . . . . .	275
10.3	Field Observations on the Influence of Weathering	278
11	WATER . . . . .	281
11.1	Theory . . . . .	281
11.2	Experimental Method . . . . .	286
11.3	Results . . . . .	288
11.4	Further Experimentation . . . . .	292
11.5	Results of Testing with Dye . . . . .	293
11.6	Conclusions . . . . .	295
12	TEXTURE, GRAIN SIZE AND ANISOTROPY . . . . .	297
12.1	Effect of Texture . . . . .	297
12.2	Effect of Grain Size . . . . .	298
12.3	Effect of Anisotropy . . . . .	299

13	STABILITY . . . . .	305
13.1	Introduction . . . . .	305
13.2	Modes of Failure . . . . .	306
13.3	Detailed Stability Analysis of Each Location . . .	310
13.3.1	Foreword . . . . .	310
13.3.2	Location Number One, (Figure 13.4) . . . . .	311
13.3.3	Location Number Two, (Figure 13.5) . . . . .	313
13.3.4	Location Three, (Figures 13.6 and 13.7) . . .	315
13.3.5	Location Number Four, (Figures 13.8 and 13.9) .	
	318	
13.3.6	Location Number Five, (Figure 13.10) . . . . .	322
13.3.7	Location Number Six, (Figure 13.11) . . . . .	322
13.3.8	Location Number Seven, (Figure 13.12) . . . . .	324
13.3.9	Location Number Eight, (Figure 13.13) . . . . .	327
13.3.10	Location Number Nine, (Figure 13.14) . . . . .	327
13.3.11	Location Number Ten, (Figure 13.15) . . . . .	330
13.3.12	Location Number Eleven, (Figure 13.16) . . . . .	332
13.4	Discussion . . . . .	334
13.5	Conclusions . . . . .	335
14	GEOSTATIC STRESS FIELDS . . . . .	336
14.1	Foreword . . . . .	336
14.2	Previous Work . . . . .	336
14.3	Theory . . . . .	338

15	SUMMARY OF CONCLUSIONS . . . . .	349
16	ACKNOWLEDGEMENTS . . . . .	354
17	REFERENCES . . . . .	356
	Appendix A : METHOD OF CASTING . . . . .	372
	Appendix B : WAVE TRAPS . . . . .	377
	Appendix C : DELAY EXPERIMENT, TEST 15 . . . . .	387
	Appendix D : EXPERIMENTATION TEST NUMBER LISTINGS . . . . .	390
	Appendix E : MODEL TESTING SHOT FIRING DATA . . . . .	392
	Appendix F : PRE-SPLIT SITE COMPOSITE PHOTOGRAPHS . . . . .	488
	Appendix G : SCALED OVERBREAK DRAWINGS - LOCATION NINE . . . . .	500
	Appendix H : LABORATORY STRENGTH TESTING RESULTS . . . . .	510

## 1 INTRODUCTION

Pre-split blasting may be briefly defined as a technique used to reduce disturbance to excavation profiles during blasting by pre-forming a continuous fracture between parallel boreholes lightly charged with decoupled explosives along the line of the required surface, (Worsey et. al., 1981).

Following difficulty with pre-split blasting on various highway contracts in Scotland, a study was initiated into the effectiveness of controlled blast techniques in discontinuous rock. This work formed part of the above study.

The work undertaken by the author was funded jointly by the Transport and Road Research Laboratory and the Science Research Council through a C.A.S.E. (Co-operative Award in Science and Engineering) award.

Out of two and a half years research, the author was employed at T.R.R.L. (Scottish branch) at Livingston for a total of six months during which he was involved in:

1. Examination and analysis of previous pre-split

blasting case histories and visits for on-site observation of the effect of pre-split blasting.

2. Appraisal of site investigation and pre-split blasting with the objective of formulating designs for contract work.
3. Monitoring of pre-split blasting contracts.

All laboratory work was performed at the Rock Mechanics Laboratories of the Mining Engineering Department at the University of Newcastle-upon-Tyne.

Due to the conflicting views (which are still held and voiced) over the varying importance of the roles played by the dynamic and gas components of explosive energy in the mechanics of pre-split blasting, it was found necessary to initially research into the actual mechanics of pre-splitting. Consequently the following three chapters are necessarily concerned with the solution of this controversy.

Although many people have touched on the field of pre-splitting and have written papers on the topic in the past, no-one (to the author's knowledge) has

researched in the laboratory on the geotechnical factors which may affect pre-splitting and only Trudinger (1973) has published on-site observations of the effect of varying major discontinuity orientation on pre-splitting in the field.

It is not possible to refer to individual sites by their names or to give locations, chainages etc. as many of the projects are still active.

The views and opinions expressed in this thesis are those of the author and are not necessarily those of the Transport and Road Research Laboratory or the Department of Transport.

## 2 SUMMARY OF PREVIOUS WORK

### 2.1 ORIGIN OF PRE-SPLIT BLASTING

The technique of pre-forming final excavation limits by pre-split blasting was first used at the Niagra Power Project (Paine et.al., 1961). The project consisted of an intake section, two parallel conduits about four miles long, an open canal 4,000 feet long, a main generating plant and a pump generating plant and was excavated in roughly horizontal massive dolomite and limestone groups. Several million square feet of rock face had to be prepared to within a tolerance of six inches, over five million square feet on the conduits (averaging 110 feet in height) alone. The contracts stipulated that rock protruding more than six inches into the final excavation from the design face line had to be trimmed back by the contractor and if any overbreak from the design line occurred in excess of six inches due to blasting inaccuracies, the contractor was to foot the bill for the excess concrete used in lining. Due to the high cost of line drilling, the total inadequacy of bulk blasting and the failure of smooth

wall blasting to sufficiently reduce overbreak in the early sections of the contracts, a new perimeter blasting technique was required.

Of the techniques used, pre-splitting gave by far the best results, the maximum drill depth of pre-split staying within the six inch tolerance being 64 feet.

The pre-split technique was developed by D. K. Holmes<sup>1</sup> as a modification of smoothwall blasting, differing from the latter in the respect that the pre-splitting was accomplished prior to the drilling and blasting of the bulk pattern rather than after.

Pre-splitting consisted of half eight ounce sticks of 40% gelatine extra taped to a length of Primacord equal to that of the hole at one foot spacings, placed in 2.5 to 3 inch holes at two foot spacings, each hole being stemmed completely with minus 3/8 inch clean stone chips. Detonation was by Primacord trunk lines or individual short delay detonators in each hole.

-----  
1 D. K. Holmes was blasting engineer for Merritt-Chapman and Scott Corporation of New York who were responsible for work sections one and five of contracts N-5 and N-3 respectively.

## 2.2 PRACTICAL FIELD USE

Since the first extremely successful use of pre-splitting at the Niagra Power Project, the successful application of the technique in both Civil Engineering and Mining has been reported by many authors and has been used in virtually every conceivable application.

On the surface it is now widely incorporated into highway rock excavation specifications in both the United States and Europe, for both stabilisation of rock slopes for safety, as reported by Hoover (1972), Falbot (1977) and Jones (1978) etc. and economy, according to Teller (1972b) and Baker (1972). The application of the technique in open cast quarrying is reported by Stenhouse (1973) and Forsthoff (1973) for the stabilization of haul roads, and for economically producing safe stable final and production faces without the necessity of scaling, in papers such as; Unknown Author (1964), Brown and Bigando (1972), Stenhouse (1973) and Johnston (1973).

Articles have been published on the successful adoption of pre-splitting in shaft sinking (Unknown Author, 1977) in order to reduce overbreak, tunnels

(Plewman and Starfield, 1965 and Holman, 1967) in order to reduce overbreak, boring down times and tunnel resistance to air flow, underground to delineate molybdenum ore from waste (Smith and Barnett, 1965) and in underground room and pillar limestone mines (Bjorn, 1969) for increasing extraction ratio and pillar strength by decreasing blast damage.

The technique has also been used in such diverse applications as the destruction of ice islands (Mellor, 1976 and Mellor et.al., 1977).

The various uses of pre-splitting, pre-split blasting patterns and suggested charge specifications are also given in a number of blasting handbooks and rock slope manuals such as 'Rock Slope Engineering' by Hoek and Bray (1977), Calder's 'Pitslope Manual' (1977) and Langefors and Kihlstrom (1978). These publications also quote the advantages and possible disadvantages of using the technique.

### 2.3 ROLE OF PRE-SPLITTING BLASTING

It is universally agreed that the utilization of pre-splitting produces cleaner, less damaged faces

than with bulk blasting and that pre-splitting significantly reduces the damage from neighbouring bulk blasts.

Bergal (1976) argues that the pre-split reduces the damaging effect of the bulk shock wave by reflection and has shown that the presence of a pre-split fracture significantly reduces blasting vibrations. However, in total contradiction both Devine (1965) and Laroque and Coates (1972) have shown that the converse is the case, and ascribe the effect to venting of explosive gases.

#### 2.4 THEORETICAL AND SMALL SCALE MODELLING

The first published theoretical work and practical research involving modelling and underground work on pre-split blasting was by Fennel, Plewman and Brown in 1966. Their theory was based on rock breakage by the dynamic component of energy release (this being the main theoretical mode of explosive fracture at the time). Pre-splitting was shown to be possible underground in adverse stress conditions and that with care, net savings using the technique could be made.

In the same year, Aso (1966) put forward a comprehensive hypothesis on the 'Phenomena Involved in Pre-splitting by Blasting'. His theory and highly complex mathematical analysis was based primarily on the initiation of the pre-split mid-distance between blast holes by the superposition and addition of their shock waves. However no actual values were given and the results of limited experimentation involving pre-splitting in mortar failed to substantiate his hypotheses.

Nicholls and Duval (1966a) performed a series of surface field trials in the presence of a high static stress field. From their results they concluded that pre-split fracturing is not initiated centrally between adjacent holes but as separate fractures at individual borehole walls which are propagated in a wedge like manner by explosion gases to connection, both expanding gases and interaction of stress waves playing important roles.

In 1967, Kutter submitted a Ph.d. thesis entitled 'The Interaction Between Stress Wave and Gas Pressure in the Fracture Process on an Underground Explosion in Rock, with Particular Application to Pre-splitting' which up to the present time is considered to be the

major contribution to the mechanics of pre-splitting. He concluded that a pre-split is formed by the connection of fracturing from adjacent holes, initiated by the dynamic shock wave and extended by the quasi-static gas pressure remaining within the shot holes. His opinion of the processes involved however, seem to have radically changed near the end of his research, as the majority of his initial work was concerned with the effect of dynamic shock waves in isolation, the quasi-static component only being simulated by hydrofracture near the end in relatively few tests.<sup>2</sup> Following his thesis, Kutter published several papers on and around the subject with Fairhurst (Kutter and Fairhurst, 1968 and 1971), verifying his initial conclusions on the mechanisms involved in pre-splitting.

Kutter's theories are further verified by Brost (1970) and Schultz (1972), who claim to have observed explosive gases entering dynamically initiated fractures, and causing their extensive propagation in both single and multiple hole testing.

In contradiction to the trend of pre-split

-----  
<sup>2</sup> No actual modelling with explosives was undertaken and therefore no direct relationship with the use of explosive blasting was formed.

publications, Griffin (1973) produced a paper entitled 'Mathematical Theory to Pre-splitting Blasting', a half theory and half empirical approach to previous dynamic theories. However, rather than basing the mechanisms on the interaction of dynamic tensile tangential shock wave components, he states that the complete shock wave is compressive in nature, pre-splitting being initiated mid-distance between boreholes by the reflection in tension of shock waves from one another.

In 1973, Katsuyama published work on 'Computer Calculations of the Effects of Pre-split on Blasting in Close Proximity to It'. Basing the main mechanics of explosive fracturing on the dynamic shock wave, he calculated for normal blasting wavelengths, that if the pre-split aperture is greater than 1 mm, wave motion will not propagate across the pre-split. For multiple fractures, he calculated that an aperture of 0.25 to 0.5 mm would be sufficient.

More recent work by Dalley and Fourney (1977) adds further confusion to the mechanisms responsible for the creation of a pre-split plane. They state that in blasting, fractures may be extended to over fifty times the borehole diameter if the gas produced by

detonation flows into the cracks and that premature crack arrest can be avoided by using long stemming columns to prevent the escape of borehole pressure. They then in contradiction state that pre-splitting is caused by the dynamic interaction of stress waves.

Work involving the surface morphology of pre-split fractures from explosive model testing in Plexiglas by Carrasco and Saperstein has shown that pre-split fractures may be formed by both dynamic and predominantly quasi-static means. However for economic pre-split borehole separations in the field, the quasi-static gas component is predominantly responsible for the pre-split, with fracture initiation at or near the borehole walls and growth to interception rather than initiation in the middle.

The most recent work on pre-splitting has been undertaken by Jones (1978). He stipulates that the dynamic component of energy release is of minimum importance in the mechanics of pre-splitting as it is reduced to an insignificant level by the combination of the low charge weights and decoupling. He has shown from model experimentation in gypsum that a pre-split may be obtained by hydrofracture alone.

## 2.5 ANALYTICAL ASSESSMENTS OF THE GEOTECHNICAL FACTORS EFFECTING PRE-SPLITTING IN THE FIELD

Although the mechanics of pre-splitting have attracted some attention in the past and present, relatively few people have worked on the varying geotechnical factors affecting the success of pre-splitting, the majority of authors working on the effect of geostatic stress fields (Nicholls and Duval, 1966a and Fennel, Plewman and Brown, 1966). More recently McCormick (1972) defined the geotechnical factors that he considered may effect blasting in general. However no practical work was included in this publication.

Field observations of the effect of weathering on the success of pre-split blasting have been reported by Hoover (1972) and Talbot (1977). They both conclude that the presence of highly weathered material leads to poor results and overbreak.

The most important publication up to the end of the seventies is by Trudinger (1973), entitled 'An Approach to the Practice of Pre-splitting in Anisotropic Rock Masses'. During pre-splitting in the construction of dam spillways in South Australia,

Trudinger observed that the main geological feature affecting the quality of the pre-split, was the relative orientation of the predominant regional foliation. From recorded measurements and further observations he concluded that where the angles between the required batters and foliation were less than twenty five degrees, pre-split results were unsatisfactory, between twenty five and forty degrees the pre-split planes followed paths partly along the foliation and partly across the fabric of the rock and where greater than forty degrees, the resulting pre-split planes occurred almost entirely across the fabric.

In addition, further work on the mechanics of pre-splitting has been published by the author (Worsey et.al, 1981).

### 3 THEORY OF PRE-SPLITTING

It is logical that a reversal to basic principles be made by considering the mechanisms involved in explosive fracturing around single shot holes before dealing with the complication of interacting multiple shot holes.

#### 3.1 COMPONENTS OF EXPLOSIVE ENERGY RELEASE

According to Johansson and Persson (1970) the process of detonation of an explosive charge is extremely complex, involving both steady and non-steady state reactions. The process consists basically of a shock wave which travels through the explosive charge at extremely high velocity, producing an extremely high pressure and temperature reaction zone in its immediate vicinity and a radiating steep fronted (short rise time) shock wave into the surrounding media. Following this reaction front, pressure decreases as the further chemical reaction and the expansion of gaseous explosive products into the hole proceeds. This process is universally accepted by the explosive and chemical industries.

The velocity of the detonation wave through the explosive or as a shock wave through rock is dependent on the confining shock velocity of that medium. As a shock wave travels faster than the seismic velocity of the medium, shock and detonation wave velocities can be expected in excess of 2.5 to 7.0 km per second. The build up of gas pressure within the borehole, produced by further chemical reaction and expansion of the gaseous products of detonation takes place within a period of milliseconds, the rate being dependent on such factors as borehole or charge size and the chemical composition of the explosive. However in one millisecond the detonation and resultant shock wave will have travelled in excess of 2.5 to 7.0 metres from any reference point along the explosive column. Therefore it can be unequivocally stated that the dynamic and quasi-static gas components of energy release may be treated as totally separate events, being separated both by type and in time.

### 3.2 ROCK FRACTURING BY THE DYNAMIC COMPONENT OF ENERGY RELEASE

### 3.2.1 Factors Affecting the Dynamic Component Magnitude

Before examining the processes of rock fracturing by the dynamic component, it is important to firstly consider the factors which may affect the size of the dynamic pulse from the moment it reaches the borehole wall to its dissipation at infinity.

The first factor which ultimately decides the initial peak magnitude of the detonation wave and ultimately that of the shock wave is the charge weight of the explosive. The total dynamic energy ( $E_d$ ) released on detonation will be proportional to the charge weight ( $W$ ).

$$\text{i.e. } E_d = k \cdot W$$

where:  $k$  is a constant of the explosive  
(per unit weight of explosive)

If we consider a spherical charge, then the peak value of the dynamic component will be proportional to the cube root of the charge weight or volume. A series of comparative studies of explosives in a range of rock types by the U.S. Bureau of Mines (Atchison and Roth, 1961, Nicholls and Hooker, 1962, Atchison and Pugliese, 1966a, Atchison and Pugliese, 1964b,

Nicholls and Duval, 1966 and Bur et.al., 1967) has resulted in equations for peak strain caused by a dynamic shock wave at any point in that rockmass, of the form:

$$e = Kc(R/W^{1/3})^n$$

where: e = peak strain

R = the distance to the shot

K = strain intercept at a scaled distance of one unit

n = weighted average slope (log-log axes) and is a function of the rock

As stress ( $\sigma$ ) can be related to strain (e) by the following simple formula:

$$\sigma = Ee$$

where: E is the Youngs Modulus of the material

Then stress:

$$\sigma = E.Kc(R/W^{1/3})^n$$

However exact formulations for the strength of a dynamic shock pulse do not exist to the best of the author's knowledge at the time of writing, although the Geothermal Energy Project at the Cambourne School of Mines is known to be working on the problem.

As the dynamic wave moves away from the explosive

charge it is subject to large pressure drops due to dynamic impedance mismatch at the explosive-air and air-rock interfaces. When a shock wave meets the boundary between two layers of differing acoustic velocity, then only a portion of the energy is transmitted, the remainder being reflected in the opposite component, i.e. compression as tension and vice-versa. The equations for transmission and reflection for any point on an incident wave form are as follows:

$$\sigma_t = \sigma_i (2/1+R) \quad (1)$$

$$\sigma_r = -((1-R)/(1+R))\sigma_i \quad (2)$$

where:  $\sigma_i$  is the incident pulse

$\sigma_t$  is the transmitted pulse

and  $\sigma_r$  is the reflected pulse

$$R = \rho_t \cdot U_{s_t} / \rho_i U_{s_i} \quad (3)$$

where:  $\rho_i$  = density of first medium

$U_{s_i}$  = shock velocity of first medium

$\rho_t$  = density of secondary medium

$U_{s_t}$  = shock velocity of secondary medium

The explosive-air impedance mismatch may be eliminated by the use of slurry charge as a replacement for cartridged charges, where complete

coupling<sup>3</sup> is impossible to achieve due to sticking problems with individual cartridges in the borehole on loading if the cartridge diameter is not significantly smaller than that of the hole. However, pre-splitting as already stated in the introduction utilises light decoupled charges, therefore a highly significant drop in dynamic pulse strength is to be expected (Atchison et.al., 1964) due to the extremely low density and acoustic velocity of air in relationship to the explosive.

On release from the explosive charge the dynamic component is a pure compressive pulse in form. This is easily indirectly verified as the air surrounding the explosive charge cannot sustain substantial tension or shear and therefore cannot allow the transmission of such components.

As the dynamic component spreads away from the detonated charge and borehole it decays, firstly due to cylindrical expansion of the wave front subject to simple square law decay and secondly by attenuation (Austin et.al., 1966, Asklof and Nylander, 1968 etc.) caused by the rock which does not act in a perfectly

-----  
<sup>3</sup> Coupling is the measure of how well the explosive charge fills the blasthole and is measured either by a straight volumetric percentage (0-100%) or by the ratio of the charge to borehole diameter.

(1968)<sup>4</sup> that tensile tangential stresses will develop at a distance of three to four hole radii from the centre of the borehole. In contradiction Selberg (1951) states that significant tangential tensile strain is developed at the hole boundary. However although Johansson and Persson credit the discrepancy between their analysis and that of Selberg to the oversimplifying assumptions of the Selberg treatment, the author feels that Selberg's initial assumptions are fundamentally wrong and that significant tensile strain at a hole boundary can only be created by the following quasi-static gas component and not by the dynamic component.

### 3.2.3 Dynamic Fracturing

According to Kisslinger (1963) and Pearson (1980) it is possible to distinguish three zones of deformation and fracturing around a detonated charged hole:-

1. A strong shock (hydrodynamic) zone immediately surrounding the hole.

-----  
<sup>4</sup> The numerical model was developed for calculating high amplitude shock wave processes in liquids.

2. An intermediate (non-linear) zone with fracturing varying from severe crushing, through plastic deformation to partial fracturing.
3. An outer (elastic) zone exhibiting predominantly radial fracturing.

However this model also incorporates the quasi-static component which is disregarded by these authors so the author therefore proposes the following mechanisms:-

In rock it is obvious that if the charge weight and coupling are excessively high then the dynamic pulse compressive peak may exceed the dynamic compressive strength of the rock and crushing (i.e. disintegration) of the rock will occur around the borehole wall. Due to the amount of energy expended in this process, the compressive peak will rapidly drop to below the dynamic compressive rock strength and the crushing process will cease. Such zones have been reported by Kutter and Fairhurst (1971) etc. An interesting phenomenon which has been observed in some blasted perspex models (depending on the explosive loading geometry adopted) is the existence of a clear zone immediately surrounding the hole, of approximately one hole radius in extent (Johansson and

Persson, 1970, Schutz, 1972 and Pearson, 1980). This effect is attributed to plastic flow by Pearson (1980) and is alleged to occur when the maximum induced stress in the rock mass exceeds its elastic limit (Hugoniot Elastic Limit) for which pressure the relationship between maximum and minimum compressive stresses, and is:

$$\sigma_3 = \left[ \frac{v}{1 - v} \right] \sigma_3$$

Above this limit the Mohr circle falls below the Mohr failure envelope and fracturing may not occur.

For granite with a uniaxial compressive strength of 135 Mpa, Pearson gives a maximum dynamic principle stress of 3.57 GPa above which a Hugoniot (annular clear zone) will exist.<sup>5</sup>

If the tensile component of the dynamic wave exceeds the dynamic tensile strength of the rock then tensile fracturing will occur. Carrasco and Saperstein (1977) have shown that for model pre-splitting in Plexiglas, fracture initiation does not occur at the borehole wall but at a short distance

-----  
<sup>5</sup> The author refrains from discussing this particular topic further as such high charge densities and coupling are purposely avoided in pre-splitting practices; where low charge densities and decoupling are used to reduce damage to the final face. Further discussion is therefore deemed irrelevant to this thesis.

away from the borehole wall and then propagates outwards. This work agrees with the previous postulations and in addition model testing solely utilising the dynamic component (Chapter Four) has shown that many of these fractures extend back to the borehole wall.

The maximum velocity of stable crack propagation is of the order of one third of the acoustic velocity of the medium (Fourney et.al., 1974 and Barker et.al., 1979). Hence the fracturing created by the outward radiating dynamic shock wave will be predominantly fresh fracturing and not produced by extension of the existing fractures, although fracturing will continue preferentially along the path of existing fractures. Therefore, the instant the tensile component of the dynamic pulse falls below the dynamic tensile strength of the medium, fracturing by this means will cease. From this point onwards the medium will act in an elastic manner and sufficient energy will have been dissipated from the dynamic pulse for it now to exist as an acoustic rather than a shock wave.

This wave will continue to decay to theoretical zero at infinity unless it confronts an abrupt change in medium or a free face where part or the whole of

the pulse respectively will be reflected in the opposite component (as previously discussed). The passage of the tensile tail of the radial component, according to Kutter (1967), if sufficient may cause minor deflectional growth of the fractures perpendicular to their original paths. The effect of the following shear wave is minimal due to its lower strength in comparison with the pressure pulse and occurrence of any fracturing will be in the form of fracture extension which will rapidly cease due to the ratio of maximum fracture propagation velocity and shear wave velocity.

This extension (L) may be given by the following equation:

$$L = \frac{x \lambda_s C_f}{2 C_s} \left[ 1 + \sum_{n=1}^{\infty} \left[ \frac{C_f}{C_s} \right]^n \right]$$

where:  $\lambda_s$  = shear wave length

x = fraction of shear wave length  
above critical shear value

$C_f$  = maximum fracture propagation velocity

$C_s$  = shear wave velocity

Kutter (1967) divided the dynamic zone of fracturing into a zone of dense radial fracturing and a zone of less dense fracturing which were well defined

in laboratory models in Plexiglas.<sup>6</sup> He states that the fractures of the dense zone are caused by tensile hoop stresses associated with the compressional wave exceeding the dynamic tensile strength of the material, and that many small fractures are initiated by the passage of this wave. These, however do not have sufficient time for growth before the wave passes on, for the reasons already given. These fractures eventually join because of residual stresses at their tips, which form rough surfaced fractures. This is in agreement with observation of fracturing by Carrasco and Saperstein (1977) and the author.

Kutter ascribes the fractures of the second zone which are continuous fractures rather than a series of smaller ones joined together and are extensions of individual fractures from the first zone, to various residual hoop and tangential stresses. However it is obvious to the author that these are in part produced by quasi-static effects<sup>7</sup> which the author admits is virtually impossible to eradicate totally, even using vented half boreholes.

-----  
<sup>6</sup> This is in agreement with the author's results and observations (Chapter Four).

<sup>7</sup> The electro-hydraulic effect used by Kutter consists of the dynamic component being created by electric discharge in water which however vapourises some of the water, producing pressurised steam and thus a quasi-static component.

The fraction of strain energy dissipated by the shock wave during the fracturing process is estimated to be approximately 10% (Fogelson et.al., 1959, Langefors and Kihlstrom, 1978, Pearson, 1980).

### 3.3 ROCK FRACTURING BY THE QUASI-STATIC GAS COMPONENT OF ENERGY RELEASE

#### 3.3.1 Calculation of the Quasi-static Component

After the passage of the dynamic component into the rock, the products of detonation still remain i.e. both gaseous and solid (small particles of explosive). Due to the high temperature produced during detonation, reaction continues until a stable gaseous mixture is reached. The explosive gases rapidly fill the borehole, applying increasing pressure to the borehole wall. Because of the relatively small time period in which peak pressure is obtained, the process can be assumed to be adiabatic in nature. Therefore the peak quasi-static gas pressure may be simply obtained if one knows the gas volume after firing in  $l/kg$ , the density of the explosive, the decoupling and

the temperature of explosion, by the following equation:<sup>8</sup>

$$PE = V_a \cdot \rho (TE + 273) / (293 \cdot D^2)$$

where: PE = peak gas pressure

V<sub>a</sub> = resultant gas volume at S.T.P.  
measured in l/kg

ρ = density of explosive

TE = explosion temperature (degrees Centigrade)

D = decoupling ratio

Peak gas pressure, along with detonation velocity and explosive temperature may also be calculated directly from the ratios of chemical components using the Pecus-Yevick equation of state. An excellent mathematically worked description of this is given by Edwards and Chaiken (1974) which has proved to give acceptably accurate results.

The ease with which the peak pressure of the quasi-static gas component may be obtained is in stark contrast with the problems involved in the direct calculation of the dynamic component, which to the best of the author's knowledge is still under investigation.

-----  
<sup>8</sup> This equation is a modified form of the equation found in Section 5.1.3 and incorporates decoupling.

### 3.3.2 Mechanisms of Quasi-static Fracturing

Once peak pressure is attained, the explosion gases begin to escape from the borehole, resulting in a fall in pressure within the hole. This escape may be effected in two separate ways; firstly by the direct escape of these gases by venting from the borehole collar after displacing any top stemming that may be present and secondly by escape of the gases into the explosively produced and natural fractures surrounding the borehole. Due to the relatively long length of time in which the quasi-static gas component of energy release is active on the rock immediately surrounding the borehole compared with that of the dynamic component, due to the latter's rapid radiation from the hole (tens of milliseconds compared with microseconds), the quasi-static component of energy release is believed to be the dominant factor controlling the breakage of rock in blasting.

Kutter (1967) showed in model blasting in Plexiglas that by statically pressurizing a dynamically fractured hole, that existing electro-hydrolically induced dynamic fractures could be extended by a factor in excess of ten. Dally et.al. (1975) found from exploding charges in thin perspex sheets that

containing the charges produced cracks which were larger by a factor of seven than those produced with the charge vented, i.e., the quasi-static component of energy release was responsible for fracture extension six times the length of dynamic fracture initiation. Further it has been shown that by notching boreholes and maximising the effect of the quasi-static gas component, fracture planes could be extended over a considerable distance (fifty times the borehole diameter - Dalley and Fourney, 1977).

It is obvious therefore that the quasi-static component of energy release is the most important factor controlling fracture extension. However the dynamic component of energy release is responsible for fracture initiation.

In model testing performed by Brost (1970) and Schultz (1972), after detonation of the charge the expanding gases were observed to enter the zone of dynamic fracturing almost instantaneously. These fractures were then seen to extend, the gases following but dropping further and further behind the propagating fracture tips. Further evidence of the penetration of the quasi-static component into the fractures surrounding the borehole is given in Chapter

Eleven by the author.

It has been suggested by Russian investigators (Barenblatt, 1962 etc.) that during the process of hydrofracture, fluid does not extend completely to the end of the crack, (see Chapter Eleven). It is therefore obviously valid to assume that the extension of dynamic fracturing by the quasi-static gas component is by a mechanism exceedingly similar to hydrofracture.

The processes involved in this can be best explained by the use of the Energy Balance Concept (Perkins and Krach, 1968). Original theory on hydrofracture was based upon elastic behaviour at the fracture tip. However according to the elastic solution (Sneddon, 1946):

$$\frac{\sigma}{p} = \frac{-2}{\pi} \arcsin(r_f/r) = \frac{1}{\sqrt{(r/r_f)^2 - 1}}$$

if a uniform pressure  $p$  is applied within a fracture, then tensile stresses approaching infinity would be created at its tip. Such a solution is of course invalid as no known material could sustain such stresses and remain relatively intact. It is obvious therefore that an elastic solution is invalid. The partial elastic energy balance solution given by

Perkins and Kretsch is as follows:

Increasing the pressure within a fracture will result in an increase in the extent of the stress altered region around the fracture (Figure 3.1), maintaining the crack in a state of elastic stability up to a certain point. However if this point is fractionally exceeded then the system will become unstable and the crack will extend slightly in radius, the stress altered region extending in unison to effect a return to stability and thus curtailing fracture extension. The differential work done in extending the fracture is the product of the volume of the fracture and the pressure increment. The change in the system's energy is accounted for by two different means. Firstly, due to the pseudo-elastic nature of the system, some of the energy will be stored reversibly as elastic strain energy. Secondly, energy is required to create extra fracture surface area, and is thus irreversibly absorbed during the change.

With this approach, the work done by the increase in fluid pressure is equal to the total energy accounted for by increase in reversible elastic strain energy and irreversible new fracture surface energy.

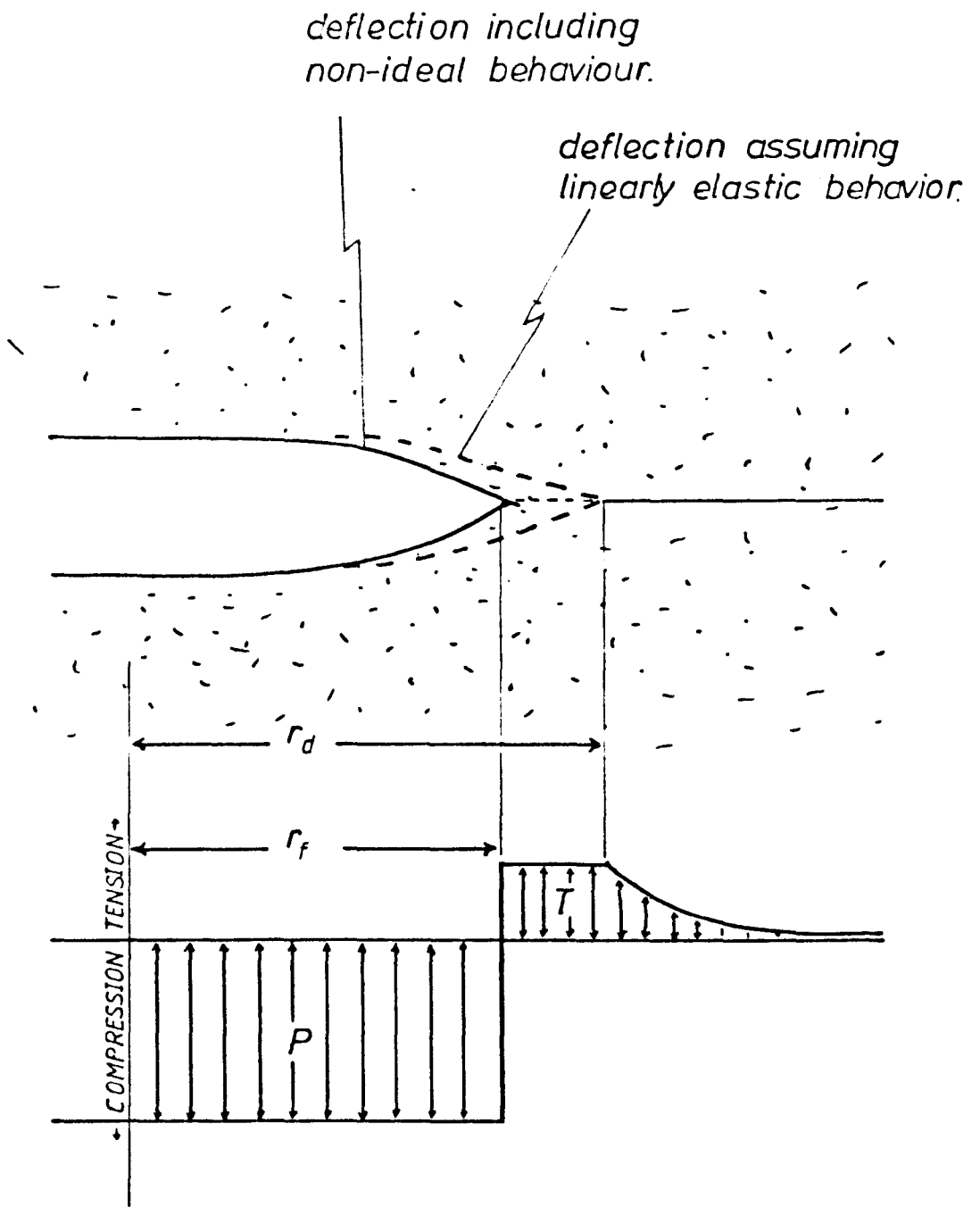


Fig. 3.1.

Fracture with damaged region stresses in the plane of the crack.

-after Perkins and Krech, 1968.

The energy balance equation (Perkins and Kretch, 1968) is given belows:

$$\begin{aligned}
 & [p-s] \sqrt{1 - \left[ \frac{p-s}{(p-s) + (s+fT)} \right]^2} \\
 & \times \sqrt{\left[ 1 + \frac{s+fT}{p-s} \right] \text{arc-cos} \sqrt{1 - \left[ \frac{p-s}{p+fT} \right]^2}} \\
 & = \sqrt{\frac{\pi a E}{2(1-\nu^2) r_f}}
 \end{aligned}$$

where: E = Young's modulus

f = Fraction of tensile strength that can be sustained across the damaged region

p = pressure applied within a crack

r = radius under consideration

$r_f$  = fracture radius

s = total earth stress perpendicular to the fracture plane

T = tensile strength of the rock

a = specific surface energy

$\nu$  = Poisson's ratio

$\sigma$  = stress in the plane of the crack

If p remains constant however the fracture can theoretically extend to infinity. This anomaly is accounted for by the drop in gas pressure within the hole due to the escape of gases into the dense zone of fracturing around the borehole wall, loss into

pre-existing discontinuities cutting or running close to the hole and by venting through the collar of the hole by displacement of any top stemming as already described. There will therefore exist a critical pressure below which fracturing will cease to propagate.

If dynamic fracturing does not extend back to the borehole wall and a 'clear zone' exists, then a selection of these fractures will be induced to extend back to the borehole wall by tensile tangential hoop stresses created during the pressurization of the borehole by the rise of the quasi-static gas component.

The equations for both induced radial, tangential and longitudinal stress around a pressurized cylindrical opening (see Figure 3.2) with internal pressure  $P$  are:

$$\sigma_R = + P r^2/R^2$$

$$\sigma_T = - P r^2/R^2$$

$$\sigma_L = 0$$

(assuming plane strain)

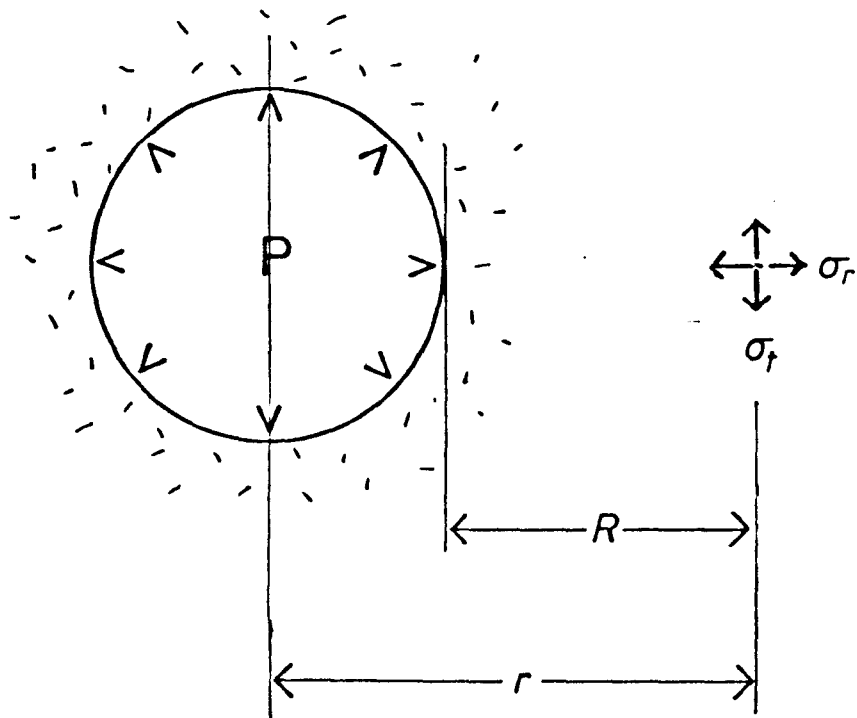


Fig. 3.2.

*Stresses at a point in the vicinity of a pressurised cylindrical borehole.*

### 3.4 THEORY OF MECHANISMS OF FRACTURE BETWEEN MULTIPLE HOLES

As explained in the previous chapter, there are two extreme views on the mechanisms of pre-splitting which are totally opposed. These are the dynamic and hydrofracture approaches, the two polarizations of thought both still being supported by various researchers and practising engineers. Before the actual mechanisms proposed by the author are given, these extremes will be discussed.

#### 3.4.1 Dynamic Approach to Pre-split Blasting

Various authors (Aso, 1966, Laroque and Coates, 1972, Griffin, 1973, Ratan and Dhar, 1976, Fries, 19 ) argue that pre-split fractures are caused solely by the interaction of the dynamic components of energy release from neighbouring boreholes.

Griffin (1973), stipulates that the pre-split fracture is initiated at the midpoint between boreholes by the 'bouncing back' of the dynamic compressive shock pulses in tension from one another. By this theory the pre-split initiated at the central

point between holes is extended back to the holes by the reflected tensile waves. This theory is obviously based on totally invalid assumptions and is impossible to sustain by using simple physical wave theory in which the addition of interfering waves occurs not reflection!

An alternative theory (Aso, 1966) is that tangential tensile hoop stresses are created (section 3.2.2) as a direct result of the radial compressive strain induced by the radial compressive stress component of the dynamic wave and that the interaction of these from neighbouring boreholes is responsible for the creation of the pre-split.

Aso considers three separate cases (see Figure 3.3) in which:

1. The rock strength is too great for the pre-split hole separations.
2. Optimum rock strength for pre-splitting exists.
3. The rock strength is far lower than the maximum for pre-splitting.

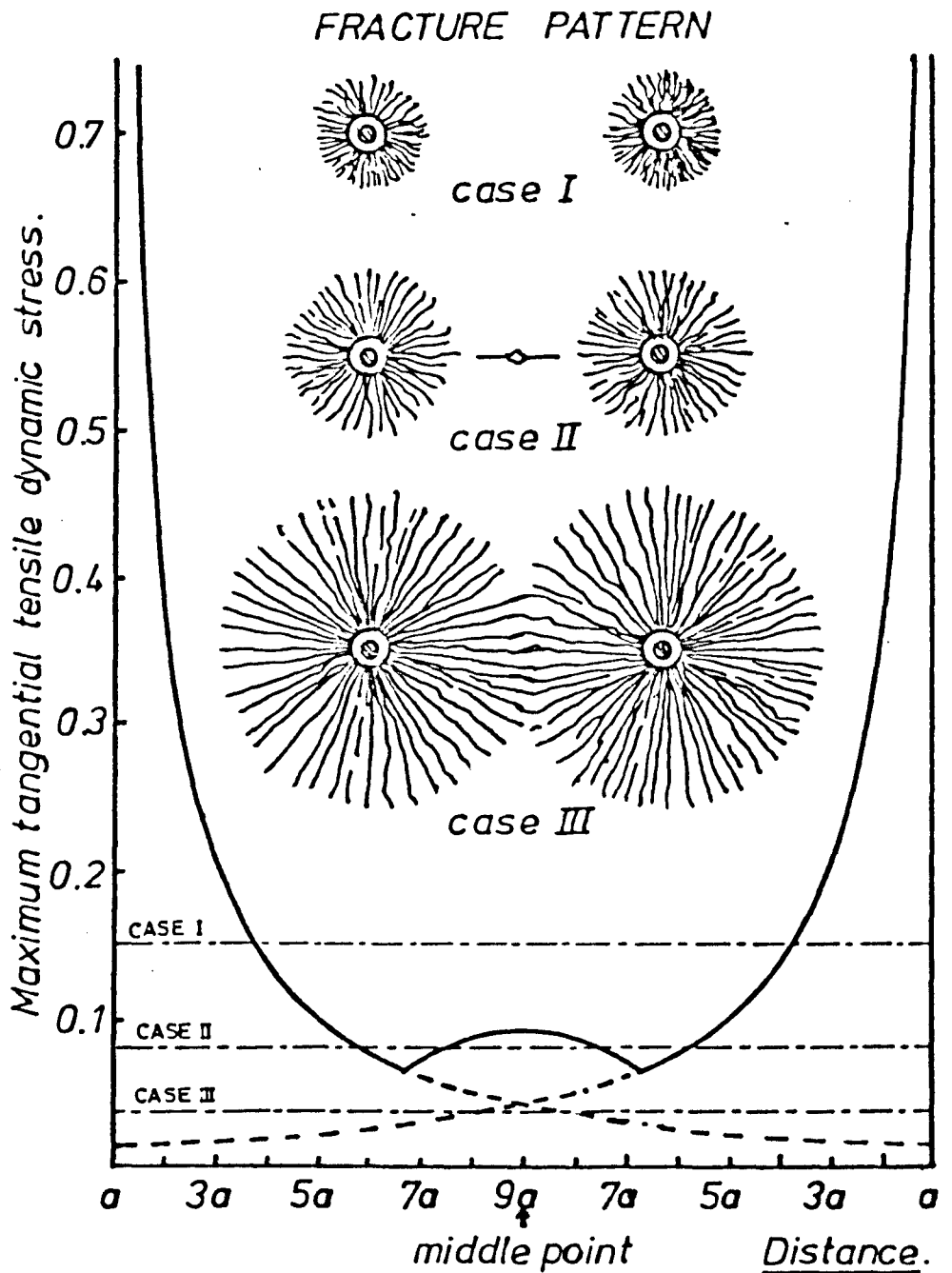


Fig. 3.3.

*Effect of rock strength on the superposition of dynamic components from neighbouring boreholes related to fracturing.*

*-After Aso(1966).*

In the first case, radial fracturing is created by the tangential tensile (hoop stress) component of the dynamic shock wave around the borehole but the borehole separation is too great for the rock strength to be overcome for fracture connection between holes. As soon as the maximum tangential tensile stress drops below the dynamic tensile strength of the rock, fracturing around the borehole ceases. At the midpoint between the holes the two dynamic waves meet and interfere, resulting in the addition of their tensile components at that point. However their sum is considerably less than the dynamic tensile strength of the rock and no further fracturing occurs.

In case two however, the rock strength is just less than the addition of the tensile components of the two waves and fracturing is initiated midway between the holes. This fracture then extends back to the larger radial fracture zones around the boreholes and a pre-split is formed between the two holes.

In the third case, the rock strength is so low compared with the charging and borehole separation that the tensile tangential component of the dynamic wave from each borehole exceed the dynamic tensile

strength of the rock for a distance of over half the borehole separation. The initial radial fracture zones around boreholes now interlock and excessive damage to the rock around the boreholes is incurred.

This hypothesis totally rules out the possibility of any contribution by the quasi-static gas component of energy release and relies on the assumption that gas pressure build up within the hole is purposely reduced to a non-active level by the use of decoupling.

However this can be proved not to be the case, as the effect of decoupling (especially that of air - see section 3.2.1) on explosive charges is to significantly reduce the peak dynamic component more than that of the quasi-static gas component.

In addition, for maximum or field pre-split borehole separations, fracturing is not initiated at the midpoint between boreholes (Nicholls and Duval, 1966, Carrasco and Saperstein, 1977) but at or near the borehole surface in agreement with the author's observations (see Chapter Four).

### 3.4.2 Quasi-static Gas Pressure Approach

It is suggested by such authors as Porter and Fairhurst (1971) and Jones (1978), that the role of the dynamic shock wave is minimal in the pre-splitting process, as the charges are specifically designed to incorporate the use of decoupling which minimises the dynamic component.

Such theories are based on the super-position of static stress fields induced by the pressurization of adjacent boreholes, resulting in more favourable fracture initiation conditions at the borehole wall in a direction along the pre-split line.

The mathematical argument by Jones (1978) (amended by the author) is as follows:

Ignoring the internal pressure of a borehole, the stresses at the surface of the borehole (assuming plain strain along the axis of the borehole) will be:

$$\sigma_T = \sigma_1 + \sigma_2 + 2(\sigma_1 - \sigma_2) \cos 2\theta$$

$$\sigma_R = 0$$

where:  $\sigma_T$  = tangential stress

$\sigma_R$  = radial stress

$\theta$  = radial angle measured clockwise from  $\sigma_2$  axis

Therefore maximum tangential stress:

$$\sigma_T^{\text{MAX}} = 3\sigma_1 - \sigma_2 \quad \text{when } \theta = 0 \text{ and } \pi$$

and minimum tangential stress:

$$\sigma_T^{\text{MIN}} = 3\sigma_2 - \sigma_1 \quad \text{when } \theta = \pi/2 \text{ and } 3\pi/2$$

If the pressure P within the hole is slowly increased then the conditions at fracture will be:

$$\sigma_T = 3\sigma_2 - \sigma_1 - P_1 = T \quad \text{at } \theta = \pi/2 \text{ and } 3\pi/2$$

where: T is the tensile strength of the rock

If a neighbouring pressurised hole, also of internal pressure P is the sole contributor of the external stress field at the first hole then the equation for an internally pressurized thick-walled cylinder is:

$$\sigma_R = \frac{P_o r_o^2 - P_i r_i^2}{r_o^2 - r_i^2} - \frac{(P_o - P_i) r_i^2 r_o^2}{(r_o^2 - r_i^2) r^2}$$

and

$$\sigma_T = \frac{P_o r_o^2 - P_i r_i^2}{r_o^2 - r_i^2} + \frac{(P_o - P_i) r_i^2 r_o^2}{(r_o^2 - r_i^2) r^2}$$

where:  $P_o$  = the external stress

$r_o$  = the external radius of the cylinder

$P_i$  = the internal pressure

$r_i$  = the internal radius of the borehole

$r$  = the radius of the point at which  
the stress is to be found

$\sigma_R$  = the resultant radius stress at a point

$\sigma_T$  = the resultant tangential stress at a point

As the external radius of the thick cylinder is

infinity and the external stress zero then this resolves to:

$$\sigma_R = + P_I \frac{r_I^2}{r^2}$$

$$\sigma_T = - P_I \frac{r_I^2}{r^2}$$

Then as  $P_I$  is positive  $\sigma_R$  is positive and  $\sigma_T$  negative:

$$\sigma_R \text{ is } \sigma_1 \text{ and } \sigma_T \text{ is } \sigma_2$$

Thus preferential splitting occurs in the direction directly between holes.

Theoretically the process is identical to hydrofracture with a single pair of diametrically opposed fractures being produced. Jones (1978) shows illustrations of this in the field. However it is extremely difficult to observe fractures that are not open in rock without the use of specialised techniques such as the use of fluorescent dyes. However in model testing (Carrasco and Saperstein, 1977 and Worsey et.al., 1981) this has been shown not to be the case and in addition it is possible to find highly fractured pre-split boreholes in the field.

The hypothesis's main downfalls are: firstly there is no room available for inclusion of the preceding effect of the dynamic component of energy release and

secondly its mechanics dictate that the presence of pre-existing fractures within the borehole surface would induce the boreholes to open along these features prematurely, excluding the possibility of a pre-split fracture. This is seen not to be the case in the field where fractures intersecting boreholes at between sixty to ninety degrees to the pre-split line have not induced failure to split.

### 3.4.3 Combination Approach to the Mechanics of Pre-splitting

A combination of both the dynamic and quasi-static components in the mechanics of pre-splitting was first suggested by Kutter (1967) and other authors since have also suggested this. However apart from work by Carrasco and Saperstein, little actual direct proof has been given. It is however the author's deep conviction that both components of explosive energy release play important roles in the formation of a pre-split. The process may be briefly described as follows:

Fracturing around each borehole in the pre-split line is initiated by the tangential component of the

dynamic wave of each shot hole produced on their detonation. Short circular dense radial fracture zones are created as these waves radiate away from the holes of their origin (as already described in single holes - see Section 3,2).

Outside this radial fracture zone the tensile dynamic wave peak drops below the dynamic tensile strength of the medium and therefore is unable to continue to create fractures although it may cause the extension of suitably orientated pre-existing fractures. Such fractures are encountered as the radially decaying waves from adjacent holes traverse their neighbouring holes, resulting in extension of the fractures parallel to the compressive radial component of the dynamic pulse and perpendicular to its tensile tangential component i.e extension occurs parallel to the line of pre-split. However maximum extension of these fractures will be a fraction of the waves' half wavelength and will be given by:

$$l = x \frac{\lambda}{2} \frac{c_f}{c_p} \left[ 1 - \sum_{n=1, \infty} \left[ \frac{c_f}{c_p} \right]^n \right]$$

for fracture propagation against the direction of dynamic wave travel and

$$l = x \frac{\lambda}{2} \frac{c_f}{c_p} \left[ 1 + \sum_{n=1, \infty} \left[ \frac{c_f}{c_p} \right]^n \right]$$

for fracture propagation with the direction of dynamic wave travel.

where:  $l$  = maximum length of fracture extension

$x$  = fraction of tangential component above  
critical tensile fracture extension stress

$\lambda$  = wavelength of dynamic pulse

$C_f$  = maximum fracture velocity in medium

$C_p$  = acoustic velocity of medium

thus resulting in fracture zones around each borehole of slightly ellipsoid form with longest axes parallel to the line of pre-split.

As the quasi-static gas component of energy release builds up, the explosion gases penetrate the fractures surrounding the borehole, extending them and the longest fractures becoming dominant at the expense of the shorter ones. The super-position of stress fields from neighbouring boreholes creates conditions more favourable for crack propagation parallel to the pre-split line and conditions less favourable perpendicular to it. The direct result of this phenomenon is to favour growth of the radial fracture zones around each successive borehole in an intensifying elliptical shape, with the longest fractures propagating at the greatest rates.

When extending radial fractures from neighbouring boreholes intersect, a through fracture between

boreholes is created. On formation, the pre-split plane opens, resulting in the venting of explosion gases which reduces borehole pressure and creates a redistribution of the stress field around the pre-split plane, such that fracturing perpendicular to the pre-split plane is curtailed.

### 3.5 THE ROLE OF THE PRE-SPLIT PLANE IN BLAST DAMAGE PREVENTION

Seismic refraction studies (Swindells, 1981, and Matheson and Swindell, 1981) on road contracts and quarry faces in Scotland has shown that ordinary bulk blasting using high explosives creates detectable disturbed zones of up to eight metres into the final face (see Figure 3.4) whereas pre-split faces show an equivalent disturbance depth of less than twenty centimetres.

There are two main theories of how a pre-split plane curtails or eliminates the damaging effect of neighbouring bulk blasting from the final face, these being; firstly reflection of the dynamic component (Katsuyama et.al., 1973 and Ratan and Dhar, 1976) and secondly by venting of bulk gases into the pre-split

Fig. 3.4.

Results of a bulk blast  
at location 9.

Illustrating bulk blast  
damage - C. Swindle  
standing at the furthest  
extent of open surface  
fracturing some 4m +  
from the face in the  
foreground. (Pre-split  
panel along line of  
stakes.)



plane (Devine et.al., 1965, Laroque and Coates, 1972, Lutton, 1977).

### 3.5.1 Dynamic Reflection Theory

Katsuyama et.al. (1973) have calculated by computer finite element techniques, the minimum separation of a pre-split fracture for complete dynamic reflection of a bulk blast to be 0.05 cm. They also quote that if multiple fractures rather than a single pre-split fracture are present then they need only have a minimum separation of 0.025 cm each. To the best of the author's knowledge no actual measurements of the openness of pre-split planes have been recorded and therefore it is not possible to verify that such openings exist although their presence under normal conditions is most likely.

However Devine et.al. (1965), Laroque and Coates (1972) and Lutton (1977) have conclusively shown that the presence of a pre-split plane between a measurement point and a bulk charge does not significantly reduce the magnitude of the bulk charge dynamic wave.

### 3.5.2 Venting of Bulk Gases Theory

The venting of bulk gases into the pre-split plane is postulated to be the key to the effectiveness of pre-splitting (Devine et.al., 1965, Jones, 1980). This view is partly supported by the author. At pre-split location number nine during bulk blasting after a previously fired pre-split trial panel (shown in Figure 3.5), bulk gases or a displacement of air and dust were seen to be emitted from the pre-split panel shortly after detonation of the bulk charge. This event was fortunately recorded on video, the sequence being shown in Figure 3.6, where by close scanning down the series of photographs these gases can be seen to be exhumed from the bottom portion of the pre-split plane nearest the bulk blast.

However the author feels that this alone is not the simple solution of the argument. Firstly with the use of pre-splitting the last row of bulk charged holes are at least a minimum of two to three metres and normally up to four metres away from the final face compared to normal bulk blasting without pre-splitting. The last row of bulk holes are used to only break rock to the pre-split face if designed properly. It is therefore obvious that the pre-split



Fig.3.5. Video recording of pre-split panel at Location 9 showing sequence of detonation of 4 adjacent panels of 6 holes each (1-2-4-3).

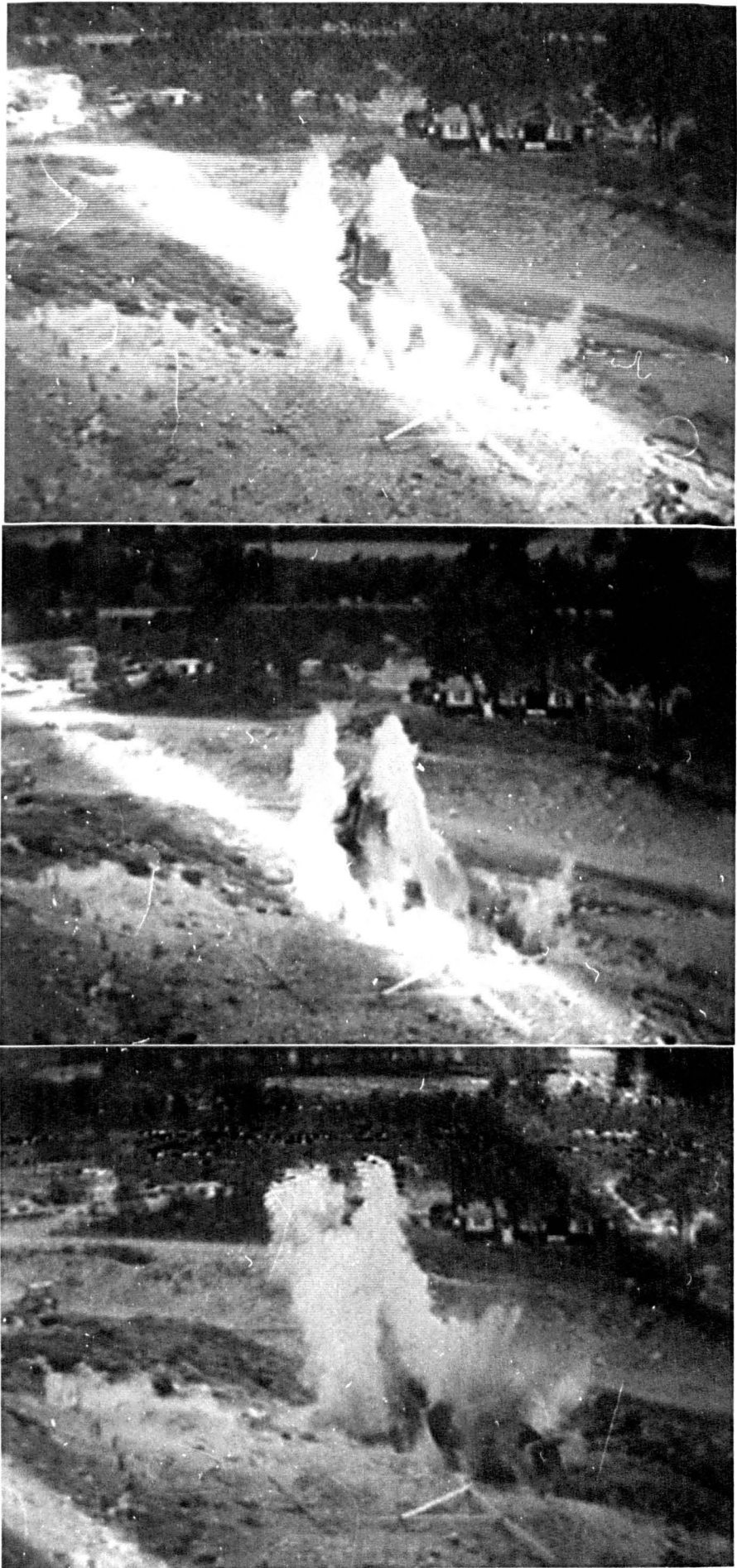


Fig. 3.6. Video recording sequence of bulk blast firing adjacent to pre-split panel in Fig. 3.5 showing gases venting from pre-split fracture. (mid-right around line of pegs).

plane has only approximately the last 50% of the depth of bulk blast disturbance (the weakest zone of damage) to contend with and contain. This fracturing would have been created by quasi-static fracture extension, which supports the above view. However the effect of the pre-split plane at this depth of bulk fracturing is thought by the author to allow opening of fractures intersecting the pre-split plane by the nature of its low shear resistance (being fractionally open). Thus the stresses at the blast fracture's previous tip are not transmitted to the opposing face and fracturing therefore terminates.

#### 4 TESTING OF THEORY BY MODEL BLASTING

##### 4.1 AIMS

In order to test the validation of individual previous theories on the mechanisms involved in pre-splitting and to verify the author's postulated theories, a series of model tests incorporating the use of explosives were devised. The ultimate aim was to derive the mechanism by which pre-splitting functions and to evaluate the relationship between, and comparative importances of gas pressure and detonation waves in pre-splitting.

##### 4.2 SEPARATION OF DYNAMIC AND QUASI-STATIC EFFECTS

In order to study the effect or relative importances of either the dynamic or quasi-static components in blast fracturing it is important to firstly eliminate the other component.

Kutter (1967) claims to have separated the dynamic component by using spark discharge apparatus in water.

However, inducing such high energy effects in water is bound to cause quasi-static pressure to build up by the vapourisation of some of the water to steam, which is enhanced by the effect of water being relatively incompressible.'

Apart from the complex apparatus and reserves needed to produce such effects on the scale used in this experiment programme and also other practical problems, there is no physical means of matching the dynamic effect of electric discharge to that of a detonated explosive within the same physical confines, i.e. boreholes of between 5/16ths and 1/10th of an inch width and three inches in length.

It is therefore felt that Kutter's experiments are unrepresentative of normal model blasting.

At the other extreme Jones (1978) attempted to isolate the quasi-static component by replacing it with hydraulic fracturing using pressurised oil. Unfortunately this is a totally static type of loading and the fracturing which would normally be initiated by the dynamic component in explosive fracturing is not present. Subsequently his tests showed that fracturing occurred along the easiest path, which was

usually parallel to the grain of the material he used rather than along the pre-split line.

It therefore can be concluded from the choice of available alternative techniques that: the only method of comparing the dynamic and quasi-static components in their independent roles of fracture initiation and extension and to quantitatively compare their effects, is to isolate each effect in testing incorporating the use of high explosive material.

As the dynamic effect is the first in order of occurrence, it was decided that this should be the effect to be initially studied. As the dynamic component is caused by the rapid detonation of the explosive, it is therefore dependent on the detonation wave which travels through the explosive. It is also dependent on the velocity of detonation of the explosive compared with the seismic velocity of the surrounding medium i.e. the relative acoustic impedances for its shape (maximum peak and duration which are inversely related). (See Plewman and Starfield (1965) and Wiebols and Cook (1965).) The dynamic component is wholly independent of the quasi-static component.

The quasi-static component is dependent on the confinement of the explosive, thus eliminating confinement will reduce the gas pressure to a minimal amount if not negating it completely.

#### 4.3 MATERIAL\_USED\_IN\_TESTING

The material chosen for use in testing was Polyester resin, a transparent 'plastic'. This material was chosen as it afforded flexibility in block size and good optical clarity at an economic price. The material was purchased from Strand Glass Plastics Ltd, and was of resin Type C. The methods and materials used in the casting of the resin into blocks, the curing and the associated problems encountered are given in Appendix A.

#### 4.4 MACHINING\_OF\_BLOCKS

After cutting to size before explosive testing, each block was subject to both top and bottom surfaces being machined flat. Also any other faces which were found to be substandard were machined by lathe.

Turning by lathe was found to give both a good flat finish and reasonable optical clarity. However, if the latter was not up to acceptable standard, a further polishing with perspex polish was undertaken.

#### 4.5 EXPLOSIVES USED IN TESTING

The main type of explosive used was PETN detonating cord (Cordtex). Unfortunately ordinary commercially available Cordtex has a charge weight of fifty grains per foot, so therefore a less powerful cord was needed.

Initially an eleven grain per foot PETN cord was experimented with, but again this was considered too powerful. Eventually four grain per foot PETN Low Energy Detonating Cord (LEDC) was obtained through ICI from Canada.

PETN Detonating Cord was used because PETN as an explosive has the relatively unique property of its detonation velocity being independent of charge diameter, its detonation velocity being approximately seven thousand metres per second.

Unfortunately one disadvantage of using such a thin explosive cord is that it is prone to misfire due to its low mass. Usually in normal blasting practice if this type of cord is to be used boosters of higher weight cord are strapped on at approximately half metre intervals. During this phase of blasting two holes misfired out of ninety one using four grain per foot cord. In both cases this was attributed to non-initiation at the detonator.

The initiation of the LEDC was by electric detonators numbers six and eight, the former being used in the majority of tests, the latter having been purchased with the eleven grain cord and were only used with the four grain LEDC when there were no number six's available.

Single strand four grain per foot PETN detonating cord was used in all series (a), (b), (c), (d) and (e) experiments.

#### 4.6 METHOD

Initial experimentation was undertaken to determine the optimum charge weights and dimensions of testing

and to obtain a "feel" for the materials used and experiments to be undertaken.

It was decided that before an attempt should be made to unravel the mechanisms involved in pre-splitting, the basics of fracture formation and extension around single blast holes should be investigated in relation to the degree of explosive coupling.

These first series of tests comprised of:

1. A series of ten single hole experiments using single strand cord, varying the borehole width from 2.5 mm (0.25 in) to 1 in (1 in) to determine the blast damage for a range of decoupling ratios (1 - 10) in 150 mm x 150 mm x 75 mm (6 x 6 x 3 in) resin blocks.
2. A similar series of five single hole tests but using half vented holes formed by sawing the blocks in two. These tests were designed to eliminate the quasi-static gas component, thus allowing investigation of the relation between the dynamic damage and decoupling ratio.

The series (b) half vented holes were constructed by drilling the required holes mid-distance between ends, near to the edges of half blocks and then machining those edges down until only half of each borehole remained in that face, the boreholes in each series of tests being vertical.

The second series of experiments were pre-splitting tests rather than single borehole tests and comprised of:

1. A series of twenty tests to determine the effect of decoupling on the maximum borehole separation for successful pre-splitting.
2. An attempt to pre-split using the technique in (b) with single cord taped to 1/8th inch half holes (as this theoretically gave maximum dynamic pulse, being the minimum size of borehole used in series (c) testing and afforded easy emplacement of the detonating cord), in order to examine the effect of the dynamic component in isolation, (four tests).

For the construction of series (d) experiments: pairs of holes of the specified diameter were drilled at specified spacings in blocks of resin. These were then machined down perpendicular to the line of the holes, from each end until two half holes remained.

The size of resin blocks generally used in experimentation were approximately three inches deep by six inches wide. The block lengths varied on the individual test requirements, varying from a minimum of three centimetres (series (d)) to a maximum of forty six centimetres (series (c)).

A final experiment (e) was performed to ascertain the role of the interaction of stress waves, by purposely excluding their interaction by delayed detonation of successive boreholes, the full theory and calculations of which are displayed in Appendix C. The test composed of three x 9.525 mm holes spaced at 38.1 mm centre with 27 micro-seconds delay increment per hole which were made by adding increments of 19 cms of detonating cord to successive holes.

A full list of test numbers for each series may be found in Appendix D and test specifications and complete blasting records in Appendix E.

Wave traps were used in all tests to significantly reduce the tensile reflection of the dynamic compressive pulse back into the block and thus reduce the effect of extra fracturing and fracture extension due to the immediate proximity of the free surfaces of the resin block. A full description of the wave traps and the associated theory behind them is given in Appendix B. The blocks with wave traps were placed in constraints for blasting.

#### 4.6.1 Constraints

Constraints were necessary for three reasons:

1. To hold the wavetraps in position.
2. To stop the rocks disintegrating and scattering over a wide area.
3. To simulate normal ground conditions in pre-splitting, i.e. semi-infinite ground extent.

The constraints were manufactured of bars of mild steel, there being two different types:-

The first constraints to be made were for six inch cubes. However, the size of block was reduced to a depth of three inches due to:

1. Lack of availability of long series small diameter drills of appropriate length.
2. Economic factors (increasing no. of blocks by a factor of two).
3. Availability of blocks due to casting time.

and therefore only one constraint was used per block. The design of the constraint for series (a), (b) and (d) is shown in Figure 4.1.

Due to the inflexibility of the first constraints a further constraint was needed when it became obvious that larger blocks for series (c) experiments were required. This constraint was fabricated of heavier mild steel bar and bolt holes were drilled to order for different size blocks, (see Fig. 4.2). The torque on the bolts was measured and was found to be considerably less than ten ft lbs, the minimum calibration on the torque wrenches available.

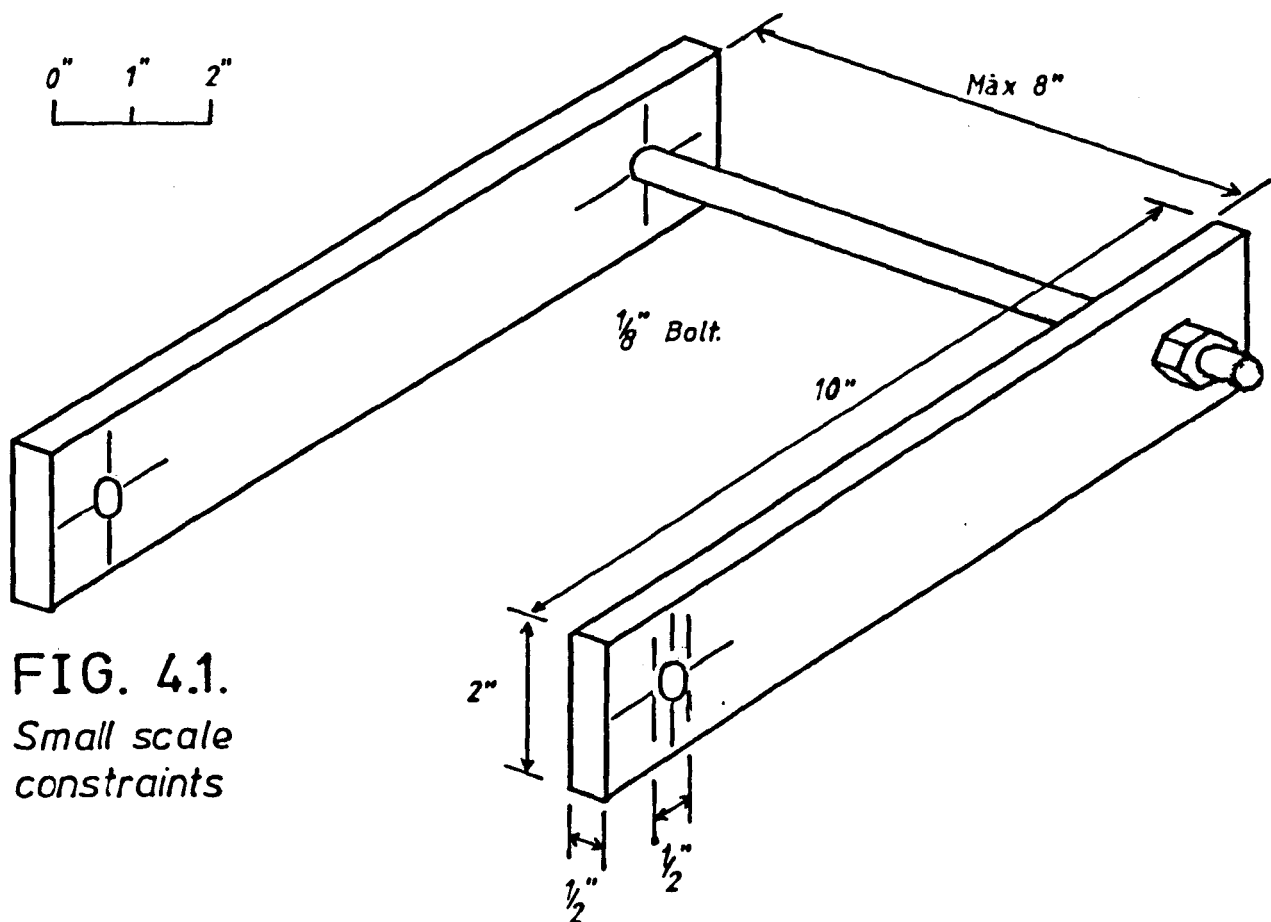


FIG. 4.1.  
Small scale constraints

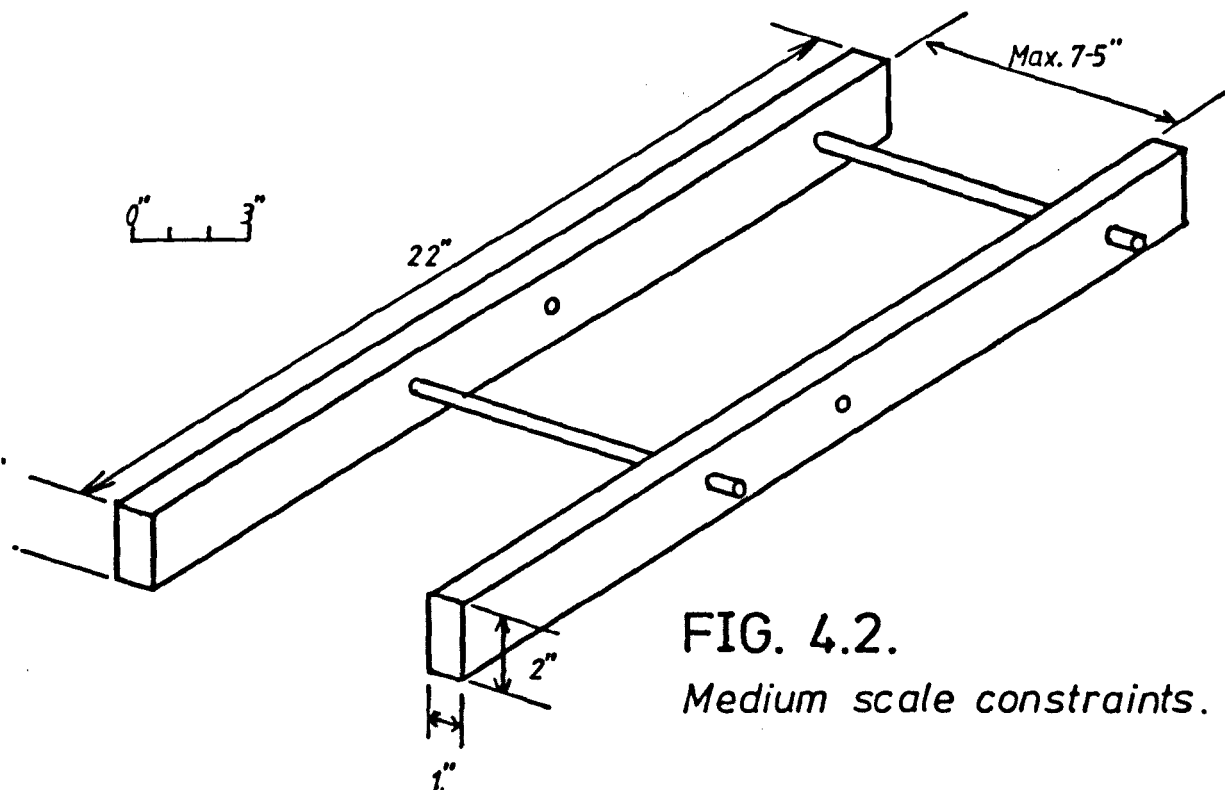


FIG. 4.2.  
Medium scale constraints.

#### 4.6.2 General Assembly

The wave traps and restraints were assembled as shown in Figs. 4.3, 4.4 and 4.5 for test series (a)+(c)+(e), (b) and (d) respectively. The blocks were transported to the departmental garage where the explosive testing was undertaken. The garage possessed the facility of a five foot deep concrete lined pit which could be covered with purpose cut railway sleepers. The explosive cord was then placed in the holes. To prevent the cord from moving either through or out of the latter two precautions were taken;

1. A piece of insulating tape was used to seal the bottoms of the holes to prevent the cord from protruding.
2. The cord was secured at the top of each hole by twisting insulating tape around the cord and then securing the latter onto the top surface of the block.

These two precautions were found to work exceedingly well.

Fig. 4.3.

Assembly for series (a),(c) and (e) experiments.  
X-section of charged block in restraints set up for blasting.

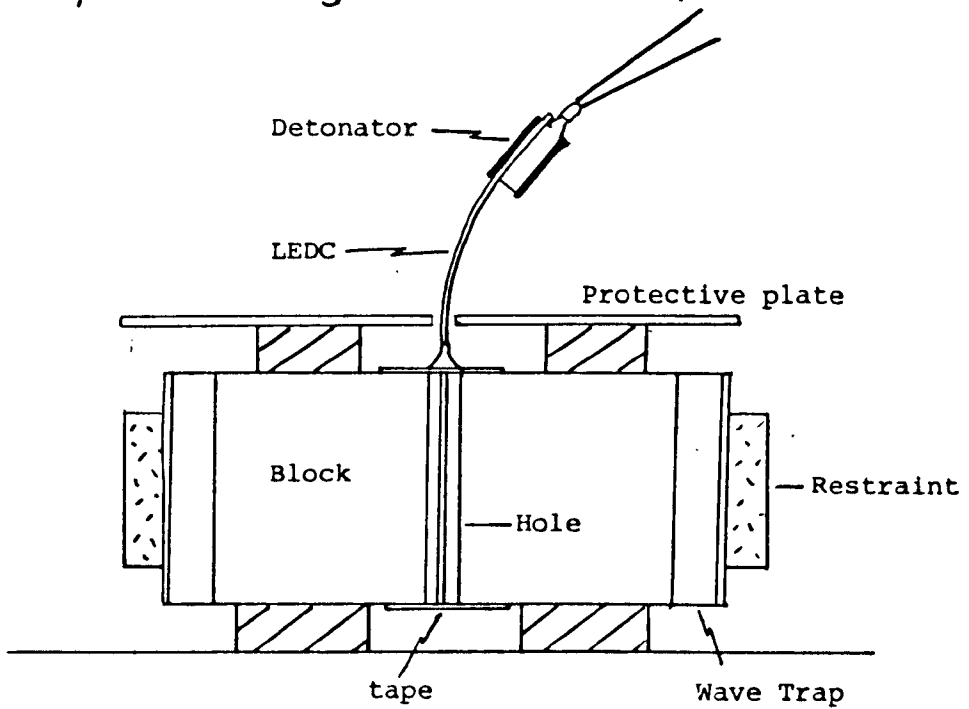
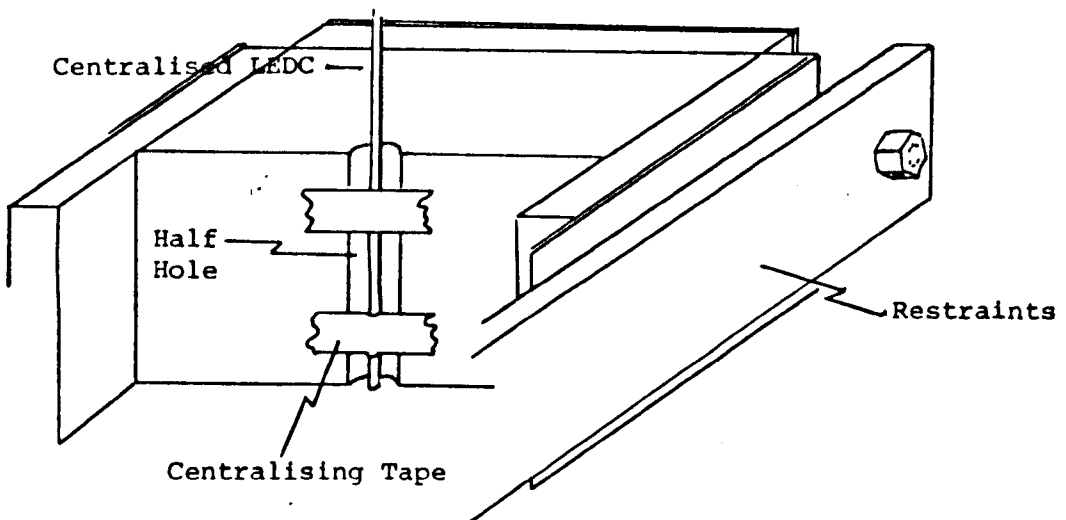


Fig. 4.4.

Assembly for series (b) experiments - minus protective plate and detonator.



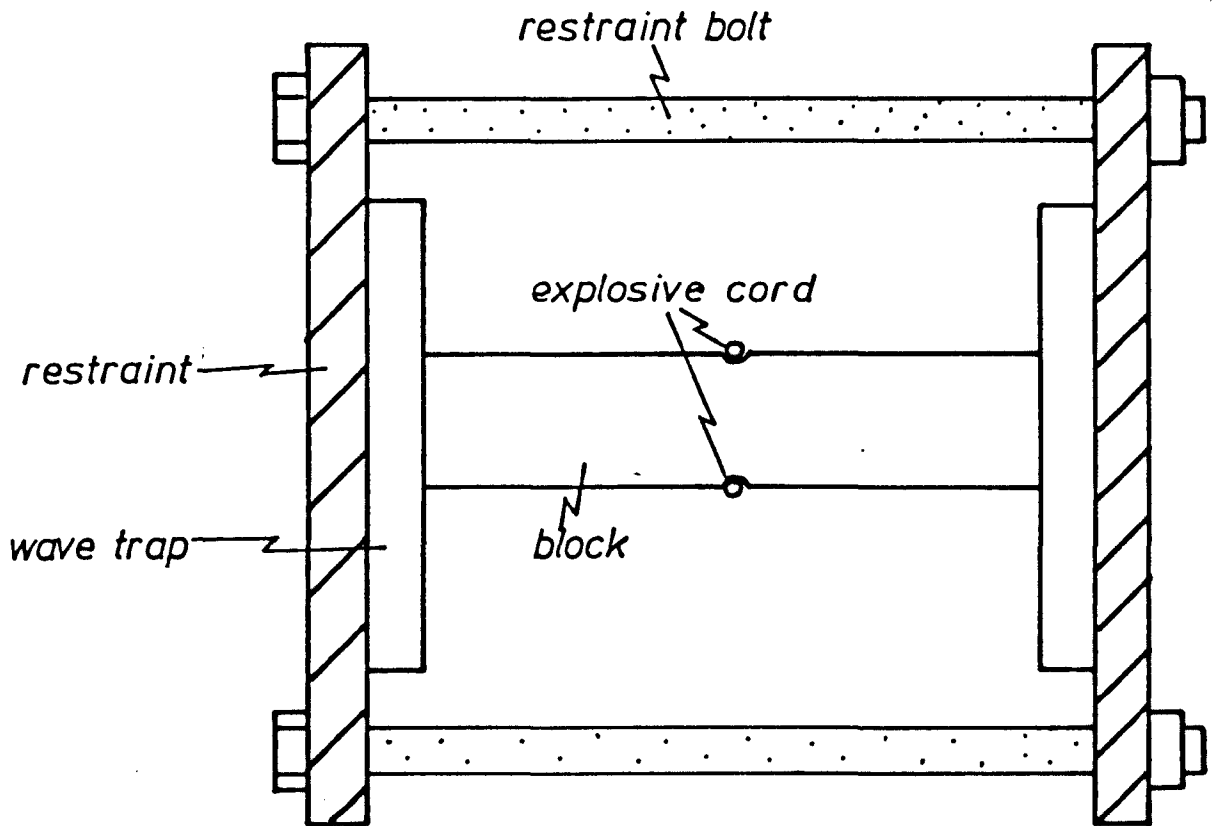


Fig. 4.5.

*Assembly for series (d) experiments with constraints and wave traps, ready for blasting.*

*Top view.*

N.B. No attempt was made to centralize the detonating cord in the hole except with the vented single hole experiments as it was not considered important. The results as discussed later appear to support this assumption. In series (b) and (d) the explosive cord was taped to the holes centrally with insulating tape as shown in Figure 4.4.

Equal lengths of detonating cord were used for ordinary multiple hole experiments (except in series (e) experiments) to ensure that detonation occurred simultaneously and congruently for each hole, the lengths of cord varying from six to fifteen inches dependent on the separation of the boreholes.

The bottom three inches of the four grain LEDC remained restrained within each hole, the excess being fed through the appropriate drilled hole in a 1/16th inch mild steel plate which was separated from the resin block by small wooden blocks. This plate was designed to protect the block from the electric detonator which was taped to the free end of the LEDC (N.B. an earlier 1/32nd inch steel plate had to be replaced very early on due to substantial detonator shrapnel damage).

The block was then placed on wooden chocks and the railway sleepers replaced over the pit. At this stage the detonation wires were attached to the detonator leads extruding from the pit and a 9v battery was brought to the site. The blast was subsequently initiated from outside, with the garage doors closed.

#### 4.7 MEASUREMENT OF BLAST DAMAGE AND FRACTURING.

##### 4.7.1 Determination of Blast Damage Zone.

A considerable amount of work has been undertaken in the past on the process of cracking in various materials around a borehole due to the detonation of an explosive charge. Research has been carried out on the relationship between the radial length of cracks and their frequency by Fennel, Plewman and Brown (1967), (see Fig.4.6). However, although their results show a good hyperbolic relationship between crack frequency and crack length, the preliminary tests by the author in polyester resin displayed very concentrated high blast damage zones which were visually distinct. The damage caused by the explosive

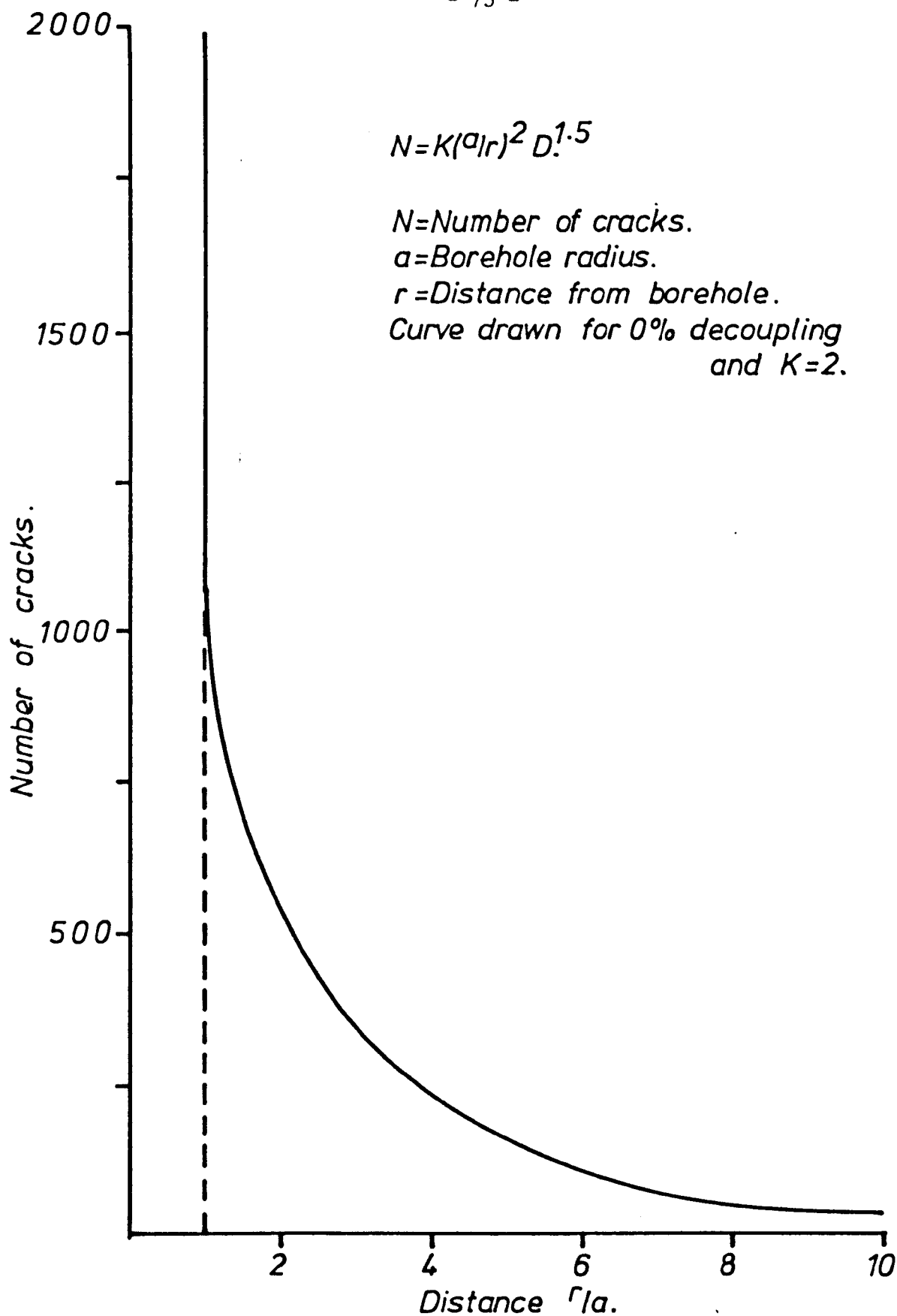


Fig. 4.6.

Relationship between the number of cracks and the radial distance from the borehole. After-Fennel, Plewman and Brown (1967).

was found possible to be categorised into two readily differentiable zones:

1. A dense zone of closely spaced fractures.
2. A zone around the first in which individual fractures from the former are preferentially elongated, (see Fig. 4.7).

#### 4.7.2 Need for Measurement and the Qualification of the Use of the Blast Damage Zone

To assess the damage caused around each hole in explosive testing some physical quantity which afforded easy measurement was required. Several of the parameters which were considered are discussed in the following:

The first obvious parameter to be considered was the maximum crack length generated by the blast. This could be easily measured from its tip to the centre or edge of the borehole. However, being a single crack from a single borehole this suffers from relative statistical invalidity if it is to represent average

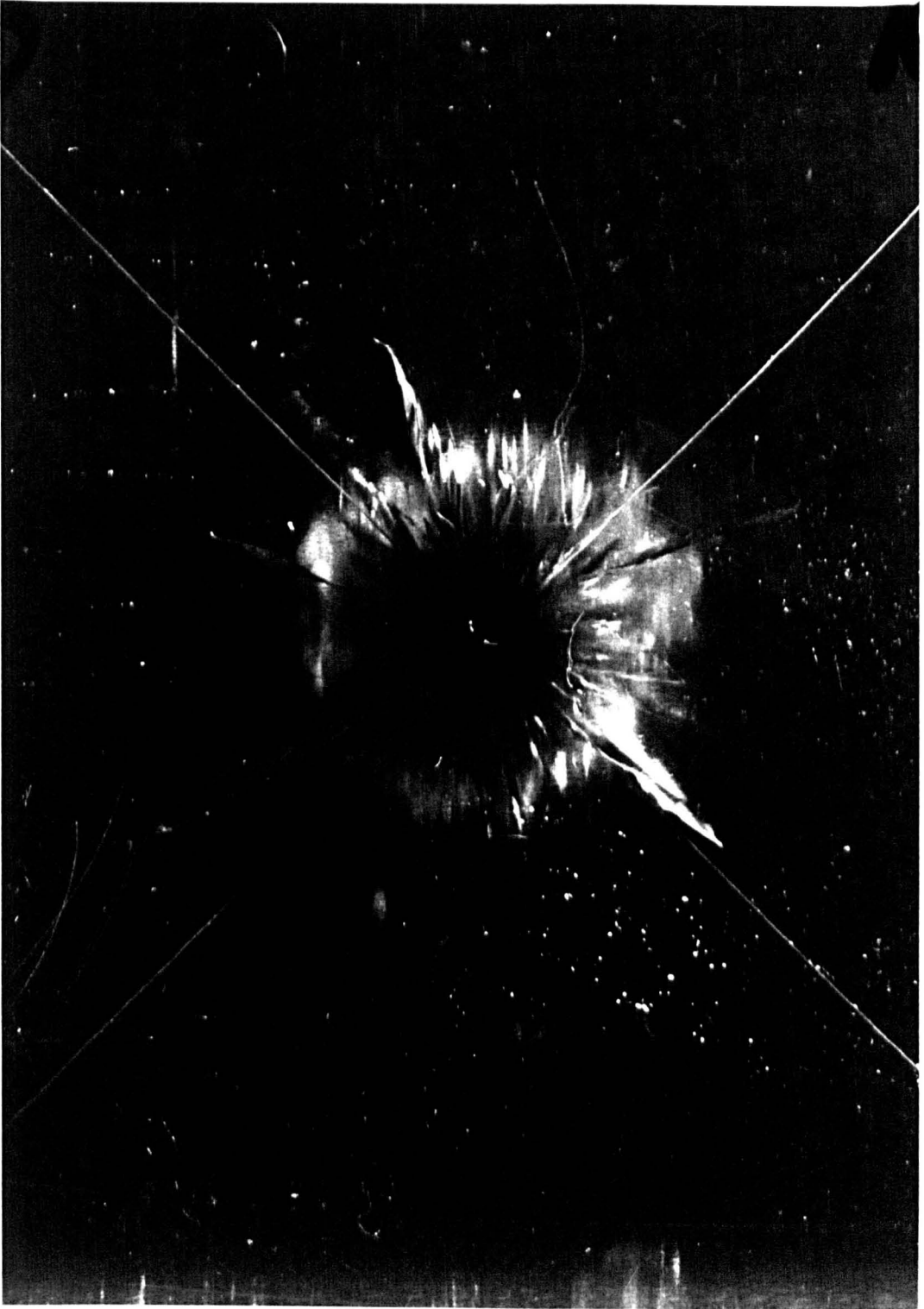


Fig. 4 .7.

Photograph of fracturing around a detonated shot hole in polyester resin, illustrating two distinct zones:

1. A circular dense zone of closely spaced fractures
2. A zone of less frequent extended fractures.

or even optimum crack length (due to imperfections in loading of the explosive cord and casting imperfections within the block etc.). To approach this would necessitate the reproduction of each test until a mean with an acceptable standard deviation was obtained. The second failing with this approach is that for low decoupling values (usually below 2.5) cracking on testing frequently reached the edge of the block, rendering the maximum crack length unobtainable.

The second parameter to be considered was the length of the  $n$ th longest crack. The main problem with this parameter is the selection of the value of  $n$ . If  $n$  was too small then it would suffer from the two above failings, but if  $n$  was too large, it would become too difficult and painstaking to locate the appropriate crack. Taking test 21 as an example, fifteen of the cracks propagated to the edge of the block in some form or other. Thus the correct value of  $n$  to be used should be greater or equal to sixteen.

The third parameter to be considered and ultimately chosen was the blast damage zone. The reasons for its choice were as follows:

1. Something that could be easily visually seen.
2. Because of the above, can be easily determined (measured).
3. Is not unidirectional (as a single crack) therefore is more representative.
4. One can take more than one reading on the radius of the roughly circular zone compared with a single crack and it is therefore more statistically valid. (E.g. if there is a weak stress field set up by the restraints this might cause elongation of cracks in a certain direction and restrain other cracking perpendicular to it. (An ellipsoid zone can be regarded as possessing the same area as a circular zone within certain limits.))

The main objection to this method of measurement is that a visual concept is not easily mathematically defined and may therefore vary from one observer to another. However, this should not increase the scatter of results if the measurements are taken by the same observer.

It thus became necessary to create a mathematical definition for the blast damage zone. A final solution to the problem was found by taking the radius in which a minimum of x fractures were present in an arc of any one y degrees. (x and y were taken as 3 and 45 respectively.) Thus:

The radius of the blast damage zone for any quadrant of 45 degrees is defined as the length of the 3rd longest vertical fracture that is present in the same quadrant.

Measurements of the longest and second longest crack lengths were also taken.

## 4.8 RESULTS

### 4.8.1 Series (a) Experiments

The results from normal single hole tests strikingly displayed the dependency of blast damage extent on borehole diameter, (see Figure 4.8). Blast damage was measured from both centre and edge of the

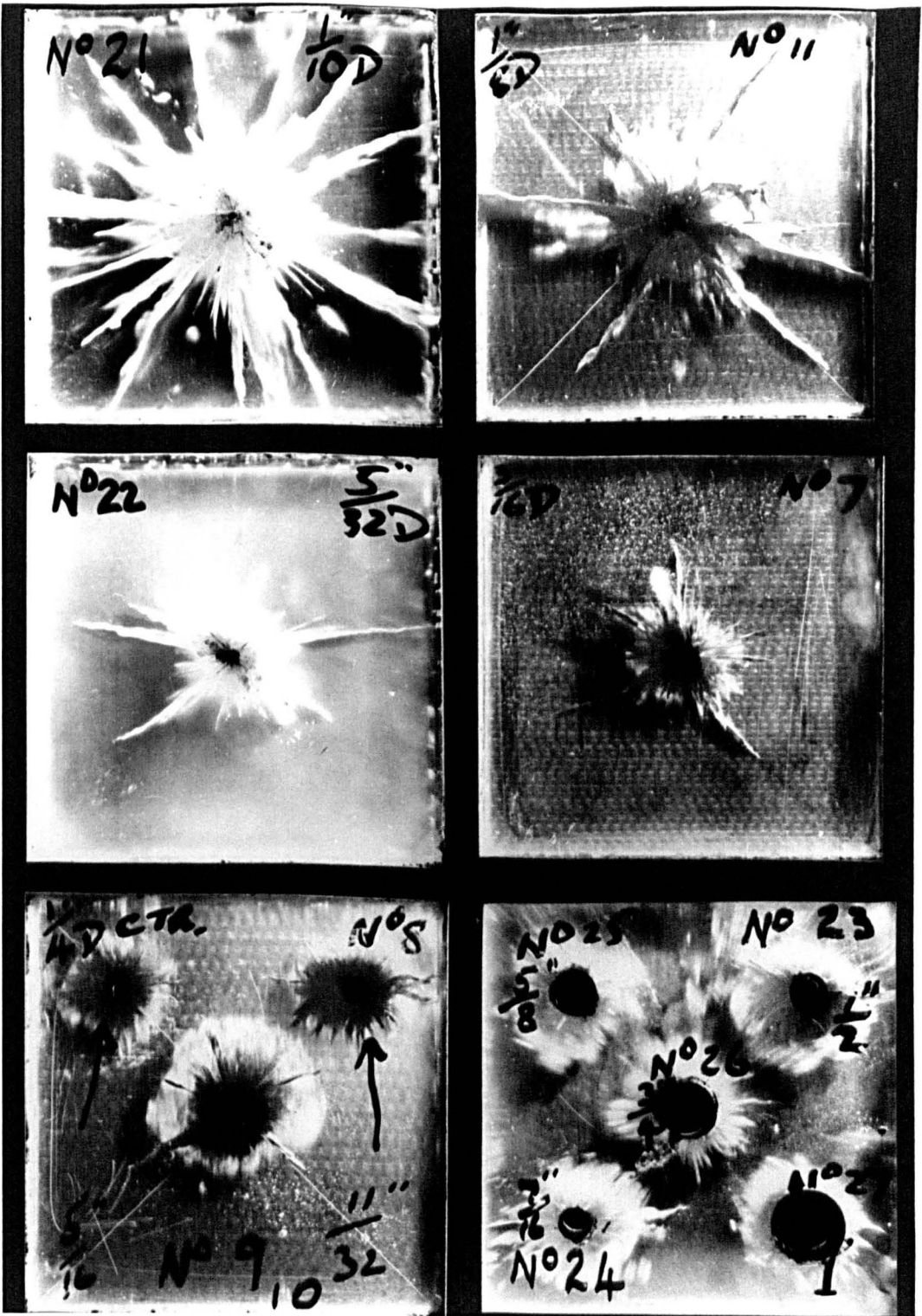


Fig.4.8.

Series (a) test results for single varying hole diameters, clearly illustrating the dependence of damage extent on decoupling. Hole sizes increasing from 2.5mm (decoupling factor 1) - top left to 25mm (decoupling factor 10) - bottom right.

borehole, but it was found that when measured from the centre, initially blast damage rapidly dropped with increasing borehole diameter as should be expected, but then levelled off and began to rise, (see Figure 4.9). Initially these results caused some consternation but this was soon explained by the following:

As borehole diameter increases, the cracks emanating from the borehole become shorter. Above a certain diameter the rate of decrease in crack length becomes less than the rate of increase in borehole diameter and thus the blast damage zone radius increases.

However, when blast damage is measured from the edge of the borehole then it fits a hyperbolic relationship with borehole diameter extremely well. This is shown in Figures 4.10 and 4.11. In Figure 4.11 the values of both damage and borehole diameter were plotted on log-log axes and a straight line fit was found to be highly satisfactory with a very low scatter of points. However this was found only to be the second best statistical fit with a goodness of fit of 94%. The best relationship only gave a 2% better fit, the remaining slight (hyperbolic) curve of the

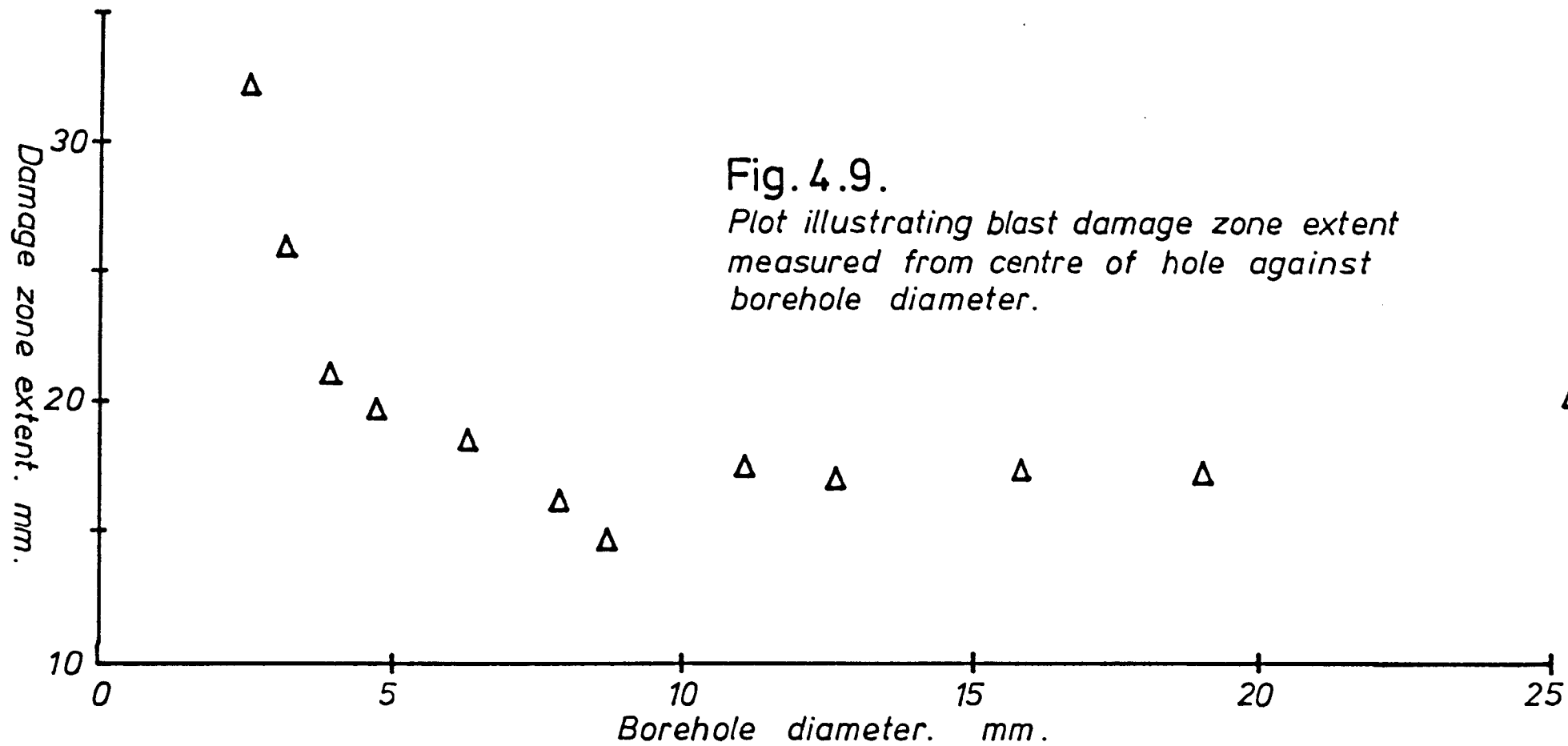
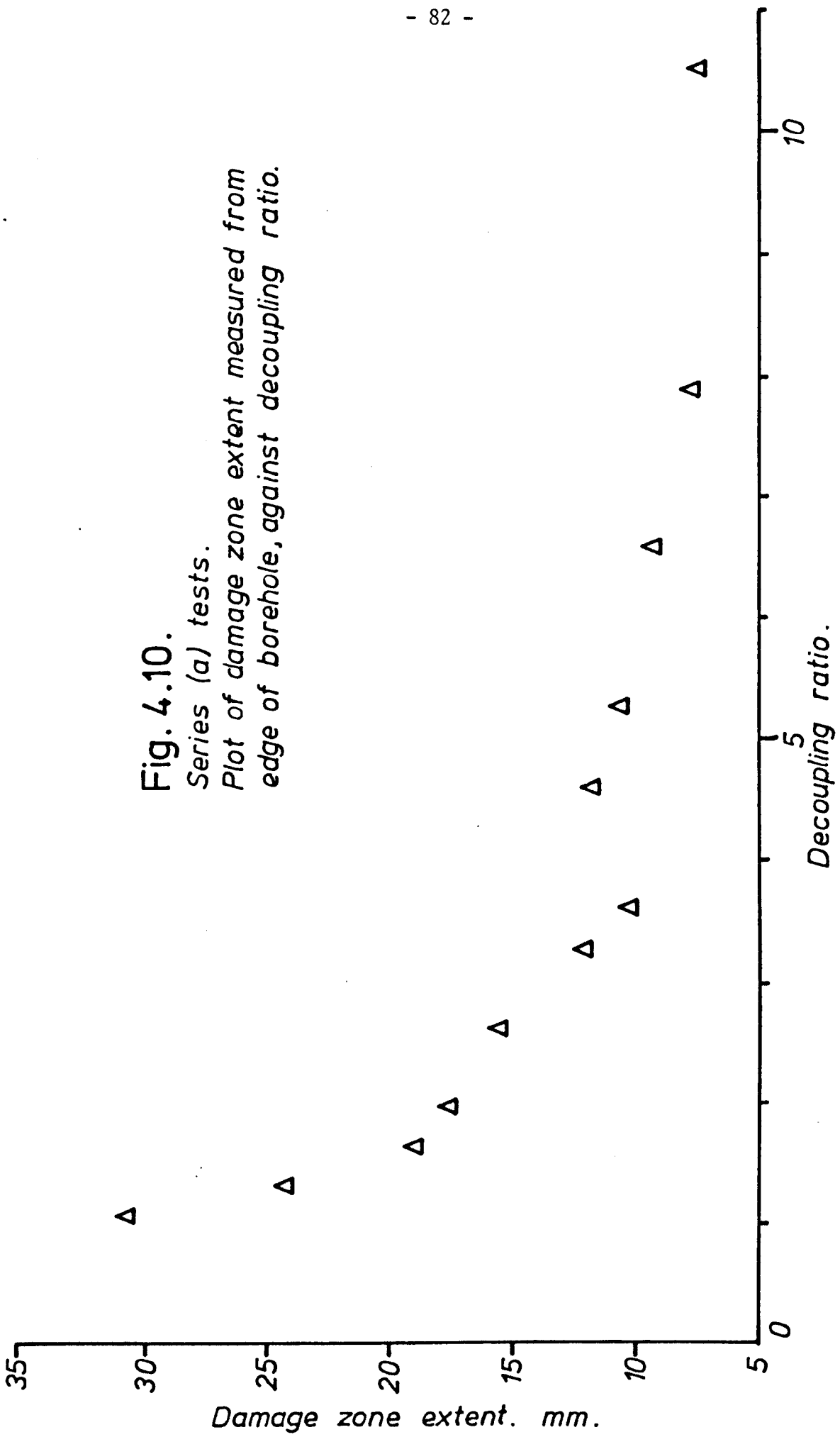


Fig. 4.9.

*Plot illustrating blast damage zone extent measured from centre of hole against borehole diameter.*

**Fig. 4.10.**  
*Series (a) tests.*  
*Plot of damage zone extent measured from*  
*edge of borehole, against decoupling ratio.*



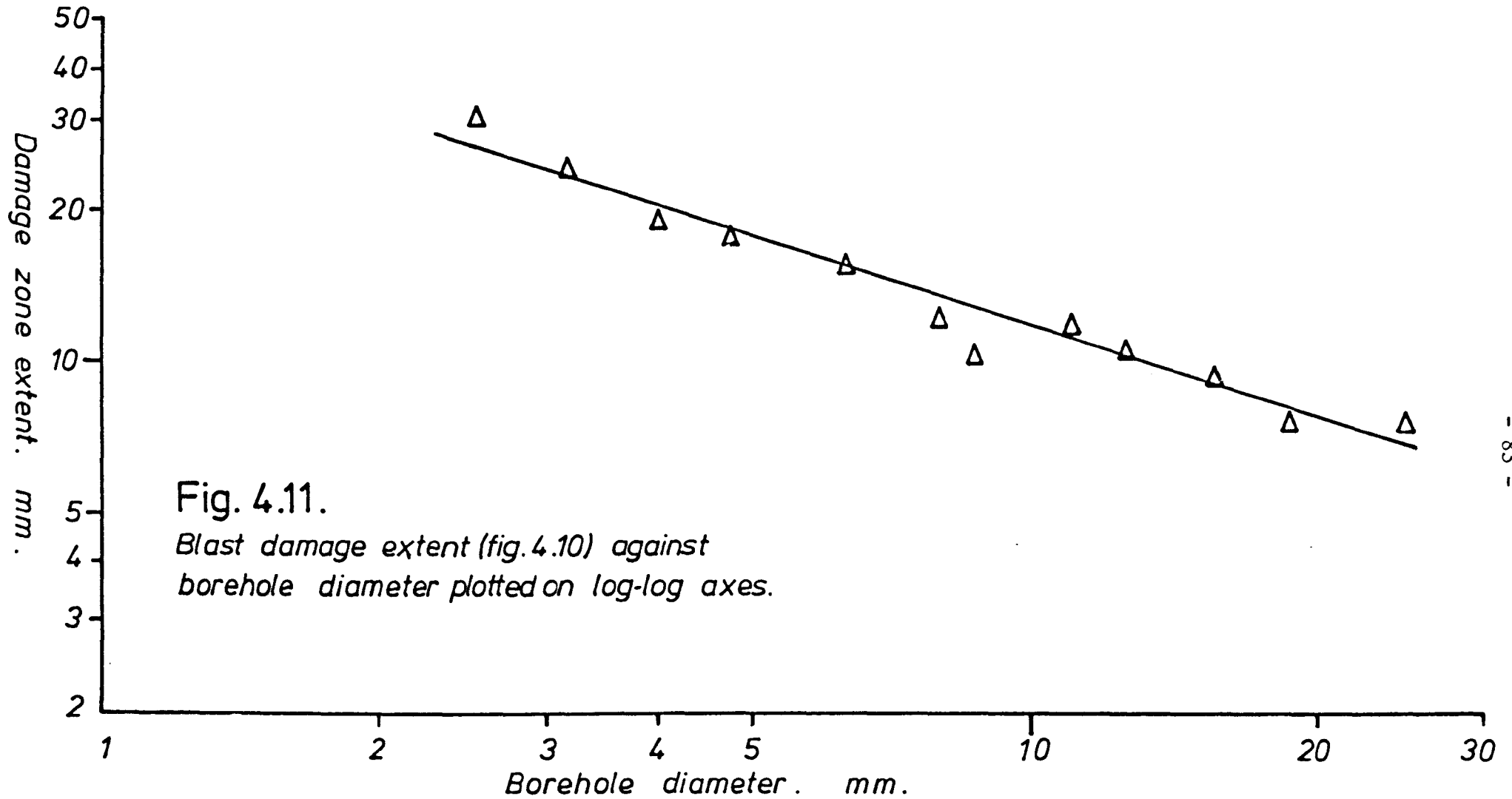


Fig. 4.11.

*Blast damage extent (fig.4.10) against borehole diameter plotted on log-log axes.*

points in Figure 4.11 giving rise to the small deviation. Thus it seems that another factor is affecting the relationship. From careful observations it is concluded that this is due to the variation in borehole size rather than having a standard sized borehole and altering the decoupling by using different charge weights, thus this is entirely a geometric effect. However from the results it can be seen that it is fairly insignificant within the experimental limits and as the effect on the points obtained is only of the order of experimental variation it can therefore be ignored. (Without specialist explosive loading facilities experimentation cannot be undertaken on the latter effect for the lower range of borehole sizes, but is theoretically possible with boreholes of a larger diameter.)

Column 1 = Test Number

Column 2 = Borehole Diameter in mm

Column 3 = Decoupling

Column 4 = Av. Blast Damage Zone Radius (from centre)

Column 5 = Av. Blast Damage Zone Radius (from edge)

7	4.76	1.97	19.75	17.74
8	6.35	2.63	18.60	15.70
9	7.94	3.29	16.30	12.32
10	8.73	3.62	14.75	10.40
11	3.18	1.32	26.00	24.40
21	2.54	1.05	32.20	30.90
22	3.97	1.65	21.10	19.10
23	12.70	5.26	17.10	10.75
24	11.11	4.60	17.60	12.00
25	15.88	6.58	17.45	9.51
26	19.05	7.90	17.40	7.90
27	25.40	10.52	20.40	7.70

Table 4.1.

A full list of blast damage values is given in Table 4.1 and the graph of maximum crack length for each individual test against borehole diameter is given in Figure 4.12, showing a similar relationship.

#### 4.8.2 Series (b) Experiments

Vented series (b) testing in which the quasi-static component was removed, provided a very small amount of fracturing/damage around the boreholes compared with normal confined tests. E.g. for 3.175 mm holes.

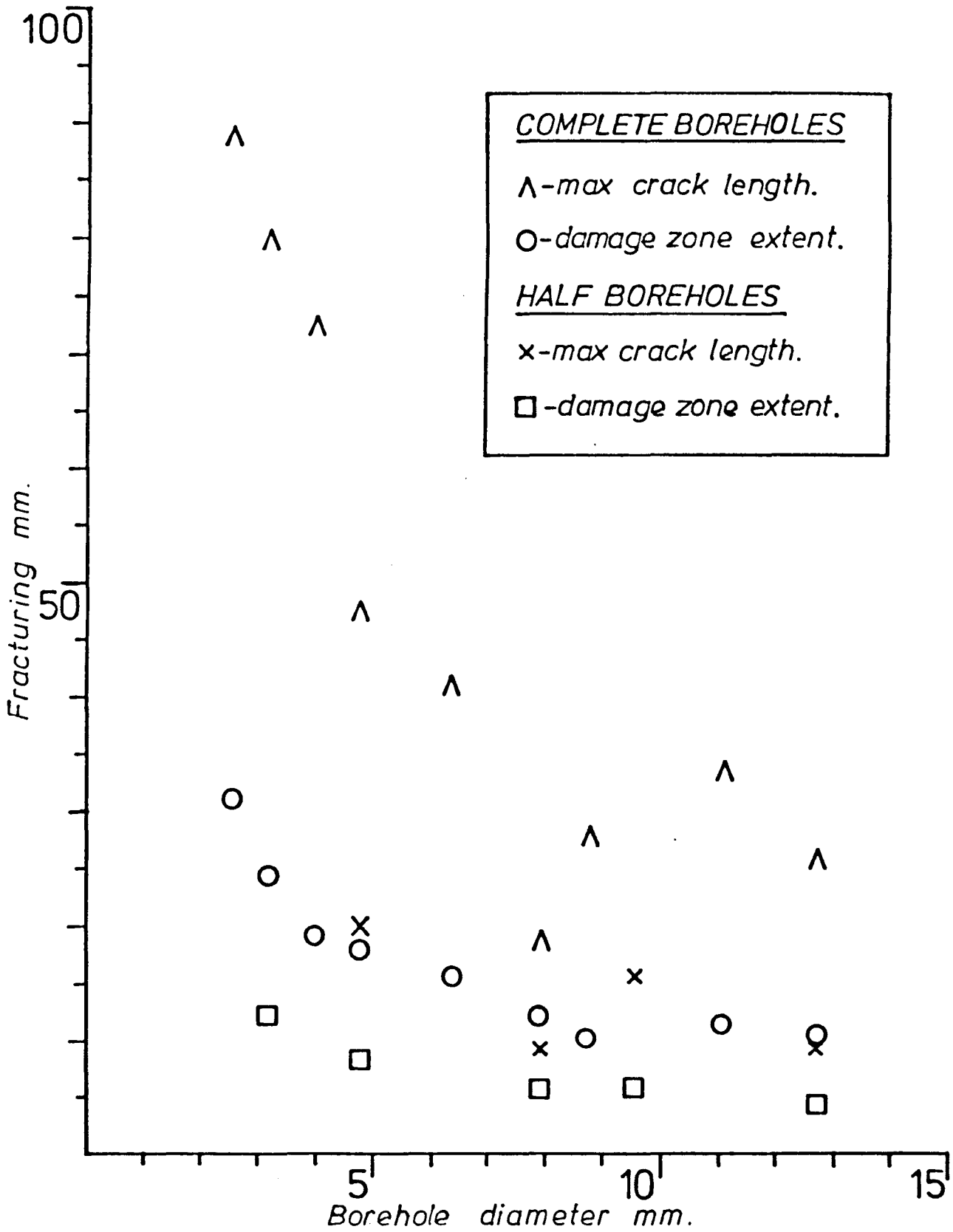


Fig.4.24 and 12.

Comparisons of maximum fracture length and damage zone extent between series (a) (complete borehole) and series (b) (half borehole) tests.

	<u>Damage Extent</u>	<u>Volume</u>
Vented	12.25 mm	150 sqmm
Normal	24.4 mm	595 sqmm

Also, virtually no elongation of cracks from the damage zone were observed. Those which were present only measured up to approximately fifteen millimetres in length, whereas elongated cracks in normal confined series (a) tests of the same borehole diameter (3.175 mm) normally exceeded 110 mm in length with a few exceeding 130 mm in length.

In these experiments the object was to eliminate as far as possible the gas pressure produced by detonation of an explosive in a confined space, thus leaving only the detonation wave from the explosive itself. Centralizing of the explosive in the half boreholes by taping was found to give consistent results, although the damage tended to be cumulative from the direction of explosive cord detonation, (see Figure 4.13). Again, an excellent hyperbolic relationship was found between borehole diameter and blast damage, (see Figure 4.14, values given in Table 4.2). The most striking feature of these experiments, as already described, was that the blast damage extent

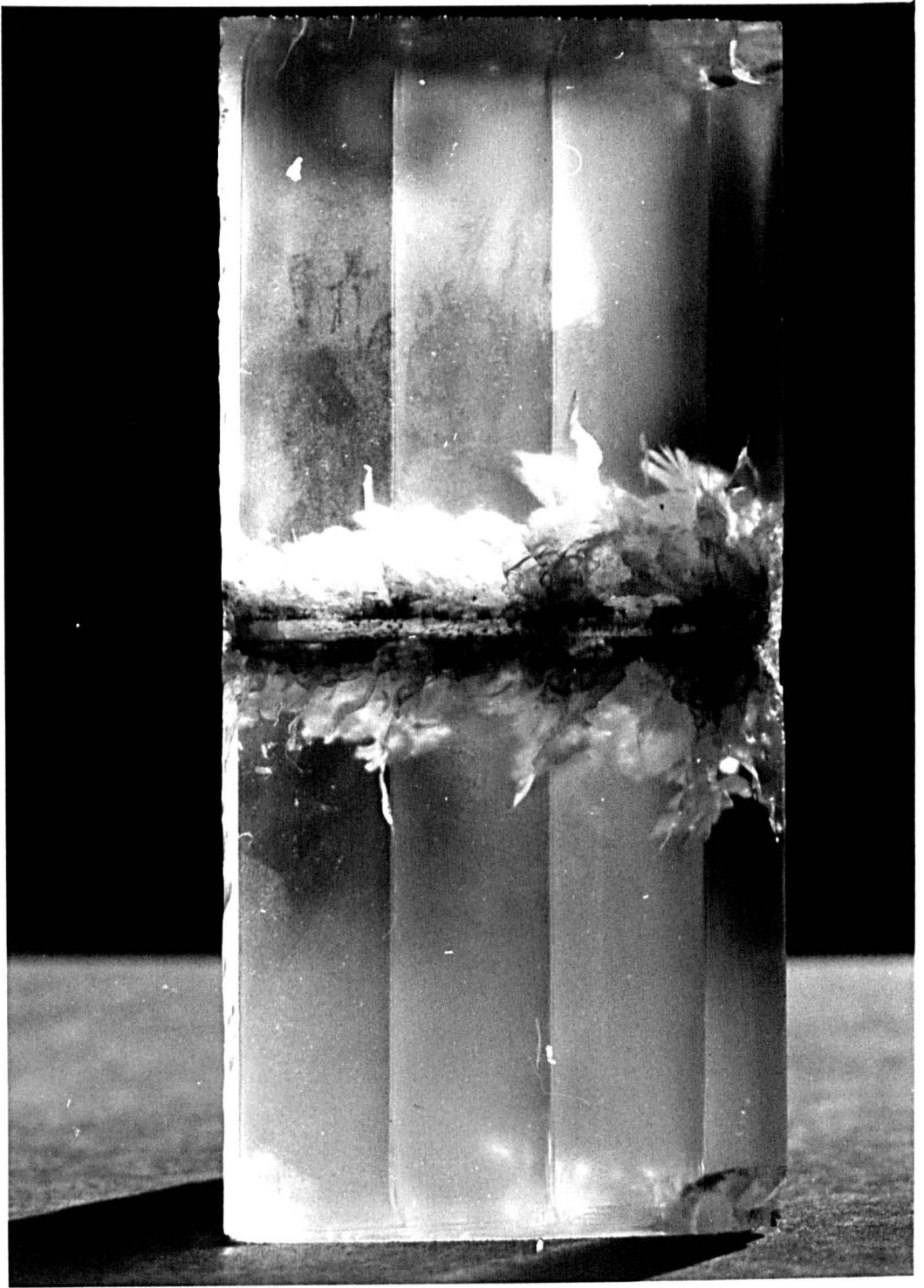


Fig.4.13.

Single vented hole series (b) test illustrating the cumulative effect of the dynamic component of a line charge (initiation from right to left) resulting in the extension of fracturing created by previous elements of explosive (fracture extension requiring less energy input than fracture creation).

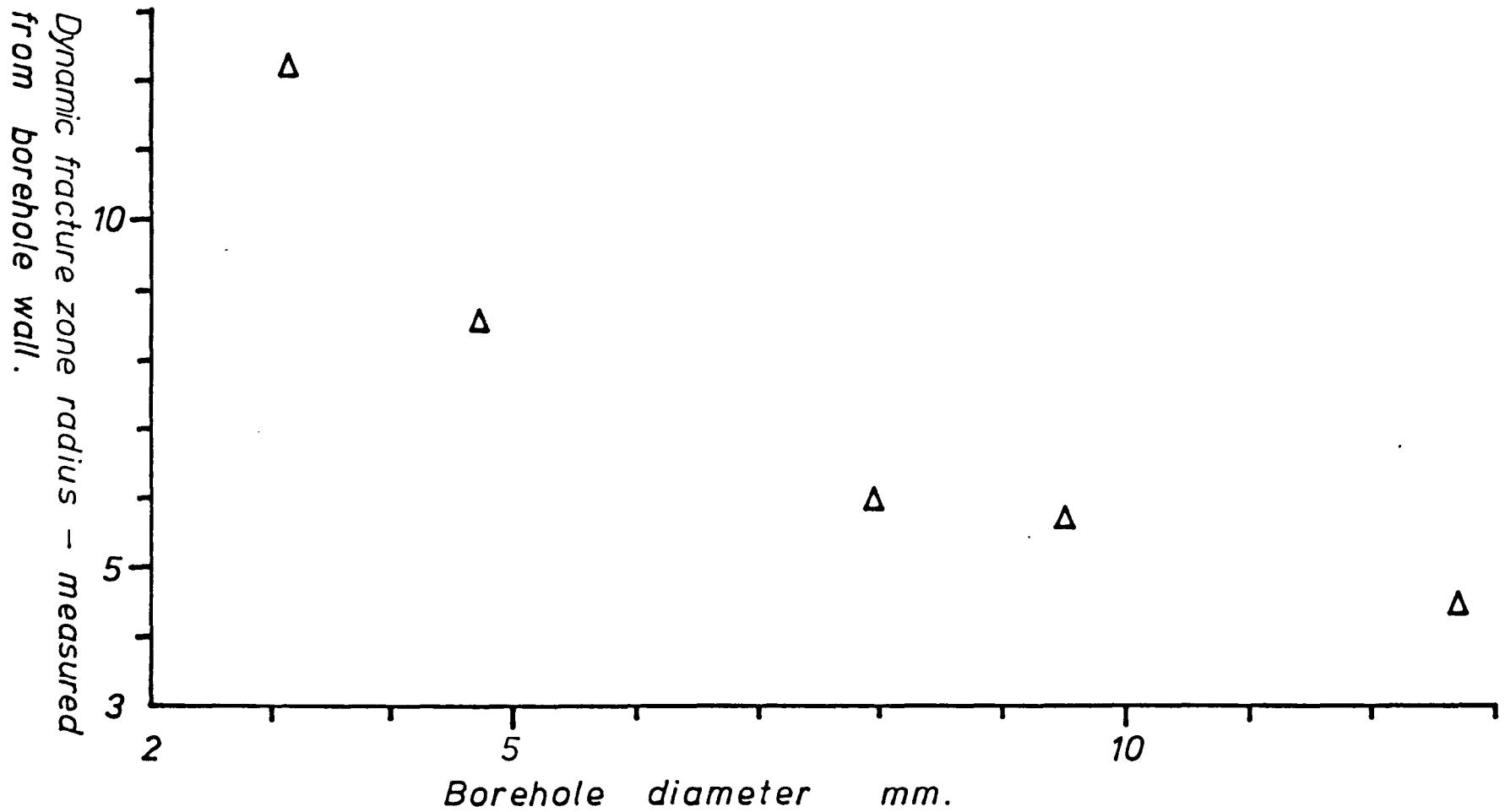


Fig. 4.14.

Plot of radius of dynamic fracture zone against borehole diameter for series (b) tests (half-vented single boreholes).

was vastly reduced, showing that although the detonation wave causes the initial cracking the majority of the fracturing is caused by the gas pressure.

Column 1 = Borehole Diameter

Column 2 = Test Number

Column 3 = Av. Blast Damage Zone Radius (from centre)

Column 4 = Av. Blast Damage Zone Radius (from edge)

3.18	33	13.84	12.25
4.76	36	11.01	8.63
7.94	37	10.00	6.00
9.63	46	10.53	5.75
12.70	47	10.85	4.50

Table 4.2.

The results of series (b) testing are also displayed, on log-log axes, in Figure 4.15. The slope of the log-log relationship is similar to that for normal single boreholes and thus these results are considered to be valid, showing the same scale relationship.

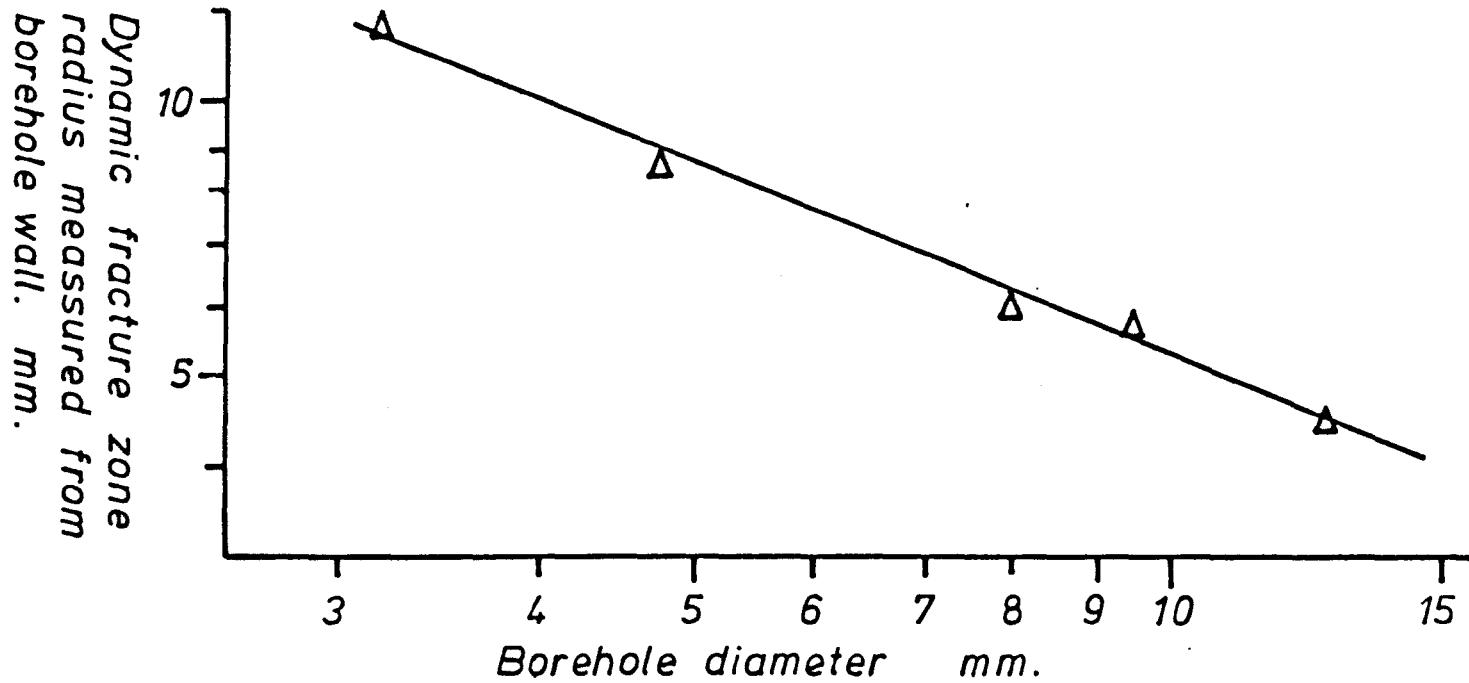


Fig. 4.15.

Graph illustrating straight line relationship between dynamic fracture zone radius and borehole diameter when plotted on log-log axes.

#### 4.8.3 Series (c) Experiments

In series (c) testing the borehole diameter was found to be the primary factor controlling the maximum successful pre-split separation. This feature is exhibited quite markedly in Figure 4.16 where the results show a distinct hyperbolic trend. When the results are plotted on log-log axes a straight regression line may be fitted, (see Figure 4.17). Although this regression is not perfect and a similar trend of results (in respect of borehole size variation) is obtained to series (a) results, comparative accuracy is well within the limits of experimental variation. The relationship derived was found to be of the form:

$$Y = A + (B \cdot X)$$

where:  $Y = \log$  borehole diameter  $\log(\text{mm.})$   
 $X = \log$  maximum separation  $\log(\text{mm.})$   
 $A = Y$  intercept = 2.57  $\log(\text{mm.})$   
 $B = \text{slope of regression } (Y/X) = -0.9$

A higher amount of blast damage (although roughly the same degree as in series (a) testing) compared with the maximum successful pre-split borehole separation was found in the course of series (c) experimentation than was originally expected. On

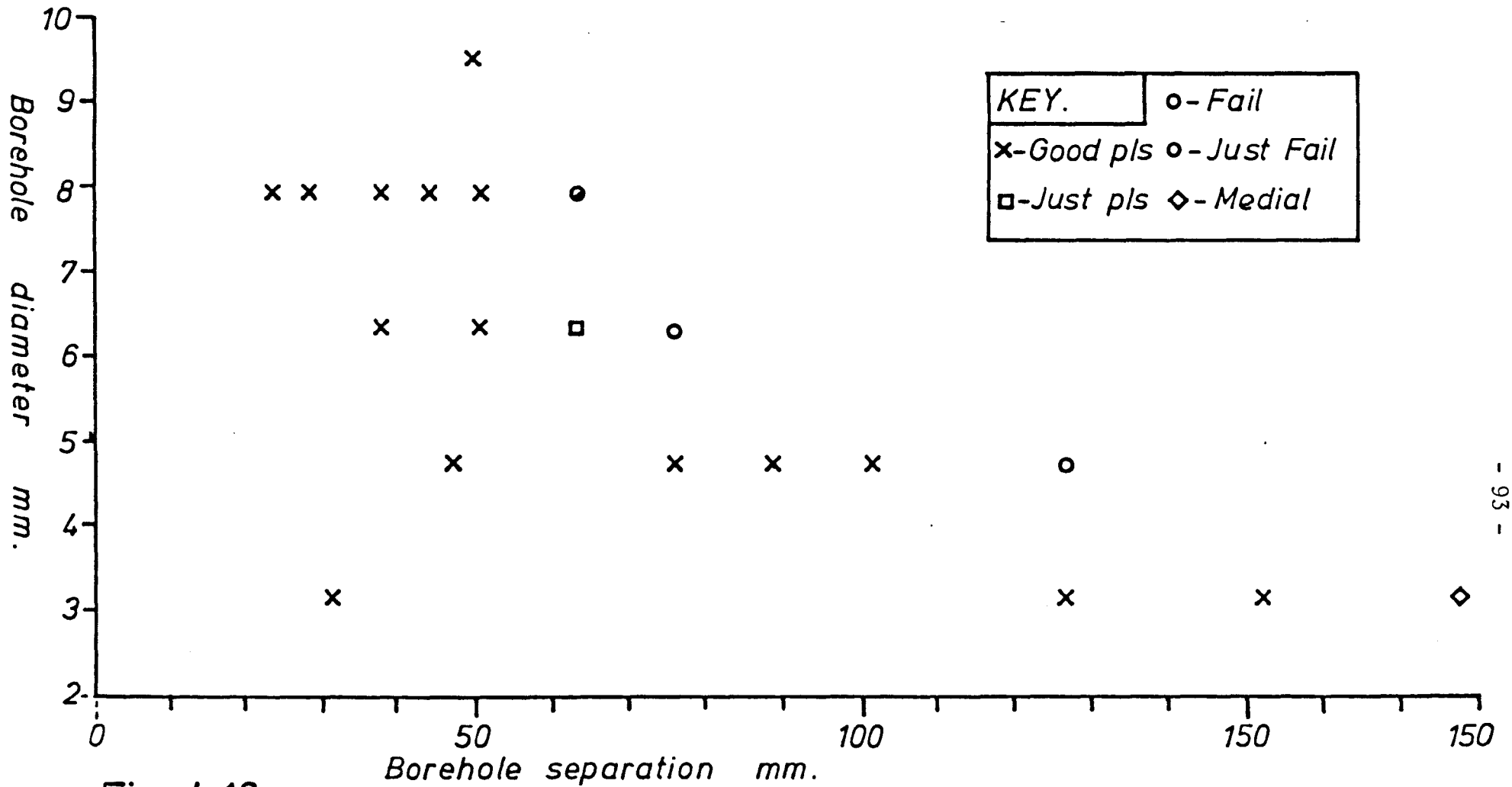


Fig. 4.16.

Plot of borehole separation against diameter for series (c) experiments.

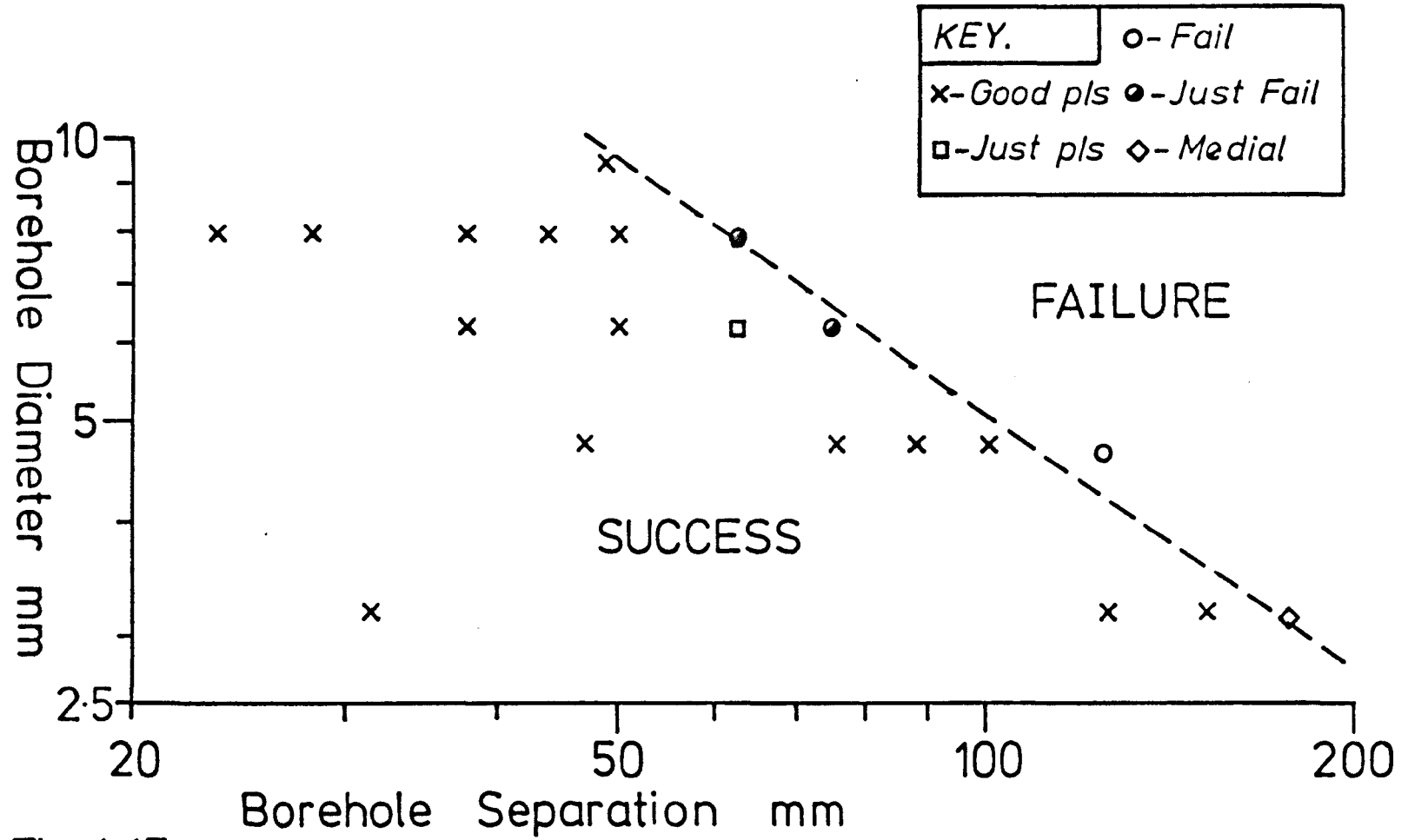


Fig. 4.17.

Graphical relationship between maximum successful pre-split borehole separation and borehole diameter (decoupling) for series (c) experiments.

reflection this is only to be expected as any minute fracturing that is present around a borehole in rock will be invisible. However when dealing with a transparent medium only a few molecules thickness of air is needed inside a crack to produce an optical reflective and refractive phenomenon which is distinctly obvious.

One possible explanation of this phenomenon is that the material is highly conducive to brittle fracturing, except that the material on inspection tends to remain fairly intact, as with similar blast holes in rock, and possess a residual strength. Therefore the original expectations may have been wrong and results obtained fair.

Approximately circular blast damage zones tending to a slight elliptical shape with the longest axis parallel to the pre-split were observed around each hole in each test, suggesting an apparent effect of interaction between successive boreholes in each pre-split test. These were slightly less circular than those obtained in single hole testing (series (a)).

Multiple splitting was seen between neighbouring

boreholes, especially where the boreholes were in closer proximity. For each borehole diameter, individual fractures from adjacent boreholes were observed to have met and coalesced approximately midway between boreholes for separations up to and including the maximum successful pre-split separation, (see Figure 4.18). Also failures to split show no fracturing to have been initiated midway between boreholes but show all fracturing to originate from each borehole, (see Figure 4.19).

Examinations of the actual pre-split surfaces using fracture morphological techniques show that in every case fracturing was initiated at or near the surface of each borehole, propagated outwards and met at a point approximately mid-distance between pairs of neighbouring boreholes. This feature is clearly shown in Figure 4.20.

#### 4.8.4 Series (d) Experiments

Only three tests were carried out, a summary of the results being included below:-

Test 34: Borehole Separation 5 cm - shattering



Fig. 4.18.

Multiple hole simultaneous initiation series (c) splitting test (near maximum successful pre-split borehole separation) clearly illustrating that no fracturing is initiated middistance between holes and that the origin of all fracturing is from the vicinity of individual boreholes.



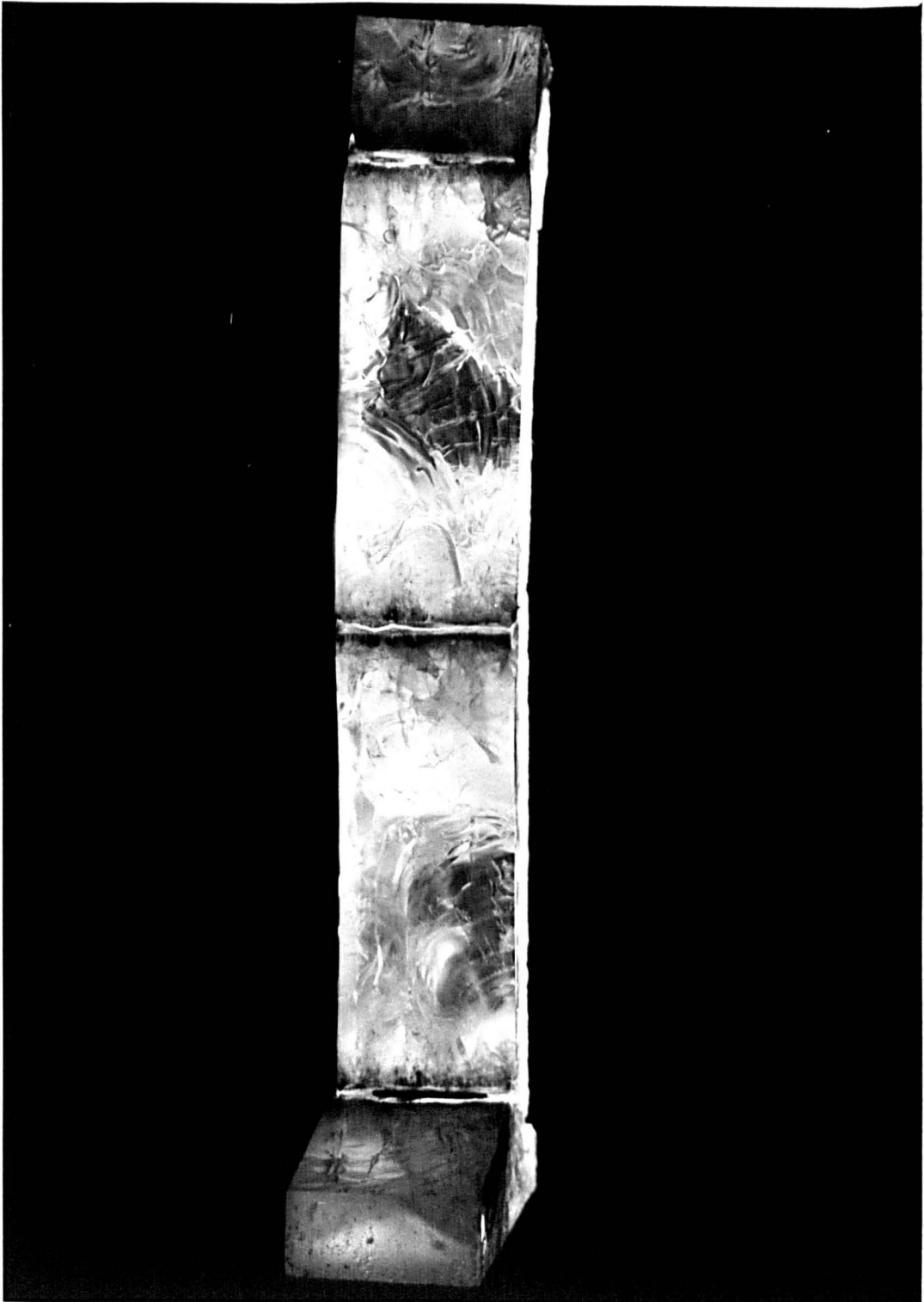


Fig. 4.20.

Photograph of pre-split produced in test 41 (series (c)) illustrating the direction of fracture propagation.

Note that fractures originating from adjacent boreholes intersect and coalesce midway between holes, fracturing is not seen to be initiated at this point.

around holes, some resemblance of a pre-split, i.e. fractures along pre-split line in middle, but are not inter-connected or not of any significant area. Block fairly intact therefore no definite pre-split.

Test 38: Borehole separation 4 cm - apparent cracking between boreholes but not completely through block, Block remains intact therefore no pre-split present.

Test 44: Borehole Separation 3 cm - high shattering and slabbing around holes, block not in two pieces, but cracks seen in backs of boreholes. Block flexes around middle and will only take moderate pressure to break. Therefore only just not split, (see Figure 4.21).

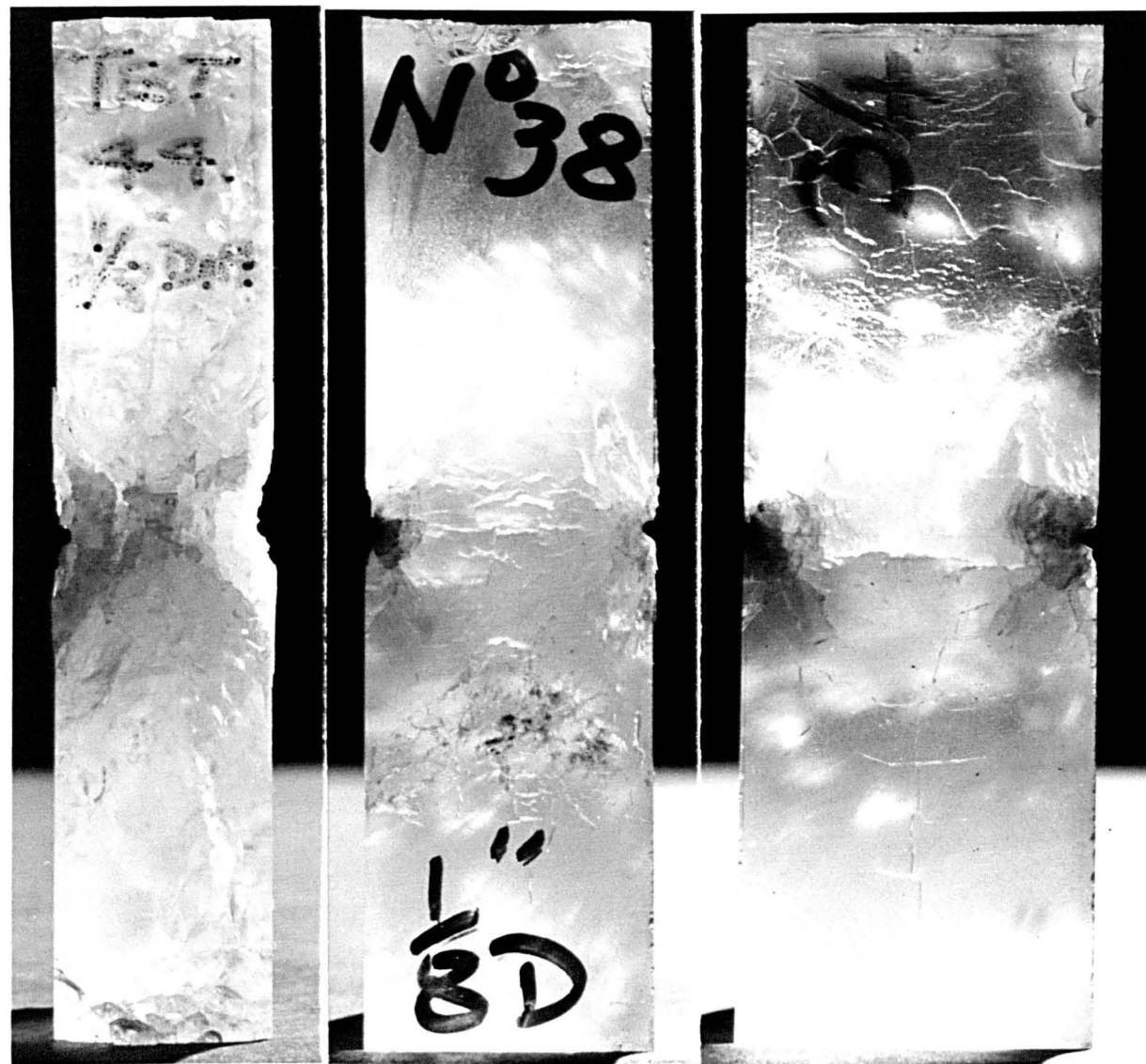
As a successful pre-split was only just not obtained in Test 44 the maximum successful pre-split was deemed just below a borehole separation of three centimetres. The photographic results of each series (d) test are to be found in Figure 4.21. It can be seen in this pre-split testing with the dynamic component isolated that some fracturing is initiated mid-distance between boreholes and extends outwards along the line of pre-split towards the holes. This

Fig. 4 . 21.

Series (d) experiments.

3, 4 and 5 cm.

Illustrating dynamic  
fracturing between vented  
pre-split holes.



feature was most prolific in Test 34 but did not extend throughout the block. However this feature is no greater in length than the fracturing around each half borehole.

#### 4.8.5 Series (c) Experiments

A 100% successful pre-split was obtained with very good breakage along the pre-split line, (see Fig. 4.22 and identical non-delay Fig. 4.23.)

The maximum 100% successful pre-split separation experimentally obtained was at a borehole separation of 50.8 mm.

#### 4.8.6 Combination of Results from Series (a), (b) and (c)

For the extent of blast damage around a single borehole - series (a) - the hyperbolic relationship obtained was of the form of:

$$Y = A + (B \cdot X)$$

where: Y = log blast damage zone extent log(mm)

X = log borehole diameter log(mm)

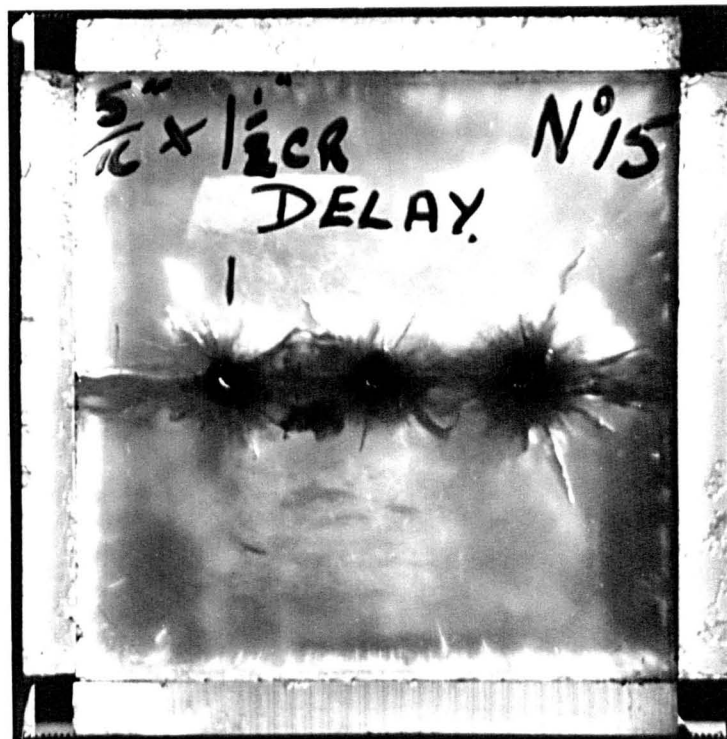


Fig. 4.22.

Photograph of delay experiment - Test 15.

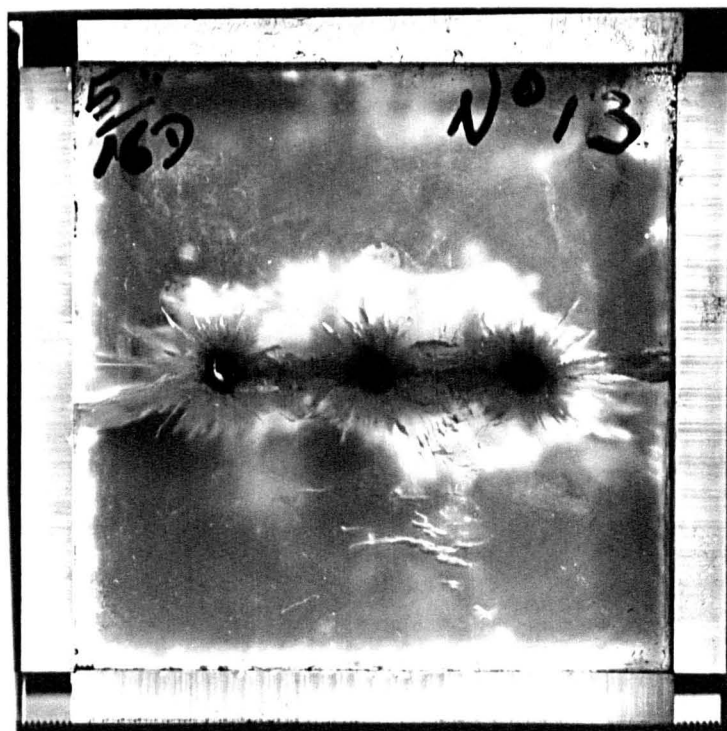


Fig. 4.23.

Photograph of identical configuration simultaneous initiation experiment - Test 13.

$$A = Y \text{ intercept} = 1.66 \quad \log(\text{mm})$$
$$B = \text{slope of regression} = Y/X = -0.589$$

The smaller zone of blast damage obtained from single vented hole testing - series (b) - was found to give a similar relationship, being described by the equation:

$$Y = A + (B \cdot X)$$

where:

$$Y = \log \text{ blast zone extent} \quad \log(\text{mm})$$
$$X = \log \text{ borehole diameter} \quad \log(\text{mm})$$
$$A = Y \text{ intercept} = 1.43 \quad \log(\text{mm})$$
$$B = \text{slope of regression} = Y/X = +0.702$$

As series (a) experiments contained both dynamic and quasi-static components whereas series (b) experiments contained only the dynamic component, then the extent of the damage zone created solely by quasi-static gas phase is thus:

$$Y = \log^{-1} (A1 + (B1 \cdot X)) - \log^{-1} (A2 + (B2 \cdot X))$$

where:

$$A1 = 1.66$$
$$B1 = -0.589$$
$$A2 = 1.43$$
$$B2 = -0.702$$

$$X = \log \text{ borehole diameter}$$

Y is in all cases greater than the extent of the dynamic blast damage component. Thus the area ratio is greater than three to one for blast damage caused by the quasi-static effect compared to that caused by the dynamic effect. As the blast damage created by the detonation wave is small compared with the total blast damage, the detonation wave is therefore not considered to be the major factor in the fracturing process around blast holes.

A comparison of maximum crack length and damage zone extent for both series (a) and series (b) experiments is given in Figure 4.24 where it can be seen that the effect of the dynamic component is far lower than the combined effects and that the greater extent of fracture propagation is caused by the quasi-static component.

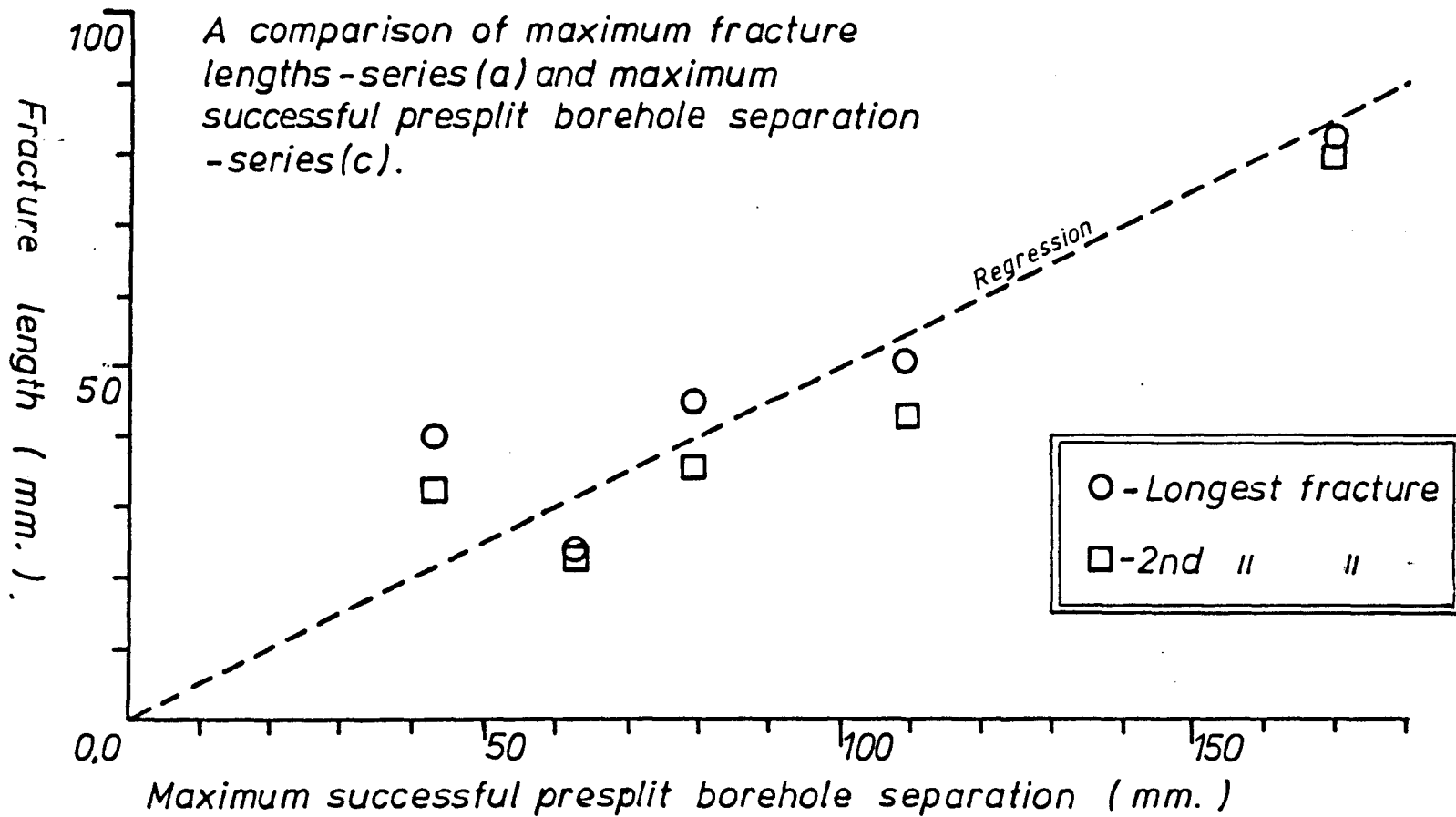
The blast damage zones and maximum crack lengths for series (c) experiments were generally seen to slightly decrease for closer pre-split borehole spacings and were at a maximum for individual holes - series (a) - or where multiple holes - series (c) - were above the maximum successful pre-split spacing. This effect is postulated to be caused by premature venting of gases into and redistribution of the stress

field around the pre-split fracture for close borehole separations.

When the two maximum crack lengths per single borehole - series (a) - were plotted against the maximum successful pre-split borehole separation - series (c) - a good straight line relationship was obtained, the regression passing through the origin, (see Figure 4.25). The slope of this line was approximately 0.5. This infers that maximum length cracks are just able to join to form the pre-split at the maximum successful pre-split borehole separation. Thus intuitively this would seem to infer that there is no or little quasi-static stress field interaction. However the points on the graph (Figure 4.25) represent the length of the longest and second longest fractures for each borehole diameter - series (a). These fractures have a random angular orientation from the borehole and therefore there must be quasi-static interaction between boreholes which aligns the longest fractures with the pre-split axis or induces the further propagation of fractures orientated in this direction.

The plotting of blast damage zone extents - series (a) - against maximum successful pre-split borehole

Fig. 4.25.



separations on log-log axes gives a straight line relationship through the origin which is illustrated in Figure 4.26. However, as this obtained relationship is well below that for overlapping blast damage zones (a straight line with a gradient of 0.5), then it can be stated that the fracture damage zone has no 'direct' influence on the maximum successful pre-split borehole separation.

#### 4.9 CONCLUSIONS

##### 4.9.1

The Pre-splitting effect is predominantly produced by the quasi-static gas pressure component, but not wholly for the previous reasons (interactive quasi-static stress fields), as the maximum crack lengths obtained for single holes are usually not significantly less than half the maximum pre-split separation for identical borehole diameters.

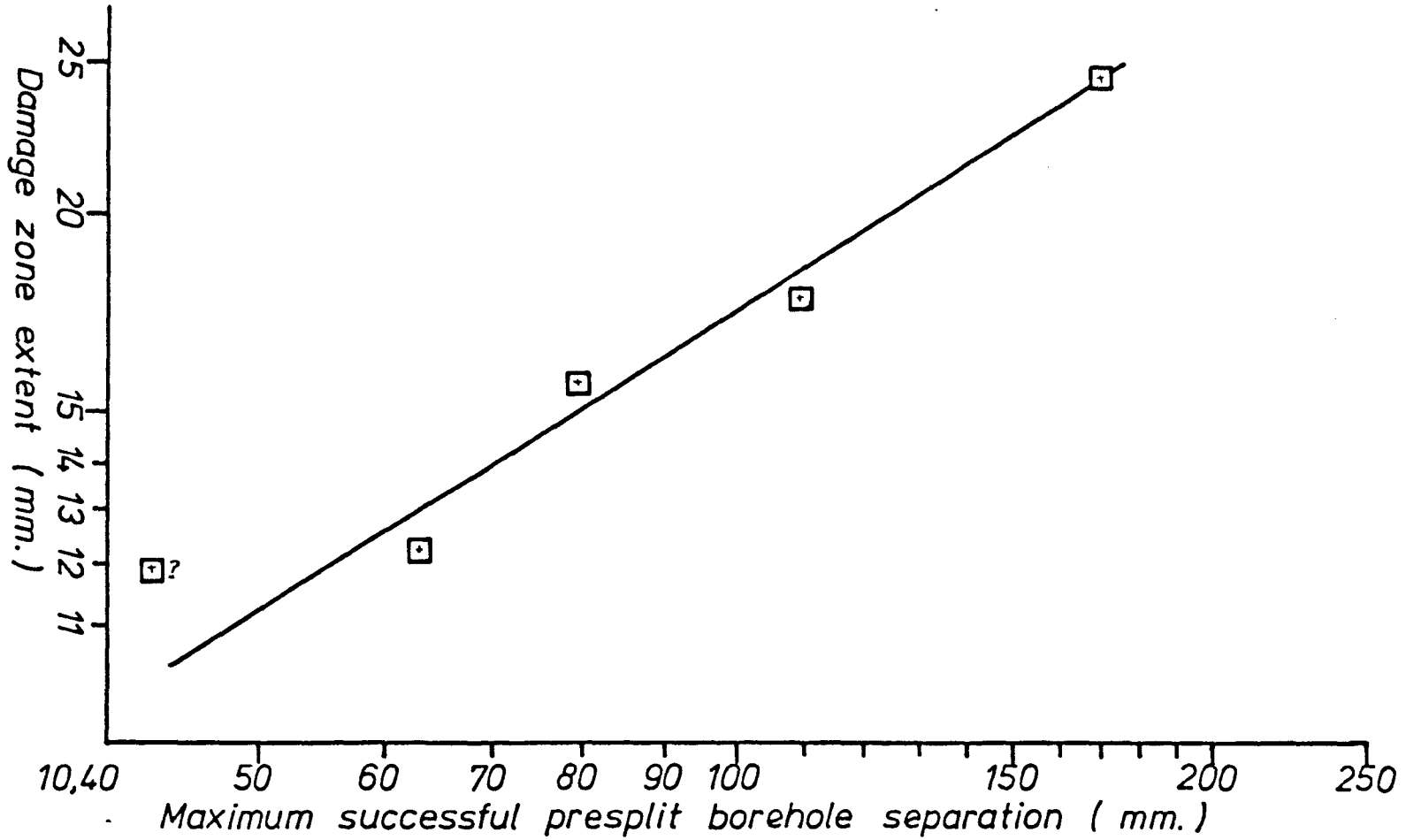


Fig. 4.26. The graphical relationship between damage zone extent and maximum successful presplit borehole separation for successively decreasing borehole diameters.

4.9.2

The extent of the damage caused around a borehole for a specified charge type and weight is dependent on the borehole diameter and thus the decoupling.

4.9.3

The size of initial damage zone caused by the detonation wave is also dependent on borehole diameter and thus decoupling.

4.9.4

As the maximum pre-split separation in experimentation for normal 3.175 mm holes is in the order of over fifteen cm and the dynamic maximum only less than three cm, then the dynamic component is definitely not the main contributing factor in the normal pre-splitting process. Also as the extent of damage zone caused by the detonation wave is small compared with that of the total damage zone (caused by the combination of both components) and the scale factor between them is a great deal larger than root

two, it can be concluded that pre-splitting between blast holes in normal field geometry is definitely not produced by the interaction or superposition of detonation waves.

#### 4.9.5

The absence of the interaction of detonation waves mid-way between boreholes does not have a significant effect on the maximum successful pre-split borehole separation.

#### 4.9.6

Examination of pre-split planes using fracture morphology analysis showed no indication that fracturing is initiated mid-distance between boreholes, but proved conclusively that fracturing is initiated at each borehole and that independent fractures from neighbouring boreholes extend outwards and generally coalesce at irregular intervals between the holes.

The process of pre-splitting may then be described as follows:

#### 4.9.7 Formation of a Pre-split

On detonation of the explosive the detonation wave travelling through the explosive column also travels outwards and on transmission into the rock becomes the dynamic component. As the tangential component of this dynamic wave is usually of greater magnitude than the tensile strength of the medium, it produces a radial fracture zone around the borehole. However, the process of fracturing the rock removes considerable energy from the dynamic pulse and it rapidly decays until it is of a magnitude less than that of the tensile strength of the medium. Therefore as a result, the extent of this radial fracture zone is small with relatively few fractures extending out from this zone and none further than a few mm, due to the consistency of the dynamic pulse.

At the same time the gas pressure in the borehole is building up by the adiabatic expansion of the gaseous products of detonation. The radial cracks already present are elongated until certain cracks which are longer start to propagate at a much higher rate and other cracking terminates. At this stage it is possible that wedging action in the cracks by the detonation gases predominates. At the same time the

stress fields from neighbouring boreholes overlap and cause a preferential line of split between boreholes. This has two effects:

1. Those elongating fractures orientated in suitable directions are encouraged/assisted by this pressure overlap to the detriment of those orientated against the field, and the former cracks then become dominant.
2. Existing fractures, not aligned with the stress field have their direction of propagation altered by the composite stress field and tend to bend towards the direction of pre-split.

Once the pre-split is complete, gas pressure is reduced and thus further fracture elongation terminates.

5 NON-GEOTECHNICAL FACTORS AFFECTING THE SUCCESS OF  
PRE-SPLITTING

5.1 EXPLOSIVE AND BOREHOLE PARAMETERS

5.1.1 Foreword

Before describing the geotechnical factors affecting the application of pre-split blasting to rock slopes it is considered important that the major non-geotechnical factors affecting the success of pre-splitting be stated and their effects described.

Without proper understanding of the non-geotechnical factors that may influence the success of a pre-split panel, it is inadvisable to infer that the occurrence of any failure is due solely to adverse geotechnical factors. For example the loading, drilling and blasting at pre-split locations three to eight inclusive were carried out under inadequate supervision and by unsuitably qualified personnel. The low quality of work undertaken is

plainly visible within the resulting faces and has in certain cases played a major role in the failure of pre-split faces, although there are generally adverse geotechnical conditions prevailing. It is therefore important to gain an understanding of the basic non-geotechnical errors that may be made and thus gain the ability to identify and correct these before serious permanent damage is initiated.

#### 5.1.2 Borehole Separation

As shown in the previous chapter, if the maximum successful pre-split borehole separation is exceeded then a failure to pre-split will occur, resulting in either underbreak or overbreak and excessive damage to the final face, dependent on the relative positioning of the bulk charge in relation to the pre-split line. For maximum successful pre-split borehole separation a maximum depth of blast fracture damage from the pre-split holes is incurred in the pre-split surface. For successive reductions of borehole separation both a smaller depth of damage and a straighter fracture between holes is induced, giving cleaner, higher integrity final faces. This effect is primarily due to the earlier connection of fracturing between the

pre-split boreholes, resulting in the venting of detonation gases which causes premature retardation of fracture propagation.

### 5.1.3 Borehole Size

Smaller sized boreholes for a standard decoupling possess a more restricted borehole separation range than larger diameter boreholes. In Europe small diameter boreholes of 100 mm down to 50 mm are used at separations of up to ten times the borehole diameter whereas the trend in America is to use large diameter holes at larger borehole separations (Johnston, 1973). Larger boreholes for the same decoupling ratio generally imply a greater amount of back damage, thus loosened rock and larger borehole separations, which allow larger amplitudes of irregularity in the final face from the intended line, although the overall shape of the faces may be the same. Therefore the degree of underbreak and overbreak in the final face will increase with the use of larger boreholes with their associated larger separations. However due to the increased separations, larger boreholes may be drilled to greater depths due to the scale factor.

#### 5.1.4 Explosive Types

There are two main classes of explosive - high and low - which refers to their detonation velocities (Dick, 1968).

High explosives are classed as explosives whose detonation velocity is greater than their seismic velocity. On initiation the explosive material decomposes at a very high rate and emits a high degree of seismic energy in the form of a shock wave. Typical commonly used high explosives are blasting gelatines and dynamites which are now virtually phased out.

In low explosives the rate of decomposition is slower than the seismic velocity and the explosive tends to burn, all be it at a high rate, rather than detonate. This low rate of decomposition is technically termed deflagration.

High explosives tend to give high seismic impulses to the rock on detonation whereas low explosives impart low seismic impulses when they deflagrate. Due to the higher energy contained within the chemical matrix, high explosives also give higher gas

pressures. Low explosives were superceeded early in this century by nitroglycerine, the base constituent of all gelitines and dynamites. The replacement of low explosives was mainly due to the higher breakage power and far superior water and damp resistance of high explosives. Low explosives are now no longer used in commercial operations and their use is mainly confined to the manufacture of fireworks.

The present concensus of opinion is that within the high explosives group there are two extremes of explosive properties. Firstly it is argued that there are high dynamic - low quasi-static (gas pressure) explosives and secondly at the other extreme low dynamic - high quasi-static explosives. This view is partly supported within the explosive industry. However, information on gas pressures and dynamic values for individual explosive brands is not readily available and that that is, is arrived at by obtuse methods.

The technical information available from which the dynamic and quasi-static components can be correctly formulated is - the volume of explosive gases at S.T.P., the explosion temperature, the velocity of detonation and the density.



temperature just after detonation and thus calculate the confined pressure of the gases after detonation of the explosive.

Taking:

normal temperatures and pressures to be initial and explosion temperatures to be resultant then

$$\frac{P_i V_a}{T_i} = \frac{P_E V_E}{T_E} \quad (2)$$

taking the unit measure of pressure as 1 atmosphere

then 
$$\frac{V_a}{T_i} = \frac{P_E V_E}{T_E}$$

$$P_E = \frac{V_a T_E}{V_E T_i} \quad (3)$$

Substituting for  $V_E$  from (1) into (3)

$$\begin{aligned} P_E &= \frac{V_a T_E}{p^{-1} T_i} \\ &= V_G p \frac{T_E}{T_i} \end{aligned}$$

However the unit of temperature used in the combined gas equation is the Kelvin and both  $T_E$  and  $T_i$  (room temperature 20 C) are usually quoted in C.

$$\begin{aligned} P_E &= V_a \cdot p \cdot \frac{(T_E + 273)}{(20 + 273)} \quad \text{where } T_E \text{ is in } C \\ P_E &= V_a \cdot p \cdot \frac{(T_E + 273)}{293} \quad (4) \end{aligned}$$

N.B. Zero degrees Centigrade is 273.15 degrees Kelvin but the common approximation of 273 is used here.

A table of the confined explosive gas pressures of some E.C.P. explosives along with their velocities of detonation may be found in Figure 5.1.

Explosive	Explosive Pressure	V.O.D.
Blasting Gelatine	17,634 A	6,000
Fortex	19,505 A	6,000
Plaster Gelatine	15,143 A	6,300
Gelamex No. 1	14,639 A	3,000 - 5,000
Gelamex	11,602 A	2,500 - 5,000
Quarrex "A"	11,625 A	2,800 - 4,500
Quarrex	8,174 A	2,500 - 4,400
Amospex	8,247 A	2,000 - 3,000

Figure 5.1

Table of Explosive Gas Pressures and Velocities of Detonation for Various E.C.P. Explosives.

To obtain the gas pressure for any hole size the following equation may be used:

$$P_B = P_E \frac{d^2}{D^2}$$

where:  $P_B$  is the borehole gas pressure

$P_E$  is the confined explosive gas pressure

$d$  is the diameter of the charge

$D$  is the diameter of the borehole

A relative means of measurement of the confined explosive gas pressure is the ballistic mortar test. In this test the explosive's quasi-static component's ability to deflect a heavy steel mortar is measured, the dynamic component giving no discernable impetus to the mortar. The ballistic mortar test is basically an empirical test for comparing different explosives. The ability of standard weights of different explosives to deflect the mortar is compared with that of T.N.T. and the strength of the explosive is expressed as a percentage of the strength of T.N.T.. In the past this strength measurement of explosives has been widely criticized by Dick (1968) and others. However as the gas component of an explosive creates a greater volume of fracturing than the dynamic component (in the absence of a free face in the immediate proximity) then both weight strength (strength % per unit weight) and cartridge or bulk strength (strength % per unit volume) are extremely

important explosive properties to be considered in the choice of explosive.

The dynamic pulse, due to its nature, is difficult to measure both directly or indirectly at a distance due to its rapid decay in amplitude around the borehole due to the leaching effect of rock breakage. However several approximate equations of detonation pressure<sup>9</sup> exist, the best of which is given by Dick (1968), i.e.

$$P = 4.18 \times 10^{-7} p C^2 / (1 + 0.80p)$$

where: P = detonation pressure in kbar

p = specific gravity

C = detonation velocity in fps

From the calculations given it is obvious that the supposition of converse extremes of dynamic and quasi-static components within the range of commercially available explosives is unfounded and thus contrary to certain belief within this country, the energy contained within the gas component increases with increasing values of the dynamic component.

.....  
<sup>9</sup> Detonation pressure, which is a function of the detonation velocity and density of the explosive, is a measure of the pressure in the detonation wave.

Thus it may be concluded that when utilising decoupling, approximately similar conditions may be obtained by both using a standard charge of a lower range strength high explosive or an accordingly reduced charge of a high strength high explosive.

#### 5.1.5 Charge Density

We can define charge density as the amount or weight of explosive per unit volume or unit length of borehole. As can be seen from Section 5.1.3, explosive type is an important factor in the selection of charge density and dictates the relative amount of explosive used, dependent on the explosive's 'strength'. The level of charge density will (for a single hole) dictate the degree of damage incurred around that hole and for a line of holes, dictate the relative maximum borehole separation for a successful pre-split (isolating and keeping constant other variables).

An excessively high charge density will cause crushing of the rock within the borehole walls and an excess of damaging fracturing around the borehole. This will lead to a less intact final face with a zone

of dramatically weakened rock apparent, especially around the boreholes. For maximum charge density (i.e. for bulk charge conditions) a disturbance zone may result of up to eight metres depth (dependent on rock conditions), with the opening up of new and existing fractures. Thus if stability is marginal, i.e. the factor of safety is say between 1 and 1.2, a weakening of the rock fabric may occur such that failure in the final face will result by either plane, wedge or toppling failure. The amount of failure produced both initially and over a period of time may be enormous, e.g. the Forth Road Bridge cuts, (Swindells and Matheson, 1981).

On the other extreme, too low a charge density will cause a failure to split between neighbouring pre-split boreholes. This is evident on the west face of pre-split road cut number three where a relatively low charging of only single strand superflex (40g/m) in 75 mm boreholes was used, (see Figure 5.2).

#### 5.1.6 Decoupling

Decoupling is the relative measure of the diameter of the borehole to that of the charge. It can either

Fig. 5.2.

Photograph illustrating line of pre-split holes having failed to produce a split at Location 3 due to ridiculously low charging in strong metamorphic rocks.



be given as a direct ratio for line charges or as a percentage measuring relative volumes for spaced charges. The decoupling ratio for a line charge is:

$$D_c = D/d$$

and the decoupling percentage is:

$$D_c = D^2/d^2 \quad \text{for linear charges}$$

and

$$D_c = (D^2 \times (L+s) / (d^2 \times L)) \times 100 \% \\ \text{for spaced charges}$$

where:  $D_c$  = decoupling

$D$  = diameter of borehole

$d$  = diameter of explosive

$L$  = length of cartridge

$s$  = spacing between cartridges

Decoupling is the inverse measure of coupling which can be calculated from the following formula:

$$C = d^2 \times L \times 100 / (D^2 (L+s))$$

where:  $C$  = coupling measured in %

According to the conclusions of work by Fogelson, D'Andrea and Fisher (1965) "Both the amplitude and duration of the dynamic pulse are significantly decreased by increasing the decoupling". In Chapter Four the effect of decoupling was conclusively shown to decrease the magnitude of both dynamic and

quasi-static components, thus reducing the amount of damage to the rock around each borehole. By using boreholes larger than the chosen charge, the dynamic component is cushioned by the high impedance mismatch of explosive to air and air to rock and the quasi-static gas pressure is lowered by the larger volume of hole than explosive.

Due to both components being affected to the same extent by the inverse square law in respect of their magnitude at any particular distance from the charge, and with the additional excess reduction of the dynamic component related to impedance mismatches, the degree of decoupling present has a greater reducing effect on the dynamic component than the quasi-static component. Decoupling may therefore be considered to be a means of preferentially reducing the magnitude of the dynamic component with respect to the gas component.

## 5.2 CHARGING

### 5.2.1 Type of Explosive Train Used

There are two types of explosive train that may be employed in pre-splitting which are; firstly a continuous uniform explosive column and secondly spaced individual charges within the borehole.

Continuous charge is available from several different explosive manufacturers. These charges usually consist of either cardboard or plastic thin cylindrical containers filled with explosive powder usually of a nitroglycerine base. Successive containers or 'sticks' may be joined by either screw threads or clips built into the ends of each charge. These are usually taped to a 'cordtex' downline which is incrementally lowered down the borehole after each stick has been attached (depending on assembled ten metre plus explosive column and placing it down a borehole being impractical).

The reason for using continuous explosive columns is that the explosive charge is uniformly spread throughout the hole and therefore there is no concentration of explosive. The Scandinavians have gone one step further by centralizing the column by the use of plastic 'feathers' to ensure that the charge

does not contact the borehole surface and thus theoretically cause extra damage at the contact.

Spaced individual charges usually consist of individual pierced charges of up to eight ounces tied to a single strand of 'cordtex' at regular intervals. Alternatively the charges can be taped to the 'cordtex' downline. This technique of spreading the charge weight throughout the borehole was the first loading technique to be adopted in pre-splitting as continuous charges were not originally available. The advantages of spaced charging are twofold; firstly it is less expensive, more commonly used and more readily available (eight ounce sticks of explosive may be used) and secondly the charge density may be easily altered by changing the charge separation without having to change the type or diameter of the explosive charge used.

However some would argue that the irregularity of charge density throughout the borehole may cause individual areas of excess damage corresponding to the positions of the individual charges, but this is not verified from observations made by the author. Also, there being no practical means of centralizing the charges within each borehole, the fracturing from each

charge would tend to be unidirectional rather than uniform if that charge was in contact with the rock of the borehole wall.

In contradiction, the results of field observations indicate that this is not the case and no visible areas of excessive or preferential fracturing were discovered in final pre-split faces produced using the latter technique except the individual zones of excessive closely spaced fracturing associated with the use and positioning of base charges. Fennel et.al. (1966) also found "No difference between stringing cartridges and having a continuous charge" from observations of experimental work underground in South Africa.

Apart from the need for proper assembly, the only detrimental factor which was discovered from field observations when using spaced charging was that it is possible for the bottom charge to lodge fast in the hole prematurely above the bottom, on charging, causing the base charge to create an excess of damage in the final face (locations one and five). This error is not easily noticeable due to the weight of the train when lowering it down a hole. It is therefore recommended that with non rigid explosive,

single or multicord charging, care must be taken that the correct length of cord is measured and marked before charging the hole rather than just lowering the explosive train into the hole until the weight of the base charge is released. Incomplete full depth loading of boreholes was obvious at pre-split localities one to eight inclusive, being most prevalent at cutting number one. Figure 5.3 clearly shows the excessive damage (crushed) zone at the positioning of the base charge far above the base of the hole.

### 5.2.2 Detonation

There are two types of detonation commercially available. These are by detonator or by 'cordtex' trunkline. For a column pre-split charge, as the V.O.D. of 'cordtex' is normally far in excess of that of the pre-split charge then the detonation can be thought of as axial. Wilbur et.al. (1965) have shown that axial detonation produces a slightly higher magnitude but a shorter duration dynamic pulse for a single column charge, i.e. the same energy is released in a shorter time by axial detonation. However due to the relatively low importance of the dynamic component



Fig. 5.3.

Photograph displaying crushed zone of rock (around 7 x 8 cm compass) in pre-split face at location 1 created by incorrectly located base charge. This has been attributed to incomplete full depth loading of pre-split holes resulting from poor charging practice.

compared to the gas component (in the absence of a free face) there is no significant difference in the end results obtained from the two methods.

For absolute accuracy in the simultaneous detonation of a line of charges in pre-splitting the proper use of 'cordtex' trunklining is far superior in accuracy than that which can be obtained using commercial detonators (0.8 to 2 milliseconds spread according to Bergmann et.al. (1977)) for the firing of each hole. However the successful use of single zero delay detonators for the detonation of individual holes in pre-splitting has been reported by Paine et.al. (1961), Lutton (1977) and Landefors and Kihlstrom (1978) and was also observed by the author at location nine. This is not a surprising result as it has already been conclusively proven in Chapter Four that the absence of the superposition of the dynamic components from neighbouring boreholes in a pre-split panel has no significant effect on either the integrity, smoothness or maximum borehole separation for a successful split.

The advantages of using 'cordtex' trunklining rather than zero delay detonators are as follows. Firstly as long as proper attention is paid to the

linkage of individual downtrains to the trunkline and it is performed in an approved manner then the likelihood of individual hole misfire is greatly reduced. If a misfire occurs it will most probably be located at the trunkline's initial detonator which will only cause detrimental effects if the pre-split and bulk charges are fired in the same blast. Secondly the chance of accidental detonation of any remaining misfired charges during mucking out will be dramatically reduced due to the absence of intact detonators within the charge.

However the main disadvantage of using 'cordtex' trunklining is its associated high airblast, making its use inadvisable in or near 'built up' areas on environmental grounds.

The pre-split charge should be fired at a minimum of fifty milliseconds before any main bulk charge within ten to fifteen metres of the pre-split. According to Matheson and Swindells (1981), from seismic refraction survey results, the zone of explosive fracturing around a standard 100 mm bulk hole may extend for up to eight metres depending on the rock conditions. Firing of the pre-split at or after the initiation of the bulk blast may result in

the damage created by the latter extending across the line of pre-split and thus lowering the integrity of the final face and thereby negating the reason for using pre-splitting in the first place. This is suspected to have occurred on some sections within localities one to eight (Jones, 1980), the proof however was never substantiated.

The recommended method of firing is well in advance (time wise) - up to a couple of days or more prior to the initiation of the bulk blast - to avoid any problems associated with a misfire.

### 5.2.3 Base\_Charges

It has become standard practice to use base charges to ensure that no toe is left on the final face (Paine et.al., 1961, Jones, 1980 etc.). Base charges of 0.5 to 1.0 kilo are normally used in holes up to 100 mm in diameter.

Their effect is to fracture the ground surrounding their placement at the base of the borehole in excess of that normally produced by the pre-split charge density.

However if it is necessary to produce the final face by more than one lift without extensive benching then the presence of shattered zones in the final face is not desired and therefore the use of base charges should be excluded in pre-split design.

The alternative is to subdrill below grade by approximately 0.5 to 1.5 times the borehole separation. The standard pre-split charge density is used throughout (except for the collar of the hole). This technique may be extended if a rock trap is required at the bottom of the face, as a clean fracture is provided to break to using 'trenching' charges which again reduces the risk of unnecessarily undercutting the toe of the face and the associated extra initial cost would reduce the total costs in the long run.

The main disadvantage of using subdrilling however is its higher initial cost compared with base charging, in that the drilling is normally much more expensive than the explosive to be contained within the hole.

#### 5.2.4 Stemming

Stemming can be used in two ways; firstly to help couple the charge better in the hole and secondly to cap the hole in order to help contain the charge and thus bring about a more efficient use of the explosive. Stemming can be of three types - sand, aggregate (e.g. hydrostone) or drilling chippings and dust.

For full length stemming Fogelson, D'Andrea and Fischer (1965) have conclusively proved that the amplitude and duration of the dynamic pulse are little affected by the presence or type of stemming. Thus the only major effect stemming has is to effectively decrease the volume of the hole and thus more greatly confine and subsequently increase the magnitude of the quasi-static component.<sup>10</sup>

It can therefore be concluded that stemming may be used combined with reduced charge density in areas where a reduced vibration level is required or to increase borehole diameter and thus borehole spacing without altering the quasi-static component and thus

-----  
<sup>10</sup> Maximum coupling by the use of the listed types of stemming cannot be achieved in practice due to the air voids between particles within the stemming even if it is compacted.

provide greater economy. There is no major discernable difference in result from the use of different types of stemming. However for hole capping, fine material should be used to reduce the hazard from the projection of coarse particles. Drilling 'chippings' are ideal for this purpose and also do not add extra cost to the work. A capping of twice the borehole separation is generally accepted in standard practice (Teller, 1972c).

### 5.3 DRILLING ACCURACY

#### 5.3.1 Borehole Layout (Marking Out)

To ensure optimum accuracy in the position of a borehole throughout its length and the maximum accuracy of face positioning, extra care should be taken during the marking out of the borehole line, especially in the marking out of each individual borehole.

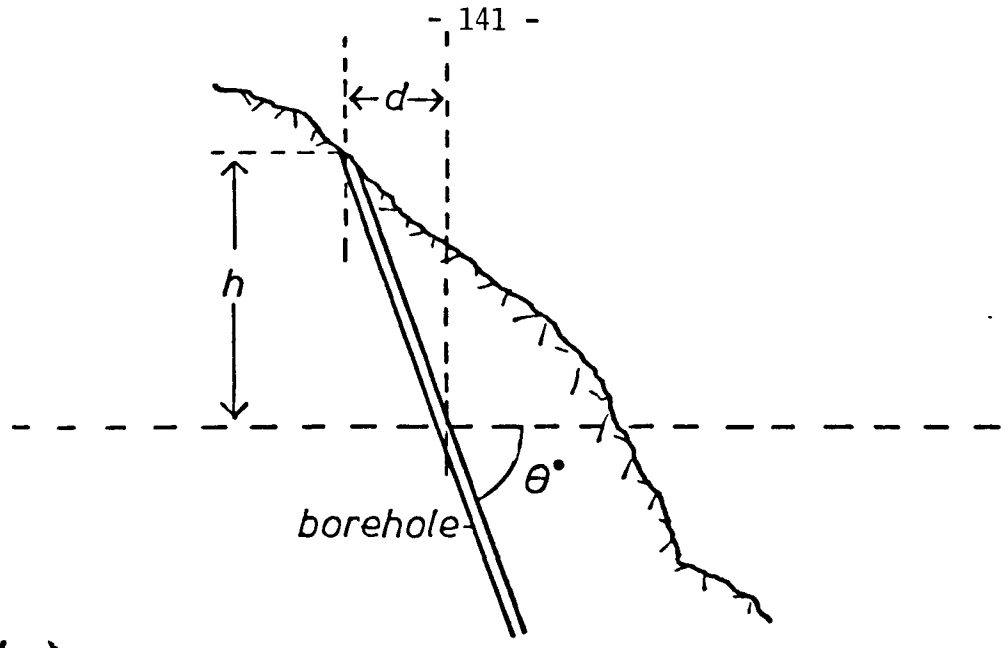
For uniform face alignment, the rise and fall of the surface should be taken into consideration and the

surface positioning of each hole should be back calculated from; the specified positioning of the toe of the face or bench, the intended face/bench inclination plus orientation and the specified borehole separation.

As can be seen in Figure 5.4a the line of the holes has to be brought back for an increase in surface elevation. If this is not done then a "bulge" in the final face will result and the pre-split may even cross the first row of bulk holes, causing damage to the face.

### 5.3.2 Drilling Platform Rigidity

To minimise borehole wander during drilling it is important that the drill rig remains stationary and does not move position or orientation. For this to be feasible the drilling rig must be seated on solid ground. It is therefore recommended that all superficial material is removed down to solid bedrock before marking out. The removal of superficial material also greatly reduces the risk of losing an individual hole due to collapse and blockage. Insufficient removal of this type of material was



(a) X-section.

$$d = h / \tan \theta^\circ$$

(b) Aerial view

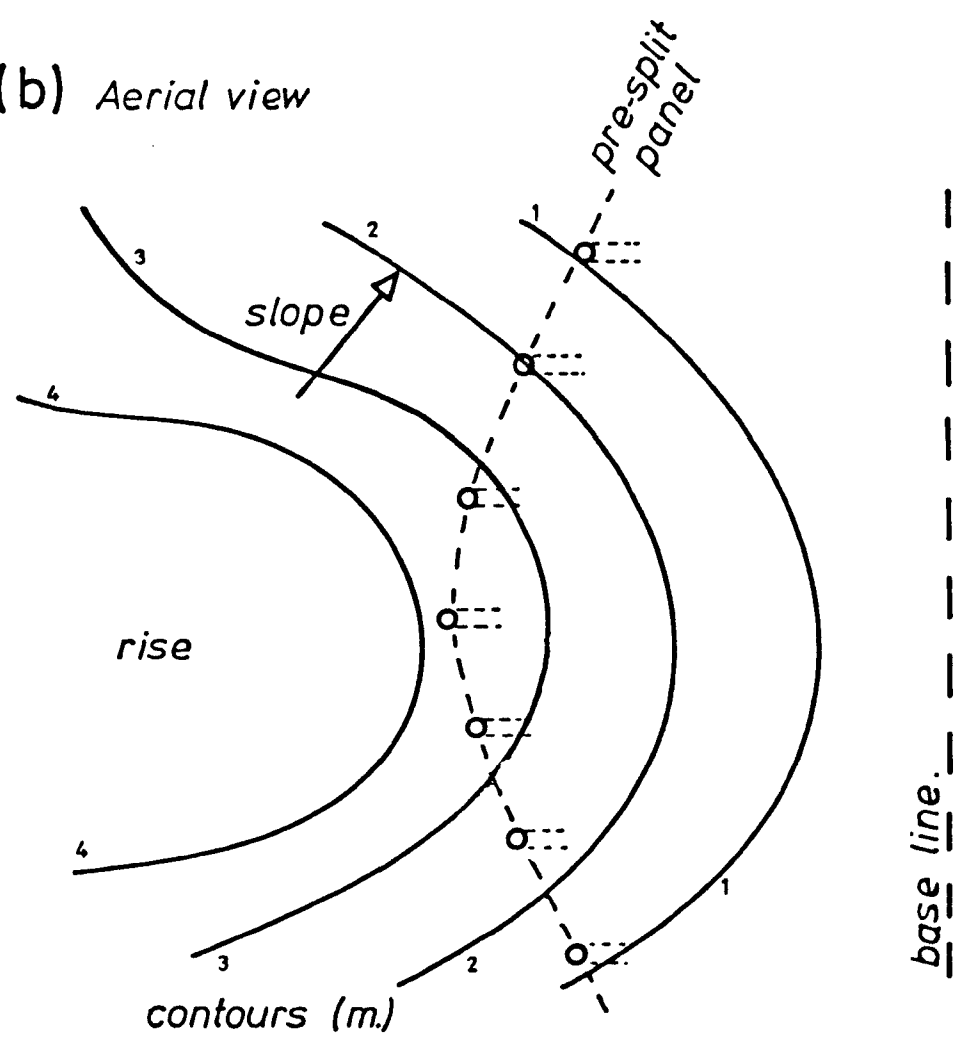


Fig. 5.4.

Effect of rise and fall in topography on the positioning of boreholes and panel layout.

observed by the author at site nine where numerous holes had to be redrilled due to poor alignment caused by drilling movement. Similar observations were made by Jones (1978) at sites three and four.

Positioning on a flat surface also reduces drilling lateral movement and drilling from a flat, solid bench allows an increase in accuracy of the alignment of the drill rigs.

### 5.3.3 Drill Alignment and Face Height

Accurate drill alignment is essential for the best pre-split results. Accurate hole positioning ensures constant borehole separation at any height along the lengths of parallel neighbouring holes and thus good results should normally be obtained. If however holes diverge, then a failure to produce a clean split will occur below where the separation exceeds the maximum successful pre-split borehole separation.

Inaccuracies in drill alignment may occur in two ways; firstly by error in drill rod dip and secondly by error in azimuth (i.e. lining up). Several methods of aligning and checking the alignment of drill bits

prior to the commencement of drilling are available and include - set squares, T bar plus inclinometer and the Drill Orientation Device (D.O.D.) (Matheson, 1979b), of which the latter is the most accurate. The dip accuracy of the borehole after drilling may be ascertained by 'torching' the hole by lowering an electric torch attached to a line down the hole and then 'sighting' it with an optical inclinometer. However the only method of accurately measuring both its azimuth and dip is by using the D.O.D. externally on a straight two metre plus length of aluminium scaffolding tube.

The effect of decreasing accuracy in borehole dip is given in Figure 5.5. However borehole deviation is not the only factor that influences the distance of deviation of the borehole toe away from the face in the horizontal plane. The actual intended borehole inclination also has an increasing effect away from the vertical as is shown in Figure 5.6 for a practical borehole inclination range of 90 down to 50 degrees.

Inaccuracies in azimuth have two similar effects to inaccuracies in dip, in that firstly and more importantly azimuth deviation may increase or decrease borehole separation between pairs of neighbouring

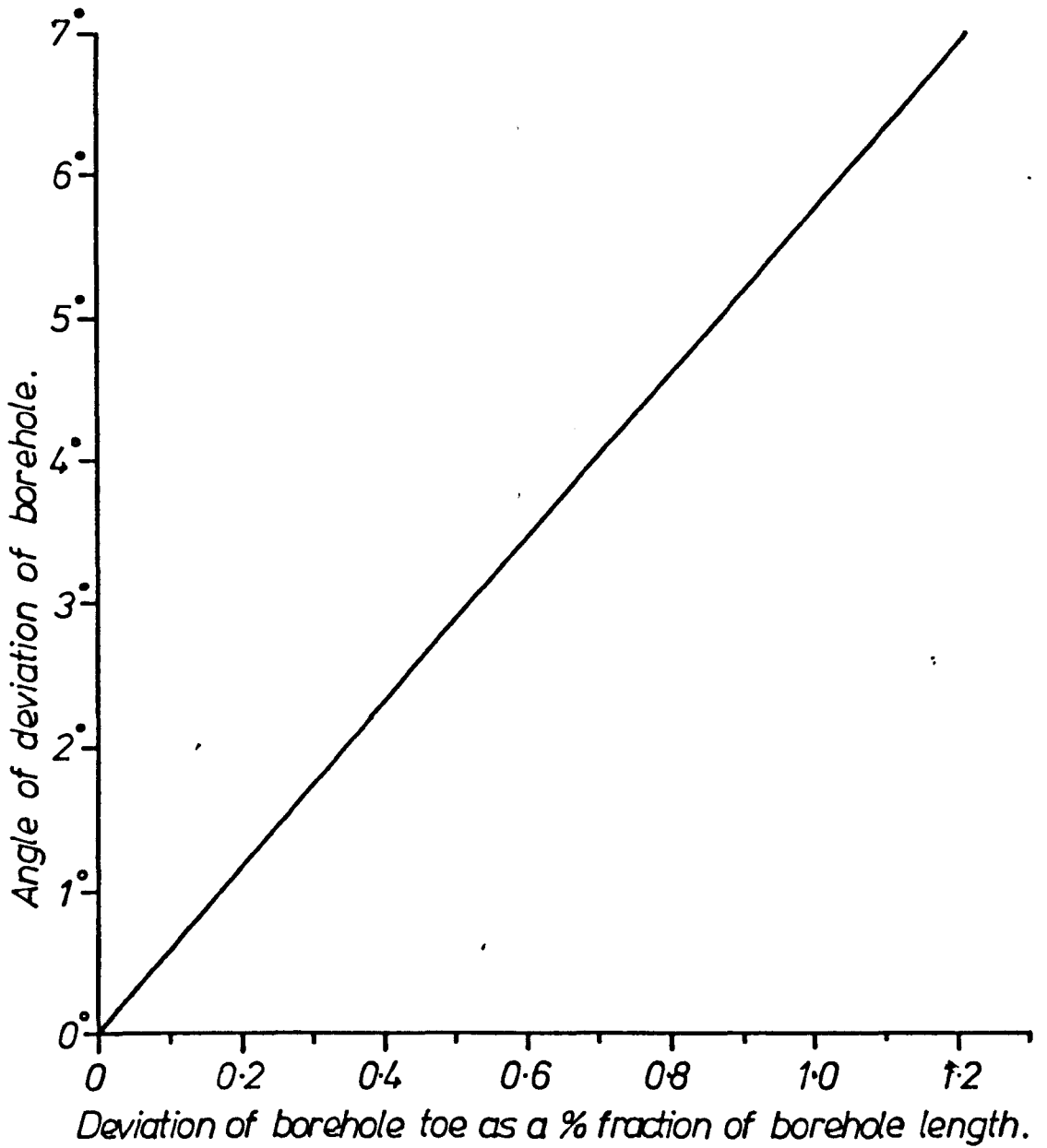


Fig. 5.5.

*Graph of relationsh between borehole toe inaccuracy and angle of deviation. (for vertical boreholes.*

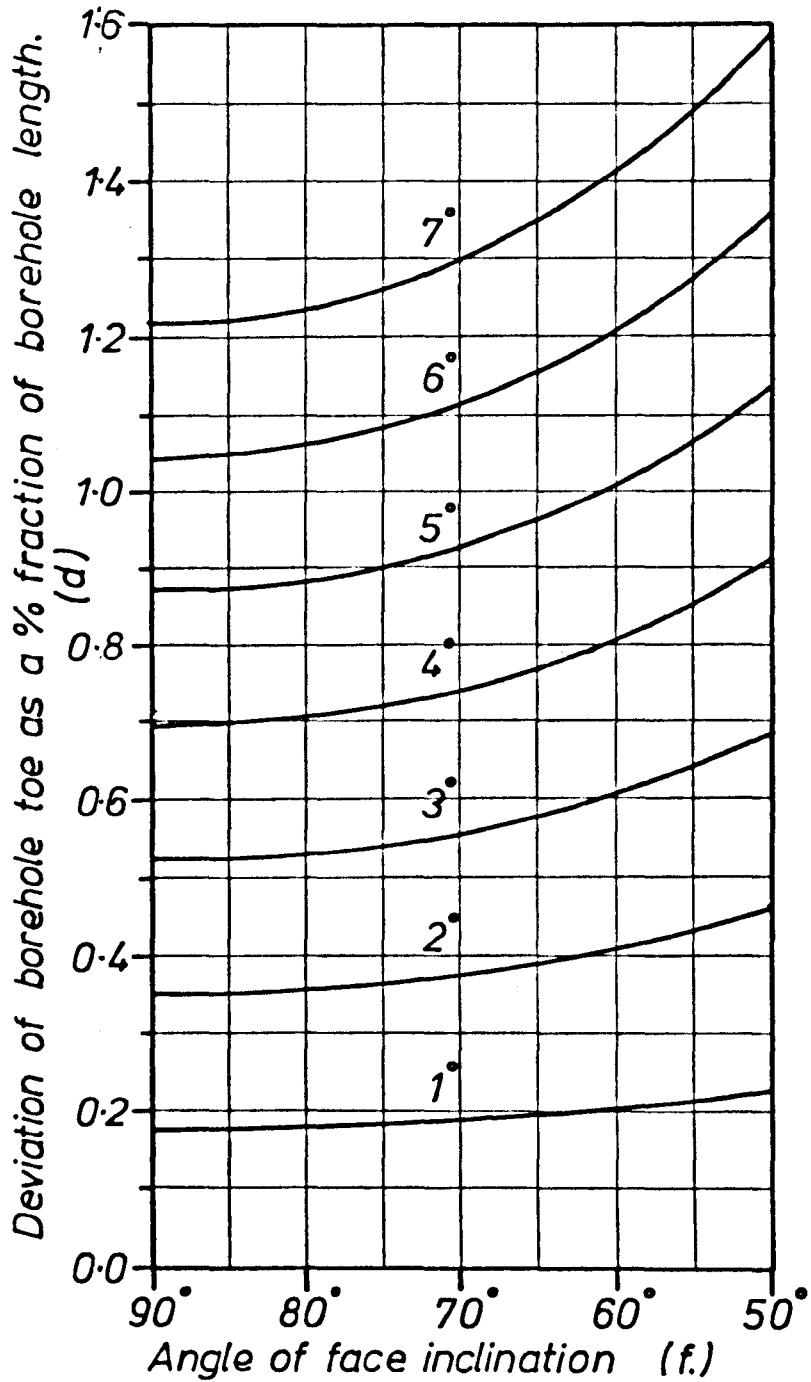


Fig. 5.6.

Chart of effect of intended borehole inclination on borehole toe deviation for various drilling angle inaccuracies.

Showing increasing horizontal deviation for decreasing face inclination.

boreholes and secondly it will cause irregularity in the line of borehole toes. However experience has shown that it is much more difficult to obtain a certain azimuth accuracy than for the corresponding dip accuracy.

Field observations made by the author conclusively prove that borehole accuracy has a pronounced effect on the final face profile. For example at site ten accurate and consistent drilling as can be seen from Figure 5.7 was noted with only azimuth deviation between panels with correspondingly good results. However at the right hand end of the second bench (from frontal view - see Appendix F) an extremely bad section of face occurs. Here the drilling was observed to be highly erratic in nature for a couple of panel lengths (approximately ten holes per panel) as is illustrated in Figure 5.8. There was no reason to believe that it was due to any other reason other than inaccurate drilling as the pre-split was located in rock which occurred in both the bench below and other panels in the same bench.

DALEK READINGS

Location 10

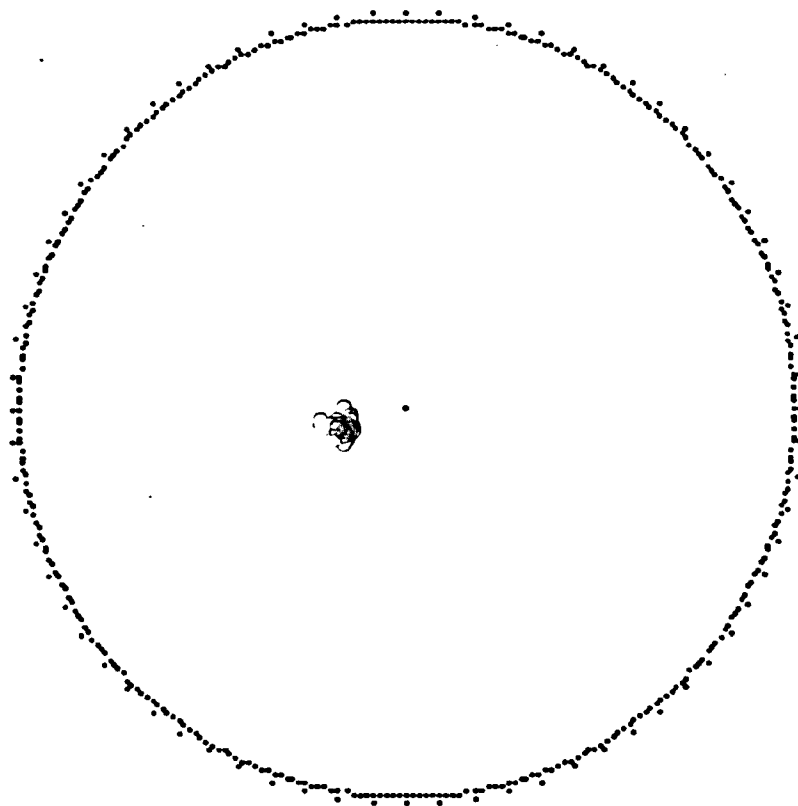
SCALE = 100°M

SCHMIDT

AZIMU

NO. OF POINTS =

24



DENSITY PLOT - SEARCH ELLIPSE = 1.00 3

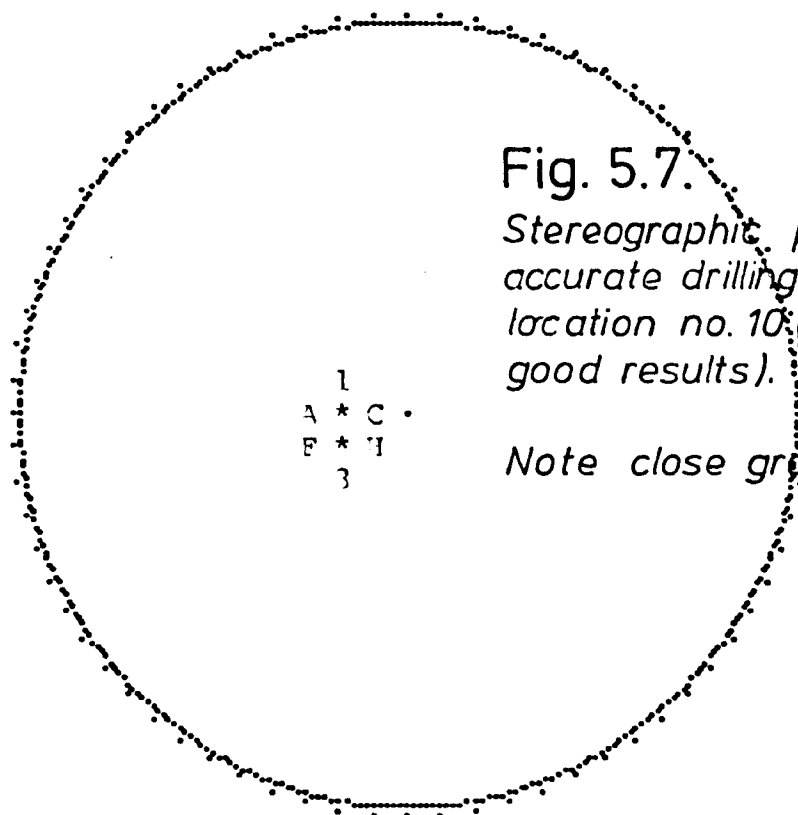


Fig. 5.7.

*Stereographic plot of accurate drilling at pre-split location no. 10 (giving good results).*

*Note close grouping.*

DALEK READINGS

Location 10

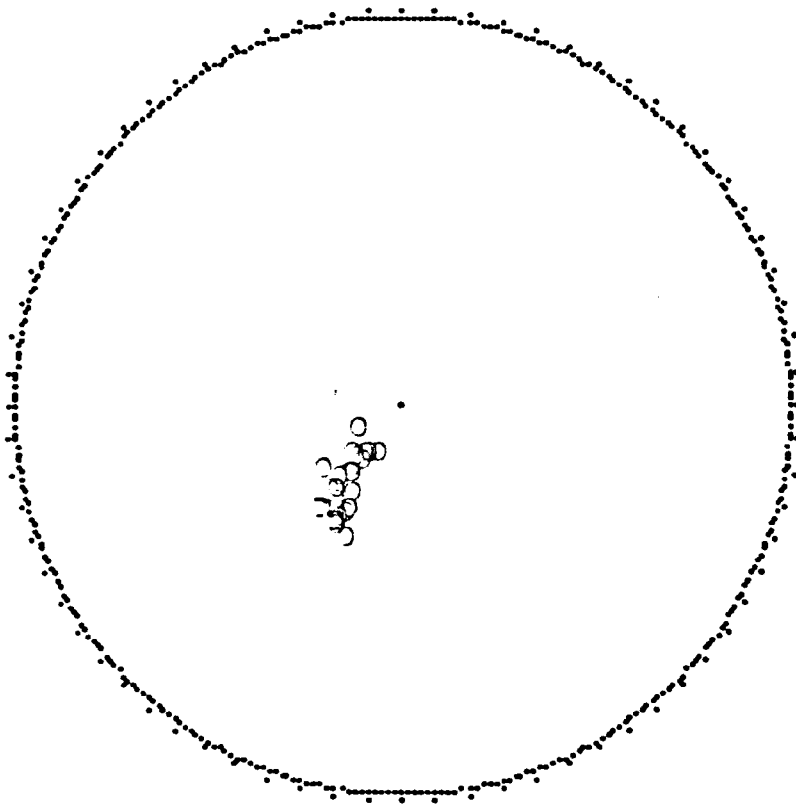
SCALE = 100:1

SCHMIDT

AZIMU

NO. OF POINTS =

27



DENSITY PLOT - SEARCH ELLIPSE = 1.00 %

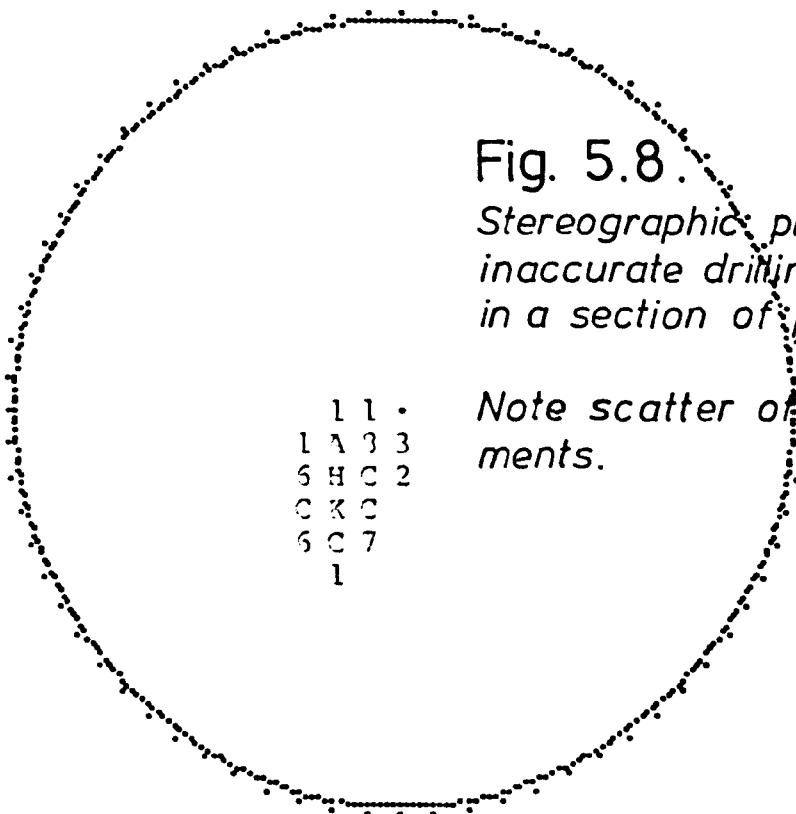


Fig. 5.8.

*Stereographic plot of inaccurate drifting resulting in a section of poor pre-split.*

*Note scatter of measurements.*

- 11.
- 1A33
- 5HC2
- CKC
- 6C7
- 1

#### 5.3.4 Borehole\_wander

The occurrence of borehole wander as shown in Figure 5.9 was present at many of the sites visited, being mainly confined to high faces. Borehole wander causes the misplacement of the borehole bottom and thus has the same effects as drilling inaccuracies. There are thought to be four main contributing factors to the degree of borehole wander which are listed in the author's order of importance. These are:

1. Face height
2. Drill bit thrust
3. Drill rig type
4. Geological factors

1. Face height was deemed the most important because as soon as a borehole was seen to start to deviate along its trace a rapid increase in 'bending' was always observed. It is therefore possible to minimise borehole wander by choosing the minimum optimum face height for which the effect is non-detrimental. Borehole deviation was seen to



Fig. 5.9.

Excessive borehole curvature resulting from excessive drilling thrust with drifter rig. (75mm hole)

be acceptable for faces not exceeding ten to fifteen metres in height for all types of drill rig.

2. Drilling thrust is deemed the secondmost important factor in borehole wander as excessive thrust leads to bowing of the drilling steel (Teller, 1972c). Borehole deviation (curved boreholes) due to excessive drilling thrust loading is easily identified in the field by the random nature of deviation direction. It is easily differentiated from borehole deviation due to geological factors as such deviations tend to "bend" in the same direction. Deviations exceeding ten degrees are common at locations three, four, five and seven where blunt drill steels and excessive pressures were allegedly used (Jones, 1980).
3. The normal type drifter rotary action rigs are commonly susceptible to drill steel flexure as the diameter of the drilling steel is normally far less than borehole diameter. Without the use of stabilisers excessive drill bit wander may occur. Down the hole hammer rigs possess larger diameter (in respect to hole diameter), hollow drill steel which is less flexible than used by drifter rigs

and due to the hammer action at the base of the hole the average compressive force on the drill steel is less.

4. If the drill bit is incident against resistant lamination of bedding dipping steeply across the path of the drill bit or if the drill bit encounters a plane of weaker resistance such as a slightly open and weathered major joint then deflection may occur, resulting in deviation along this feature. Examples of this were observed at sites three, four and seven. Further pivotal changes in direction of the drilling bit may be induced by the penetration of alternating hard and soft layers (Trudinger, 1973 and Pritchard-Davies, 1970). As the drill bit penetrates obliquely through a band of soft rock to a band of hard rock, pivoting of the drill bit occurs in the weak rock, (see Figure 5.10a). However the opposite effect (see Figure 5.10b) occurs when drilling through hard rock into soft rock and is of a smaller magnitude due to the drill bit being partially restrained by the harder rock. Thus the deviations do not cancel out and hence the overall deviation in a foliated rock with numerous alternating bands of hard and soft rock tends

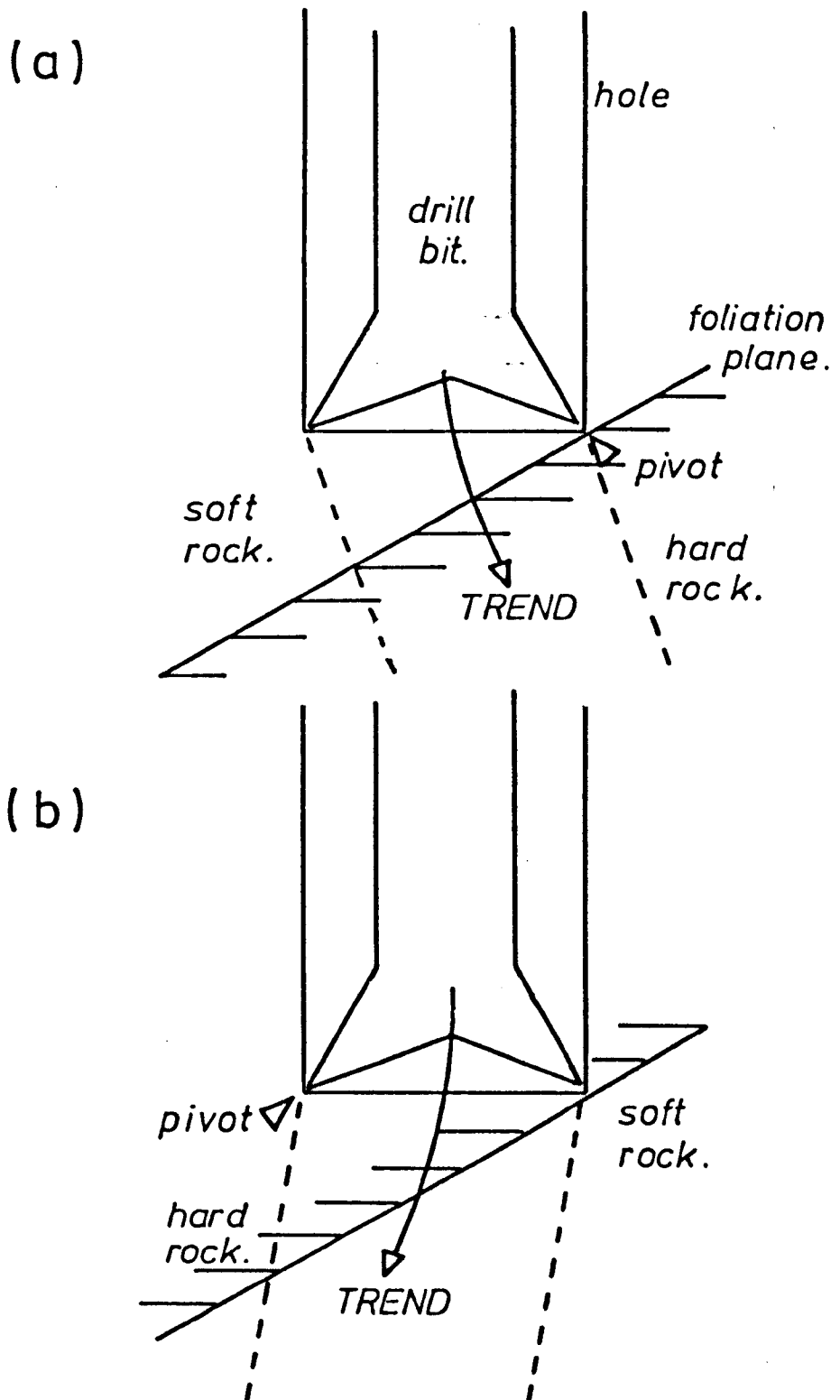


Fig. 5.10 a & b.

*Possible mechanisms for deviation of drill holes - after Trudinger (1973).*

towards the normal to the foliation. This latter effect was observed in the high portion of the successful pre-split face at location nine. Borehole deviation produced by geological rock foliation can be easily identified and separated from bad drilling practice as the deviations tend to be uniform and the boreholes remain roughly parallel whereas for the latter random deviations are the rule.

#### 5.3.5 Measurement of the Effect of Drilling Inaccuracies on a Pre-split

To quantify the effect of drilling inaccuracies on the resulting slope profile it is essential that the face chosen possesses a good splitting index (Matheson, 1979a) and thus traces of boreholes (half-barrels) in order to obtain the required results. In addition a spread in borehole bottom positioning accuracy is required. For these two reasons a relatively successful pre-split with a high face is required and accordingly the pre-split face at location nine was chosen.

With the use of scaffolding bars erected against the face and with the aid of measuring tapes, profiles of the rock face between neighbouring hole traces in the face were recorded and are displayed in Appendix G.

The areas of overbreak and underbreak from adjacent pairs of holes were then measured in the horizontal plane from the reconstructions. The resulting values of underbreak and overbreak measured in square centimetres were then plotted against their delimiting borehole separations in metres (Figure 5.11a and 5.11b) and their summation can be seen in Figure 5.12.

Although there is a fairly wide spread of points on both Figures 5.11a and 5.11b, the overall trend for greater overbreak and underbreak for increasing borehole separations is apparent. These results also show quite markedly that there is no damaging effect caused by boreholes wandering too close together. On the contrary (and contrary to popular belief) overbreak and underbreak rapidly decrease below the standard borehole separation (for location nine 100 mm holes charged with Trimobel 4 were spaced at 1 m centres). In addition no evidence of excess damage due to the higher charge concentration is apparent in

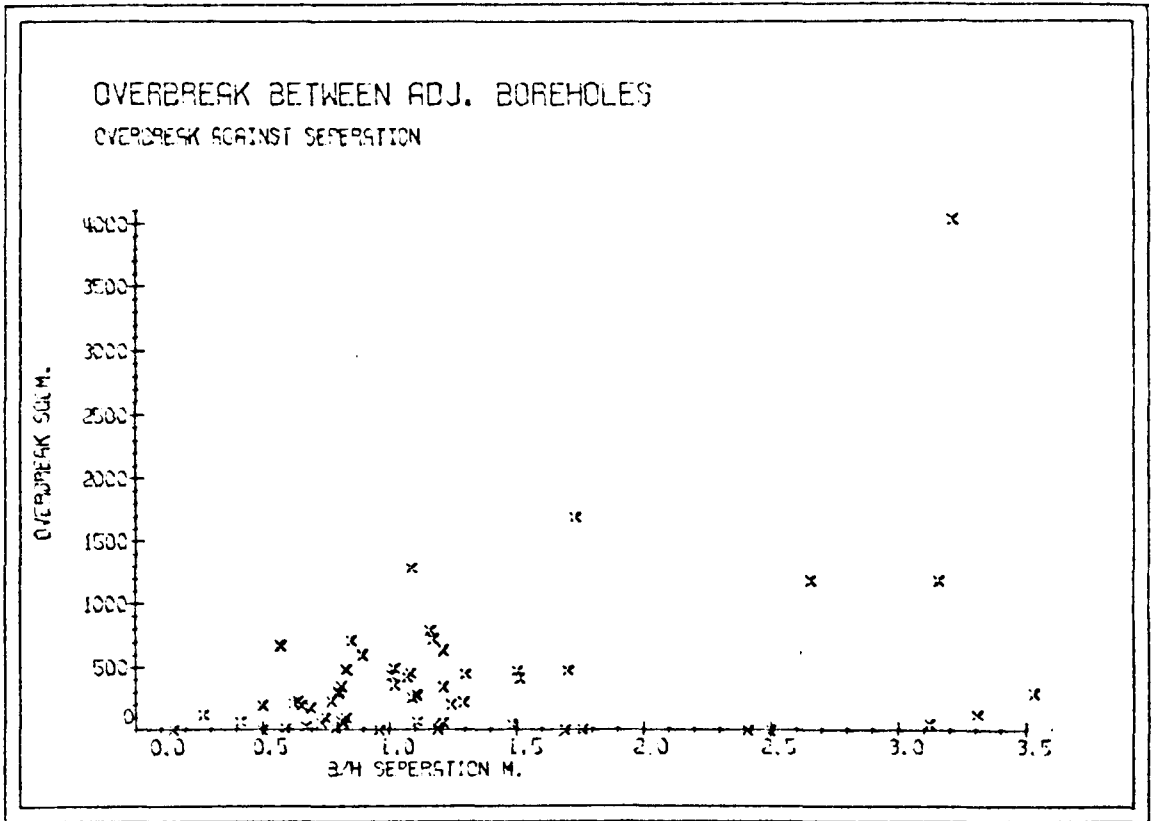


Fig. 5.11a. - Plot of overbreak component against borehole separation. Field measurements from pre-split location no. 9.

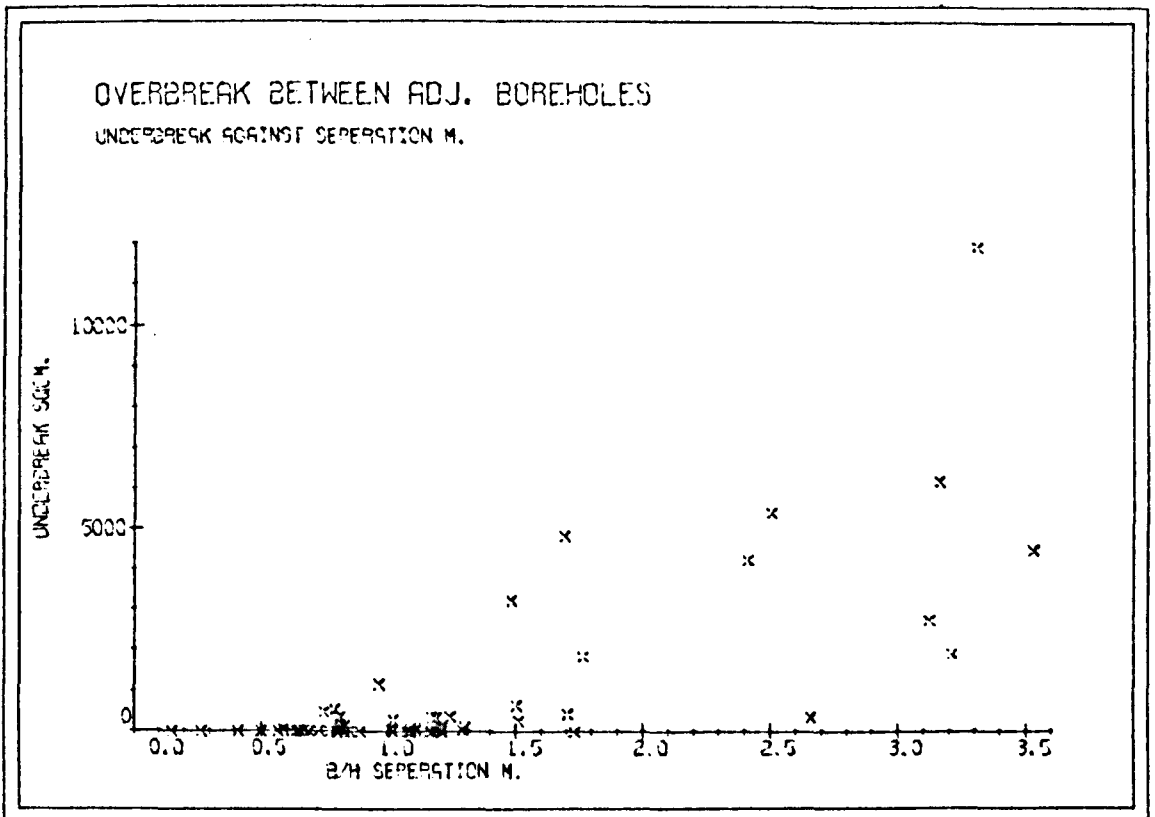


Fig. 5.11b. - Plot of underbreak component against borehole separation. Field measurements from pre-split location no.9.

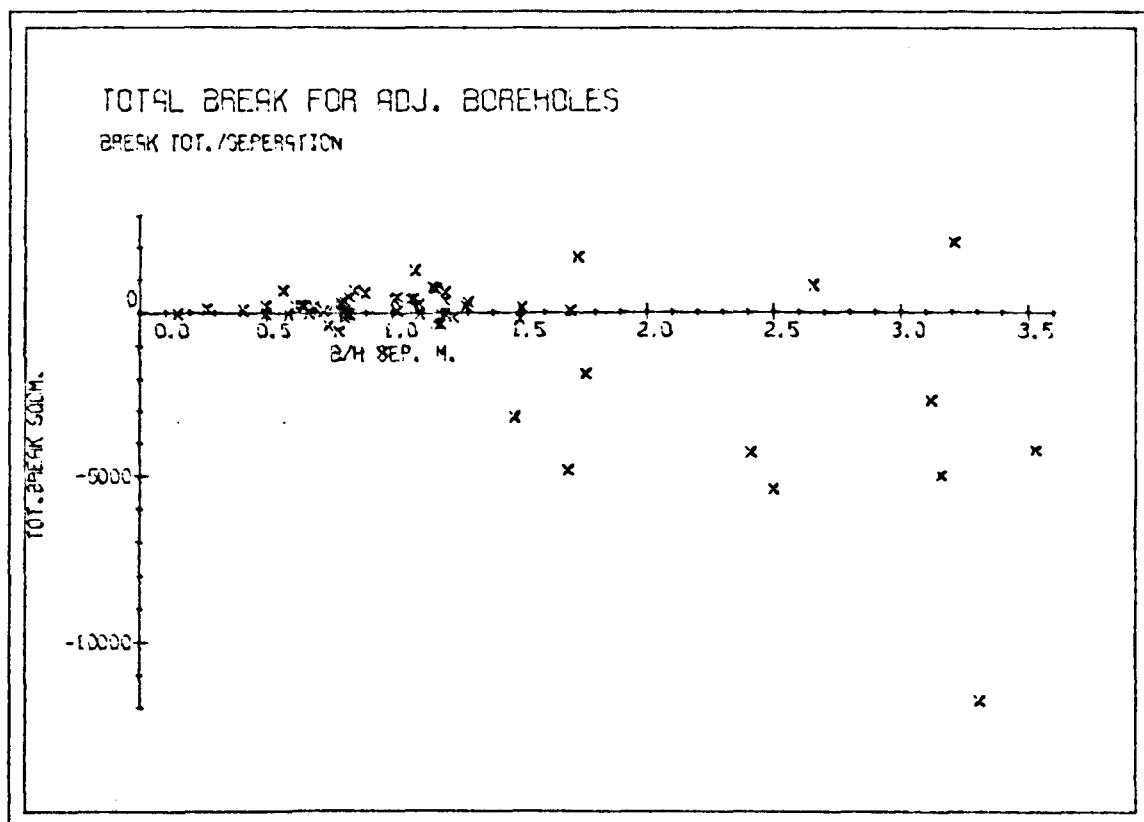


Fig. 5.12 .

Plot of Net breakage between individual boreholes against borehole separation.

Illustrating fairly clean profiles for up to a borehole separation of ~1.2m. above which major irregularities may occur. Underbreak being more predominant than overbreak.

Field measurements from pre-split location no.9.

any of the locations examined and these reduced borehole separations in fact give the impression of reduced damage. This observation may be explained as follows:

Due to their reduced separation the boreholes may be linked earlier by the pre-split fracture and thus the stress situation will be altered in their immediate vicinity earlier, this causing the premature termination of propagation of radial fractures perpendicular to the pre-split line, thus reducing damage to the intended face and producing a straighter split between boreholes.

From Figure 5.12 (the total breakage against borehole separation) it can be seen that although overbreak is predominant below a borehole spacing of 1.4 m, above this value underbreak is prevalent generally - resulting in large toes. The spread of values of breakage can be seen to fan out with increasing borehole separation in the shape of a wedge.

The spread of results in each of the three graphs represents the geotechnical influences at location nine which were predominantly the presence of minor

Jointing sub-parallel to the face, which in certain cases the breakage to which has reduced both underbreak and overbreak and in other cases has marginally increased overbreak by the fracturing to jointing just behind the line of the final face.

#### 5.4 PROXIMITY OF BULK CHARGE

The separation of the pre-split panel from the bulk charge at all points is essential for a successful final face to be achieved on completion of mucking out after blasting. The bulk charge should be close enough to the pre-split line to produce adequate breakage of the intermediate ground but should be separated from that line to give sufficient protection to the final face from the power of the bulk blast.

If an inclined pre-split panel is used then care should be taken to ensure that the toe of the last line of bulk holes does not infringe within the minimum acceptable limits of separation, (see Figure 5.13a). If necessary these bulk holes should be inclined at the same inclination and azimuth as the pre-split boreholes (Figure 5.13b) or short bulk holes should be drilled in between the bulk and pre-split

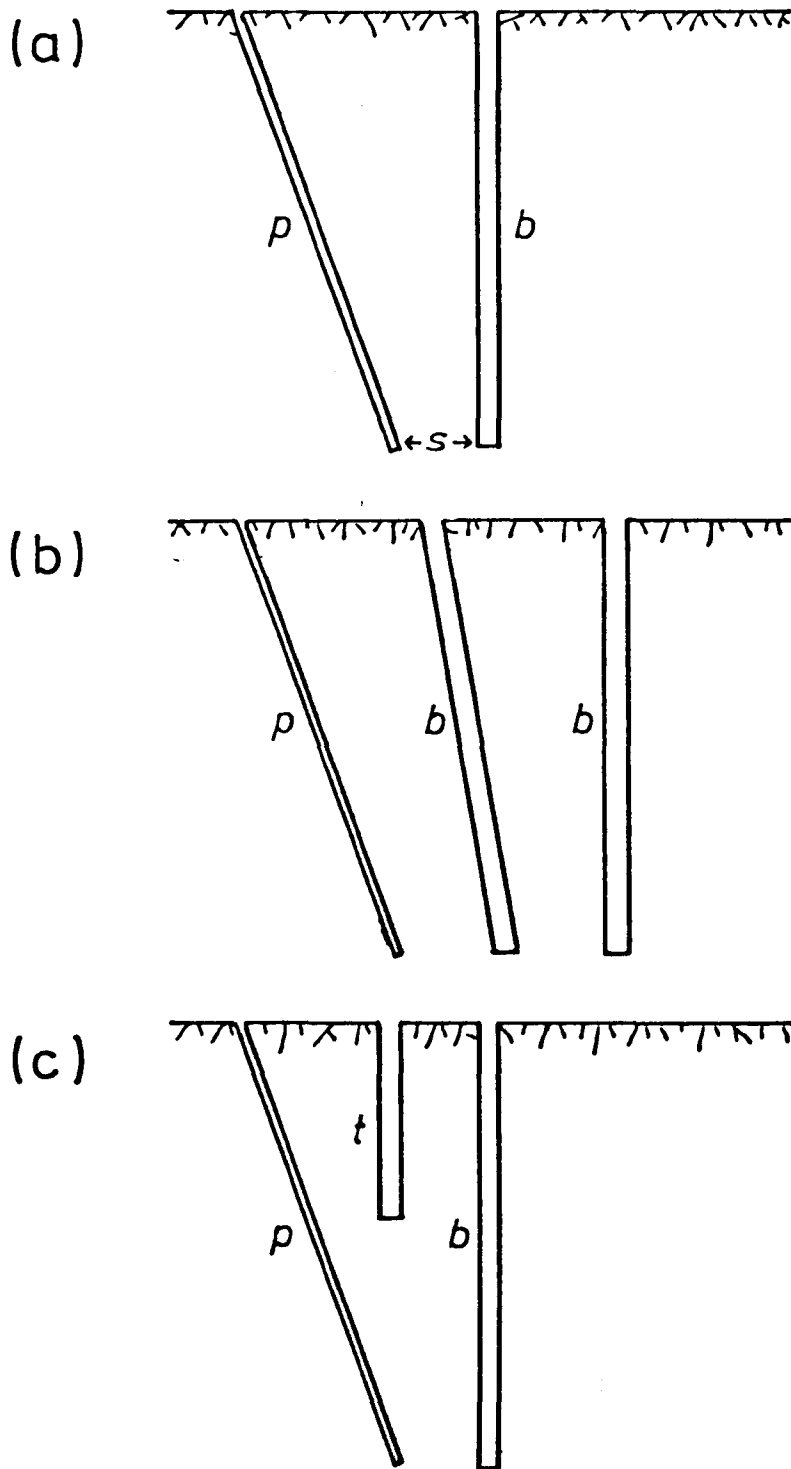


Fig. 5.13 a,b&c.

Diagram of different bulk blasting techniques and borehole configurations for use with pre-splitting.

*p* = pre-split line,

*b* = bulk holes,

*t* = 'pop' holes.

holes in order to ensure breakage of the intermediate top wedge of rock (Figure 5.13c).

For surface operations the minimum distance between pre-split and bulk blast holes recommended by the author is two metres or twice the pre-split borehole separation (whichever is the greatest) and the maximum distance is half the optimum bulk hole separation. If the bulk charge is large then the maximum separation should be used and also a reduction in charge density (kg per m or lb per ft) of the last row should be considered in order to protect the final face.

Another important consideration is the accuracy in the drilling of the bulk charge holes and particular care should be taken in the drilling of the last row before the pre-split panel and holes should not be charged if they come within two metres of the final face.

Bulk holes have been observed to cross the pre-split panels at location two to eight inclusive by Talbot (1977), Jones (1978) and Matheson (1980) where the accuracy of bulk hole alignment was low, creating extensive zones of damage within the final faces and

negating the effect of the pre-splitting. Misfired bulk holes were discovered in the final face still full of pink ANFO prill by Jones (1978) at locations three and four and intact bulk holes which presumably had misfired were also discovered by the author.

The objective of using the pre-splitting technique is to create a relatively undisturbed stable clean face of planar nature rather than a highly disturbed uneven unstable bulk face, therefore any pre-splitting should be carefully designed with that of the bulk blasting and not as totally separate issues.

## 6 THE EFFECT OF SINGLE DISCONTINUITIES (EXPERIMENTAL)

### 6.1 THEORY

The most striking result obtained from the work undertaken in understanding the mechanisms involved in pre-splitting is the amount of fracturing and its extent around the borehole compared with the maximum pre-split separation. This effect is not expected or explained by trying to describe the mechanism involved by either dynamic stress wave interaction or by hydrofracture alone.

The resolution in two dimensions of the resultant pattern of fracturing that is obtained by splitting in polyester resin, is that of marginally overlapping approximately elliptical zones of fracturing, with the largest axis of fracturing parallel to and in line with the axis of the pre-split, (see Figure 6.1).

If one were to assume the mechanisms which are involved in pre-splitting as those which have been previously given as correct, then the zone of fracturing around each borehole in a simultaneously

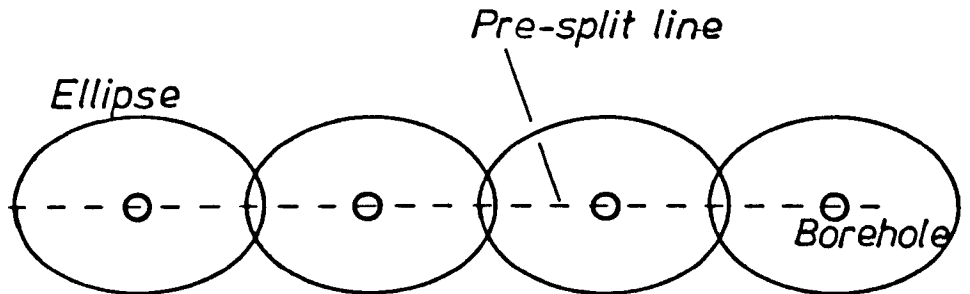


FIG. 6.1. ...  
Inter-fingering of elliptical fracture zones.

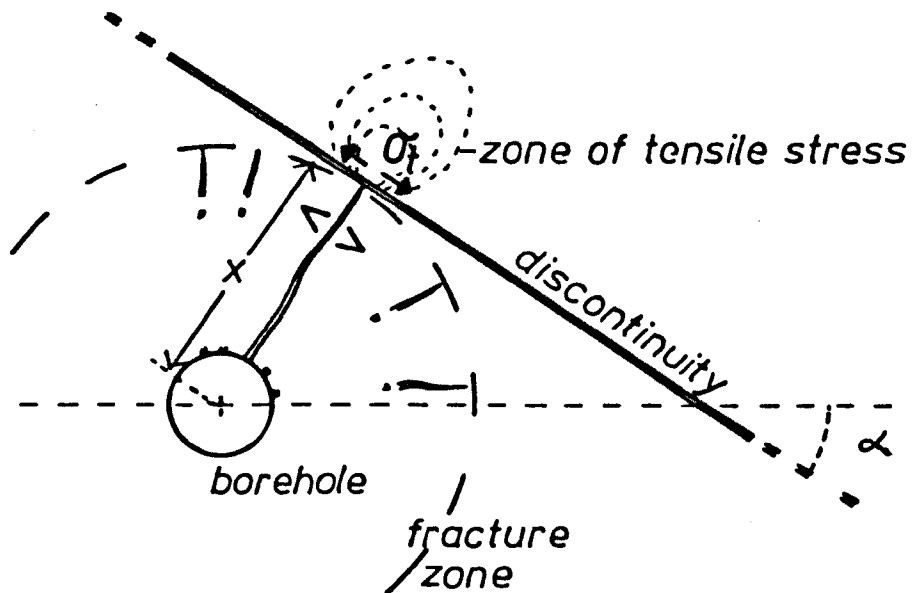


FIG. 6.2.  
Expanding fracture zone around borehole with first fracture to breach discontinuity opening.

detonated pre-split line will originate as a circle, and then gradually assume an elliptical form as it expands, the rate of change in ratio of the lengths of the axes of the ellipse increasing slowly with the area of the zone.

Now consider the presence of a single discontinuity at an angle  $\alpha$  to the pre-split line, and a distance of  $x$  from the borehole concerned, (see Figure 6.2). The first fracture within the expanding elliptical zone to breach the discontinuity will cause slight shearing motion along the discontinuity, assuming that it has no considerable shear strength, which may be caused by high cohesion or high shear strength. For shearing:

$$\sigma_w > \sigma_t$$

where  $\sigma_w$  is the normal force across the opening fracture caused by the wedging action of the gas.

$$\sigma_t = \sigma_N \tan \phi + C$$

where:  $\sigma_t$  = shear strength of the discontinuity

$\sigma_N$  = normal force acting on discontinuity

$\phi$  = angle of friction of the discontinuity  
interfaces

$C$  = cohesion along the discontinuity

Also  $\sigma_N$  may be reduced by these gases of detonation migrating into the discontinuity, depending on its openness.

This shearing along the discontinuity is due to an opening of the fracture which is in turn caused by the wedging action of the explosive gases against the fracture walls. Opening of the fracture will allow extra explosive gases to flow into the fracture, further pressurising the fracture walls (up to the pressure within the borehole itself), causing a redistribution of the stress field around it, and will result in it becoming the dominant fracture, suppressing the growth of other fractures, (see Figure 6.3).

If a pressure  $P$  is exerted on the walls of the dominant fracture then the force exerted on a neighbouring fracture will be  $\sigma_p$ , where  $\sigma_p$  is a function of the distance from the dominant fracture.

If  $\sigma_p \times \sin w > -(\sigma_t - T)$  propagation will cease where  $\sigma_t$  is the tensile stress at the fracture tip, normal to the fracture, and  $T$  is the tensile strength of the rock.

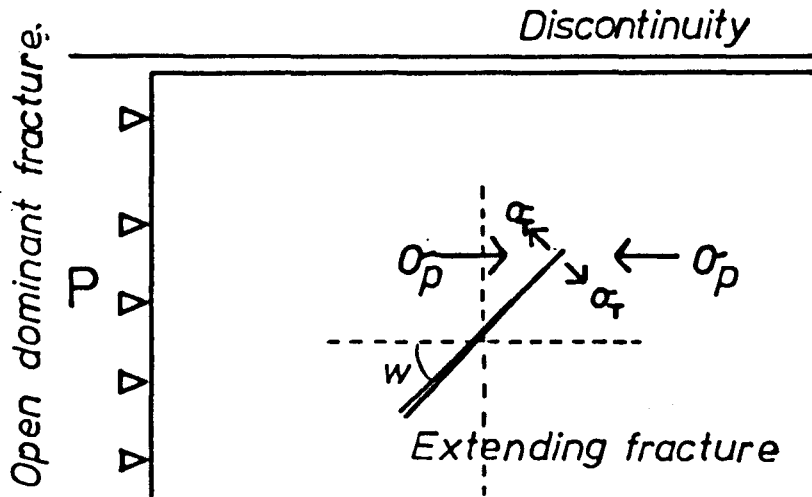


FIG. 6.3.

*Effect of open pressurised fracture on an adjacent extending fracture.*

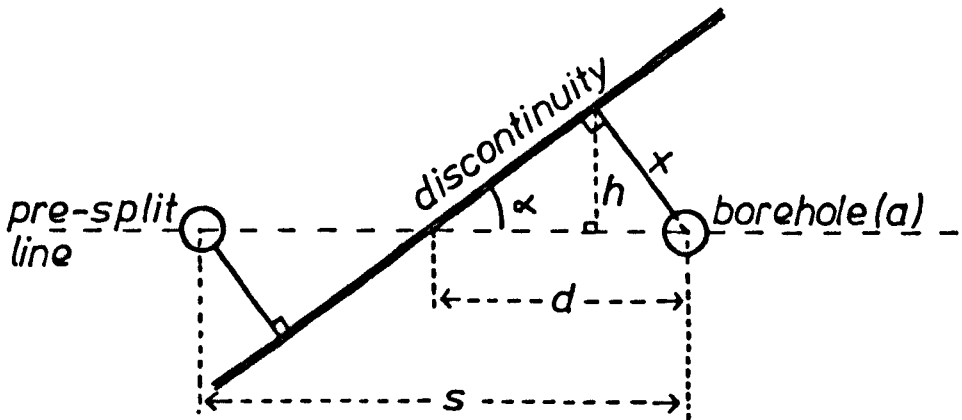


FIG. 6.4.

*Simplified pre-split with discontinuity and dominant fractures.*

*Diagram of the geometry involved in the formulation of theoretical overbreak e.t.c.*

The shearing action along the discontinuity will also theoretically create tensile forces in the rock opposite the dominant fracture, a tensile 'stress bulb' being created. This may influence the extension or direction of growth of fractures under propagation from a neighbouring simultaneously detonated blast hole located on this side of the discontinuity, or may even induce failure in the discontinuity wall if the tensile stresses created exceed its tensile strength.

Due to the geometry involved, this dominant fracture will be orientated perpendicular to the discontinuity, or sub-perpendicular by a few degrees towards the pre-split line, say  $y$  degrees where  $y$  is dependent on the geometry of the ellipse of fracturing around the borehole involved.

It is postulated that the fracture zone will be more elliptical for borehole separations near the limits of a successful pre-split, and conversely more circular in shape for closer borehole separations. However, the degree of deviation of the dominant fracture from the perpendicular to the discontinuity is mainly dependent on the positioning of the discontinuity in relation to the borehole, and thus the state of growth of the fracture zone when it

reaches the discontinuity.

Thus the first, and subsequently dominant breakage between adjacent boreholes, bisected by a discontinuity, will be directly perpendicular to that discontinuity from the hole, then travelling along the discontinuity's length to where the next borehole has fractured to it. From this statement it is obvious that the orientation of the discontinuity to the pre-split line and the positioning of the discontinuity in respect to individual boreholes will greatly affect the degree of underbreak and overbreak obtained, and also determine the smoothness/regularity of the final face.

By simplifying the fracture ellipsoid to a circle the maximum irregularity and overbreak may be readily calculated, (see Figure 6.4):

Let:  $x$  be the shortest distance from hole to joint,  
the angle of incidence of joint to line of pre-split  
be  $\alpha$  and the distance from intersection to hole be  $d$ .  
Then:  $x = d \sin \alpha$  .....(1)

Thus the measurement of maximum departure  $h$  of the resultant face from the desired face is:

$$h = x \cos \alpha$$

substituting for x from (1)

$$h = d \sin \alpha \cos \alpha$$

As the area of a triangle is given by half its base x height, then the area of maximum overbreak between hole and the joint will be:

$$d/2 \times d \sin \alpha \cos \alpha$$

therefore:

$$\text{Area} = (d^2 \cdot \sin \alpha \cos \alpha) / 2 \quad \dots\dots(2)$$

This function gives a maximum for a value of  $\alpha$  of forty five degrees for a constant d, equal to or less than half the borehole separation. Examples of this geometric effect on irregularity and overbreak/underbreak are given in Figure 6.5

Still considering a circular fracture zone, the approximate maximum distance that the zone may reach a discontinuity away from a borehole will be equal to half the borehole separation (providing reasonable borehole separations are used). Therefore overbreak may only occur for values of x equal to or less than half the borehole separation.

$$\text{i.e.} \quad \text{for } x < s/2$$

where s is the borehole separation. For maximum possible overbreak h must also be at a maximum value.

$$\text{i.e.} \quad h = x = s/2$$

but

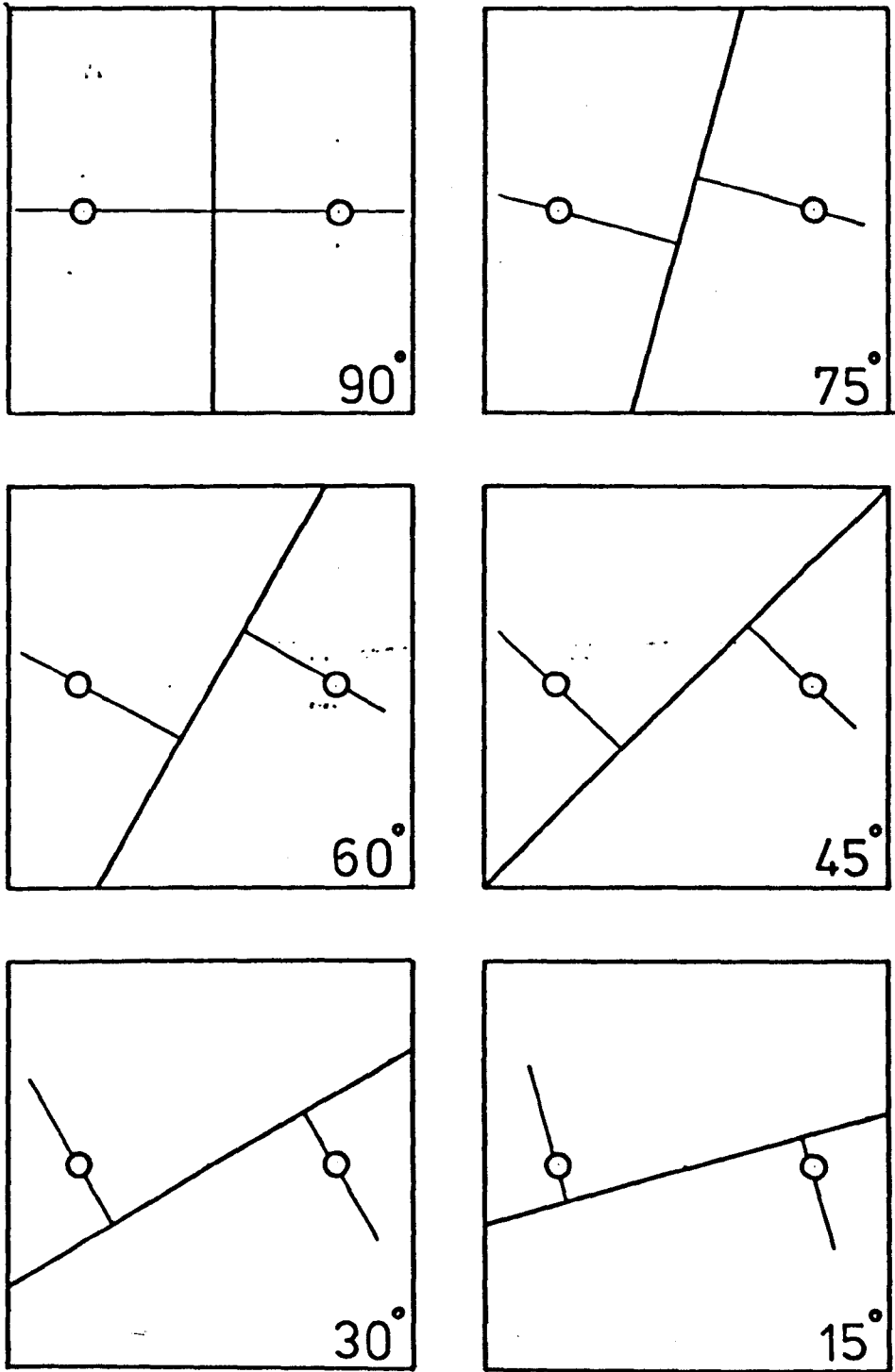


FIG. 6.5.  
Geometry of fracturing between boreholes with varying bisecting discontinuity orientations.

$$h = x \cos \alpha$$

therefore

$$\cos \alpha = 1$$

and therefore

$$\alpha = 0^\circ$$

but

$$\sin \alpha = x/d$$

therefore

$$d = \infty$$

Thus maximum overbreak will occur with parallel discontinuities to the pre-split line which are located at half the borehole separation away from the pre-split line. Therefore, the overbreak caused by a single discontinuity within the confines of:

$$x < s/2$$

will give the asymptotical functions:

$$\text{Overbreak area} = d^2/2 \sin \alpha \cos \alpha$$

and

$$\text{Max overbreak} = s^2/8 \tan \alpha \quad (\text{see Figure 6.6})$$

NB This solution is for analysis in 2 dimensions only.

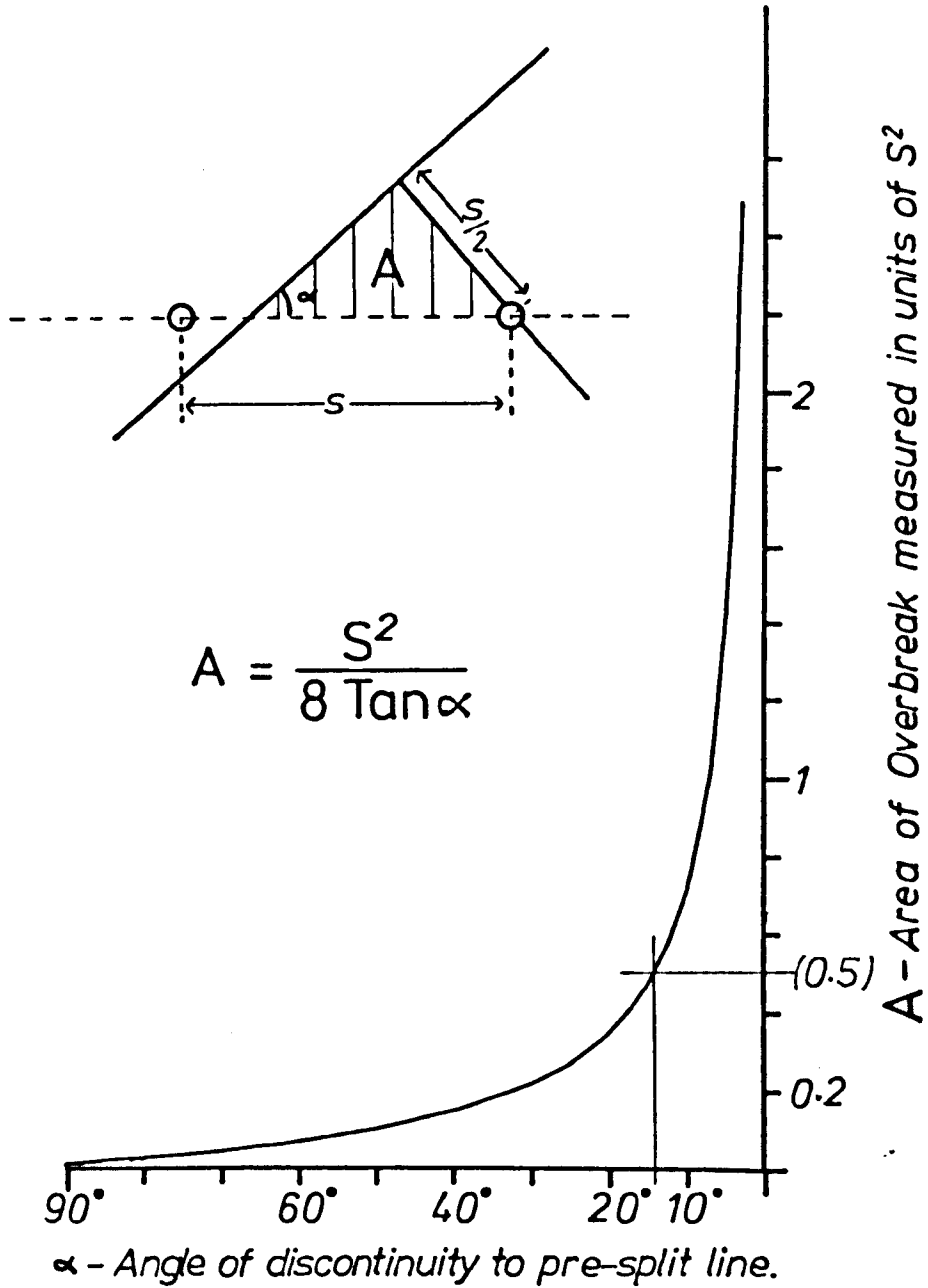


FIG. 6.6.

Graph of the maximum possible overbreak measured in square optimum borehole separations for a single discontinuity intersecting the presplit line at  $\alpha$  degrees.

6.2 AEEECI ON THE SUCCESS OF A PRE-SPLIT

For maximum overbreak, fracturing from each borehole will join with the discontinuity behind the line of the intended face. Although a pre-split fracture may be formed, the rock will be loose and the integrity of the face low. On excavation this rock will be removed to the discontinuity. The discontinuity itself may take over the role of the pre-split behind the intended face, protecting the rock behind. Thus all traces of the pre-split half barrels and thus intended pre-split face will be lost.

It is therefore essential to find out at what angle of discontinuity to borehole line the effect of loosing half barrels due to overbreak is completely eradicated.

Using the constraints  $d < s$  and  $x < s/2$

As  $\sin \alpha = x/d$

then  $\alpha = \sin^{-1}(x/d)$ .

Substituting for maximum values of  $d$  and  $x$

$$\alpha = \sin^{-1} s/2s$$

$$= \sin^{-1} 1/2$$

therefore  $\alpha = 30^\circ$

A complete graph of discontinuity intersection angle against maximum number of half barrels lost by one discontinuity (in two dimensions) is given in Figure 6.7.

It can be seen from Figure 6.7 that the curve of this function becomes asymptotic exceedingly quickly below fifteen degrees, and that extensive fractures within ten degrees of the pre-split line will cause a virtual extinction of the proposed final face and the half barrels within it.

### 6.3 EXPERIMENTATION IN RESIN

It was decided to initially continue explosive model testing using Polyester resin blocks, due to the fact that there were a small number of blocks and a quantity of resin which had remained unused from the first phase of model blasting. The transparent qualities of the medium also made it highly suitable for examination of the fracturing and breakage processes in detail.

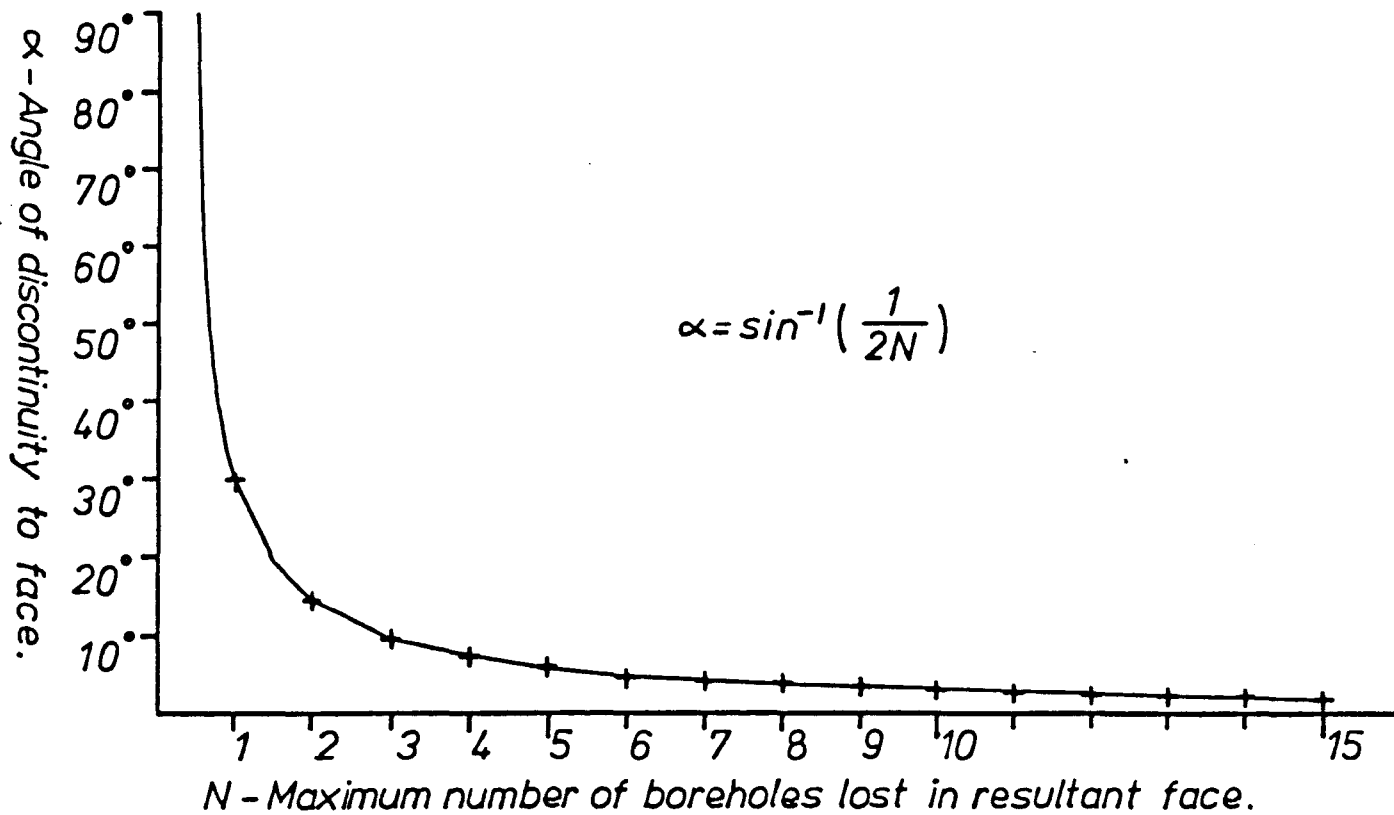


**FIG. 6.7.**

*The theoretical effect of the angle of a continuous single discontinuity on the maximum number of half barrel lost in the final presplit face.*

### 6.3.1 Method

A borehole diameter of 3/16 inch and separation of three inches were chosen as suitable dimensions from the results obtained during previous model blasting tests. It was decided to use three holes of the stated diameter and spacing, with a single machine sawn discontinuity positioned midway between each pair of adjacent holes, the width of the saw cuts being taken into account when marking out the hole positions. Accordingly a block length of ten inches was chosen, block dimensions being 10 x 6 x 3 inches. The saw cuts were left, as fairly good matching of surfaces was achieved and machining of these faces was deemed an unnecessary expense.

A series of seven experimental tests were constructed in this manner, incorporating successive increments of fifteen degrees to the discontinuity to pre-split line intersection angle from zero to ninety degrees. In all seven tests the blocks, including wave traps, were restrained identically to first phase model tests, and were similarly loaded with four grain per foot PETN detonating cord and initiated for simultaneous detonation from a single electric detonator. The usual precautions against detonator

shrapnel damage were taken. Full blasting records are given in Appendix D and E.

### 6.3.2 Results

All tests provided breakage between each three holes. The results of blasting are shown in Figures 6.8 to 6.14. The results of each model blast backed up theoretical postulation of dominant open fractures being formed roughly perpendicular to, and vented into the discontinuity present. The fracture zones are also shown to be circular/ellipsoidal in shape, except at their contact with discontinuities where the fracturing is curtailed.

Few fractures were actually seen to cross the discontinuity concerned and these were extensions of the dominant fracture or fractures across the discontinuity, (see Figures 6.12 and 6.13). Notably this effect was only encountered in tests where the discontinuity to pre-split line angle was equal to or less than thirty degrees. In contradiction however, in test 57, (Figure 6.14), which incorporates two discontinuities parallel to the pre-split line (one on either side) no fracturing was seen to propagate

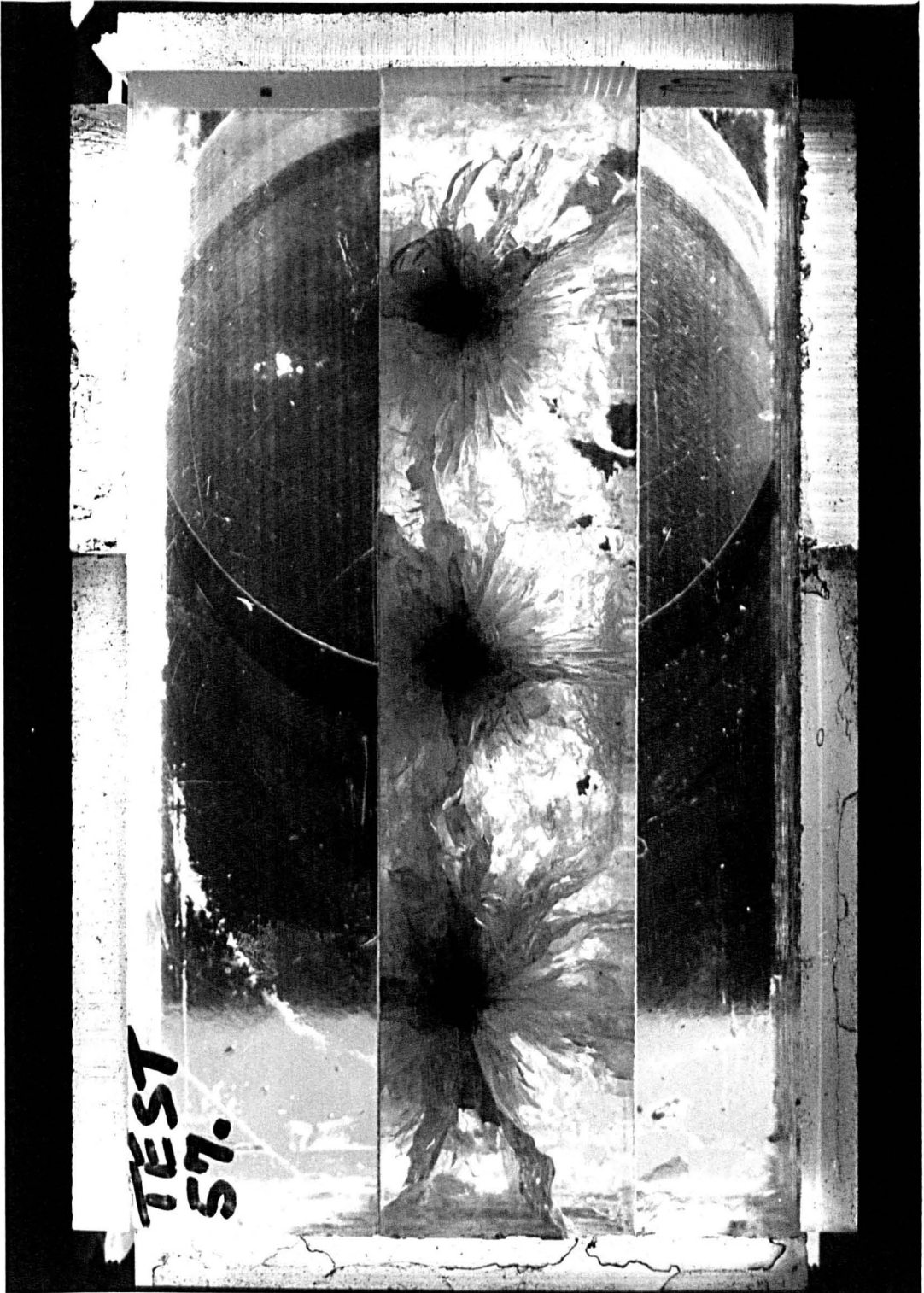


Fig. 6.8 .

Test 57 - pre-split test in resin with single discontinuities.  
Discontinuity intersection angle =  $0^{\circ}$ .



Fig.6.9.

Test 54 - pre-split test in resin with single discontinuities.  
Discontinuity intersection angle =  $15^{\circ}$ .

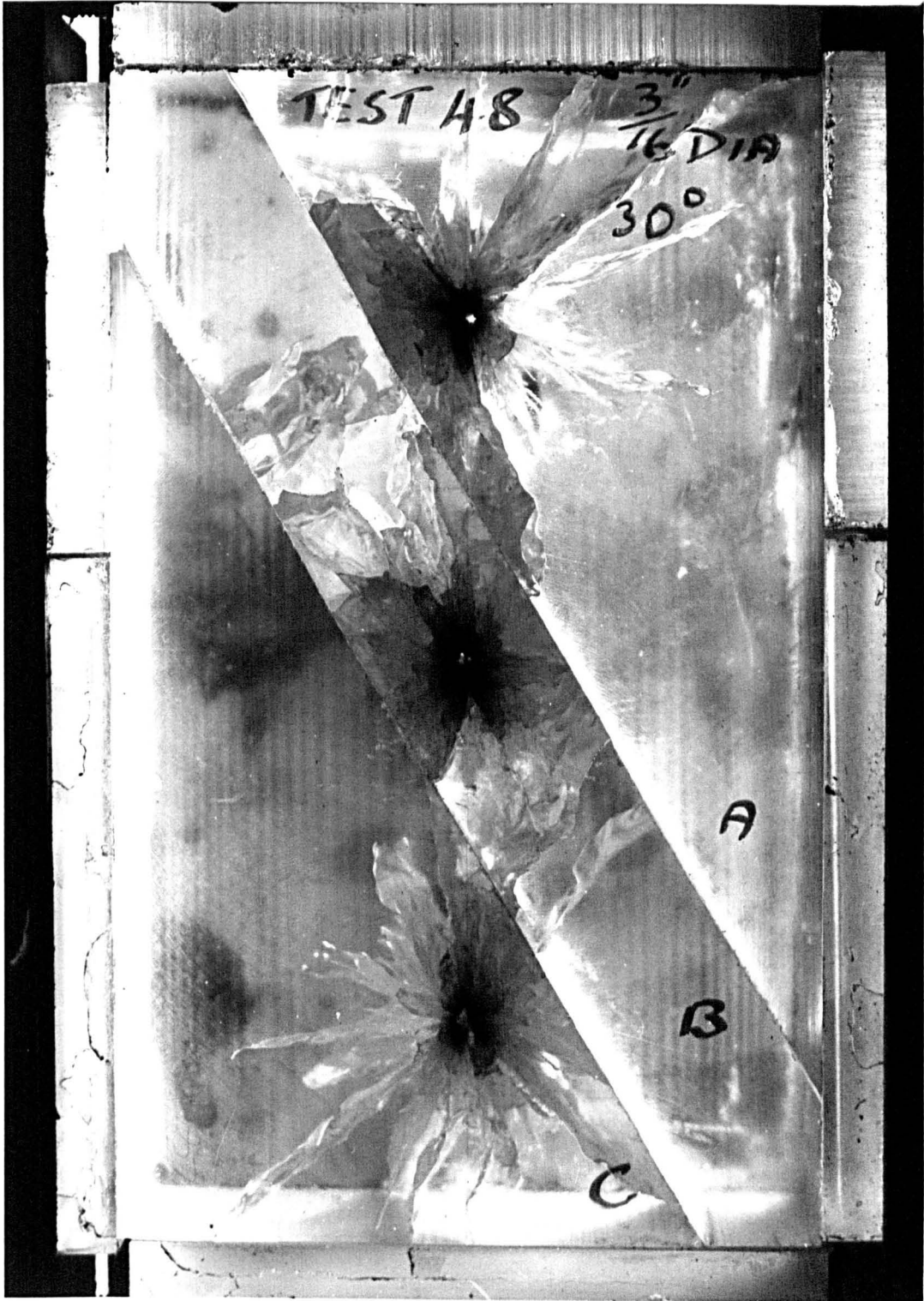


Fig. 6.10.

Test 48 - pre-split test in resin with single discontinuities.  
Discontinuity intersection angle =  $30^{\circ}$ .

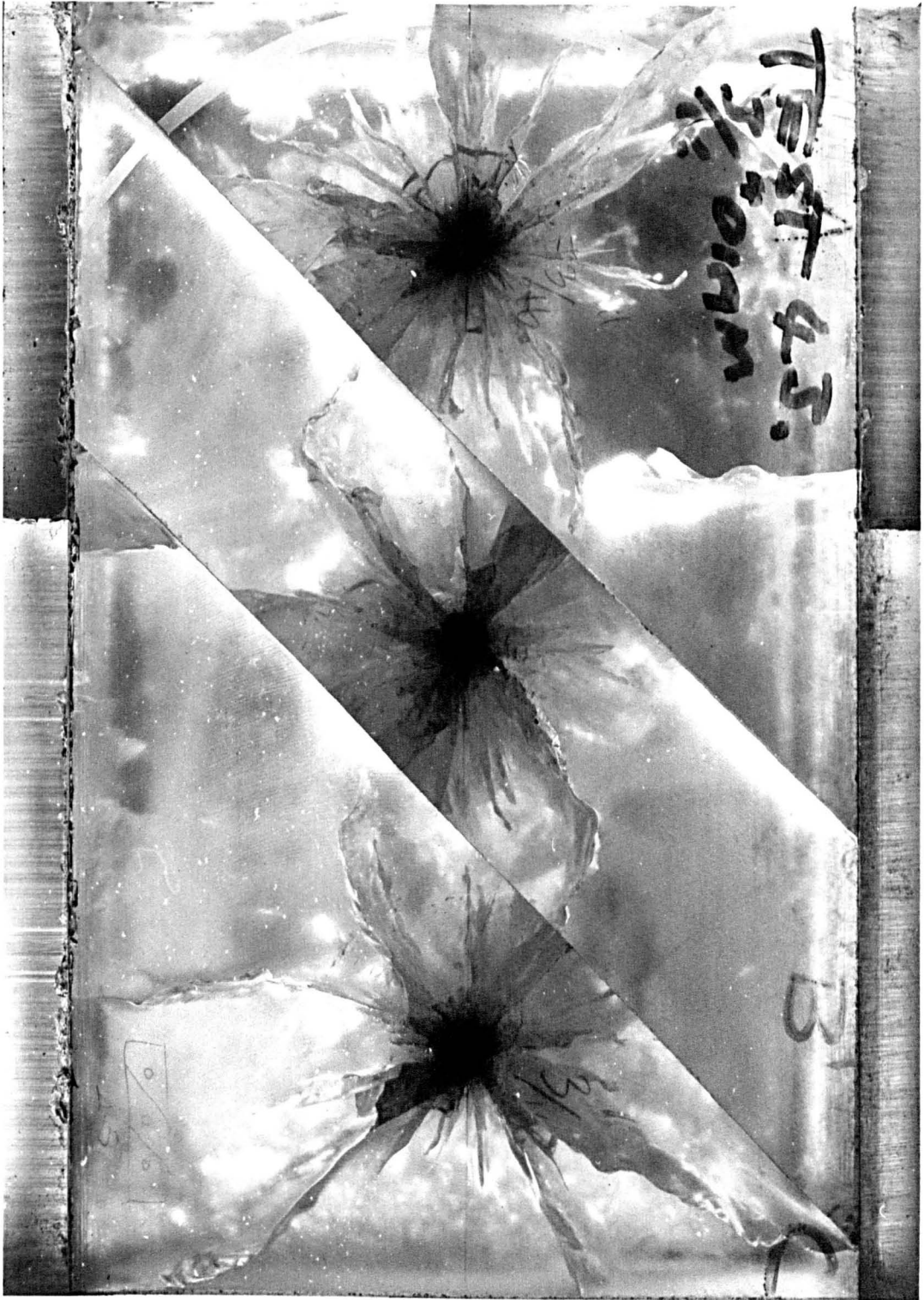


Fig. 6.11.

Test 43 - pre-split test in resin with single discontinuities.  
Discontinuity intersection angle =  $45^{\circ}$ .

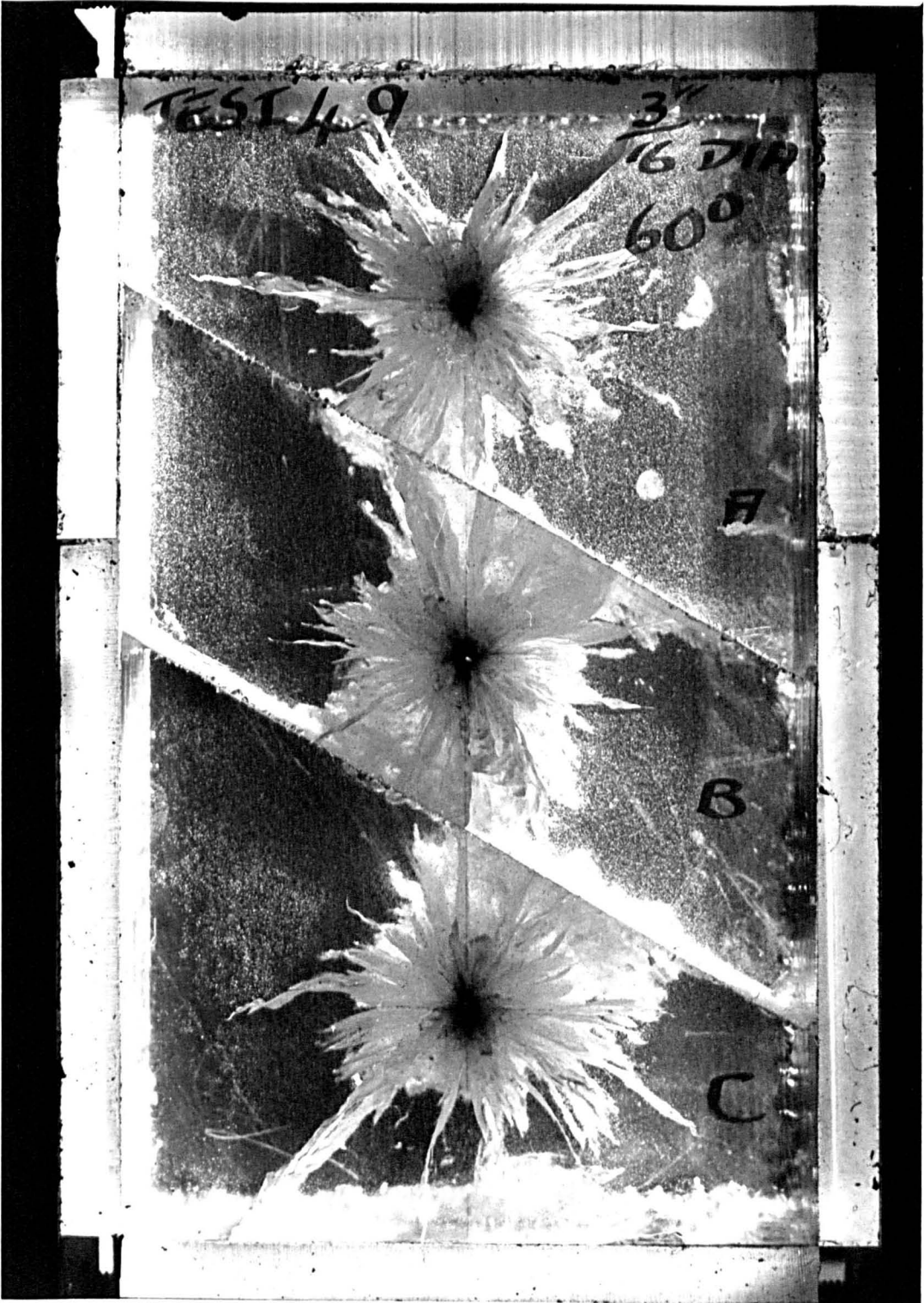


Fig. 6.12.

Test 49 - pre-split test in resin with single discontinuities.  
Discontinuity intersection angle =  $60^{\circ}$ .

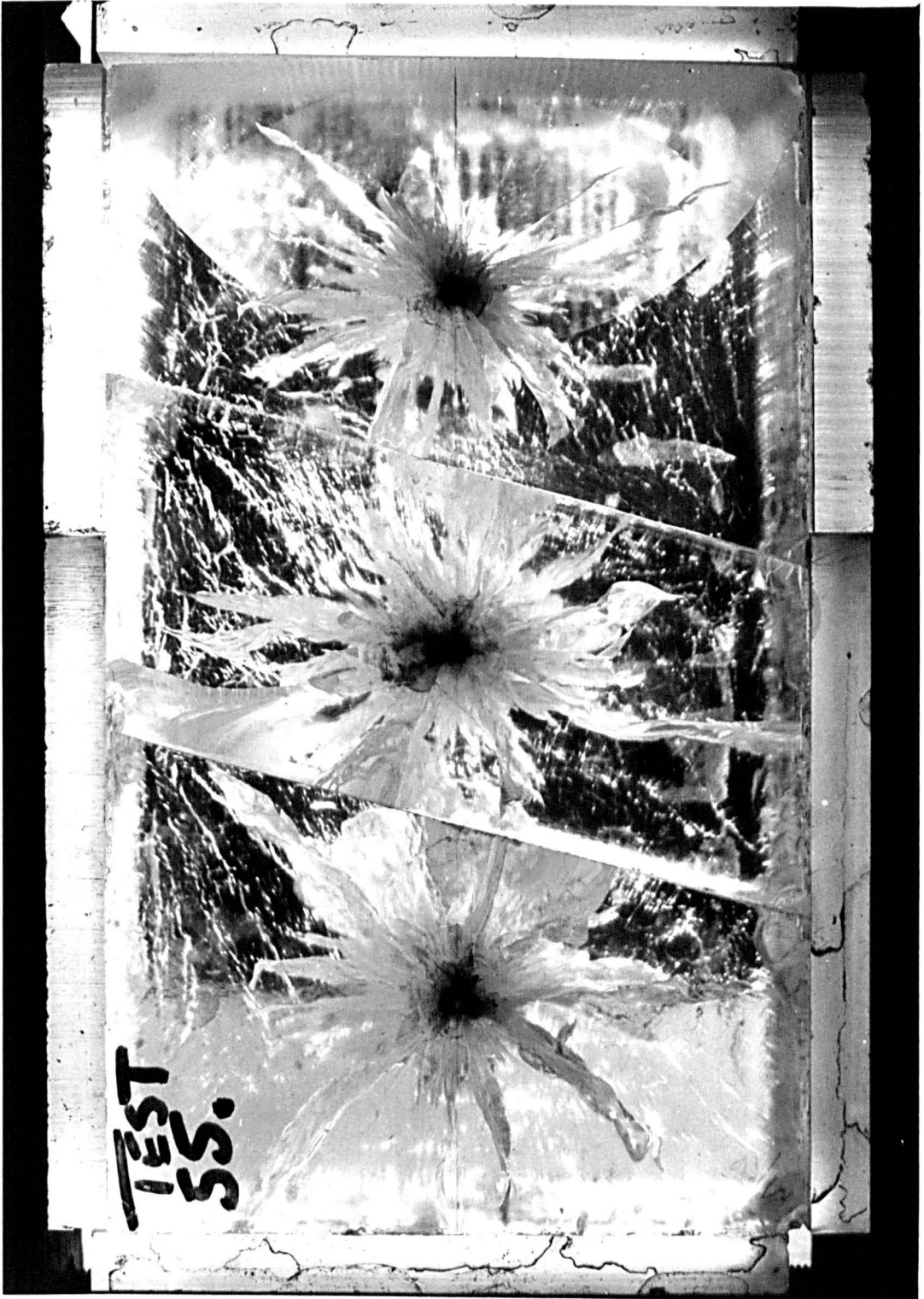


Fig.6.13.

Test 55 - pre-split test in resin with single discontinuities.  
Discontinuity intersection angle =  $75^{\circ}$ .

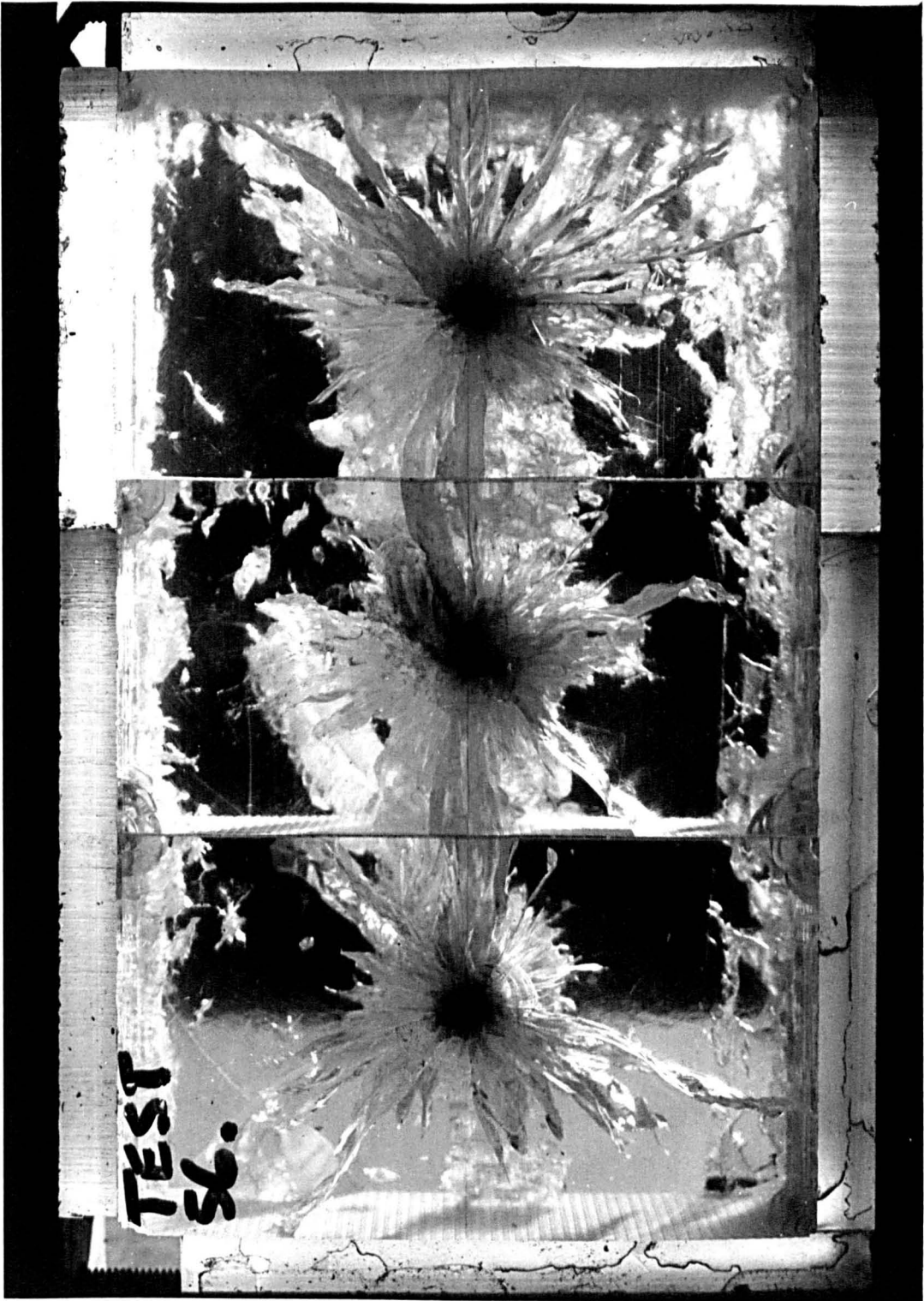


Fig. 6.14.

Test 56 - pre-split test in resin with single discontinuities.  
Discontinuity intersection angle =  $90^{\circ}$ .

further than the discontinuities, which acted as perfect pre-splits themselves in a sense, confining fracture damage to the shothole side. This contradiction may tentatively be explained by the fact that in tests 48 and 54 (thirty and fifteen degree discontinuities respectively) the discontinuities are separated by less than half of the borehole spacing.

Test No.	Angle	Separation/Borehole Spacing
48	30	0.49
54	15	0.26

The fracturing within these slabs has possibly been initiated by the high tensile stresses in the discontinuity surface, built up at the intersection of a dominant fracture and the discontinuity by the shearing of the discontinuity walls, which in turn is produced by the opening of the dominant fracture or fractures under the force of the explosive gases, (see Figure 6.2). This, coupled with the lower tensile strength of the thinner slabs of Polyester resin located between the joints and the close proximity of the holes to the discontinuities induces failure, whereas in the remainder of the tests with

interdiscontinuity thickness in excess of half borehole spacing, the strength is too high and the blast holes due to the geometrical factor are located further away from the discontinuity, resulting in lower tensile forces being created at the discontinuity. This explanation is backed up by examination of these fractures by fracture morphological techniques, which show the fractures to have been initiated at or near the discontinuity/dominant fracture interface, and to have propagated in a direction away from the borehole concerned. Fractures were not found to pass over single discontinuities.

In resin testing with discontinuities, the dominant fractures were observed to only have minimal effect on the suppression of the connection of other extending fractures with the discontinuity concerned. However, suppression of the 'opening' of other fractures was achieved. The former effect becomes increasingly apparent with decreasing discontinuity orientation angle and resulting reduction of the separation of the discontinuity and hole. This is attributed to the greater driving force behind the extending fractures, due to their proximity to the borehole and the corresponding shorter time interval after detonation.

This gives a higher driving pressure within the borehole and thus the opening of the dominant fracture will have less of an effect. Also the length of the dominant fracture will be shorter and thus have a smaller effective area of influence.

Overbreak was defined as any ground in the tests within the pre-split line that is surrounded, i.e. separated from intact ground by the connection of a discontinuity and blast fracture, the ground in this case being resin. The amount of overbreak was measured orthogonally between the two end holes in square millimetres.

Table 6.1

Angle (degrees)	Overbreak (sq mm)
0	5,904
15	3,042
30	2,597
45	2,360
60	1,491
75	1,385
90	998

Pre-splitting with Discontinuities in Resin.

Total area of overbreak obtained per pre-split side  
for discontinuity borehole line angle from zero  
to ninety degrees.

Maximum overbreak was found to occur for acute angles of discontinuity to pre-split line and conversely minimum overbreak was concurred when the discontinuities were orientated perpendicular to the pre-split line. This conforms well with the theory for maximum possible overbreak postulated previously, but clashes to some extent with theory for the geometric constraints of the tests. The results of overbreak are given in Table 6.1, and displayed in Figure 6.15.

The values of overbreak obtained were significantly higher than those geometrically calculated on the basis of theory, (see Figure 6.22) and also no underbreak was obtained contrary to the postulated theory based on dominant fracturing. This excess of overbreak and absence of underbreak is generated by a combination of three factors.

Firstly, as has been already stated, the dominant fractures failed to suppress other neighbouring blast

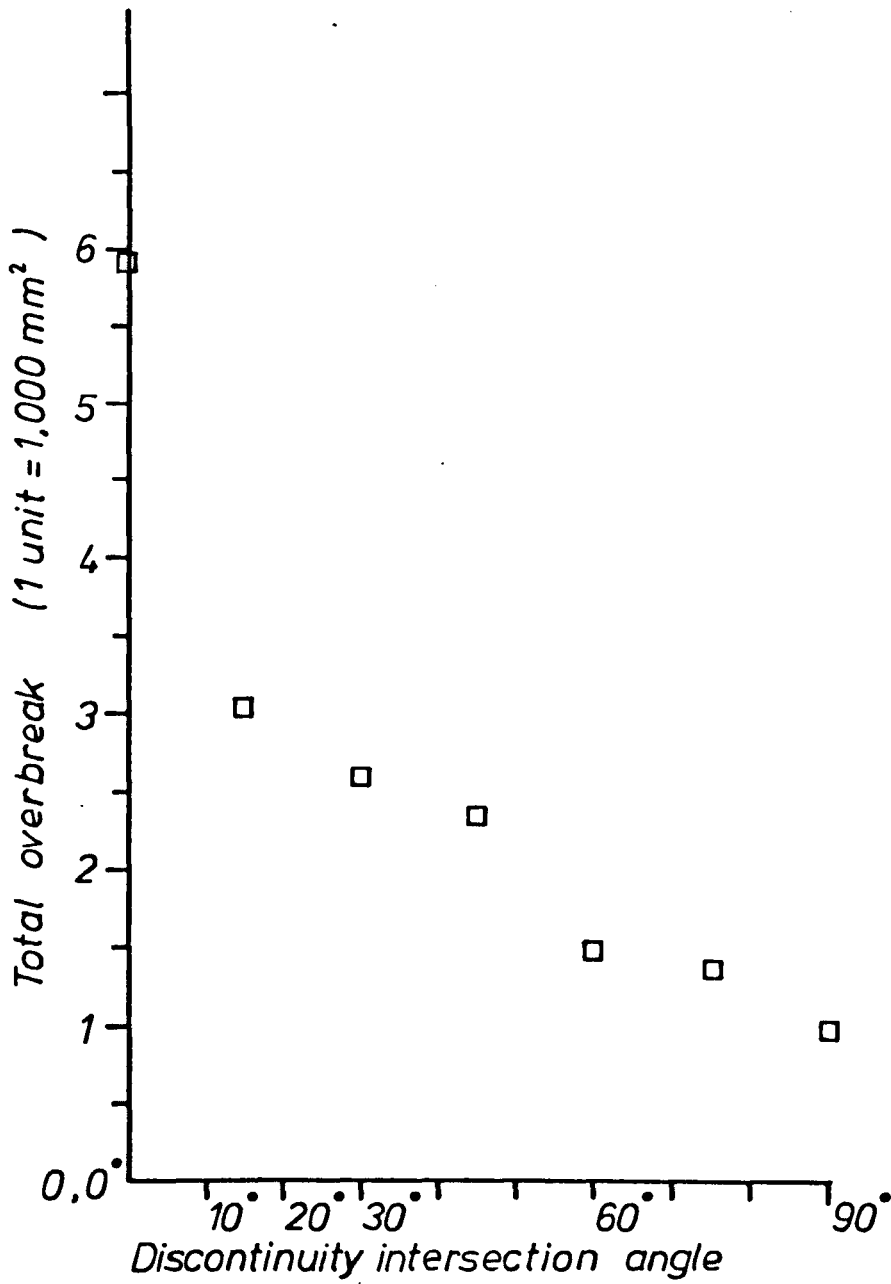


FIG. 6.15.

*Graph of overbreak obtained in resin testing with single discontinuities for various values of intersection angle.*

fractures sufficiently to inhibit their connection with the discontinuity. The result is that a fan shaped zone of straight fracturing from the borehole to the discontinuity is formed, with the dominant fracture positioned approximately central. The effect of the fractures within this fan on either side of the dominant fracture are to increase overbreak on the side furthest away from the pre-split line, and to decrease underbreak on the side nearest.

Secondly, fracturing across discontinuities which were at or under a separation of half the borehole spacing, (tests 48 and 54), also caused an excess of overbreak than was predicted.

Thirdly, as shown most markedly by test 43, (see Figure 6.11), certain fractures are seen to suddenly change direction and deflect towards the intersection of a dominant fracture from an adjacent borehole with the discontinuity. This 'secondary' effect, although not totally unexpected, was of a far greater magnitude than was originally conceived. This feature alone almost totally eliminated the possibility of underbreak and greatly increases overbreak.

The combination of the above three effects results

in a zone of fracturing between each borehole dictating the degree of overbreak, which will equal approximately half the area of this zone, over double that predicted by theory. The width and thus the area of this zone (refer to Figure 6.15) increases with decreasing values of discontinuity intersection angle down to approximately thirty degrees, where the integrity of the pre-split begins to diminish. At an angle of fifteen degrees the pre-split becomes a wide zone of fracturing and no evidence of half barrels will remain. At this stage and below the pre-split may be termed as a failure on the degree of overbreak alone.

N.B. The setting of the spacing of the discontinuities as bisecting adjacent boreholes has most certainly changed the conditions for maximum overbreak, most widely in the tests incorporating discontinuity intersection angles less than forty five degrees. However, it is obvious that the trend of the degree of overbreak produced for decreasing discontinuity intersection angles is qualitatively valid for any fixed separation of discontinuity planes, and thus over a sizeable length of actual pre-split face is valid for even a distribution of discontinuity spacings.

#### 6.4 EXPERIMENTATION IN ROCK

Due to the relatively high misfire rate that had been obtained using four grain cord, and the 'drying up' of its supply source, it was replaced by larger and more consistent eleven grain PETN detonating cord, which was more readily available. This change warranted an increase in the size of individual model tests, and due to the size of test now involved, the use of Polyester resin became economically prohibitive and a new test material was needed.

A decision to continue model testing in rock was made in order, firstly, to verify the results obtained in resin testing and secondly, and more importantly, to use a material which was 'granular' in nature with flaws, and more typical of the material pre-splitting in the field than the isotropic, homogeneous, artificial medium of Polyester resin.

After a wide search for a suitable rock type, Springwell Sandstone, which is a carboniferous sandstone from the Springwell Quarries was chosen for the following reasons;

1. It was a readily available material from a nearby

source.

2. Offcut slabs of suitable thickness were available at a relatively low cost.
3. It is a 'granular' homogeneous rock with extremely consistent strengths and moduli.
4. The rock is of medium strength and other properties, and therefore was not an atypical rock to use.
5. Springwell Sandstone has been regularly used in the department and there was a large amount of data on the engineering characteristics of the rock readily available.

The rock cutting equipment at Newcastle was limited to a slice of eleven inches depth which restricted the thickness of sandstone slab to be acquired. The stone eventually purchased was rough 5.5 to 9.5 inch thick slabs which were cut down at the department to rectangular blocks of an approximate size of 24 x 9 x 6 inches each. The exact individual sizes for each test are given along with the blasting data in

Appendix E.

6.4.1 Method

Initially, a series of tests were carried out to determine a suitable borehole spacing and charge density, (tests 50 - 52). A borehole diameter of 0.375 inches was chosen from a selection of sizes. This choice was mainly governed by the availability of long series masonry drills of sufficient length.

From the results of this initial testing, a borehole separation of four inches and a charge density of twenty four grains per foot were adopted for each of the five vertical boreholes used.

Single joints/discontinuities bisecting each successive pair of holes were incorporated into the main testing, as previously used with testing in resin.

To avoid needless repetition of results and to fill in some of the gaps in the data from testing with discontinuities in resin, the angle discontinuity to pre-split line was decreased in increments of ten

degrees from ninety to ten degrees (with the exception of seventy degrees, which was accidentally missed out).

The discontinuities were again machine sawn with the width of cut of the rock sawn taken into account when marking out the hole positions, which were drilled prior to the discontinuities.

The blocks were restrained for blasting in a specially constructed constraint of two feet square internal dimensions, which consisted of welded six inch 'I' section steel girder and tensioning bolts. The complete set up can be seen in position within the pit in Figure 6.16.

Equal lengths of single strand eleven grain PETN detonating cord, doubled over and taped, were used for simultaneous detonation produced by a single electrical detonator in each test. Due to the increased amount of explosive used and resultant air blast, dampened sacking was laid over each test. This precaution proved quite satisfactory.

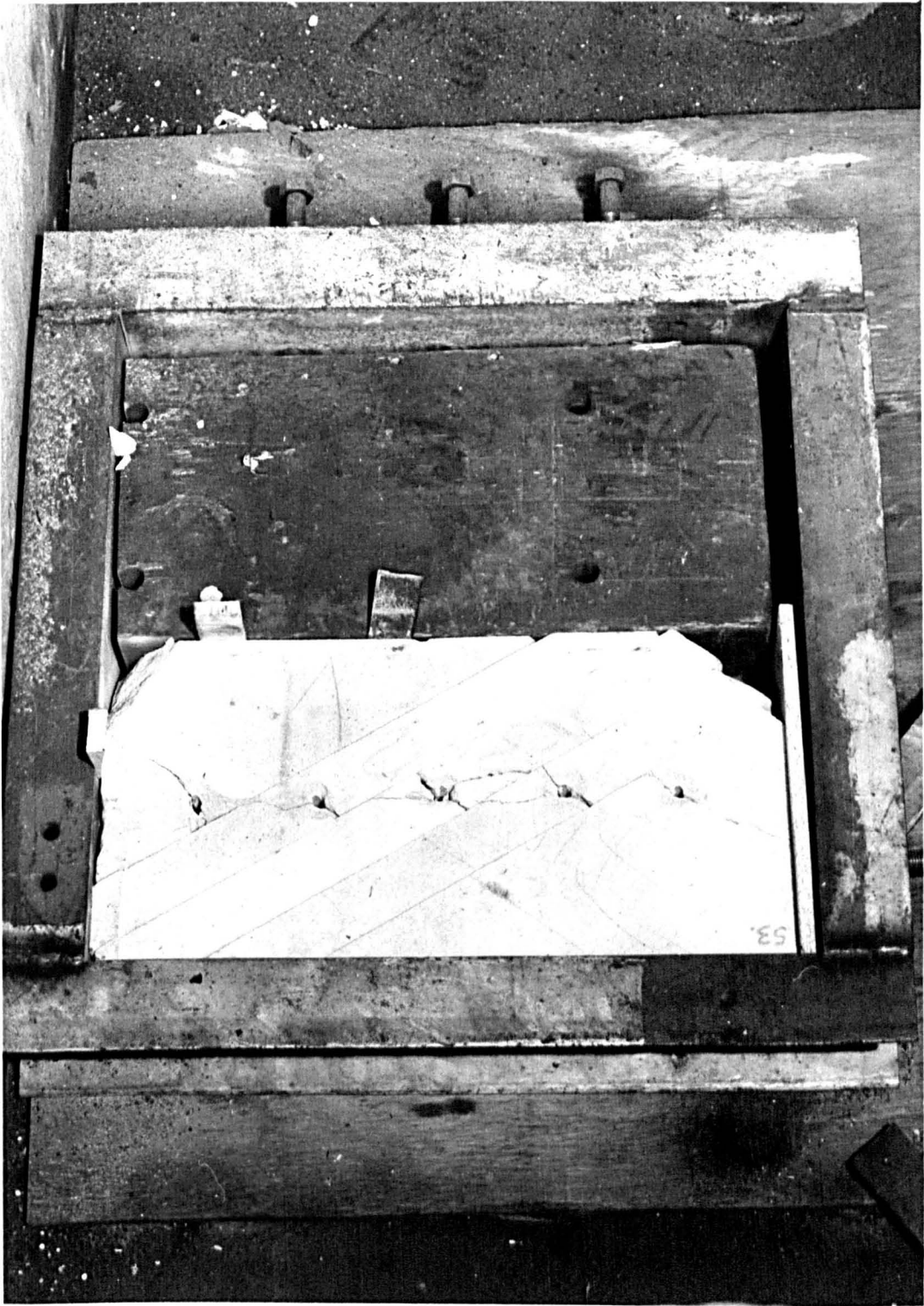


Fig. 6.16.

Heavy steel restraint used for simulation of 'near infinite ground' during model blasting in rock. Illustrating test 53 in position shortly after blasting.

#### 6.4.2 Results

A full photographic record of the results are displayed in Figures 6.17 to 6.21, and the full record of each test can be found in Appendix D and E.

As in resin, all tests provided breakage between all holes. Testing in sandstone gave results similar in nature to those achieved in resin except in some instances, which will be discussed later.

The main most immediately noticeable difference was that the degree of visible fracturing was far less than that encountered in previous resin testing. This effect was most marked in tests with discontinuity intersection angles above fifty degrees, in which a general maximum of only three fractures were observed per borehole attempting to cross between boreholes. The dominant perpendicular (to jointing) fractures and their associated deflected counterparts were the most distinct. It is thus supposed that the more brittle nature of the Polyester resin is more conducive to extensive fracturing and multiple fracture propagation, whereas the sandstone, due to the presence of vast numbers of microfractures and flaws, is more conducive to the singular propagation of

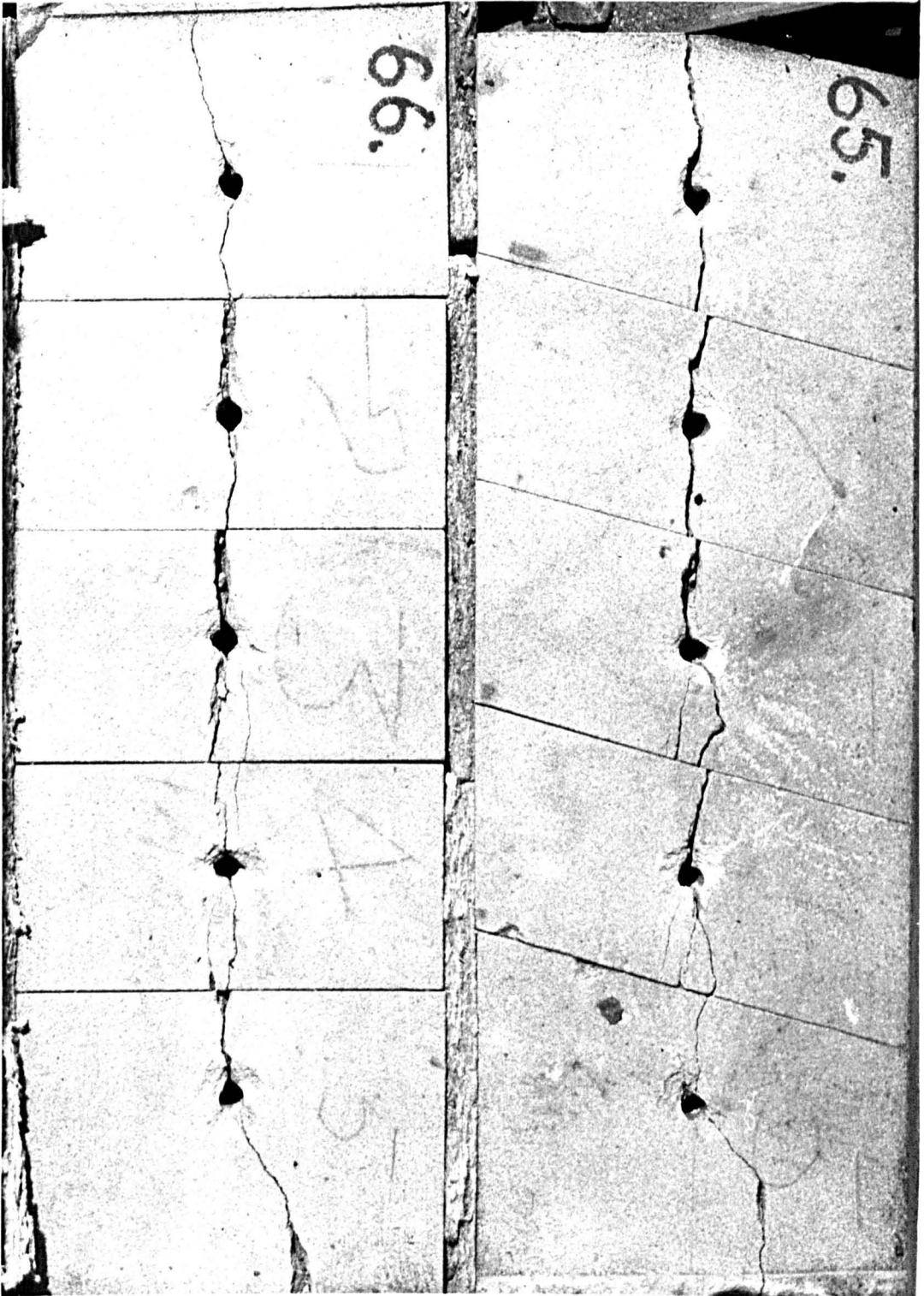


Fig. 6.17.

Pre-split tests in rock with single discontinuities.

Test 65 - discontinuity intersection angle =  $75^{\circ}$ .

Test 66 - discontinuity intersection angle =  $90^{\circ}$ .



Fig.6.18.

Pre-split tests in rock with single discontinuities.

Test 59 - discontinuity intersection angle =  $60^{\circ}$ .

Test 60 - discontinuity intersection angle =  $50^{\circ}$ .

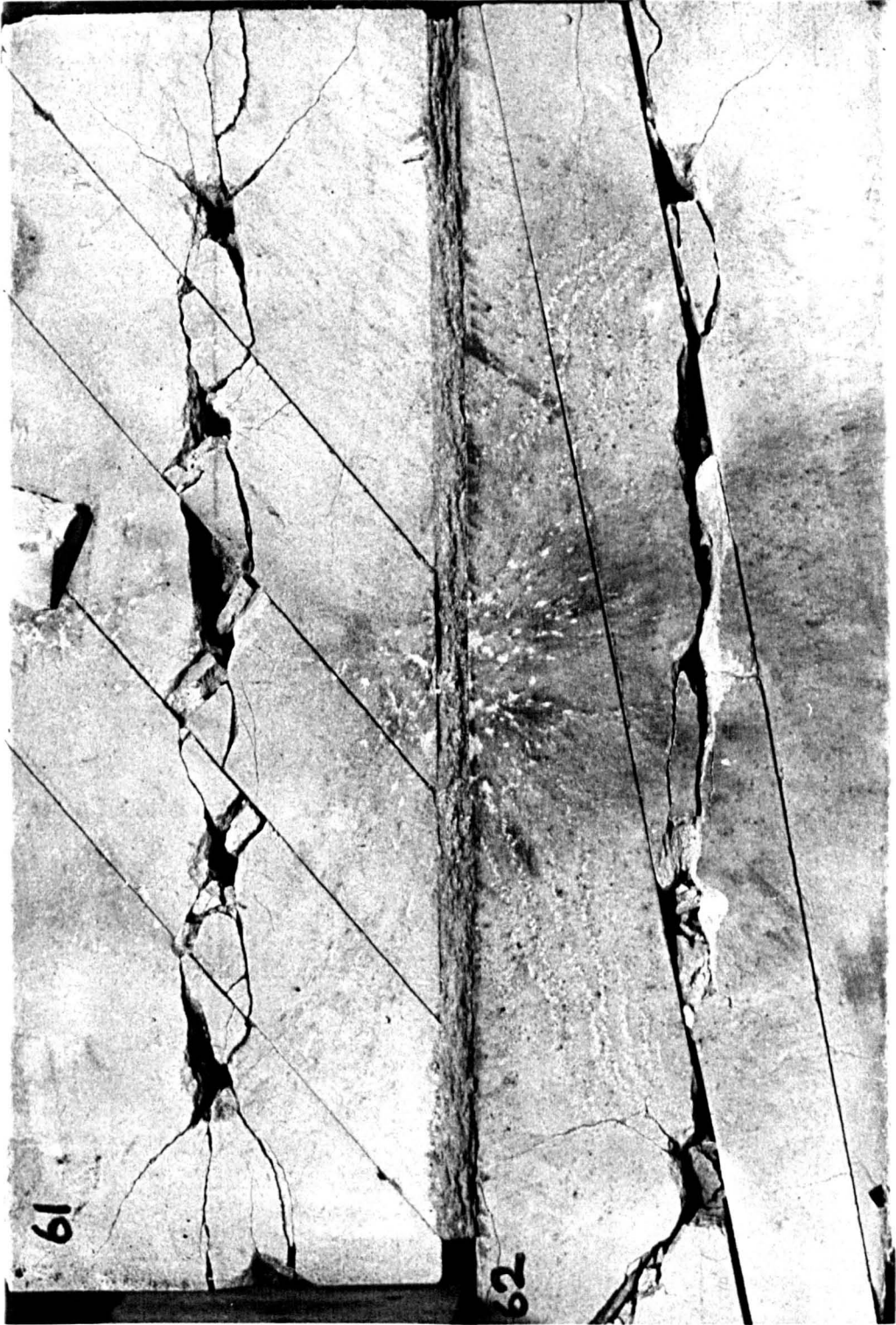


Fig.6.19.

Pre-split tests in rock with single discontinuities.

Test 61 - discontinuity intersection angle =  $40^{\circ}$

Test 62 - discontinuity intersection angle =  $10^{\circ}$



Fig. 6.20.

Test 53 - pre-split test in rock with single discontinuities.  
Discontinuity intersection angle =  $30^{\circ}$

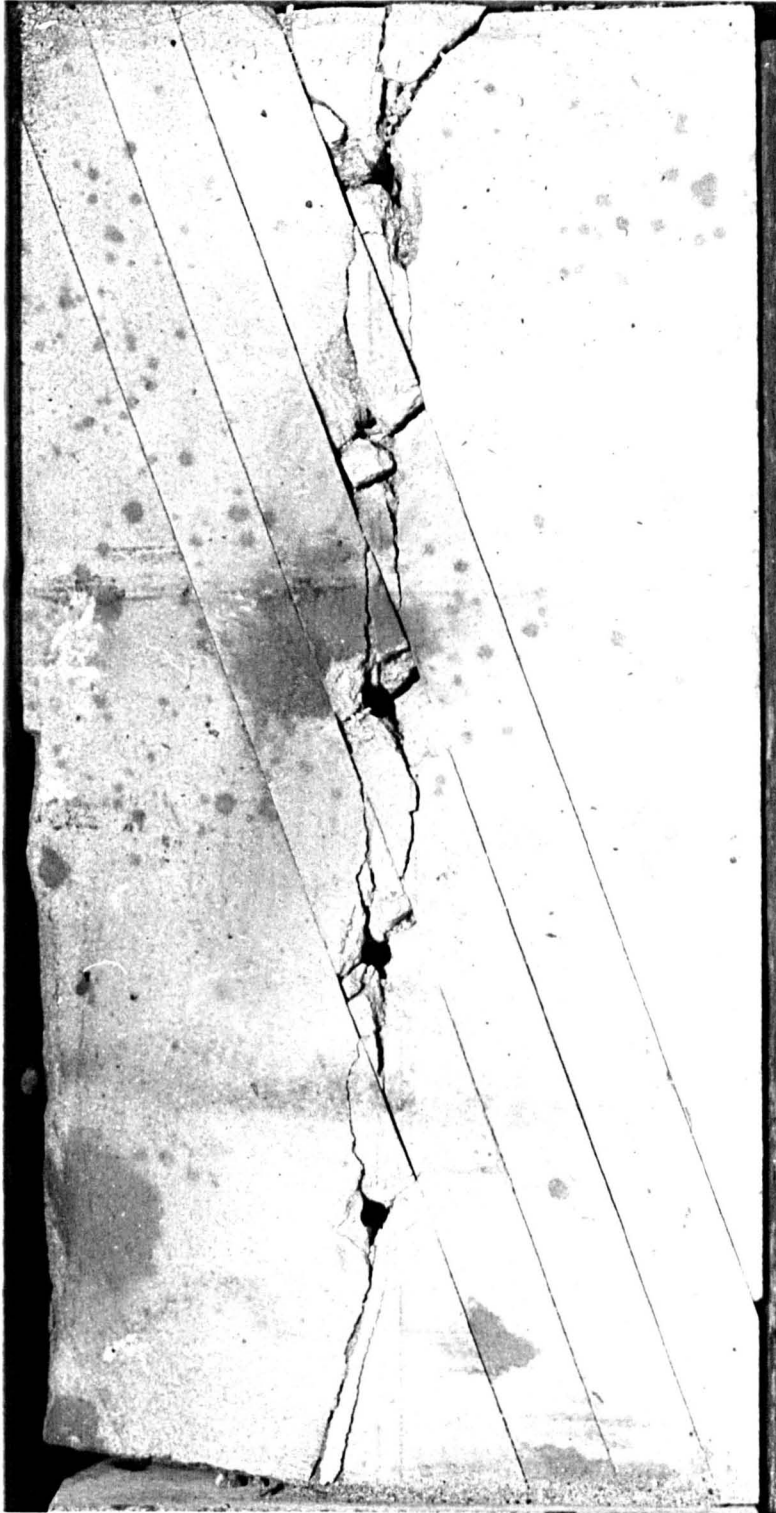


Fig.6.21.

Test 58 - pre-split test in rock with single discontinuities.  
Discontinuity intersection angle =  $20^{\circ}$

dominant fracturing and the associated suppression of other sub-parallel fracturing. In addition, the transparent nature and optical clarity of the Polyester resin blocks allow every fracture 'open' or 'closed' to be seen, even if they are not linked to the surface. Only a fracture wall separation of a few molecule diameters of air are required for sufficient optical refraction.

From comparison of sandstone and resin testing results, these fractures although present in sandstone are not of major importance and therefore in the resin testing results only distract from the dominant open fracturing of zero strength.

On the dismantling of the blocks for storage the top surfaces of the blocks were seen to be wholly representative of the fracturing at different levels throughout the blocks, the blast fractures present being vertical in nature, although in some cases a certain amount of undulation in their surface was observed. The fracture walls however, were of a notably lower strength than the intact rock, pieces frequently scabbing off from their surfaces, revealing closed fractures behind. This would tend to support the findings in resin testing of other fractures being

produced around the borehole, but not being as extensive and not connecting with all "free surfaces" as seen with the dominant open fractures.

Less suppression of other fracturing was seen in tests with discontinuity angles less than fifty degrees, but these were never seen to be as extensive as in resin testing.

Secondary "deflected" fracturing connecting with the intersection of dominant fractures and joints was far more evident, and these fractures were present for discontinuity angles from ten up to and including eighty degrees, (see Figure 6.17).

Direct breakage across single discontinuities was not present in testing in sandstone. This may be attributed to two factors. Firstly the sandstone is less brittle than the Polyester resin, in that fracturing once initiated is likely to travel with a lower (scaled) velocity than in resin. Secondly, the number of discontinuities per test were reduced from one per pair of boreholes down to one every two pairs of boreholes below twenty degrees, due to the problems of accurately sawing and drilling at the tolerances involved, this having the effect of more widely

spacing the discontinuities.

Maximum overbreak again occurred at the minimum discontinuity intersection angle of ten degrees and was at a minimum when the discontinuity and hole line were mutually perpendicular. The results obtained are given in Table 6.2 and are graphically represented in Figure 6.22. (The value of overbreak for ten degrees was doubled since the number of discontinuities was halved in this test - 62.)

Table 6.2

Discontinuity Intersection Angle	Overbreak
90	1,848 mm
80	3,184 mm
60	8,451 mm
50	15,104 mm
40	11,426 mm
30	6,022 mm
20	6,438 mm
10	16,870 mm

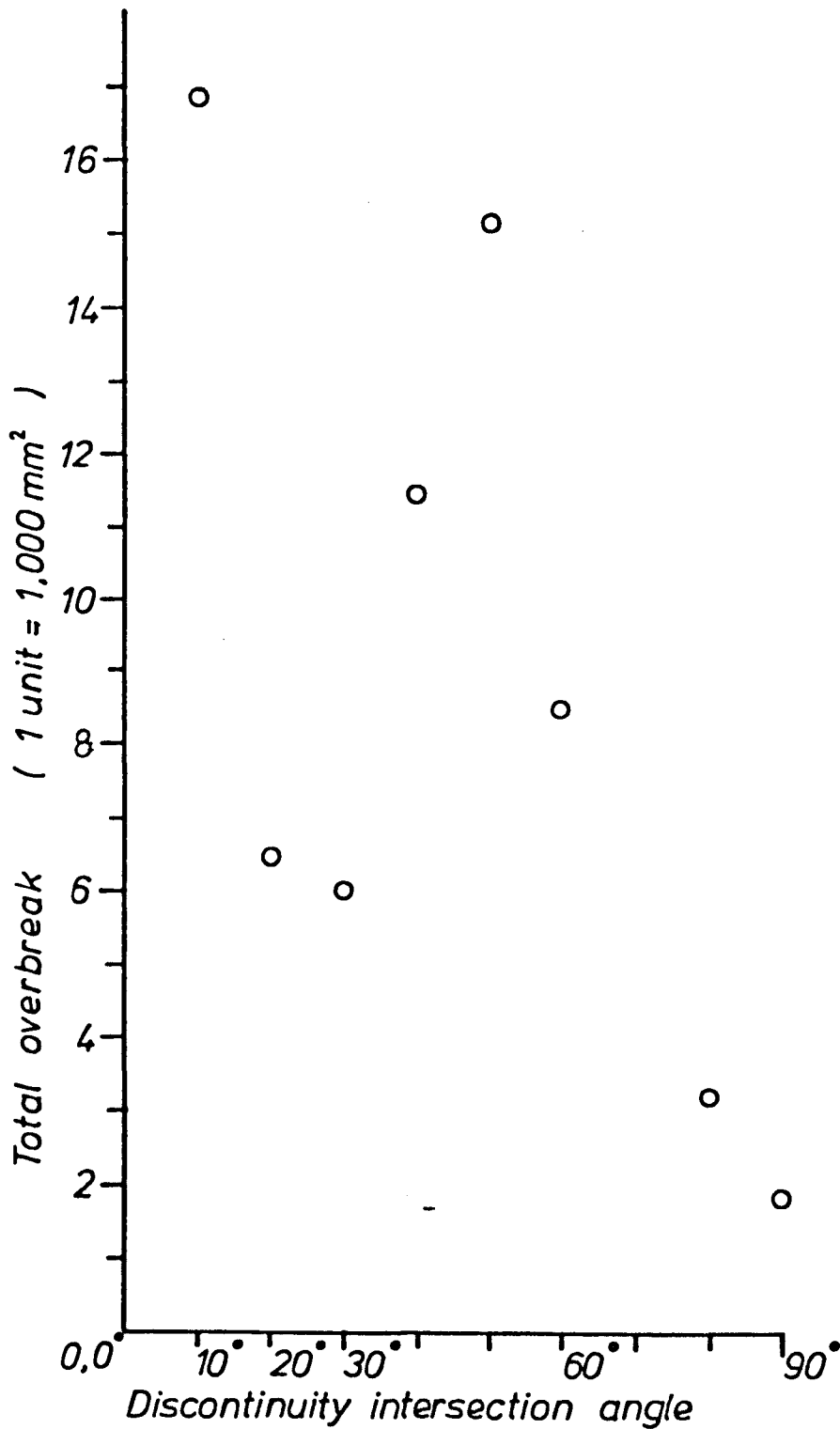


FIG. 6.22.

Values of overbreak obtained in sandstone testing with single discontinuities, for various intersection angles.

Table of the total overbreak per side of pre-split line obtained for changing discontinuity intersection angle whilst testing with single discontinuities per pair of boreholes in Springwell Sandstone.

However, the type of overbreak distribution for resin testing was not incurred. Due to the fact that no fracturing transgressed discontinuities, an overbreak peak for a test value of discontinuity intersection angle of fifty degrees was obtained. For the joint positioning constraint used this is only to be expected, due to the geometric constraint imposed, (see Figure 6.5) and a theoretical peak of overbreak should occur at a discontinuity intersection angle of forty five degrees. A scaled comparison of the amounts of overbreak produced by testing in both resin and sandstone, with the theoretical predicted overbreak curve (incorporating the given constraints) given for different values of discontinuity intersection angle is displayed in Figure 6.23.

The graph clearly illustrates the importance of the secondary (deflected) fracturing in increasing the overbreak from that theoretically predicted. The higher overbreak which is shown by the resin and its exponential distribution, is due to fracturing

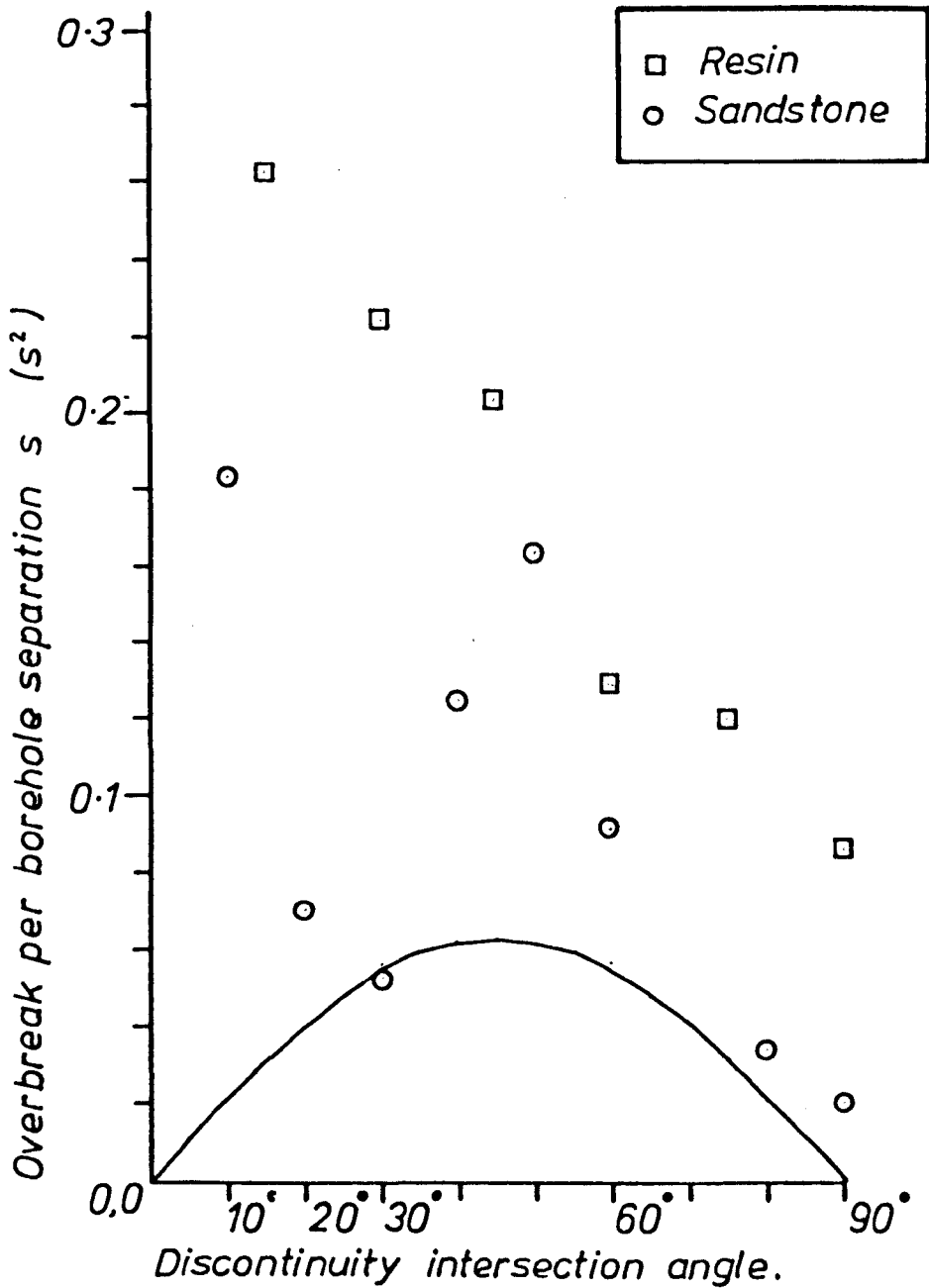


FIG. 6.23.

*Single Discontinuities.*

*Graph of scaled overbreak per hole for resin and sandstone tests including the theoretically predicted overbreak curve based on dominant fracture and discontinuity geometry.*

occurring across successive joints, due to their close proximity for acute angles of discontinuity intersection, coupled with the more extensive fracturing to discontinuities. Because of these effects the results can be likened to values and trends of the maximum possible overbreak graph given earlier, (see Figure 6.7).

#### 6.5 EXPERIMENTATION IN CONCRETE

So far, only the effect of vertical discontinuities on vertical pre-split lines had been experimentally deduced. However, in field situations the presence of jointing which is perfectly vertical, or whose orientation is such that the line of intersection between joint and proposed excavation limit is parallel to the boreholes within the pre-split panel, are isolated. Therefore, it was decided that a limited number of experiments to discover the effect of discontinuity; vertical deviation (dip), and orientation on a pre-split should be undertaken for completeness.

Due to the size of test required and the technical problems involved with the sawing of discontinuities

at widely varying orientations, coupled with the associated size of cutting disc required (far in excess of what was available), it was decided to change from using sandstone to using concrete. The reasons for choosing concrete were as follows:

1. Jointing can be easily placed in the blocks at any orientation required, by casting the blocks in layers.
2. The eradication of having to trim the blocks to size and shape.
3. Comparatively low cost of concrete.
4. Concrete can be considered as a fairly homogeneous artificial sedimentary rock.

#### 6.5.1 Method

Two wooden casting moulds were constructed to produce concrete blocks twenty four inches long, nine inches wide and six inches high, to fit the constraints used for blasting previous sandstone

tests. From consultation of the Concrete Design Manual a concrete mix of four parts building sand to one part cement by weight was used. All blocks were left for at least twenty eight days before blasting, for curing purposes.

An initial series of four trial tests using 3/8 inch vertical boreholes and single eleven grain cord were performed to find the optimum successful borehole separation. The result of these tests showed the pre-splitting effect to start to fade at a borehole spacing of 4.5 inches. A borehole separation of four inches was accordingly chosen for the main testing.

Two values of discontinuity dip, forty five and thirty degrees, and orientations of zero, forty five and ninety degrees, to the pre-split line were picked to give a representative selection of discontinuity orientations, thirty degrees dip being selected to assess the effect of lower angle discontinuities. The combinations of these values gave six separate tests in all.

Successive layers of concrete were cast at a thickness of 2.5 inches, with the exception of initial and finishing casts. Immediately after pouring, each

layer of liquid concrete was vibrated using a vibrating probe in order to settle the concrete and to release any remaining trapped air. The moulds were then left for twenty four hours and thin sheets of paper were laid down to form a joint between the cast and its successor. The different orientation angles of the discontinuities for each test were achieved by orientating the casting box at the appropriate angle before casting commenced.

Six 3/8 inch boreholes per test were drilled vertically at four inch centres, with the blocks restrained in testing position using a portable drill. Each hole was loaded with equal lengths of single strand eleven grain cord, and detonated simultaneously by a single electric detonator. As with the sandstone tests, damp sacking was placed over the specimen before firing to reduce the airblast.

#### 6.5.2 Results

A full photographic record of the results is given in Figures 6.24, 6.25 and 6.26, and the specifications of each test are given in Appendix E.

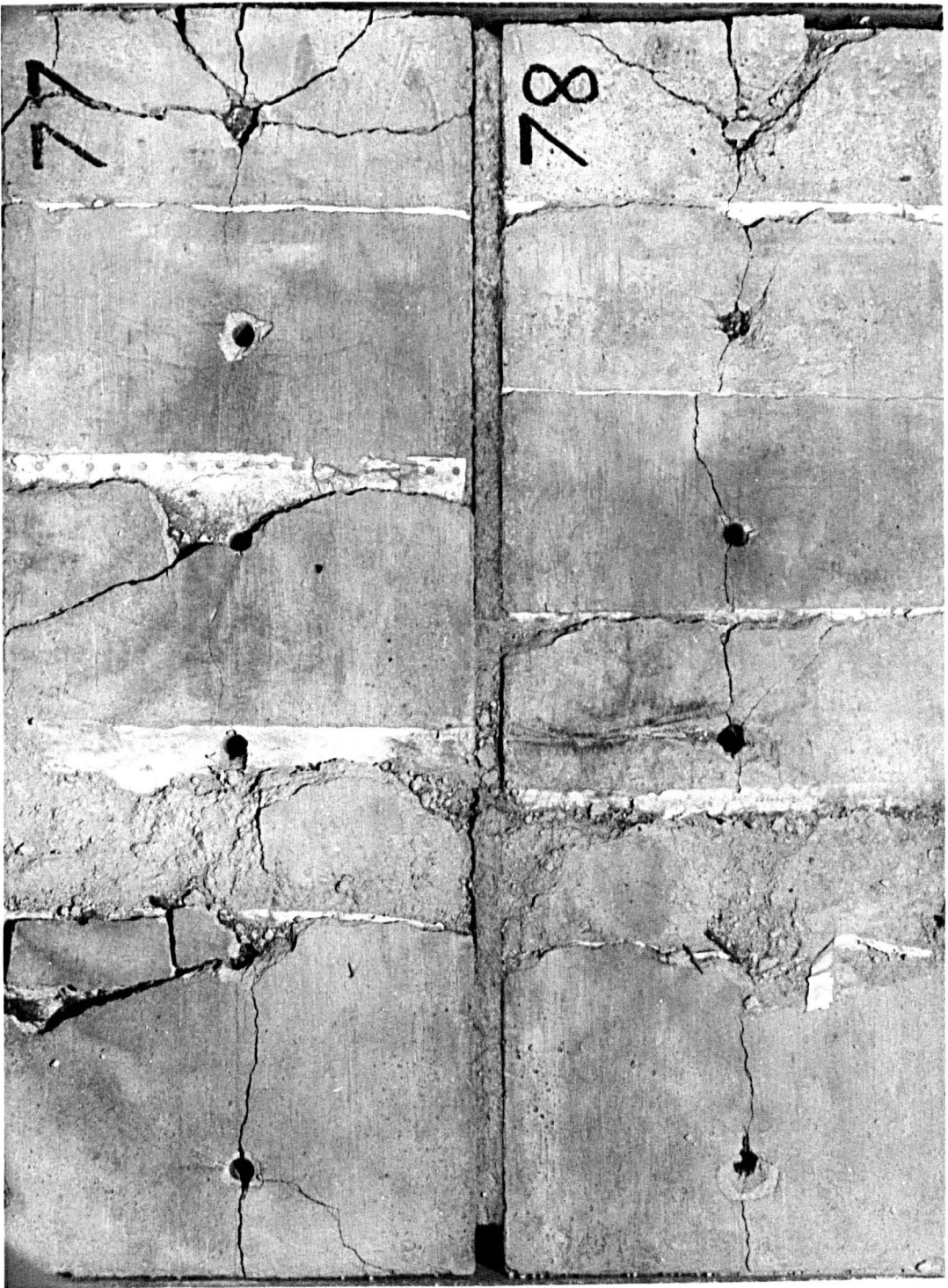


Fig.6.24.

Pre-split tests in concrete with regularity ( $2\frac{1}{2}$ " ) spaced discontinuities.

Test 77 - discontinuity strike intersection angle =  $90^{\circ}$ , dip= $30^{\circ}$

Test 78 - discontinuity strike intersection angle =  $90^{\circ}$ , dip= $45^{\circ}$

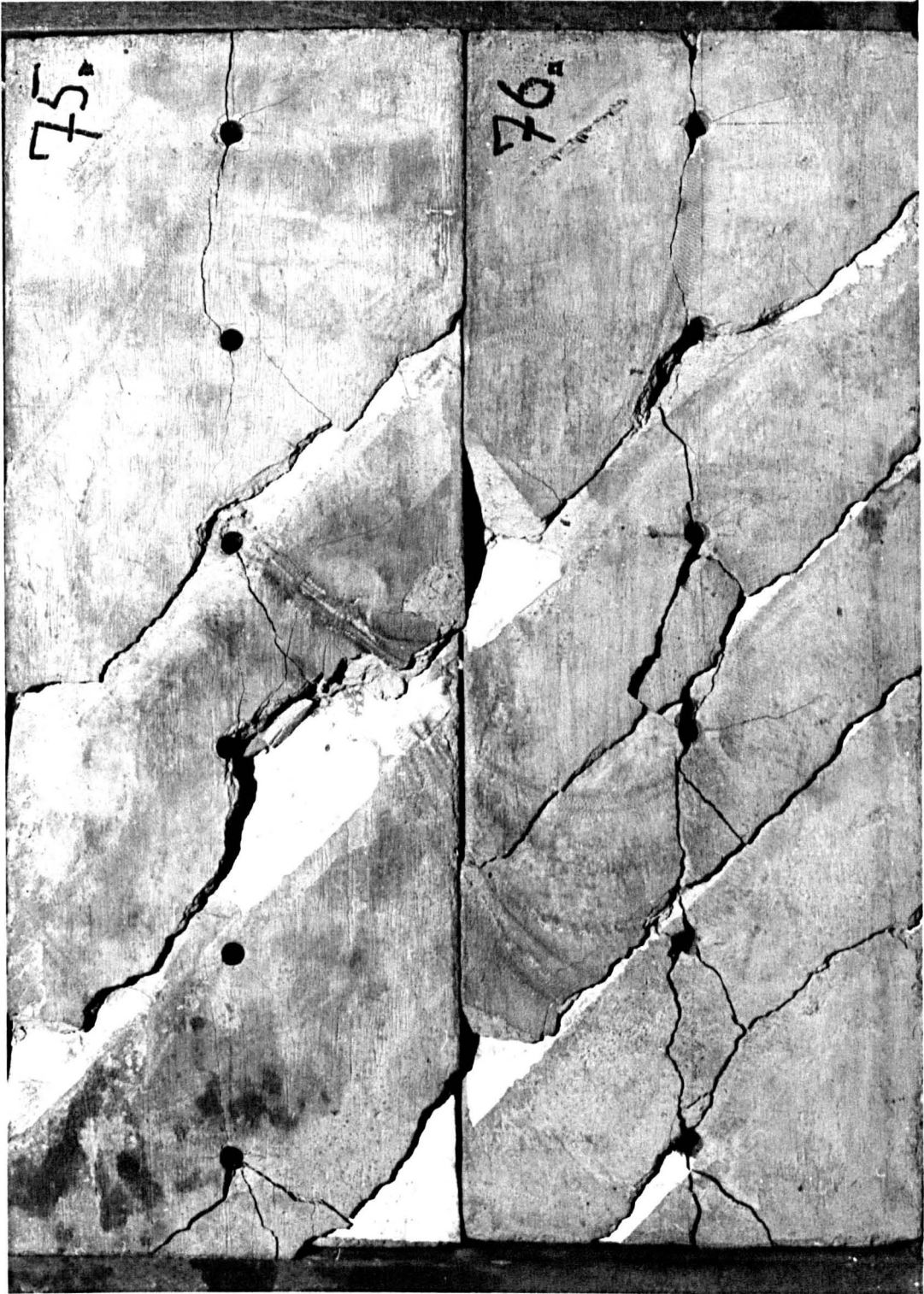


Fig. 6.25.

Pre-split tests in concrete with regularity ( $2\frac{1}{2}$ " ) spaced discontinuities.

Test 75 - discontinuity strike intersection angle =  $45^{\circ}$ , dip= $30^{\circ}$

Test 76 - discontinuity strike intersection angle =  $45^{\circ}$ , dip= $45^{\circ}$

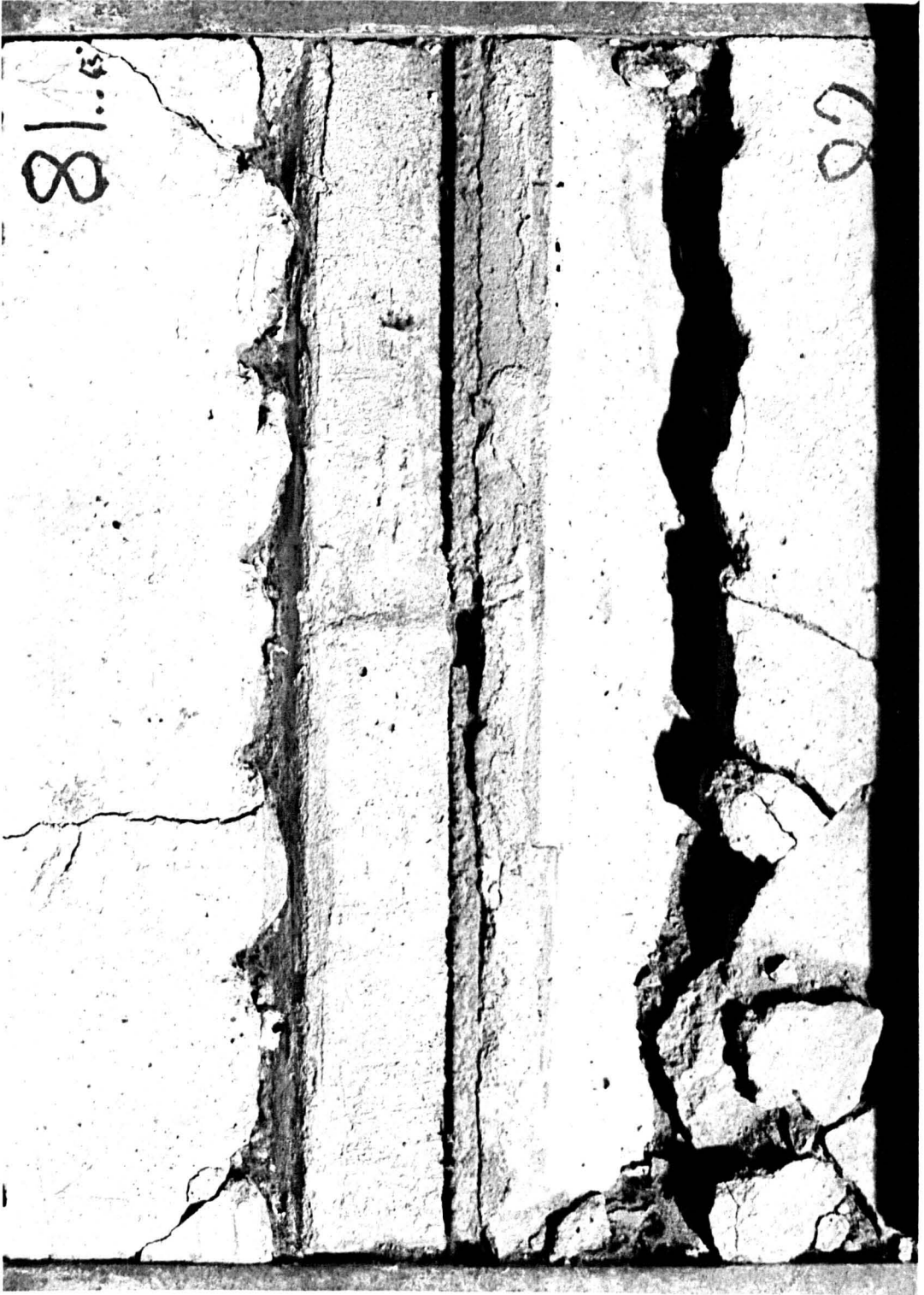


Fig. 6.26.

Pre-split tests in concrete with regularity ( $2\frac{1}{2}$ " ) spaced discontinuities.

Test 81 - discontinuity strike intersection angle =  $0^{\circ}$ , dip= $45^{\circ}$

Test 82 - discontinuity strike intersection angle =  $0^{\circ}$ , dip= $30^{\circ}$

The first, most noticeable result was that there was a failure to split between certain holes in tests 77 and 75, with other examples of weak splitting present. In both cases one or both of the holes were positioned relatively close to the top emergence of a discontinuity, and both were in tests with discontinuities dipping at thirty degrees to the vertical. This signifies that there was some vertical heave in the specimen caused by explosion gases venting into the less well constrained thirty degree discontinuities. This argument is backed up by a small amount of noticeable movement along joints in test 75.

In tests 77 and 78, (Figure 6.24), incorporating thirty and forty five degree discontinuities dipping parallel to the pre-split line, no undue effect was observed, other than a slight undulation on the pre-split line causing fracturing from neighbouring boreholes not to line up exactly across discontinuities. Also small amounts of overbreak were seen at the surface of the block where the upper joint walls were fractured near holes. These fractures however, terminated at the joint and were absent in the layers beneath.

Unfortunately, one layer in both tests 77 and 78 failed to set properly, due to prior hydration of some of the cement used and resulted in very low strength. This can be seen clearly in Figure 6.24.

In tests 75 and 76, (Figure 6.25), incorporating thirty and forty five degree discontinuities striking at forty five degrees to the pre-split lines, two predominant effects were seen. Firstly, an irregular direct split was formed between holes. This feature extended throughout the depth of the testing blocks of concrete and was by far the most dominant feature of the test. Secondly, fracturing from individual boreholes ran directly towards the discontinuities, and was perpendicular or sub-perpendicular to the latter by up to fifteen degrees in the direction of the pre-split axis. This is best illustrated by test 76.

Tests 81 and 82, (Figure 6.26), show a strong but slightly irregular/uneven pre-split with no sign of direct fracturing to discontinuities, although from the size of the fly rock produced in each test there are indications that this has occurred within the removed material only. However, no evidence of this was found in the corresponding bottom layer, therefore

overbreak is only present at the surface on the updip side of the pre-split line in both cases. In the field this effect would only cause slight overbreak at the top of the face for outward dipping discontinuities, and no overbreak would occur for inward dipping discontinuities. On the dismantling of the blocks the individual layers were found to be highly unstable, especially in the forty five degree dip test, as was only to be expected.

## 6.6 CONCLUSIONS

Fracturing around a pre-split borehole extends outwards in an elliptical shaped zone. In the presence of a vertical discontinuity the first fracture within that zone to reach the discontinuity will become the dominant fracture. Due to the geometry involved this fracture is perpendicular to the discontinuity or sub-perpendicular by a few degrees towards the pre-split axis.

The high degree of fracturing in resin testing signifies a zone of weakened material which is not immediately visible in rock testing, although the fracturing is present but not open.

The quantity of overbreak, although primarily produced by dominant (perpendicular) fracturing to jointing, is higher than theoretically predicted. This excess is caused by secondary fracturing linking up with dominant fracturing from adjacent boreholes. This secondary fracturing also eliminates the bulk of any underbreak.

For single jointing the maximum overbreak possible is highest for low discontinuity intersection angles and is at a minimum for jointing orientated perpendicular to the line of pre-split.

Overbreak becomes noticeable, with individual half barrels being lost from the final face, for discontinuity intersection angles below thirty degrees. A complete failure to pre-split will occur for values at or below fifteen degrees where two or more half barrels per continuous discontinuity will be lost. This effect is rapidly accentuated below an intersection angle of ten degrees.

The presence of discontinuities below ninety degrees to the intended face will cause a slight reduction in the maximum possible successful pre-split borehole separation.

Discontinuities that are less than forty five degrees to the vertical will cause less overbreak than their vertical counterparts, overbreak occurring primarily at or near the surface.

Discontinuities at less than thirty degrees to the horizontal may allow explosion gases to vent into their lengths, thus causing slight ground heave in the upper strata. Flyrock from the surface may also be produced if no top stemming is used.

Low angle discontinuities have no effect on the path of the pre-split fracture. However, if they are intrinsically unstable in the final face orientation, stability problems may affect the outcome of the pre-split.

The type of fracturing to look for in site investigation for pre-splitting is large scale planar discontinuities of similar angle of dip to the proposed pre-split and which possess intersection angles at around or under fifteen degrees. If fractures of these specifications are present in sufficient numbers, the pre-split will fail and a high degree of overbreak will be incurred. Also a stability analysis for the final face should be undertaken at this stage.

## 7 EFFECT OF SINGLE DISCONTINUITIES - FIELD OBSERVATIONS

### 7.1 BOREHOLE FRACTURING TO JOINING

#### 7.1.1 Field Data Recorded

The major measurements taken were the inclination and azimuth of:

- (a) The pre-split face
- (b) Blast fracture to joint (the break)
- (c) The discontinuity See Figure 7.1

The length of break to the discontinuity and the discontinuity outcrop extent out of the face were also measured.

A total of 453 sets of measurements were taken, 2,265 in all (including minor measurements), random samples being taken from all pre-split locations one to eleven inclusive.

These parameters were chosen in order to verify the

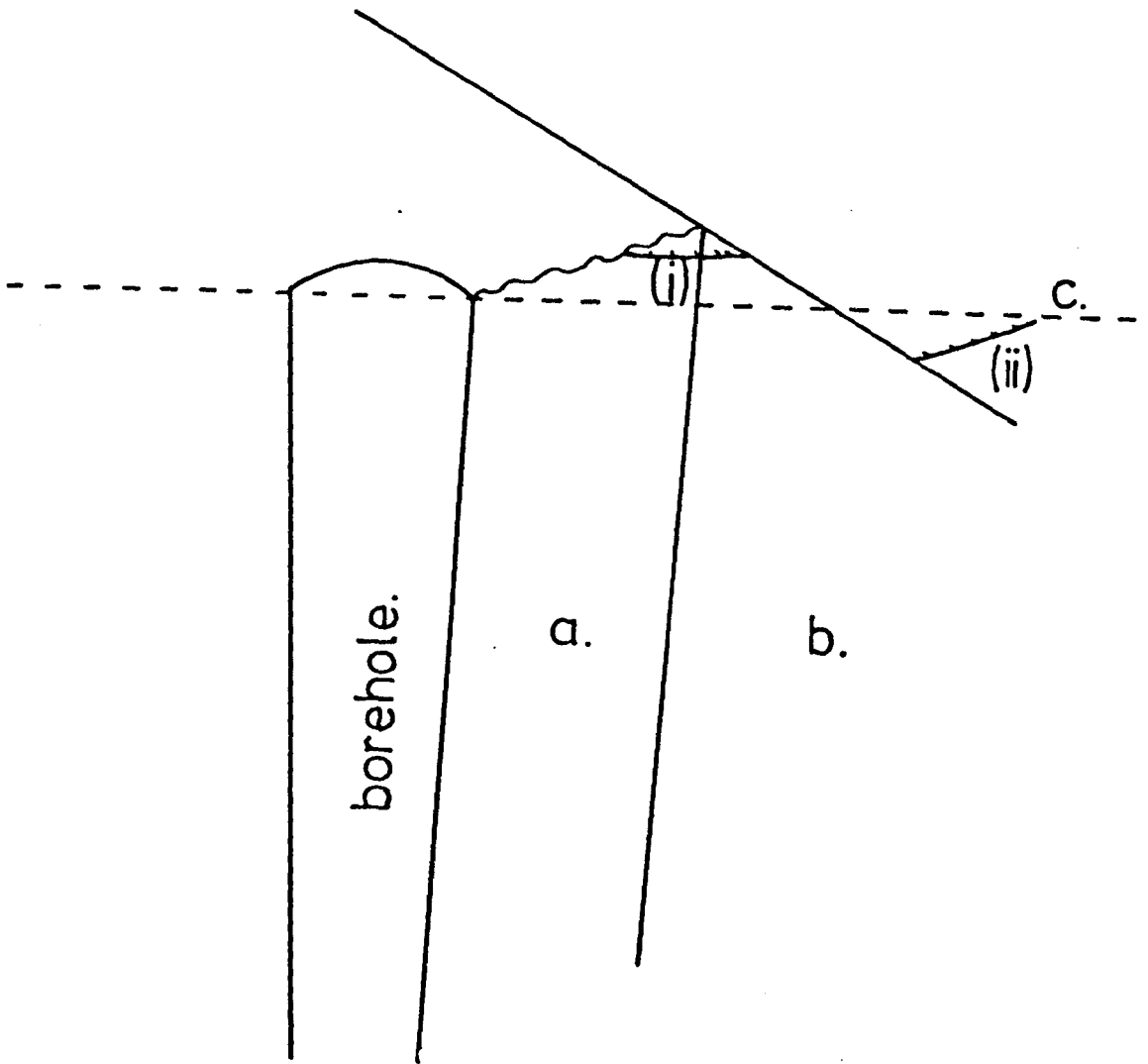


Fig. 7.1.

Diagram of orientation measurements take in the field of :

(a) break to joint.

(b) discontinuity (joint).

(c) line of pre-split.

results of model testing and to examine in detail the processes involved when pre-splitting in the presence of discontinuities in the field. The processed data required for each set of measurements as illustrated in Figure 7.1 were:

- (i) Angle of breakage to jointing
- (ii) Angle of intersection of the  
discontinuity with the final face

where both (i) and (ii) are the acute angles measured.

These results were obtained by using a computer program devised by the author working on the principle of vector analysis.

### 7.1.2 Results

The raw data results/output from the computer program; break to joint angle and joint-face intersection angle are plotted in Figure 7.2. To give a better visual assessment of the data the points are roughly contoured as percentage occurrence from the base of the graph from ten to fifty percent as displayed in Figure 7.3 (the question marks reflect insufficient data for contour calculation).

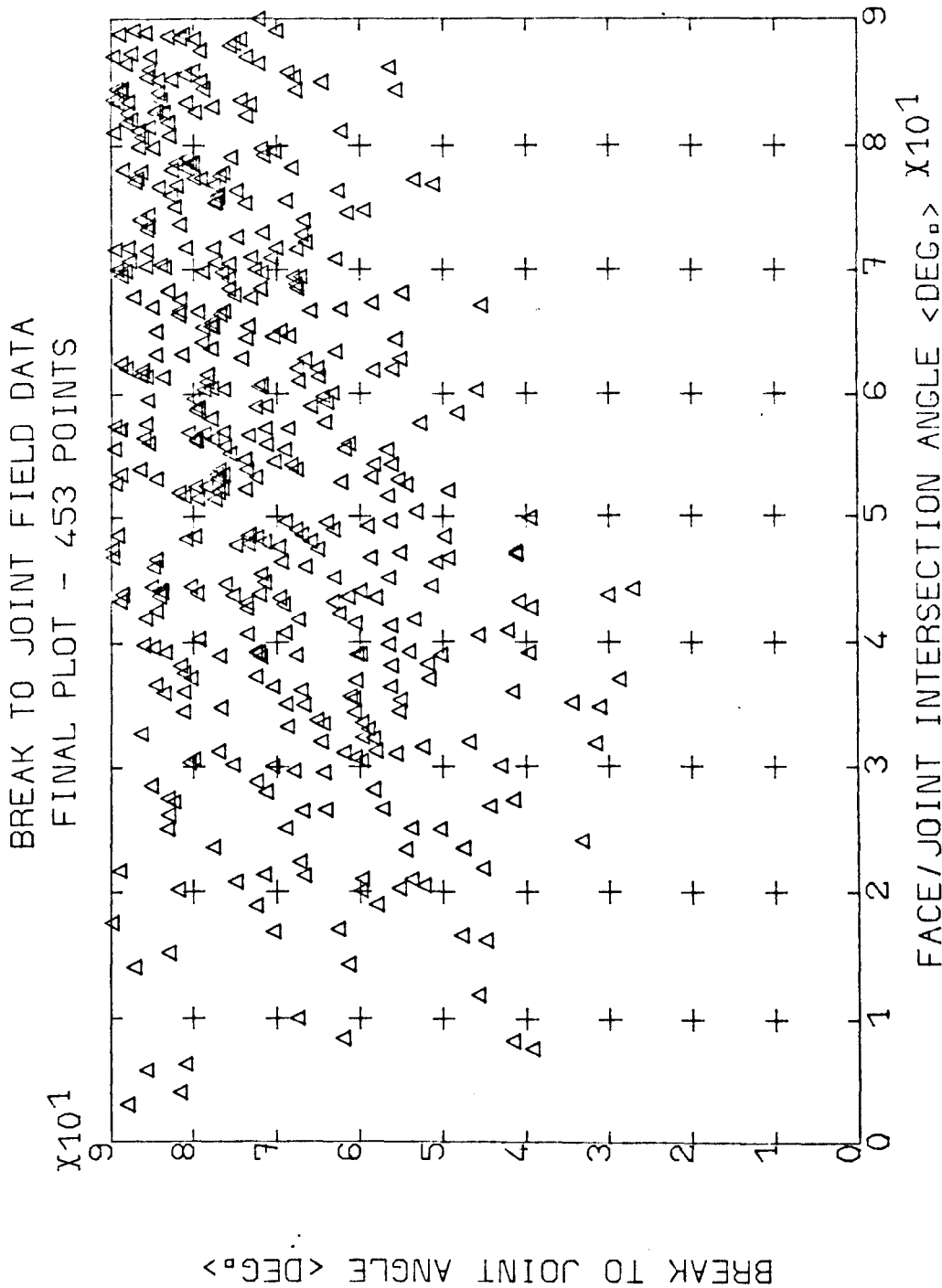


Fig.7.2.  
Plot of break to joint field measurements.

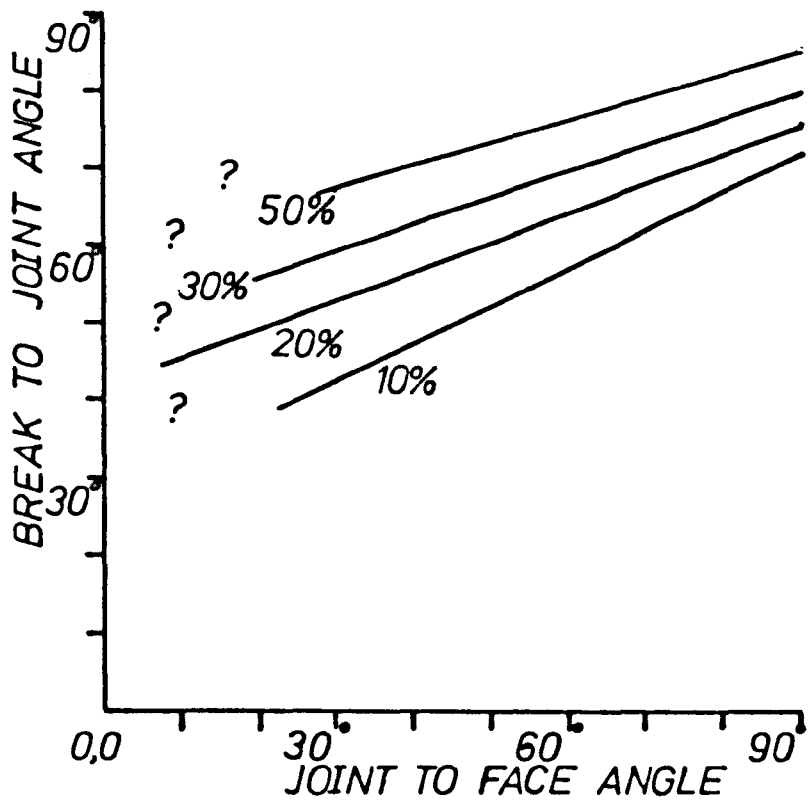


Fig.7.3.

*Contoured break to joint data plot  
(fig.7.2.)*

*Percentage occurrence measured from  
joint to face angle axis.*

*? - denotes absence of data points  
due to pre-split failure for low joint  
to face angles.*

### 7.1.3 Summary\_of\_Results

From Figures 7.2 and 7.3 there are three distinct observations and deductions which may be made:

Firstly the majority of data points lie at or near the ninety degree break to Joint angle. This infers that the predominant fracturing from pre-split boreholes to neighbouring discontinuities is approximately perpendicular to the discontinuity. Also these fractures (breaks) become increasingly sub-perpendicular, tending to the direction of the line of pre-split with decreasing joint-face intersection angle.

Secondly there is a greater spread of points for the lower values of joint-face intersection angle. This may be attributed to secondary fracturing as observed and described in the previous chapter (Chapter Six) which is non-existent for joint-face intersection angles of around ninety degrees but is more prevalent between thirty and sixty degrees from the results of model testing.

Thirdly and finally the relative thinning out of results i.e. their lower occurrence for low joint-face

intersection angles, especially below a value of fifteen degrees reflects an absence of half barrels in the final face at these values and thus the progressive failure of the pre-split down to a value of fifteen degrees where total failure of the pre-split occurs.

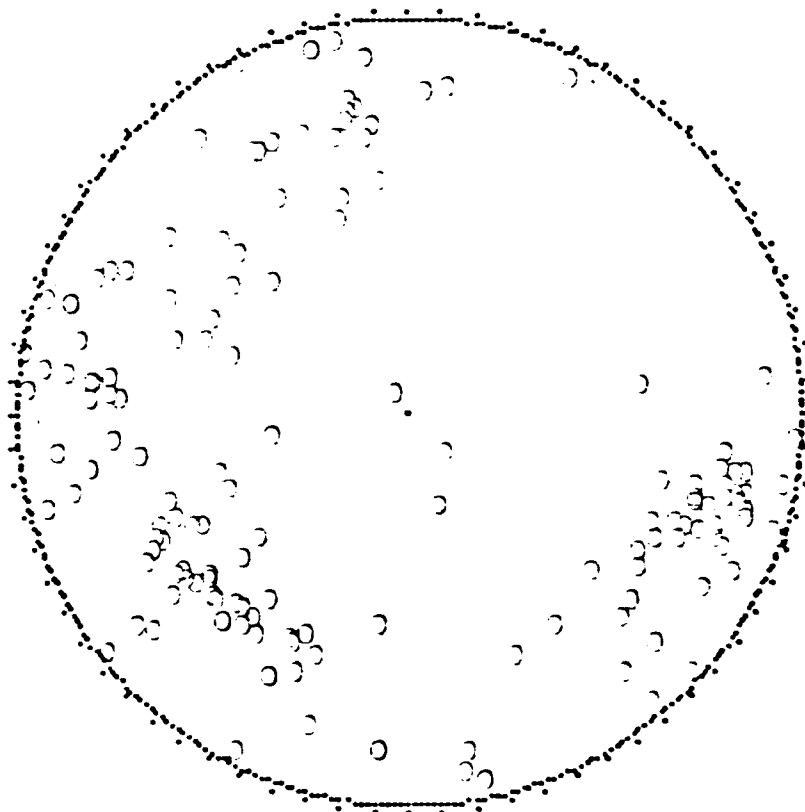
## 7.2 EFFECT OF JOINT INTERSECTION OF BOREHOLES

The intersection of pre-split boreholes along their trace lengths by individual jointing whether closed, tight or cemented was conclusively demonstrated to have no major observable detrimental effect on the pre-splitting process in the field. This is most apparent and best displayed at pre-split location number nine, where closely spaced 'foliation jointing' is orientated at approximately ninety degrees to the line of pre-split (as displayed in Figure 7.4, a computer stereographic plot (Matheson, 1981) of joint densities) and was observed often cutting pre-split boreholes along their length but with no observable effect. At this location excellent pre-split results were obtained with a pre-split index<sup>11</sup>

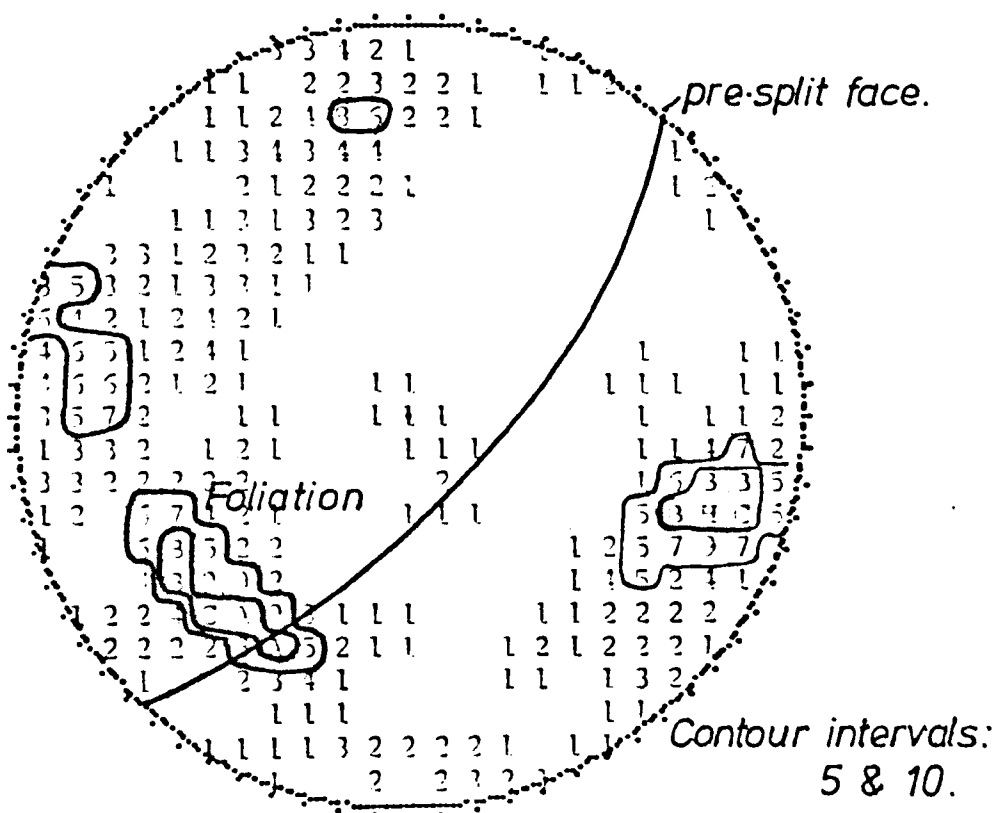
-----  
<sup>11</sup> The pre-split index (after Matheson, 1980) is the percentage length of borehole half barrels visible in the final face and thus can be used as an assessment of the

Fig.7.4.

Stereographic plot of discontinuity field measurements -Location 9 - illustrating foliation perpendicular to pre-split.



DENSITY PLOT - SEARCH ELLIPSE = 1.00 3



of over 95%.

### 7.3 EEECT DE THE CONTINUITY DE DISCONTINUITIES

It was immediately noticed that small scale discontinuities i.e. those less than 20 cm in extent have little effect on the outcome of the final face, although their presence may cause a slight weakening of the face. However, the effect of medium (above 20 cm) and large (above 5 m) scale discontinuities on pre-split success may vary according to the intersection angle from minor to major importance.

A comparison of their relative effects may be made from Figure 7.5 and 7.6 where the effects of medium and large scale discontinuities are shown respectively. Both photographs were taken of separate portions of the same face at pre-split location number two. Here the discontinuity set in question strikes to within fifteen degrees of the face line.

The medium scale discontinuities shown in Figure 7.5 in conjunction with the other discontinuities present have caused a total failure of the pre-split

-----  
11.(cont'd)relative success of a pre-split.

Fig. 7.5.

Photograph illustrating the effect on the integrity of the final face of interconnected medium scale discontinuities at location 2 which intersect the pre-split line at less than  $15^{\circ}$ .

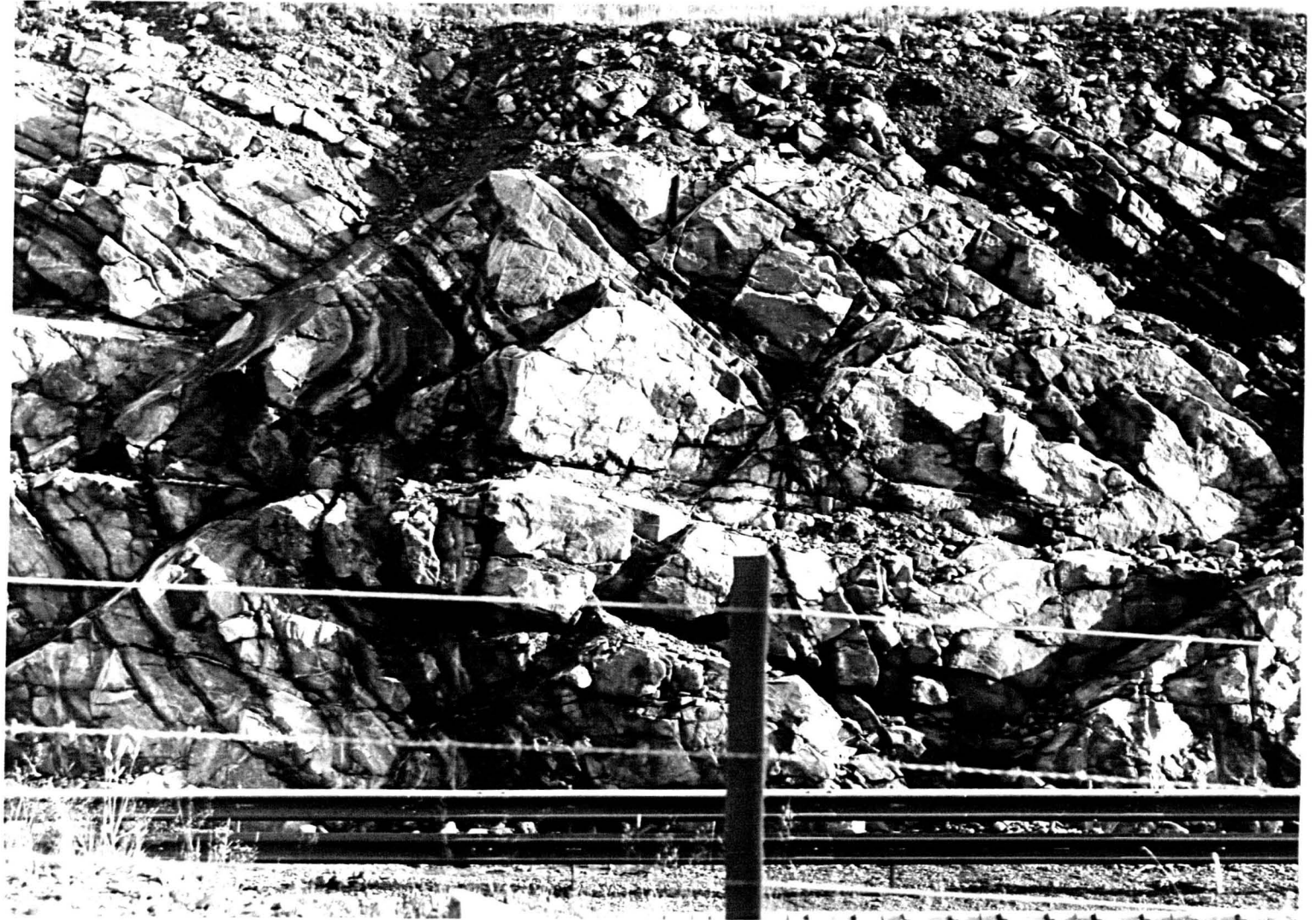


Fig.7.6.

Large scale planar discontinuity (location 2) striking within  $15^{\circ}$  of the face line resulting in failure to pre-split with the final face breaking back to the discontinuity for over 5m of its length.



face with virtually no half barrels left visible in the resultant face. The final face is blocky in nature, reflecting the extent of continuity of the discontinuities and sits at a slightly lower angle of repose than designed.

In contrast the presence of the large scale continuous discontinuity shown in Figure 7.6 (of the same set) has caused the individual pre-split holes to break back to it, resulting in the final face following this feature cleanly for some 5 m with a complimentary splitting index of zero. Here the resultant face has more integrity than in Figure 7.5 and is more stable. This effect is further discussed in Chapter Seven.

At the other end of the discontinuity intersection angle scale both large and medium scale joints which intersect the final face at an angle of ninety degrees have no effect on the final pre-split face, as can be seen from Figures 7.7. Here at pre-split location number nine a splitting index of over 95% was recorded with minimal overbreak and underbreak, which generally only occurred in the toe of the face.

Fig. 7.7.

Successful pre-split  
with minimal over-  
break at location 9.  
Dominant jointing/  
foliation is orientated  
perpendicular to the  
final face.



#### 7.4 LARGE SCALE DISCONTINUITIES ACTING AS PRE-SPLITS

If large scale fractures are present in the immediate proximity of a design face then when either bulk or pre-split blasting is sufficiently close, breakage will occur back to these surfaces, resulting in them becoming the final face on completion of excavation.

Many examples of this feature were observed by the author in the field, these large scale discontinuities acting as 'pre-splits' in their own right, as for example shown in Figure 7.6. In order to ascertain their actual effect on the fracture disturbance process Swindells (Swindells,1981) carried out a seismic refraction blast damage survey on a particular dominant feature at pre-split location number nine which is shown on the left hand side of Figure 7.8. At the time of photography a previously fired pre-split trial panel in the background was in the process of being excavated after a bulk blast which had also broken back to the massive discontinuity in question (on the left of the picture). The results of his seismic survey showed that the degree of measureable damage due to the bulk blast behind this plane was comparable to that of the

Fig.7.8.

Large scale discontinuity (left) at location 9 having reacted in a similar manner to a pre-split trial panel (centre-right) during bulk blasting operations.



pre-split plane, i.e. less than 20 cm. Therefore this discontinuity plane, although closed had effectively acted in the same manner as the pre-split plane.

It is therefore obvious that if such features exist at a favourable orientation within rock to be excavated, then these large scale features should be mapped and utilised whenever possible as ready made pre-split planes during blasting operations.

## 7.5 CONCLUSIONS

Field observation primarily confirms the results obtained in laboratory model testing and the hypotheses made based on those results. In addition a better understanding of the processes involved has been acquired. From the observations made within this chapter and in consort with the previous chapter it may be concluded that the most important geotechnical factors affecting the success of the application of pre-split blasting to rock slopes are discontinuities and their geometries.

## 8 THE EFFECT OF MULTIPLE DISCONTINUITIES AND THEIR FREQUENCY

### 8.1 THEORY

The results of the previous experimental chapter have shown that although fractures from a pre-split borehole cannot cross single discontinuities, they may in the presence of two sufficiently closely spaced discontinuities, cross at least the first. From these results it would seem that the predominant factor determining fracture extension across multiple discontinuities is their separation.

From the results of resin testing, the fractures observed to cross discontinuities were orientated perpendicular to a discontinuity and originated at its edge. These fractures were seen to be in line with dominant fractures and can thus be presumed to be their extension.

The mechanism for failure across the joint has been described earlier, (see Section 6.1), the opening of the dominant fracture causing shearing of the

discontinuity, thus forming a tensile stress bulb in the face opposite to the dominant fracture, (see Figure 6.3). For a tensile strength of the inter-discontinuity slab lower than the tensile stresses produced, failure will occur normal to the direction of maximum tensile stress. Thus fracturing will be formed perpendicular to the joint surface and will propagate in a direction normally away from the joint. This feature becomes the extension of the dominant fracture and so long as the previously stated conditions hold, this fracturing will continue to propagate through other discontinuities of the same set. As the only fracturing to cross discontinuities is dominant fracturing then the shape of any overbreak will be dependent on the combined geometry of these fractures and the positioning plus intersection angle of the discontinuities. The amount of overbreak obtained will depend also on how far the dominant fractures can be propagated.

The maximum length of dominant fracture propagation will be dependent on two factors; firstly, it will depend on the maximum radius of the fracture zone for a single borehole in non-jointed similar material, and secondly, it will be affected by the fracture frequency and the actual fracture positioning. The

thinner each individual layer of rock is between successive discontinuities, the lower their tensile strength and thus the further the fracture will be able to propagate.

## 8.2 METHOD

The testing using multiple discontinuities per pair of boreholes, was a continuation of testing with single discontinuities in Sandstone. Therefore the same borehole specifications were used, which were:

Borehole diameter = 0.375 inch

Borehole inclination = vertical

Borehole spacing = 4 inches

Charge density = 2 x 11 grain cord

Identical sized blocks of sandstone were used, along with the same marking out and cutting techniques. A standard discontinuity intersection angle of sixty degrees was used throughout testing (with the exception of test 70). All jointing was vertical.

The testing undertaken followed two overlapping paths; firstly, with testing designed to determine the effect of discontinuity frequency/spacing, and secondly, testing designed to determine the effect of

multiple discontinuity positioning. In the first line of testing, individual tests were undertaken with two, three and four joints per pair of boreholes (tests 63, 68 and 69) at joint spacings of 2.00, 1.33 and 1.00 inches respectively.

The second line of testing composed of three tests incorporating twin discontinuities per pair of boreholes. These were separated as follows; equidistantly (test 63), equidistantly between boreholes (test 64), and 1.33 inches from each borehole.

A further test was designed to explore the effect of multiple discontinuities at varying angles, including discontinuities bisecting individual boreholes. In this test the boreholes were drilled with the block restrained after sawing the discontinuities.

All tests were loaded and fired in an identical manner to previous testing in sandstone, (see Section 6.4.1). The exact specifications for each test, along with their blasting records are given in Appendix E.

### 8.3 RESULTS

A photographic record of the results obtained is given in Figures 8.1, 8.2 and 8.3.

Taking the results obtained from the fracture positioning experiments, dominant fracturing was seen to cross the discontinuities nearest the borehole concerned but was observed to terminate at the discontinuity located immediately before the next borehole. This occurred in every test, and was even the case in test 67, where the discontinuity slabs containing the holes were half the width of the fractured slabs.

A possible explanation that the fracturing should cease there, is that the slabs containing each borehole are under axial compression caused by the gas pressure within the borehole and open dominant fracturing, which is perpendicular to the jointing.

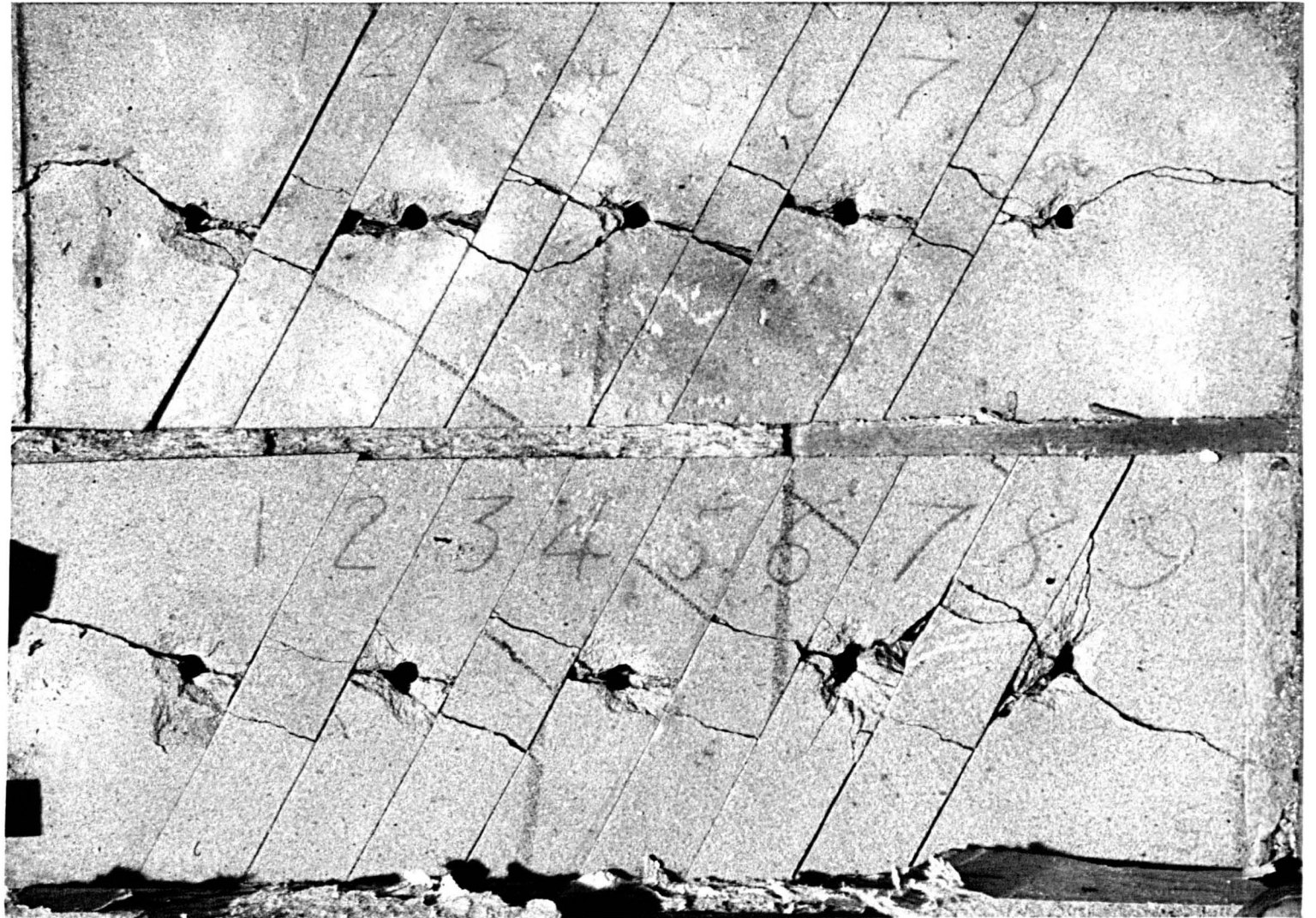
The results from increasing joint frequency were similar, in that for all fracture frequencies used, the dominant fracturing from each hole extended in all cases up to the discontinuity prior to the next hole. All fracturing across jointing was seen to be

## Fig. 8.1.

Tests 64 and 63.  
Effect of multiple  
discontinuities on  
pre-split success and  
overbreak.

Discontinuity inter-  
section angle =  $60^{\circ}$ .

Note: dominant  
fractures crossing  
discontinuities at  
right angles.



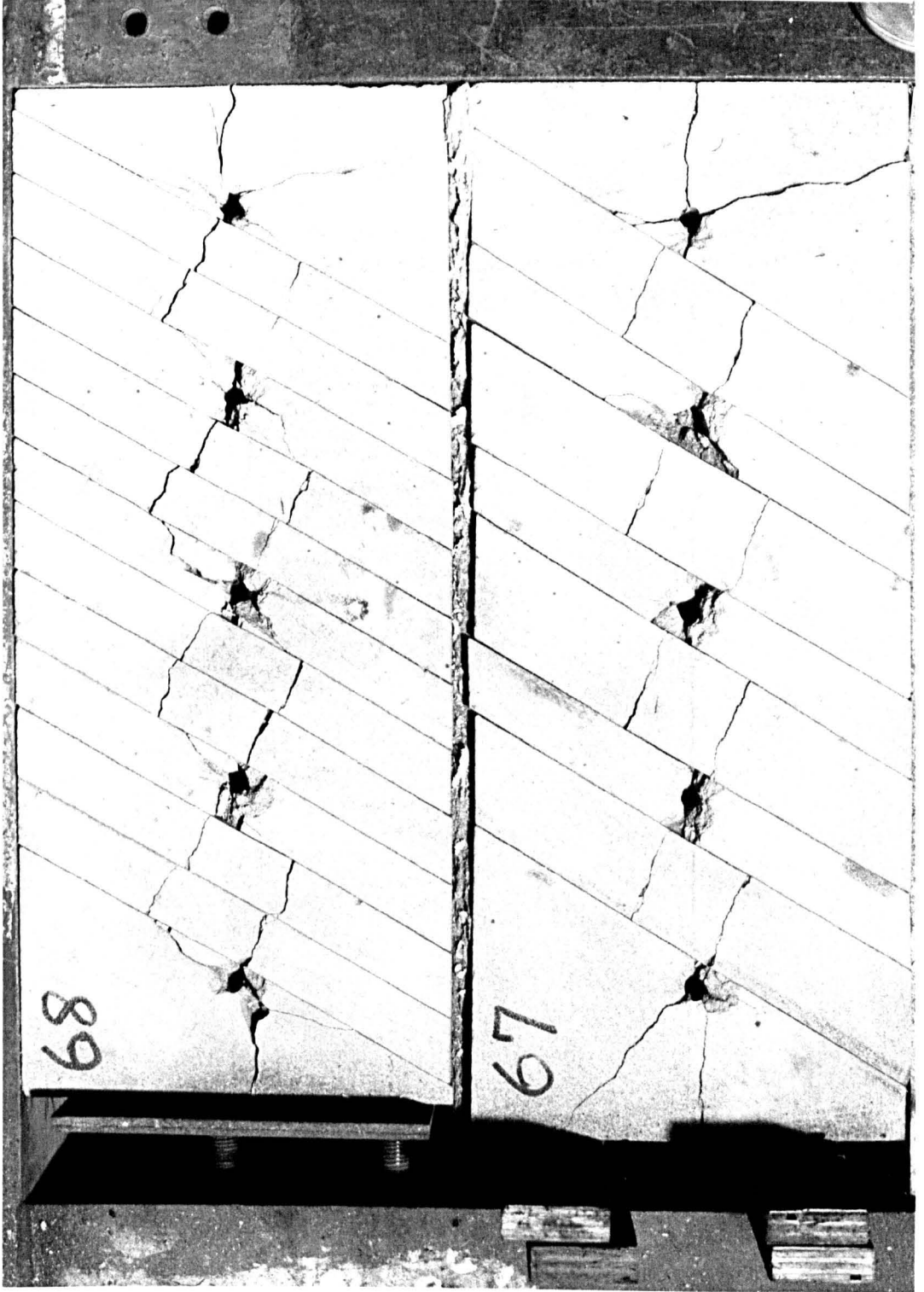


Fig. 8.2.

Tests 68 and 67.  
Effect of multiple  
discontinuities on  
pre-split success  
and overbreak.

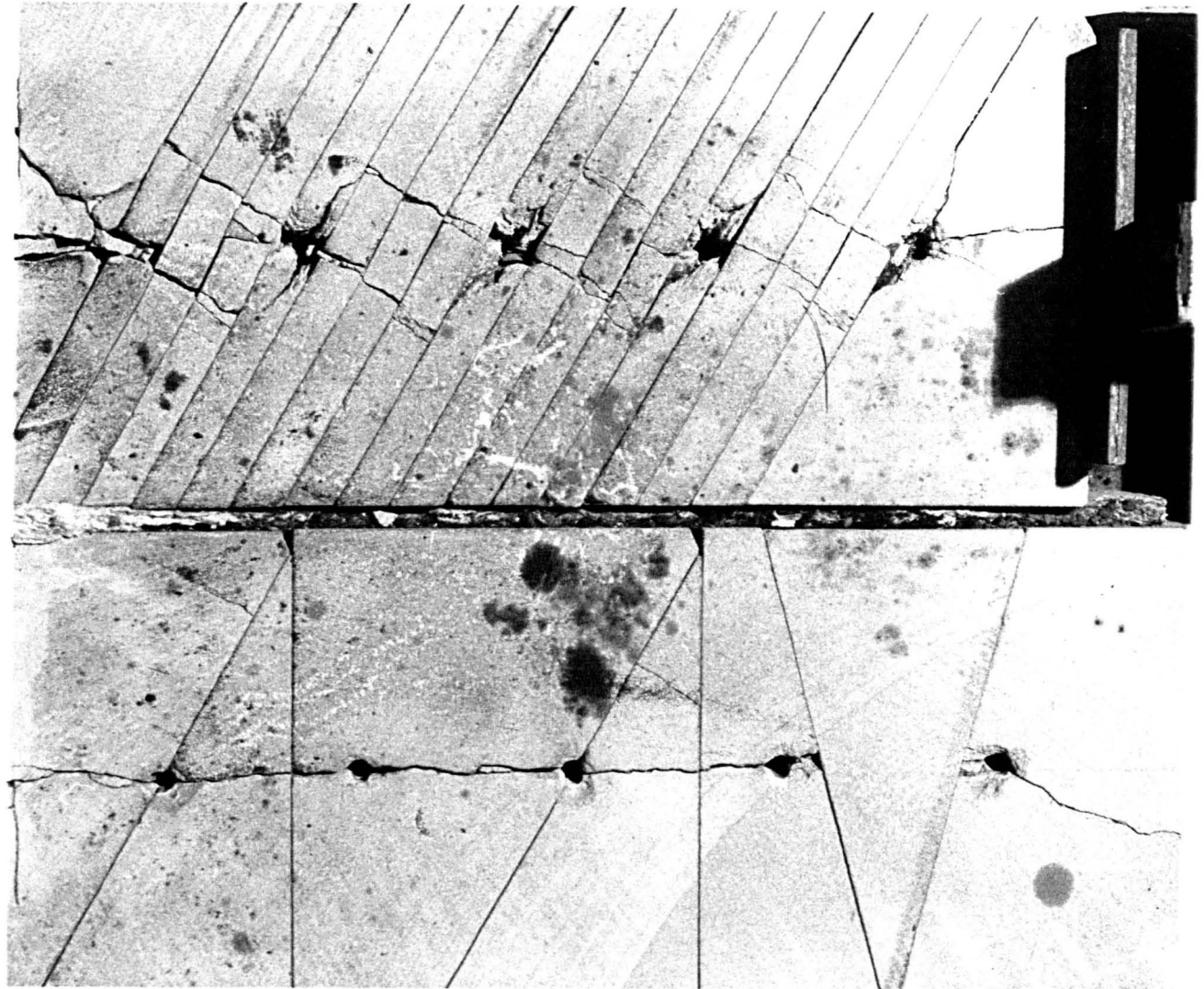
## Fig. 8.3.

Test 69.

Effect of multiple discontinuities on pre-split success and over-break.

Test 70.

Effect of multiple discontinuities with varying orientations and of discontinuities intersecting boreholes on pre-split success.



perpendicular as in previous tests.

Secondary fracturing was seen in most cases to link up with dominant fracturing. However, the higher the fracture frequency, the lower the volume of rock enclosed by the secondary fracture and conversely the higher the volume of rock enclosed by the dominant fracturing.

In all tests the majority of overbreak was caused by the dominant fracturing, which was seen to extend for a length nearly as far as the pre-split borehole separation in test 69. Overbreak volume increases from single to multiple discontinuities, for increasing discontinuity frequency but this increase rapidly tails off for values at and above four discontinuities per borehole spacing.

In test 70 fracturing between boreholes was achieved for jointing bisecting boreholes, although the splitting power from that borehole is noticeably reduced (see middle borehole, Figure 8.3). However, for jointing with similar intersection angles but opposing directions, a failure to split between holes was produced.

## 8.4 FIELD OBSERVATIONS

### 8.4.1 Measurements

To ascertain the effect (if any) of discontinuity frequency on pre-splitting in the field, it was decided to take scan lines at individual pre-split localities where other geotechnical factors such as instability were not dominant and compare these results with the actual success of the pre-split.

This however presented somewhat of a problem in that there is no exact method of measuring the success of a pre-split directly, as it is difficult (if not impossible) to distinguish between the pre-split path and other fracturing, (predominantly caused by the bulk charge) and natural discontinuity surfaces present within the rock. This problem is created by the pre-split not only inducing new fracturing along its path but also utilising the pre-existing joint network within the rock mass.

A final solution to this problem was achieved by using an indirect method - the splitting index

(Matheson, 1980) where the splitting index is the measure of the percentage length of pre-split half barrels left visible in the final face.

The scan lines taken varied from 4 m to 30 m in length dependent on the continuity of the splitting index within each location, the latter being measured at a later date from photographs of the exact localities involved. These measurements are displayed in Figure 8.4 in which pre-split success (splitting index) is plotted against fracture frequency (or intensity).

#### 8.4.2 Discussion of Results

The first obvious and main observation that may be made from Figure 8.4 is that there is no discernable statistically valid relationship between splitting index and fracture intensity, the almost random spread of points confirming this. However a slight decrease in splitting index for the higher values of fracture intensity is just discernable. This is thought not to reflect a reduction in pre-split success but has been logically concluded by the author to reflect a weaker face (i.e. a greater number of discontinuities will

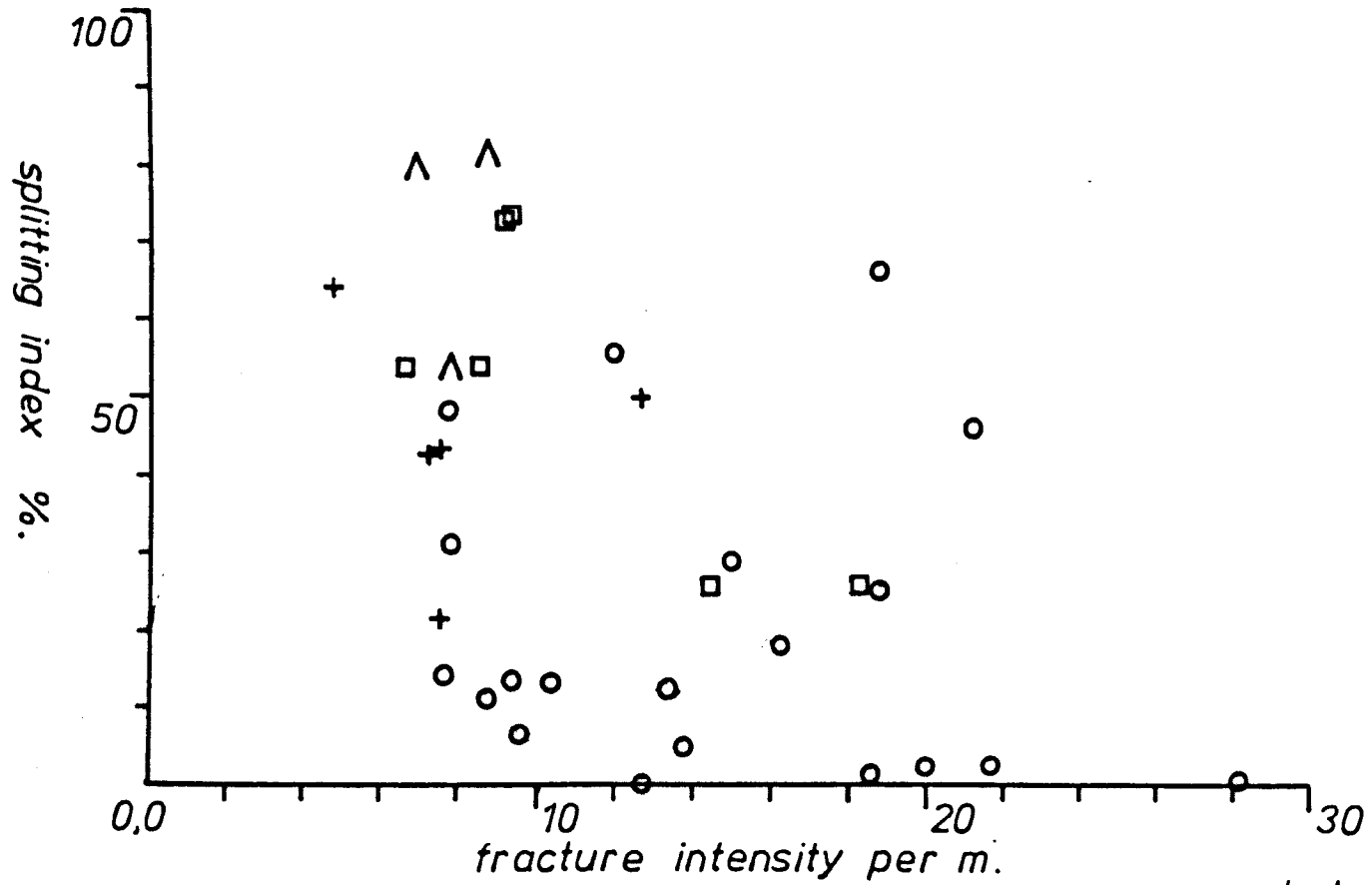


Fig. 8.4.

Plot of pre-split success [splitting index] against fracture frequency.

<u>symbol</u>	<u>location</u>
○	1
+	8
□	9
△	11

result in a reduction of overall strength in a rock mass) which results in the traces of half barrels becoming more prone to removal on excavation. This was observed to be the case during excavation at pre-split location number nine where an over enthusiastic Priestman 150 Mustang operator attempted to remove parts of the face of a pre-split trial panel, scabbing material from the pre-split plane and thus reducing the splitting index.

It is also a possibility that instability was reflected in the wide spread of points in Figure 8.4. However extreme care was taken in the choice of measurement localities and only the relatively most stable locations (i.e. location numbers one, eight, nine and eleven) were included in the survey, (see Chapter Thirteen).

## 8.5 CONCLUSIONS

Pre-splits may be produced in ground with a high dominant discontinuity frequency, provided that the intersection of the discontinuity set with the pre-split axis is not below the guide given in the previous chapter.

The amount of overbreak obtained is highly dependent on the orientation of the discontinuity set involved. Maximum overbreak will occur for low intersection angles and minimum overbreak for sets of discontinuities perpendicular to the pre-split. The degree and shape of the overbreak due, is almost entirely a geometric effect. No underbreak will occur.

The quantity of overbreak caused will increase for increasing values of joint frequency, but will level off rapidly at and above four discontinuities per borehole separation.

Pre-splitting may be achieved even if holes are intersected by a discontinuity, as long as it is closed. However, a reduction in the splitting ability of that hole is incurred.

From field evidence it may be concluded that increasing fracture intensity does not have any serious effect on pre-split success and that there is no discernable relationship between these two factors.

## 9 ROCK STRENGTH

### 9.1 IMPORTANT CONSIDERATIONS

Considering a blast is something of a 'dynamic' event in respect of its time scale, the relevant parameters for the deduction of optimum charge densities for blast boreholes in homogeneous rock are the dynamic compressive and tensile strengths, the dynamic strengths of rock being higher than their static strengths.

The dynamic compressive strength is only relevant to the crushing of rock in the borehole wall which is indicative of over charging and under decoupling. However such high enough charging and coupling to produce crushing is purposely avoided in pre-split practice in order to keep the degree of blast damage to a minimum and thus protect the final pre-split face and therefore the dynamic compressive strength of rock is irrelevant within the pre-splitting process.

Although research has been undertaken in the field of dynamic compressive strength testing a lack of

information exists on dynamic tensile strength testing. This can most probably be attributed to both the difficulty in acquiring the tensile dynamic strength compared with the compressive dynamic strength and the associated high cost due to the sophisticated equipment which would be required. Due to these factors the dynamic tensile strength is also of little use to the practical blasting engineer.

The normal strength parameters which can be easily and relatively inexpensively obtained are the 'static' tensile and less importantly in this case the 'static' compressive strengths.

With these considerations in mind it was obvious that testing should be undertaken to determine the effect of static rock strength on the maximum successful pre-split borehole separation for a standard charge density and borehole diameter.

## 9.2 LABORATORY TESTING

### 9.2.1 Materials

It was considered important that to obtain a reasonable understanding of the effect of rock strength in the pre-splitting process it was essential to perform tests in the maximum number of varying rock types and strengths. Also the availability of stone in suitable dimensions was an important factor in this choice. However, due to the number of tests required in each rock type and the corresponding time available, the minimum number of rock types in order to produce a valid representation of results was used. The following six materials were chosen:

Springwell Sandstone (as used in Phase 2 Testing)

4:1 mix Concrete (as used in Phase 2 Testing)

Dolerite (Whin Sill)

Creetown Granite

Dolomitic Limestone (Permian)

Shelly Limestone (Permian)

A brief description of these materials may be found in Appendix H along with source locations and both tensile and compressive strengths.

### 9.2.2 Experimental Method

Single strand 2.31 gm/m (11 grain per foot) P.E.T.N. cord was loaded in open ended 3/8 inch hammer drilled holes positioned in line at constant spacing in rough blocks of approximately six inches thickness. In each test explosive cord per hole was of equal length and the free ends were detonated by a single detonator to ensure instantaneous detonation of the charges in each hole.

Split blasting was continued in each rock type until both a failure to split and a success had been recorded for successive decreases of borehole separation.

Cores of intact rock were then taken from the test specimens and/or unblasted blocks (depending on the availability after testing) in order to fabricate compressive (84 x 42 mm diameter) and tensile Brazilian Dice (42 mm diameter x 21 mm thickness) strength test specimens. The results of the subsequent strength testing for each material are given in Appendix H.

### 9.2.3 Results

A complete list of tests and rock descriptions with compressive and tensile test results can be found in Appendices D and H.

Graphs of the combined results of each test indicating rock type are displayed in Figures 9.1 and 9.2 in which pre-split borehole separations and success are plotted against tensile and compressive strengths respectively. As would be expected, both figures show that the maximum successful pre-split borehole separation decreases with increasing tensile and compressive strengths. Each figure shows a hyperbolic relationship between maximum successful pre-split borehole separation and strength, all points of the former except for the Whinstone tests fitting onto a single curve. Surprisingly the compressive strength values give as good a fit as the tensile strength values even though the spread of strengths is inferior.

In an attempt to quantify the relationship it was decided that the two variables might be simply inversely proportional to each other. The inverses of the strengths were then plotted against maximum



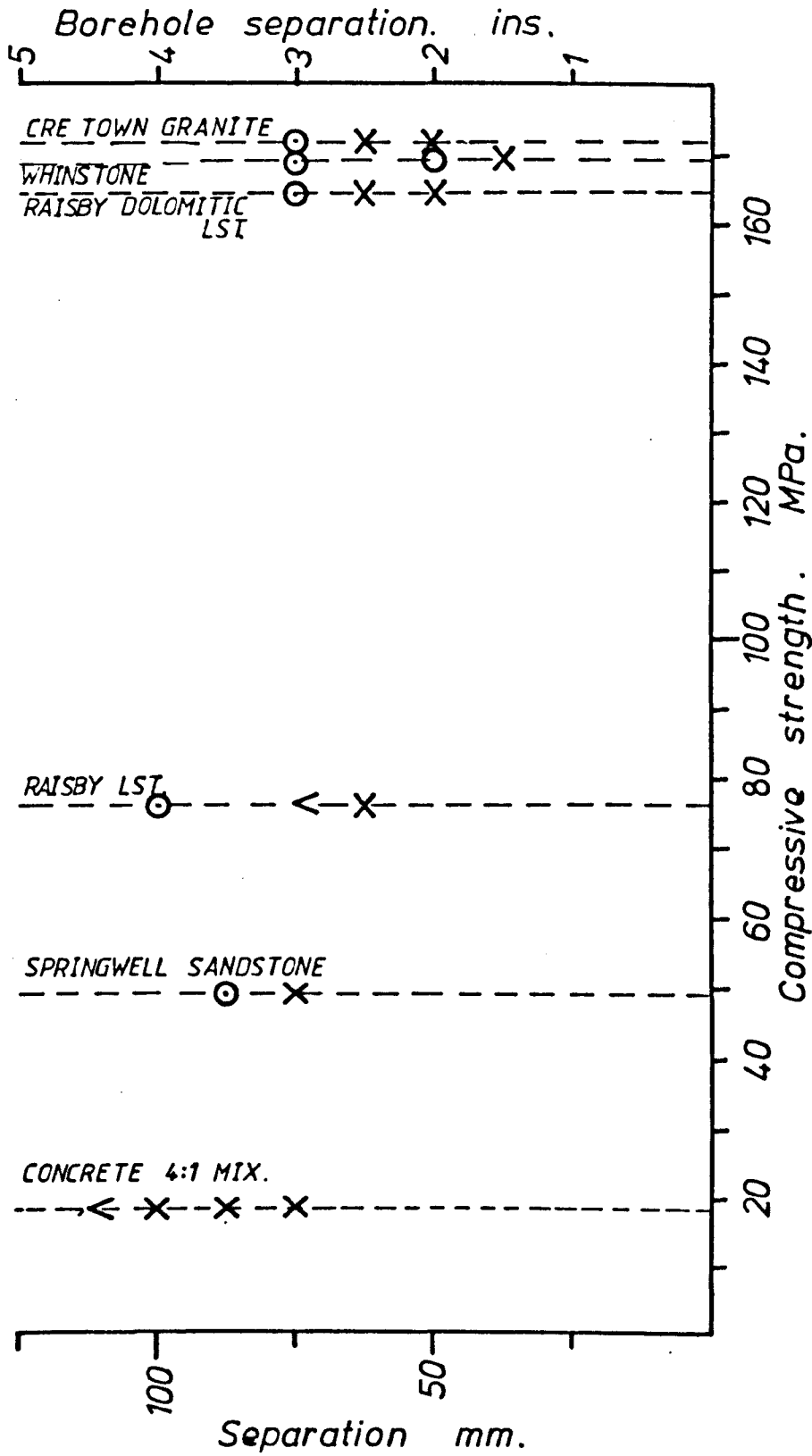


Fig. 9.2.  
Plot of borehole separation against compressive strength for each test: denoting success of pre-split, and rock type.

successful pre-split borehole separation for each rock type and are displayed in Figures 9.3 and 9.4 with better results. In Figure 9.3 it can be seen that each rock type with the exception of the Whinstone fits closely to a straight line with:

Y axis intercept (A) = 6.35 cm (2.45 ins)

Slope (B) = 8.01 cm MPa

Giving the relationship:

$$Y = 6.35 + 8.01T^{-1} \text{ cm}$$

where: Y = maximum successful pre-split borehole separation

T = tensile strength

However the Whinstone value of Y is only 66% of the predicted value from the above relationship and lies well below the regression line in Figure 9.3. Initially it was thought that there had been exceptional circumstances or some mistake but on rechecking the blasting data sheets and the actual specimens it was shown that the Whinstone was unusually resilient and resistant to blasting.

Although it did not possess the greatest compressive strength of the rocks tested, it possessed by far the largest tensile strength (see Figure 9.1). On visual re-assessment of the blast damage around

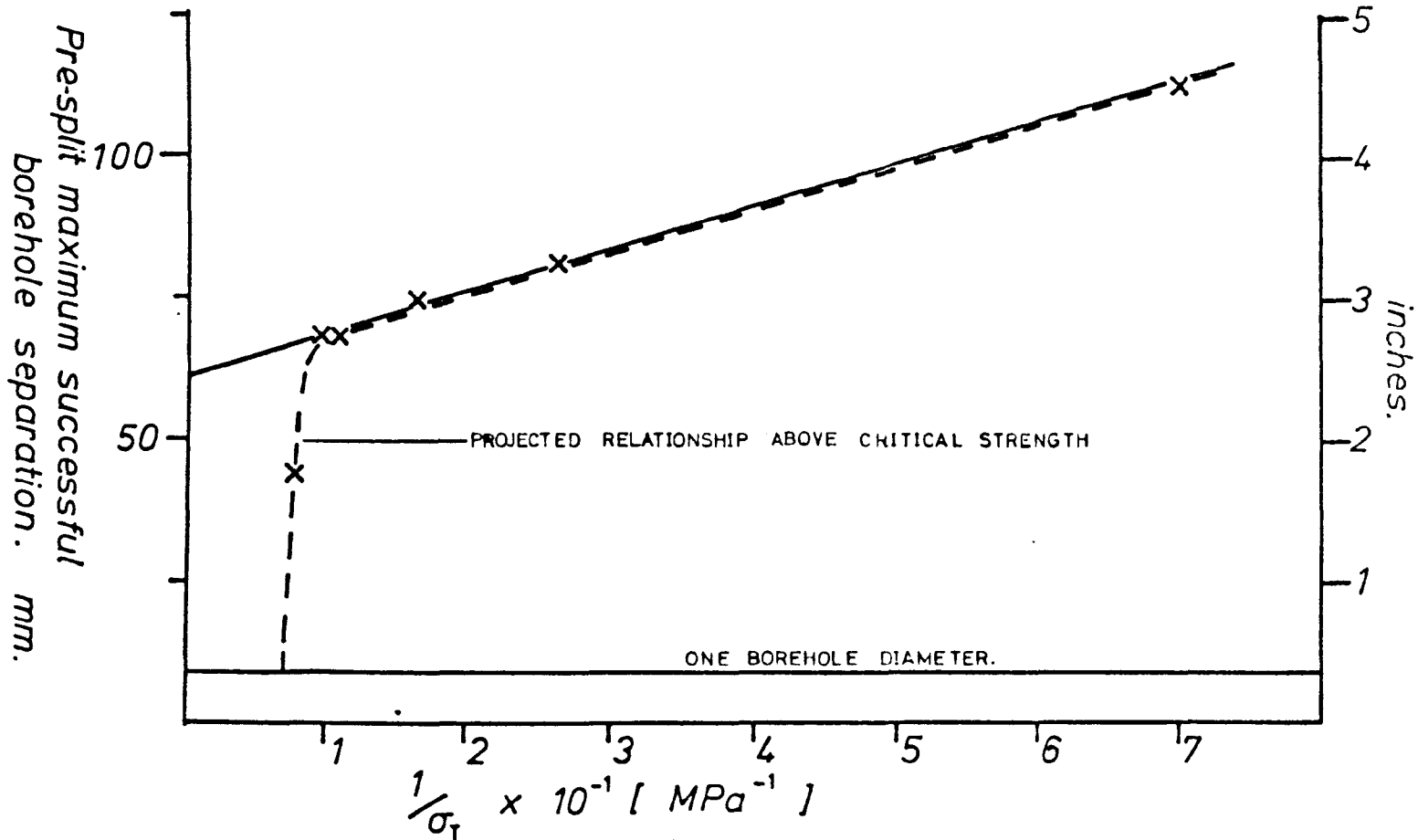


Fig. 9.3.

Graph showing the inverse relationship between maximum successful pre-split borehole separation and rock tensile strength.

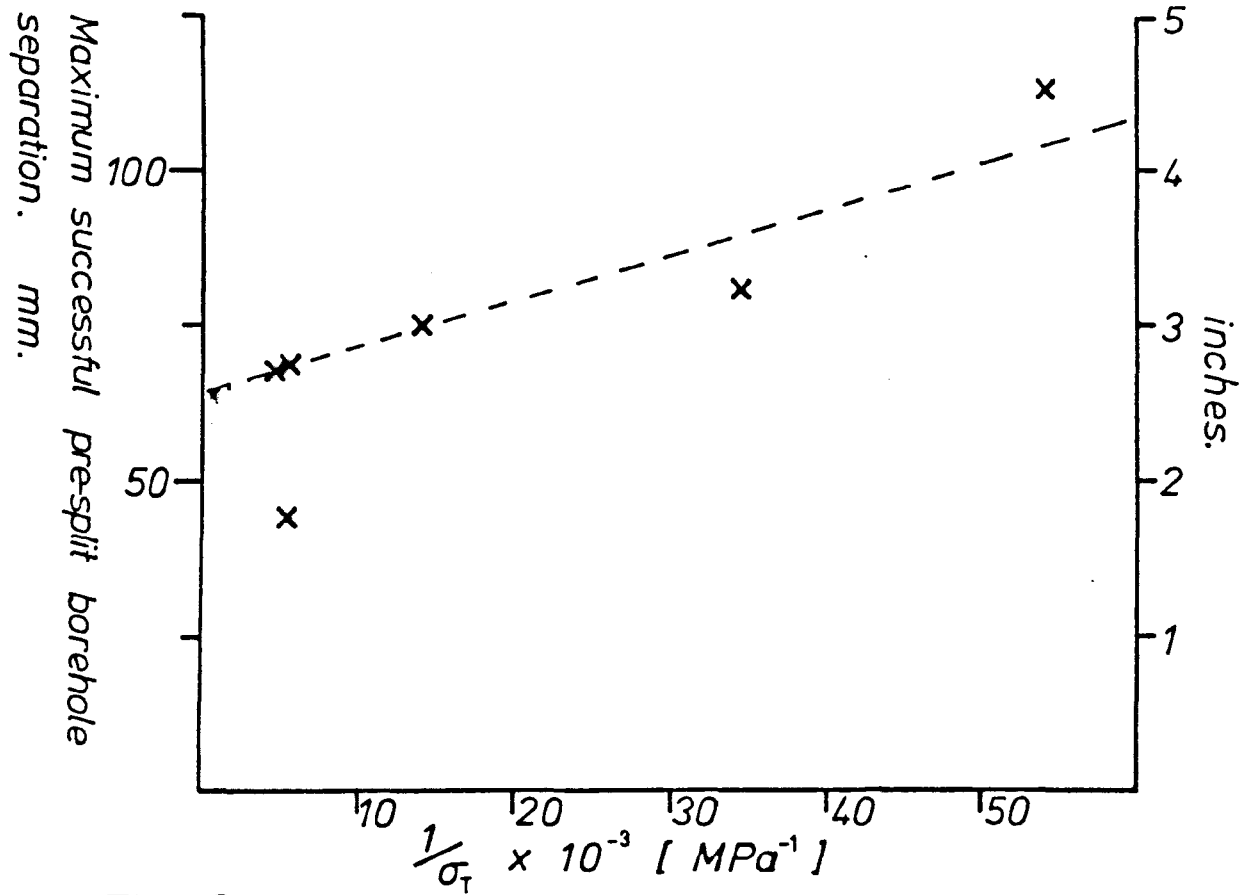


Fig. 9.4.

Graph illustrating approximate inverse relationship between compressive strength and maximum successful pre-split borehole separation.

each borehole it was discovered that in both unsuccessful and successful whinstone pre-split tests no damage other than a pre-split fracture where present could be detected.

It is reasonable to assume that there comes a limit to the strength of a rock that can be pre-split, it being impossible for the straight line relationship to reach the Y axis otherwise a maximum successful pre-split borehole separation of 8.01 cm at a tensile strength of infinity could be obtained. The relationship must therefore at some point deflect from the straight line of Figure 9.3 to the reciprocal of the tensile strength axis. However it cannot reach this axis in practice due to the finite diameter of the boreholes. It is suggested by the author that the path of the relationship for 0.9525mm (0.375 inch) holes loaded with single eleven grain (2.31 gm/m) P.E.T.N. cord defects sharply downwards at a tensile strength of approximately 11 MPa and passes through the whinstone maximum successful pre-split borehole separation point values.

Figure 9.4 for compressive strength values shows a similar effect but a greater spread of results. However this is only coincidental and due to a tenuous

link between tensile and compressive strengths and therefore the compressive strength should not be used in design etc. especially when a better relationship between maximum successful pre-split borehole separation and tensile strength exists.

### 9.3 EFFECT OF PRE-SPLITTING ON INSITU STRENGTH

#### 9.3.1 Method

The effect of rock strength on pre-splitting having already been explored it was decided to find what effect the pre-split has on the insitu rock strength. As any disruption to insitu rock will be affected by the disruptive presence of individual holes, three compressive test and three tensile test specimens were taken from test No 58 around the end borehole at the following centre spacings - 30 mm, 44 mm and 65 mm.

Test 58 was chosen as Springwell Sandstone is an extremely homogeneous rock and strength testing in the Department has shown it to have extremely consistent strengths and moduli. In addition test 58 offered a

sufficiently large 'intact' piece of rock for the drilling of cores at suitable distances from a pre-split borehole. Tests were carried out using standard sized cylindrical specimens (84 x 42 mm diameter - compressive, 21 x 42 mm diameter - tensile).

### 9.3.2 Results

The results of compressive and tensile testing are as follows:

Distance	Compressive	Tensile
30	38.98 MPa	2.85 MPa
44	42.88 MPa	3.20 MPa
65	44.75 MPa	3.20 MPa
intact	48.82 MPa	3.80 MPa

These results are graphically displayed in Figures 9.5 and 9.6. Both tensile and compressive strengths show a decrease for decreasing distance from the pre-split hole. However at the distance of half the borehole separation there is only a reduction of six

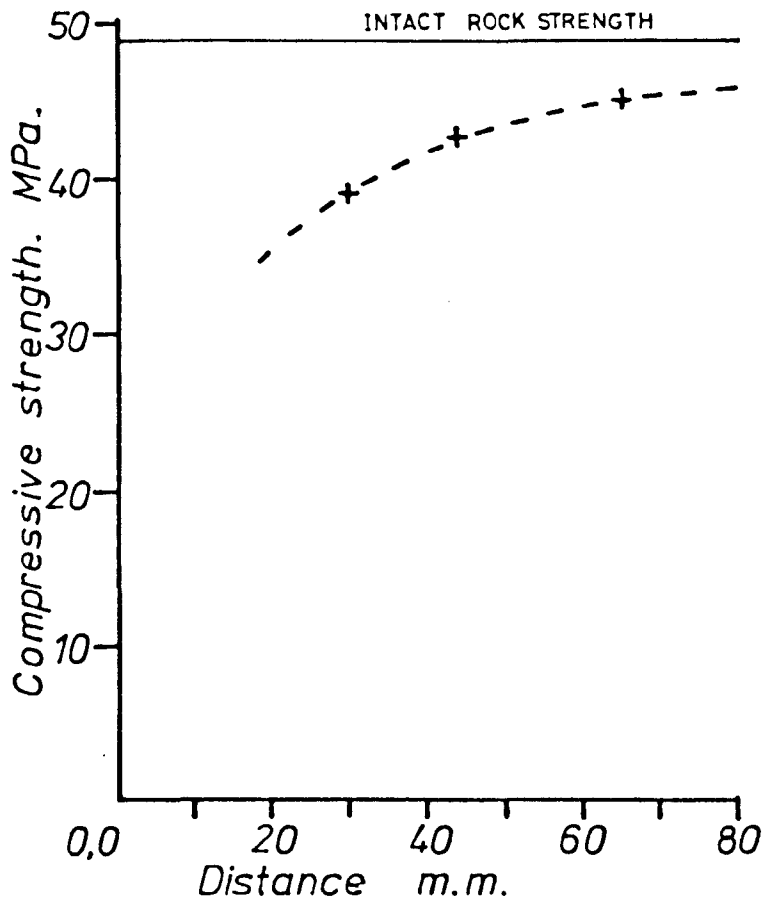


Fig. 9.5.

Graph of the proximity effect of a pre-split borehole on comp. strength [Springwell sandstone]

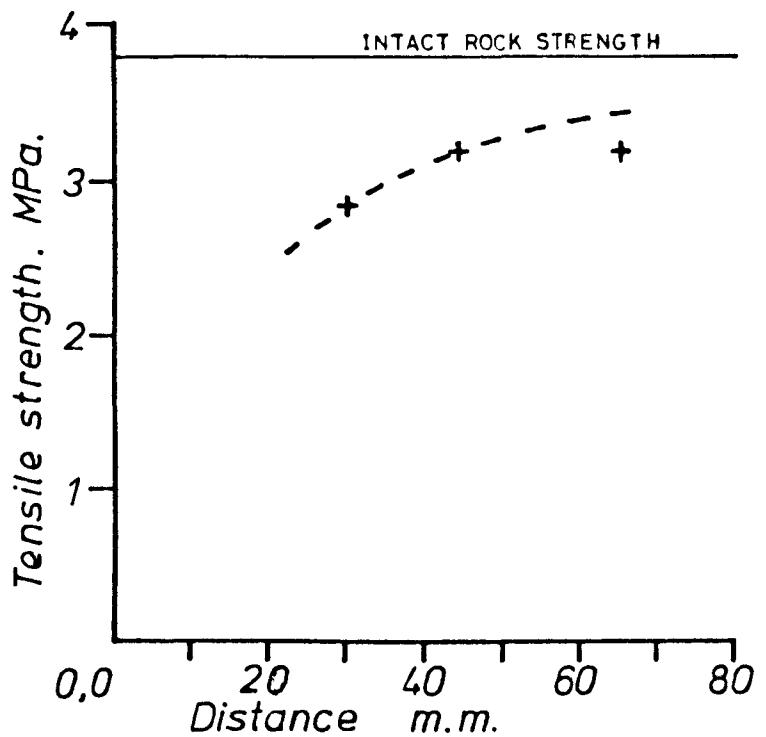


Fig. 9.6.

The same but for tensile strength.

and eleven percent respectively. It can therefore be concluded that any substantial lowering in rock strength along the pre-split line will be confined to the immediate vicinity of the pre-split boreholes and the rest of the face will remain relatively unaffected back from the pre-split line.

## 9.4 FIELD DATA

### 9.4.1 Method

Strength testing was carried out in the field using a portable point load testing rig on each rock type at successive localities. The testing was carried out under the guidelines suggested by Reichmuth (1967) and tensile strengths were calculated from the equation:

$$S_t = K_s P/h^2 + K_b P$$

where:  $S_t$  = tensile strength (Pa)

$P$  = applied load at failure (N)

$h$  = height (distance between  
loading points, m)

$K_s$  = shape factor

$K_b$  = relative brittleness index (m)

$K_s$  was taken as  $0.7 h/w$  (for Prisms)

and  $K_b$  as 1550 (m )

where:  $w$  = width of specimen (shortest) (m)

#### 9.4.2 Results

The number of tests taken, the mean point load tensile strengths and their population standard deviations for each rock type and their localities are given in Figure 9.7. Due to the fact that some specimens failed at very low loads along microfissures and cemented joints etc. the means and standard deviations are shown for both with and without these results. The loading densities and charge layouts for each site are shown in Figure 9.8.

#### 9.4.3 Discussion of Results

As can be seen from Figure 9.8, the loading densities vary enormously between sites, the lowest by far being for sites one to eight inclusive. However at these sites the strongest rocks are found as illustrated by Figure 9.7 (these sites were also the least successful). The best pre-split results from these sites were obtained at cutting number one which

Site No.	No In	X	St. Dev.	No Ex	X	St. Dev.
1	26	13.28	14.53	13	24.26	13.43
2	21	29.80	20.41	19	32.67	19.34
3 (Gneiss)	20	24.00	13.76	20	24.00	13.76
3 (Felsite)	5	41.32	13.55	5	41.32	13.55
4	28	22.56	13.14	27	23.26	12.86
5	26	24.52	18.42	20	31.01	16.08
6	23	22.11	12.69	23	22.11	12.69
7	21	25.69	19.78	18	29.37	19.02
8	16	27.77	15.91	13	33.35	12.05
10 (upper)	10	10.22	9.95	8	11.30	10.02
10 (lower)	11	9.09	5.17	10	9.82	4.85
11 (upper limestone)	21	14.13	8.57	15	18.83	5.04
11 (middle limestone)	8	26.41	8.24	7	29.34	2.98
11 (middle mudstone)	13	4.67	1.08	13	4.67	1.08
11 (middle sandstone)	5	2.36	0.71	5	2.36	0.71
11 (lower limestone)	19	16.94	5.00	19	16.94	5.00

Figure 9.7

Table of Results from Point Load Testing in the Field

In = including low failure values

Ex = excluding low failure values

All initiation by cordtex trunklining.

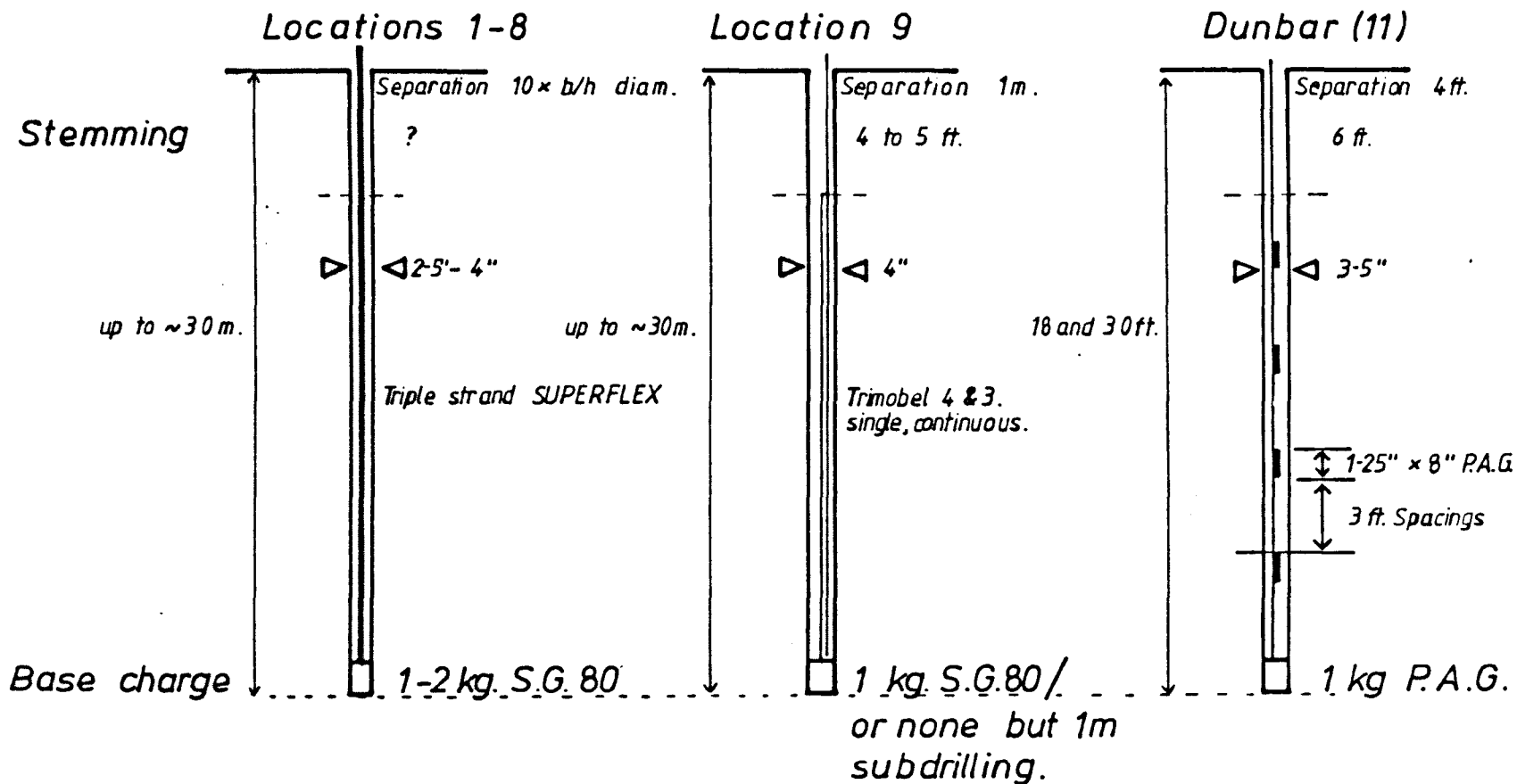


Fig. 9.8.

Diagram of pre-split charge layouts for individual pre-split locations.

Location 10:  
 Little information available.  
 borehole diameter 4"  
 borehole spacing 1m.

has the lowest rock strength of this group of pre-split locations. In contradiction, excluding low failure values there are three other sites which have lower tensile rock strengths, two of which, numbers three and four, the application of pre-splitting to the final faces has proved very unsuccessful.

As shown in Chapter 5 (Figure 5.2), at location three pre-split boreholes in gneiss were observed to have failed to connect, the results of pre-splitting being on the whole very poor. However the best results were observed to have been obtained in a felsite intrusion (sill) orientated with the major discontinuity planes dipping at an angle into the line of the carriageway.

These contradictions seemed initially to be insoluble, but on close examination it was decided that the jointing structure within the rockmass was playing a decisive role. It was discovered on revisiting location three that all of the accessible felsite which was present in the rock trap or reposed against the face was hand sized in dimensions and bounded by three flat joint sets which were roughly mutually perpendicular with no fresh surfaces. From the size of felsite block encountered it would be very

difficult for a 100 mm borehole not to cut at least one of these interconnected discontinuities at any point along the borehole's length. In comparison, the gneiss in which pre-split failure occurred is massive in nature with few discontinuities and boreholes were observed to be rarely cut by discontinuities except in the case of the main 'bedding' which cuts across the holes and not along their length (as illustrated in Figure 5.2).

Examining the point load tensile strength data obtained from gneisses at location number one it is obvious that the small scale closed flaws, 'cleavage' planes and cemented small discontinuities are widely disseminated throughout the rockmass in great numbers as 50% of the random samples failed at extremely low loadings due to their presence.

Essentially it is the author's opinion that generally the rock strength at locations one to eight due to the general failure of the pre-split and the high occurrence of intact borehole lengths in some of these faces, was too high for the charge densities and borehole separations used. Infact the use of triple strand superflex gives a low charge density and resultant quasi-static gas pressure incurred compared

with those used at locations nine to eleven although the exact charge densities are not available for location ten (see Figure 9.8).

At location eleven (Dunbar Quarries), excellent pre-splits were obtained in the upper and lower limestones, excessive back damage and a general loosening of the face by opening up of fissures was observed in the middle beds within the mudstone and silty sandstone horizons. From consultation of Figure 9.7 this should not be totally unexpected as their tensile strengths are extremely low - 4.67 and 2.36 MPa respectively compared with means of 10.22 and 16.94 MPa for the upper and lower limestones.

## 9.5 CONCLUSIONS

The tensile strength of rock may affect the success of a pre-split panel if it is too high for the pre-split charge to totally overcome.

From laboratory experimentation there is a definite inverse relationship between 'static' tensile rock strength and the maximum successful pre-split borehole separation. However this relationship does not hold

above a critical tensile rock strength (which may be different for differing borehole diameters, charge densities and explosive types). where the dynamic component may be insufficient to fracture the borehole wall, the effect being to rapidly reduce the maximum successful pre-split borehole separation above this value.

From field results it has been shown that the presence of abundant micro-fissures, flaws and small scale interconnected jointing dramatically increases the maximum successful pre-split borehole separation. In such conditions the importance of the intact tensile strength of the rock in the determination of the success of a pre-split is dramatically reduced.

## 10 WEATHERING

### 10.1 WEATHERING PROCESSES IN RELATION TO THE ROCK MASS

The effect of weathering (chemical) on insitu rock is to weaken the fabric through mineral decomposition and by the breaking up of the matrix through mineral recrystallization e.g. Feldspar to Kaolinite and Sericite etc.

The jointing within a rock mass plays a major role in the weathering process, as weathering generally permeates strata through the system of discontinuities, progressively attacking the rock of the joint walls until just cores of rock remain between joints. Weakening of joints by the associated reduction of their cohesion and also opening may occur, thus an increase in permeability is common which in turn leads to intensification of the weathering process.

Eventually, through weathering the rock may become completely altered so that it possesses the strength of a soil but still retains the texture and 'fabric'

of the original rock. The overall effect of weathering is thus a reduction in strength and stability of the strata involved.

## 10.2 EEECI DE WEATHERING AND RECOMMENDATIONS

All weak weathered material which is rippable should be removed before drilling to prevent the loss of holes due to borehole collapse in the upper regions of the holes, which may be located in 'loose' weathered material).

Normal practice in pre-split blasting is to use a constant charge density throughout the borehole length, with the exception of the top 1 to 1.5 m of hole with, (in some cases), the provision of a base charge. It is critical to ascertain the depth as well as the degree of weathering as boreholes may 'bridge' both highly weathered ground and intact strata.

Consider a borehole within a pre-split panel surrounded by extensively weathered weak material in its upper half and intact stronger unweathered rock in its lower half, (see Figure 10.1a). If a charge density for the hole is calculated or selected on the

(a). Normal Practice.

(b). Recommended Practice.

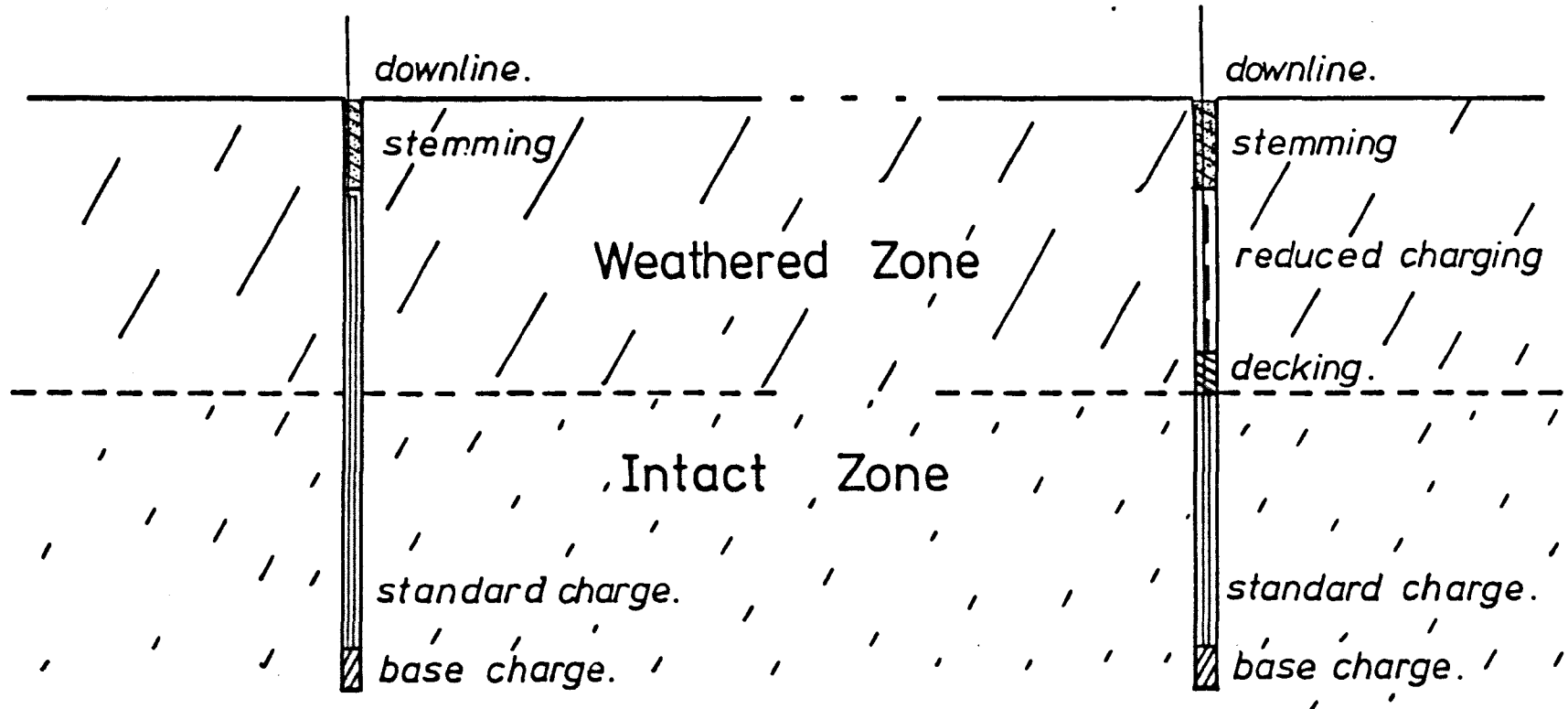


Fig. 10.1.

Diagram of normal (a), and recommended (b), charge string layouts for blasting in rock with sizeable weathered zone.

strength of the intact rock, then the upper portion of the hole within the weathered strata will be overloaded and excessive damage will be likely to occur on detonation, especially in respect of opening the joints, reducing cohesive strength and thus correspondingly that of the surrounding rock mass. In extreme cases slight ground heave may be encountered and it may become necessary to dispense with any top stemming to negate this effect. A weakening of this ground may result in extensive instability problems at the top of the final face.

Conversely if the charge density for the hole is calculated or selected on the strength of the weathered portion of the strata, then the lower half of the borehole will be undercharged. Here failure to pre-split may occur, resulting in either a toe or excessive damage from the accompanying bulk blast.

If such a contrast between weathered and unweathered zones exists then they must be treated as differing rock types or horizons and the charge density along the borehole lengths should be varied accordingly, with a reduction of charge density within the weathered ground.

The reduction in charge density at any one point will reduce the degree of dynamic damage to the borehole wall, producing smaller and shorter radial fractures for quasi-static extension which in turn will be reduced. To diminish the influence of the gas component from the more highly charged lower portion of the pre-split holes a small amount of decking (say 0.5 to 1 m of tamped clay-sand mix) may be introduced at the approximate 'interface' of the weathered and unweathered zones, (see Figure 10.1b).

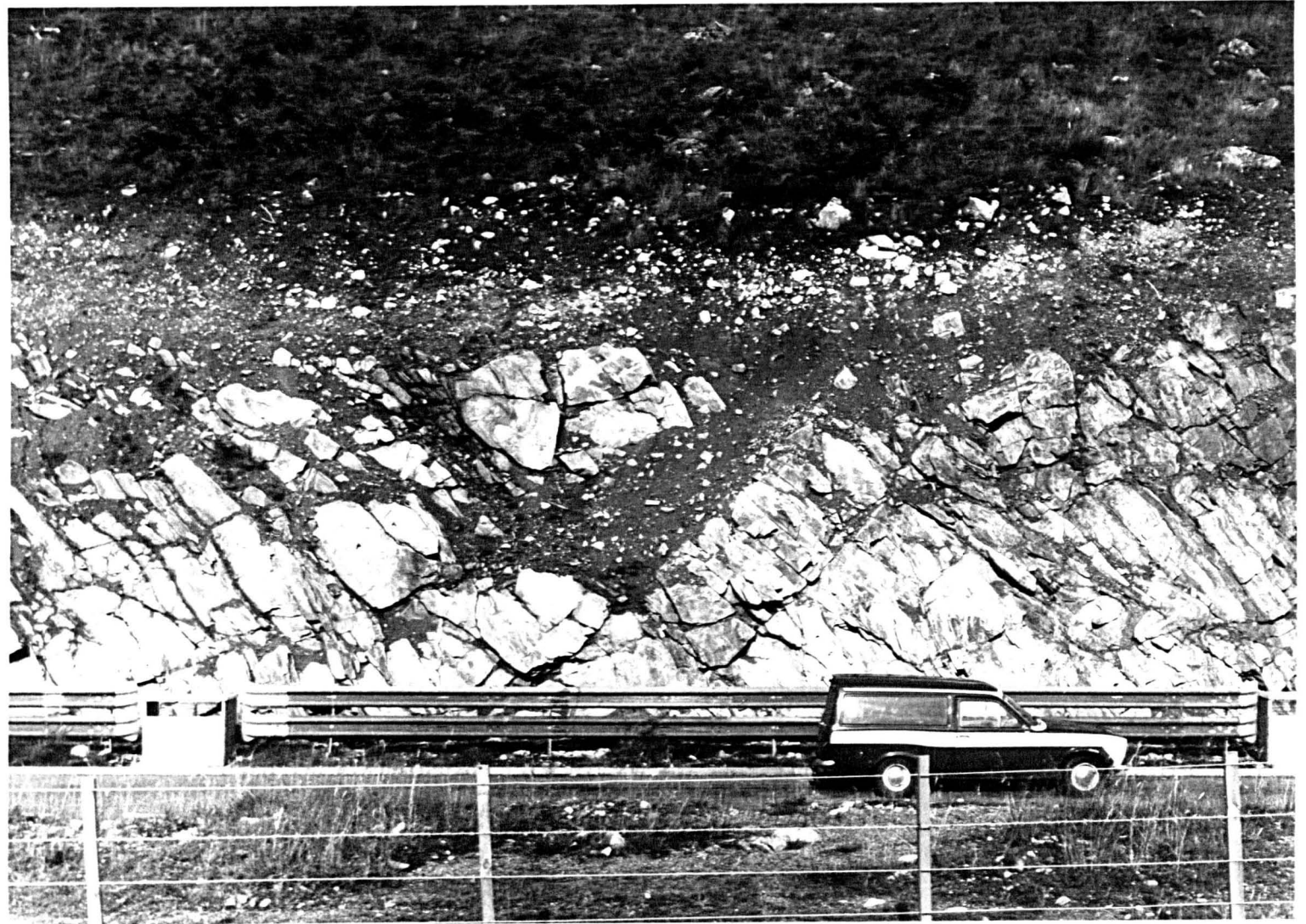
### 10.3 FIELD OBSERVATIONS ON THE INFLUENCE OF WEATHERING

The effect of weathering and the absence of reduced charging in the weathered zones can be clearly seen at rock cuttings one, two and five. Here wedge and plane failure has predominantly occurred in the upper regions of these pre-split faces where the opening of discontinuities is the most marked. Talbot (1977) attributes the failure to produce a clean split in the upper portions of these faces (locations one, two, five etc.) to the presence and degree of weathering, (along with other factors). (See Figure 10.2.)

It is however important to note that the upper

Fig. 10.2.

Highly weathered rock at location 2 in the upper portions of the face in certain areas has shown to be totally unsuitable for obtaining reasonable pre-split results, giving rise to both excessive backbreak and instability.



areas of the pre-split plane should theoretically produce the best face. This is due to the fact that borehole deviation and drilling inaccuracies are minimal compared to the foot of the pre-split. A major contributor to the failure to pre-split in these areas can be attributed to the degree of weathering present.

## 11 WATER

### 11.1 THEORY

The free water content within a rock mass should be considered as an important constituent of the strata. It may affect its strength and/or stability and even the seismic velocities of the medium. Leaving aside the main stability problems arising in certain situations which may be accentuated by the presence of excess water, by far the most important factors controlling the effect of water on the process of pre-split blasting are the actual level of the water table and the ease with which the water is allowed to pass through the rock mass, in relation to the pre-split boreholes. The important items which should be considered can be broken down to the following:

1. Height of the water table in relation to the base level of the boreholes.
2. Rate of filling of the boreholes.
3. Rate of flow of water through each borehole.

If there is the possibility of there being water present then care must be taken of at least items (1) and (2). If water is present and drains into the boreholes, filling them, the explosive used must be water resistant and the charges fired on the same day as loading to avoid water saturation of the explosive or deterioration due to leakage through any protective seal.

Deterioration of the explosive charge will result in a reduction in strength, (both seismic and gas pressure) with the possibility of misfire in some water susceptible explosives. Generally the lowest water resistant explosives are the low strength ammon-gelignites and n.g. powders whereas the higher strength gelignites have superior water resistance, (Dick, 1968). If there is water flowing through the boreholes the pre-split charges should be fired without delay as the effect of flowing water is more detrimental than that of static water.

With charges consisting of individual sticks of high explosive attached to cordtex downlines or with charges of single or multiple strands of flexible high explosive cord, the Specific Gravity of the explosive

train should exceed 1.0 (S.G. of water). If this condition is not met within top stemmed holes slowly filling with percolating ground water the charge will tend to float up the borehole with the rising water, resulting in a charge concentration near the top and a possible absence of explosive at the bottom. This will result in excess damage at the top of the intended face and if a weathered zone is present it may be excessively loosened. This portion of the face is the most important in a stability sense as maximum damage may occur due to the falling of rock from the higher regions of the face. Conversely the fracturing at the base of the hole will be drastically reduced and failure to pre-split at this point may occur resulting in an unbroken toe of rock at the base of the pre-split.

If a base charge is incorporated in the explosive train then the point along the borehole's length at which it rests will concede excessive damage on detonation resulting in a pocket of highly fractured rock at this point in the final pre-split face.

Boreholes drilled in 'impervious' strata may become unexpectedly filled from surface or subsurface water, as was observed by the author at site nine. Here

water was observed to have drained into the pre-split boreholes over a period of one to two days from direct drainage from the layer of overlying Glacial Till and/or subsurface rivulets at the Quartzite/Gneiss and Glacial Till interface. Rapid filling was observed during wet periods.

The second effect that a column of water around an explosive charge in a borehole has is to effectively increase the coupling and thus increase the 'fracturing' power of the explosive charge. This is effected in two ways:

1. Water is a far more efficient medium than air for the transmission of pressure pulses and sonic waves as it is denser than air and thus, as it possesses a higher acoustic velocity it therefore produces less damping. Due to this higher sonic velocity a better impedance match between the explosive and water and also between the water and rock is achieved, allowing a substantially higher proportion of the dynamic pulse to be transmitted into the borehole wall and thus into the rockmass. The combined effect will be to increase the amplitude of the dynamic pulse, thus giving rise to a more extensive zone of dense radial

fracturing in the rock around the borehole before the quasi-static gas pressure component takes over in crack propagation.

2. water unlike air (or any other gas for that matter) is relatively incompressible, therefore the decoupling of the explosive is dramatically reduced and thus a far higher gas pressure will be achieved after detonation of the explosive column. This will induce the formation and extension of fracturing far beyond that which could be expected for a water free case. However on the detrimental side to fracture development water instead of gas would be forced into the cracks around the borehole wall, the water due to its high surface tension (molecular attraction) and higher molecular size would infiltrate these fractures at a reduced rate and thus maximum quasi-static wedging efficiency would be lost.

In order to deduce which theoretical factor is dominant in practice or whether the opposed factors cancel each other out, experimental testing incorporating the use of water filled boreholes was devised.

## 11.2 EXPERIMENTAL METHOD

For ease in measurement of fracturing a reversion to polyester resin blocks was made, for reasons which have been previously stated (Chapter Four). Two tests were devised using 6.35 mm (0.25 ins) and 4.76 mm (3/16 ins) diameter holes (tests 84 and 85 respectively). These hole diameters were chosen as previous results from decoupled single borehole testing incorporating these borehole diameters (Chapter Four) gave good correlations to the overall trend (i.e. they did not give atypical results).

The holes were drilled centrally in individual polyester resin blocks of dimensions: 150 x 127 x 75 mm (6 x 5 x 3 ins). The blocks were then assembled with wave traps and constrained as specified previously in Chapter Four. Single four grain PETN explosive cord was then positioned in each hole with approximately one centimetre protruding through the base of the blocks. The base of the hole in each test was then sealed with water resistant sealant (see Figure 11.1) and the end of the explosive cord was likewise sealed to prevent moisture attacking the explosive within. The holes were then filled with water and left open at their tops, a protective plate

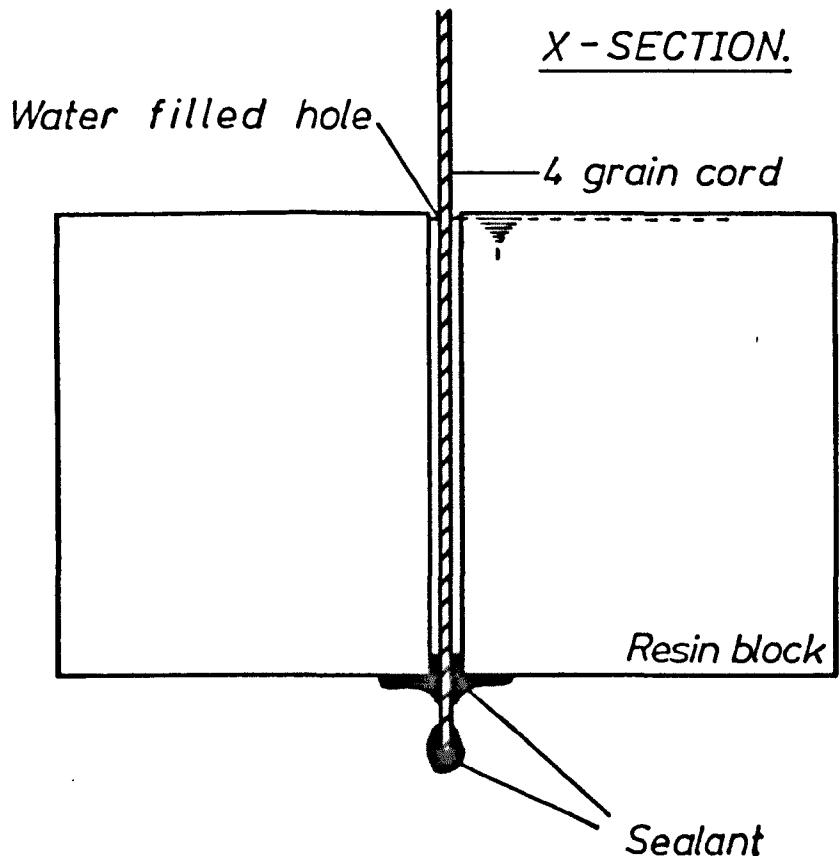


FIG. 11.1.

*X-Section of water coupled tests  
84 and 85.*

was placed above each block to shield it from detonator fragments as in previous standard procedure and the tests were fired separately.

### 11.3 RESULTS

Both water coupled tests 84 (6.35 mm) and 85 (4.76 mm) shown in Figure 11.2 produced higher degrees of blast damage than their air coupled counterparts illustrated in Figure 11.3. The extent of the damage zone produced was also greater than that produced by test 21 (2.54 mm) also shown in Figure 11.3 - the smallest hole size air coupled test (2.54 mm being the minimum size of hole available into which the four grain cord could easily be inserted). The values of blast damage zone extent obtained in water coupled tests along with those from the previously mentioned air coupled tests and the curve of the relationship between blast damage zone extent and borehole diameter are displayed in Figure 11.4.

The higher extent of blast damage zone in tests 84 and 85 compared with test 21 would tend to suggest that there is a higher degree of coupling of the explosive to the resin with the use of water,

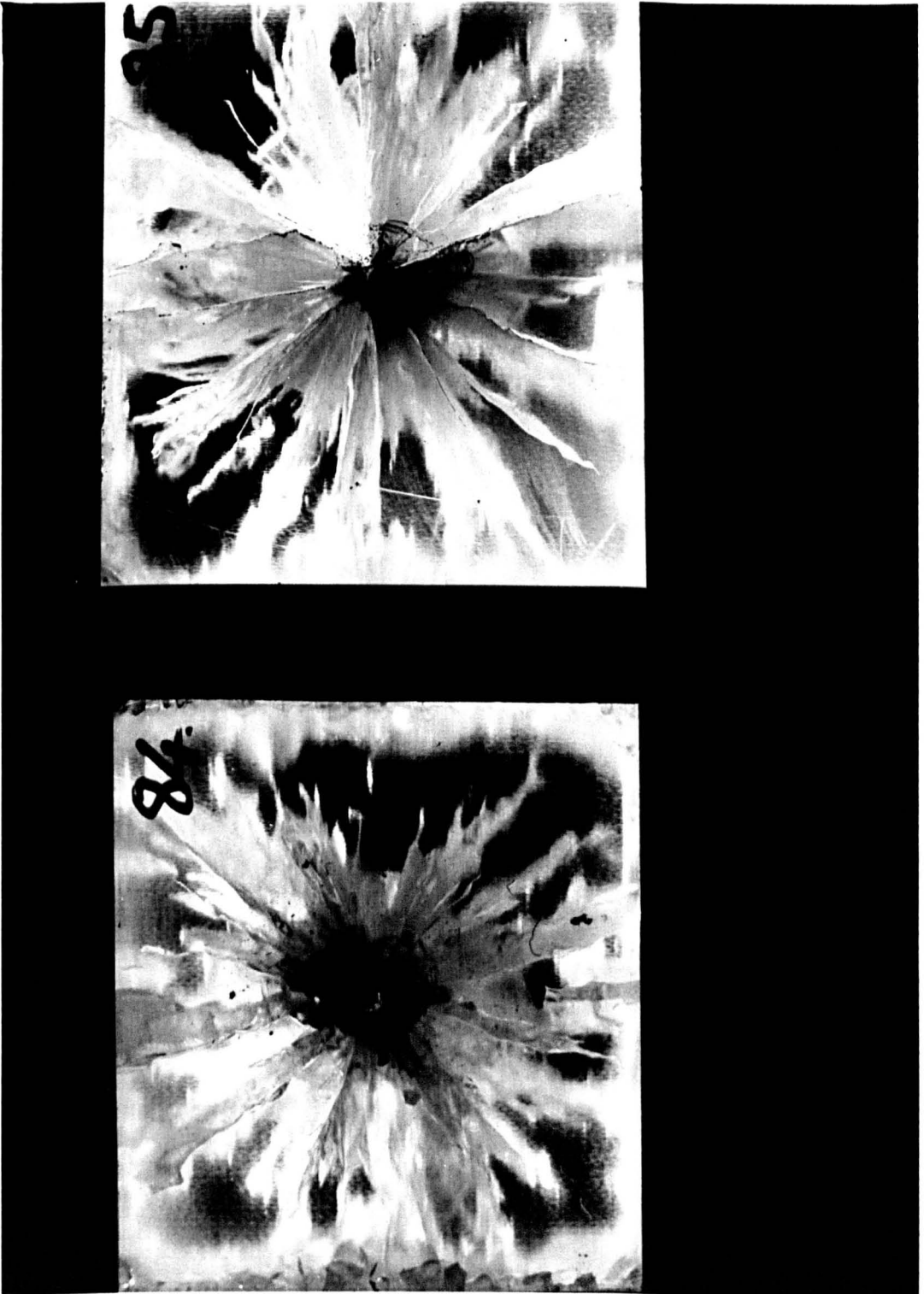


Fig. 11.2.

Fracturing produced in water coupled tests 84 (6.355mm hole) and 85 (4.76mm hole) indicating reduced effect of hole diameter for water coupling. Compare with figure 11.3. Block size 150 x 125mm.



Fig. 11.3.

Air-coupled counterparts of tests 84 and 85 - tests 7 and 8 respectively with maximum coupling test No. 21. Block size 150mm square.

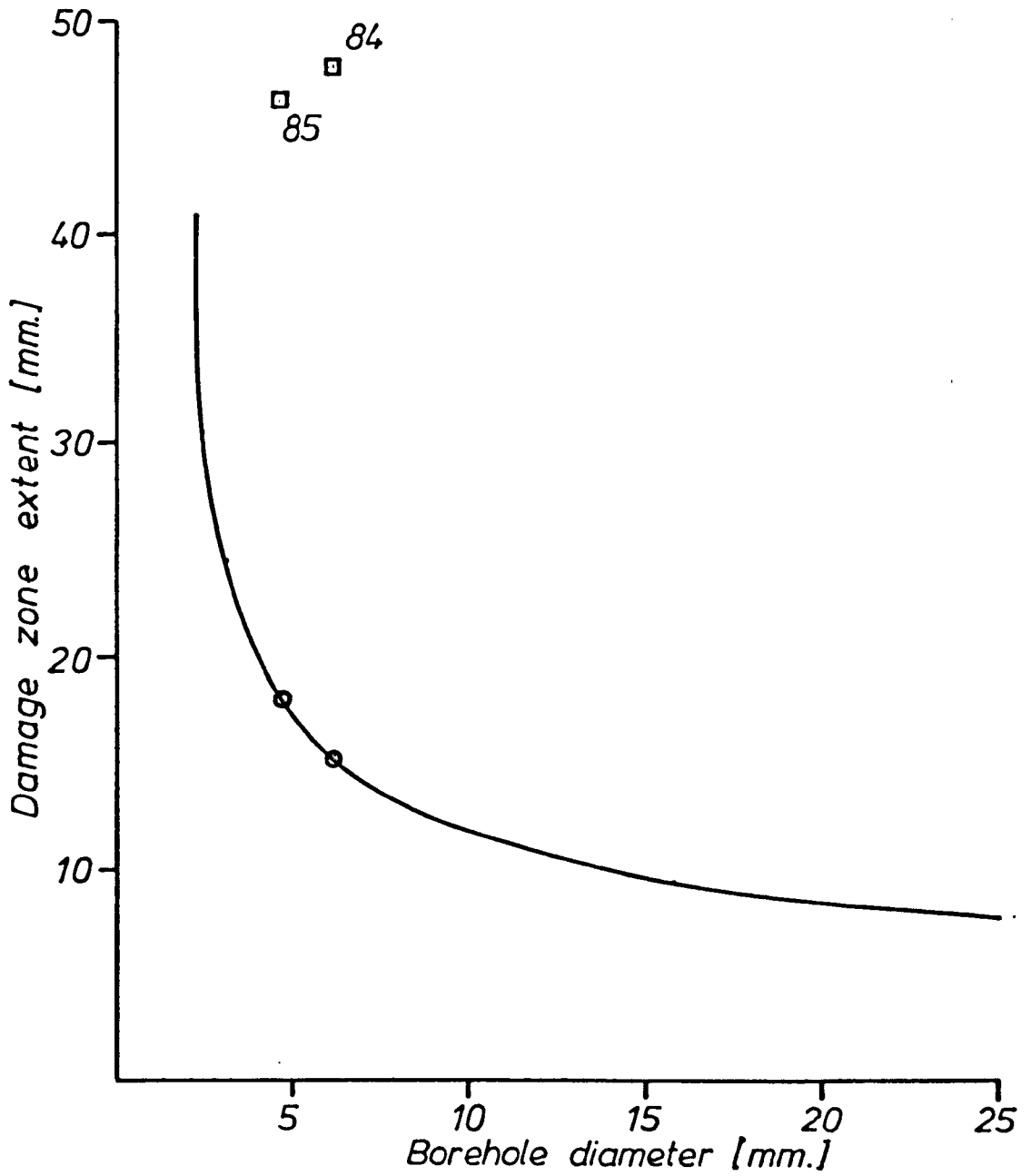


FIG. 11. 4 .

*Results of water-coupled tests 84 and 85 plotted with their air-coupled counterparts and related decoupling/damage zone extent curve.*

therefore it can be supposed that even a relatively thin layer of air around an explosive charge will reduce its rock breaking power. It is thus suggested that the use of water in a borehole maximises coupling.

#### 11.4 EURIHER EXPERIMENTATION

Although these experiments had conclusively proven water to be an efficient coupling agent, the basic mechanisms of fracture formation with water coupling had not been established. From the resulting 'marginally' higher magnitudes of explosive damage obtained during the water testing compared with that of the previous 'full' coupling test (21), it is obvious that similar if not identical fracture mechanisms are prevalent. Thus this new line of model testing gives an ideal opportunity to discover the actual mechanisms involved in explosive fracture propagation (Chapter Three).

In order to discover how far a fluid will effectively penetrate a relatively 'constricted' blast fracture induced by the dynamic component of energy release and pressurise that fracture inducing further

fracture propagation, the following experiment was devised.

Identical specifications to test 85 were adopted in every respect except that water was replaced by blue coloured cellulose based dye (Spectra colour layout and identification fluid) which had a measured surface tension of 0.45 poise (the surface tension of pure water being 1.0 poise). This dye was chosen as it was readily available and also possessed a surface tension approximately half way between that of water and 'gas'. After detonation the block was photographed using an orange filter in front of the camera lens in order to accentuate the penetration of the blue dye into the blast fractures surrounding the borehole.

#### 11.5 RESULTS OF TESTING WITH DYE

As can be seen from Figure 11.5 (test 86) the dye managed to penetrate along only a fraction of the fracture lengths. However the surfaces of one fracture, which spanned the shortest width of the block (127 mm), can be seen to be coated with dye. This fracture on close observation was open with its fracture surfaces laterally parted. This suggests



that the dominant factor affecting the penetration of dye into the blast induced fractures around the borehole is their aperture.

The maximum depth of dye penetration into the block from the hole, excluding the previously discussed open fracture was 20.4 mm and the average value 12.7 mm. The maximum crack length observed was 77 mm and the average blast damage zone extent 55 mm. Therefore the dye has penetrated up to a depth of 37% of the blast damage zone extent.

Another important factor to note is that the dye showed no marked preferential injection along the longest fractures except where these had reached a free surface and thus been allowed to open.

## 11.6 CONCLUSIONS

1.

The introduction of water into a borehole has the effect of fully coupling the explosive to the rock.

2. The effective pressurised diameter of the borehole

is increased during the quasi-static phase by fluid injection into the fractures radiating out from the borehole. This has the effect of further fracture extension.

3. Fluid is not injected into the full length of each fracture after detonation. From results of model testing an injected length of only 37% of damage zone extent was found, the dominant factor controlling the penetration being fracture aperture.
4. Fluid injection is limited to the immediate vicinity of the borehole where the highest elastic strain occurs during the quasi-static phase of fracture propagation.

## 12 TEXTURE, GRAIN SIZE AND ANISOTROPY

### 12.1 EFFECT OF TEXTURE

The texture of a rock has no real effect on the pre-split itself other than would be caused by rock strength but may affect the general appearance of the final fracture surface as follows:

A glassy homogeneous texture to the rock along a fresh fracture surface will highlight any morphological fracture features such as ribbing, stepmarks and hackle marks (Carrasco and Saperstein, 1977). The less homogeneous the texture becomes the more the amount of these features which may be readily detected decreases. For example schistose or gneissose material due to its 'crystalline' nature with the majority of crystals aligned in one direction tends to destroy all morphological features due to the roughness of fracture.

## 12.2 EFFECT OF GRAIN SIZE

The grain size of a rock again has no noticeable effect on the pre-split process itself except at extreme sizes such as a conglomerate where the sizes of the individual clasts approach the pre-split borehole separation or if a high porosity is present due to poor infilling of voids in a very well sorted or poorly graded sediment of coarse grain size.

For the former case the relative strengths of the matrix and clasts will be of importance and also their ratio of occurrence. In this case the path of the split between holes will tend to circumvent the individual clasts if the strength of the matrix is sufficiently low and an irregular face will be created with individual loose clasts protruding.

For the latter case excessive damage (crushing etc.) may occur in the immediate region around the borehole, but due to the excess void volume the maximum successful pre-split borehole separation will be reduced by the rapid dramatic drop in borehole gas pressure as the gas vents into the voids.

However the main effect of grain size noted from

field observations was again on the determination of the presence of fracture (morphological) patterns in the final pre-split face. For very fine grained rocks such as quartzite (see Figure 12.1) conchoidal fracture patterns and radiating ribs were seen to emanate from individual boreholes, proving that fracture initiation is at or near the borehole wall and that fracturing extends radially outwards from the boreholes to interconnect. As grain size increases, the frequency of occurrence of the features decreases, e.g. the fine grained upper lavas at location ten showed some conchoidal fracturing emanating from individual boreholes (Figure 12.2) but the lower coarse amygdaloidal lavas showed no indication of any such features being present. As the grain size approaches the relief height of these 'delicate' features then they become totally obliterated, the fractures extending along the coarse intergranular boundaries of the rock involved.

### 12.3 EEEECI DE ANISOTROPY

Any anisotropy in rock will effect the strength, moduli and other properties, giving differing values in different directions.



Fig.12.1.

Fracture patterns on pre-split plane in fine grained metamorphosed quartzite at location 9.



Fig.12.2.

Conchoidal blast fractures emanating from pre-split borehole in fine grained rhyolite at Location 10.

For instance, in strongly bedded or foliated rock the direction of maximum tensile strength will be parallel to the foliation or bedding planes and the minimum tensile strength perpendicular to the foliation or bedding, the converse holding for compressive strength. It is therefore obvious that the maximum possible successful pre-split borehole separation, i.e. the 'ease' of pre-split, and the degree of damage around a pre-split blast hole will also be dependent on the orientation of the pre-split line in respect to the foliation.

In an anisotropic rock mass, the direction of maximum dynamic crack formation and length due to the detonation of a charged borehole around that borehole will be perpendicular to the orientation of the minimum tensile strength, i.e. along the plane of natural 'cleavage' of the rock. Conversely the direction of minimum dynamic crack formation and length will be perpendicular to the maximum fracture orientation and maximum tensile strength.

Due to the combined effect of the more extensive cracks produced by the dynamic component and lower tensile strength for fracture propagation parallel to the foliation, the quasi-static gas component of

energy release will preferentially extend fracturing of this orientation. These combined factors will therefore precipitate the expansion of the zone of fracturing around the borehole in an elliptical form with the major axis parallel to the foliation or bedding etc.

It is obvious from the above that the direction of maximum successful pre-split borehole separation will be parallel to the foliation or cleavage of the rock.

However, at location nine where both the foliation and dominant jointing strikes perpendicular to the pre-split face, no detrimental effect to the latter was observed, although results from seismic investigations gave a peak particle velocity directional ratio of 3:1 (Swindells, 1981) along and across the foliation respectively. A clean sound pre-split face was observed with concentrated fracture damage extending only a matter of centimetres back into the face around the remaining half-barrels. The exact details and figures may be obtained from Swindells (1981).

It may therefore be concluded that any anisotropy within the rock mass may partially or wholly act with

close similarity to 'continuous' extent dominant jointing, and that a direct analogy may be made with the mechanisms and results described in Chapter Six.

## 13 STABILITY

### 13.1 INTRODUCTION

It is obvious that if a design face will be intrinsically unstable due to the discontinuity geometry and configuration within the rock mass then on excavation any pre-split that has been formed within the rock mass at that boundary will be partially or wholly destroyed.

Due to the geometry involved and the statistical probability of the position of occurrence of a daylighting discontinuity surface or intersection of discontinuity surfaces above the maximum angle of natural repose (i.e. friction angle) the top portion of the intended face will invariably fall on excavation. The intensity of major failure surfaces etc. will dictate how near to the base of the face is the level to which collapse will occur.

## 13.2 MODES\_OF\_FAILURE

There are three main modes of failure that require consideration. These are:

1. Plane failure
2. Wedge failure
3. Toppling

The general conditions for failure in each of the above three modes are as follows:

1. Plane failure, (Hoek and Bray, 1977) - see Figure 13.1:
  - a. The plane on which sliding occurs must strike parallel or nearly parallel (within approximately twenty degrees) to the slope face.
  - b. The failure plane must 'daylight' in the slope face. This means that its dip must be smaller than the dip of the slope face.

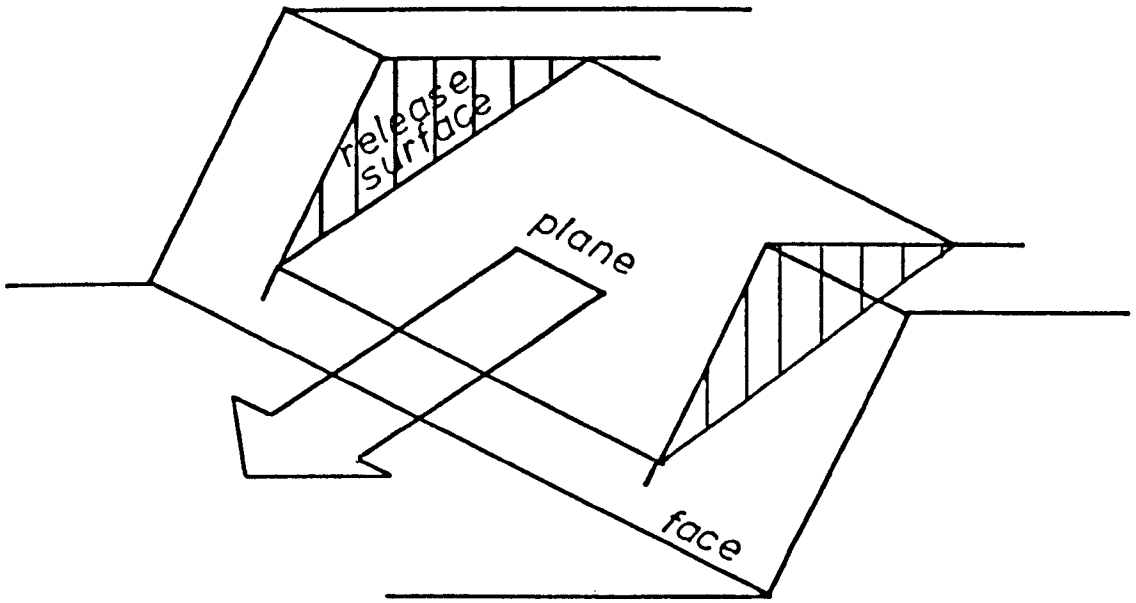


Fig. 13.1.  
*Plane failure.*

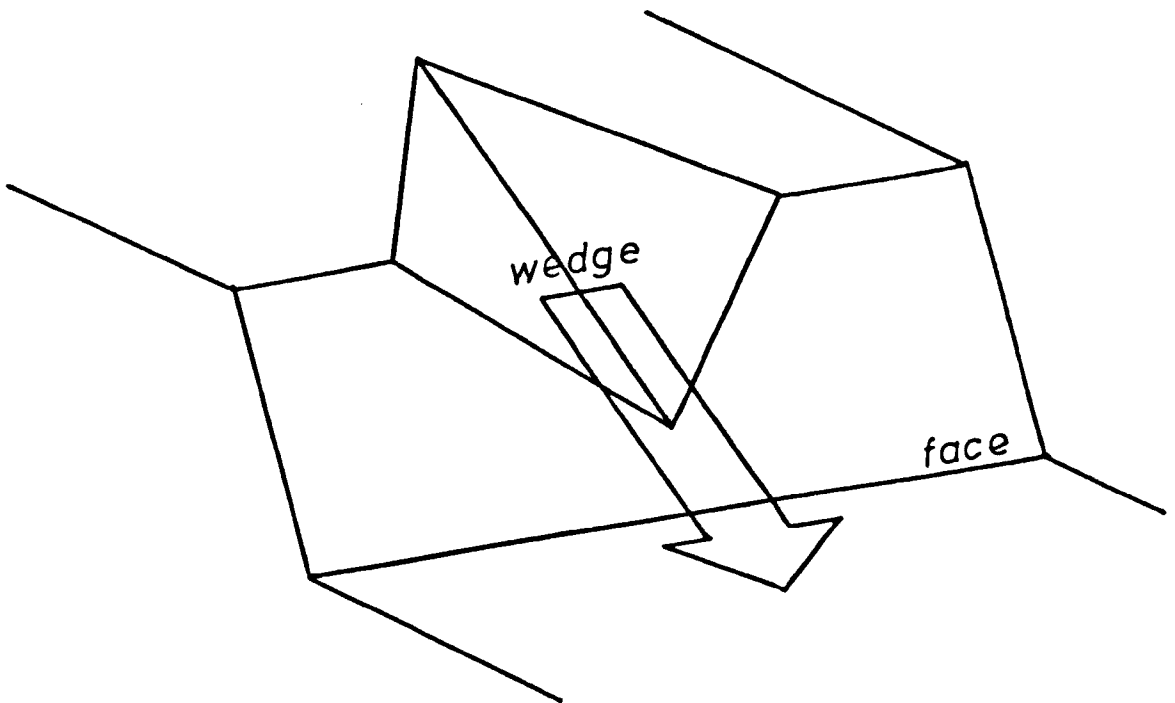


Fig. 13.2.  
*Wedge failure.*

- c. The dip of the failure plane must be greater than the angle of friction of this plane.
- d. Release surfaces which provide negligible resistance to sliding must be present in the rock mass to define the lateral boundaries of the slide. Alternatively, failure can occur on a failure plane passing through the convex 'nose' of a slope.

2. Wedge failure - see Figure 13.2:

- a. The dip of the line of intersection of two continuous joints or joint sets must exceed the angle of friction of the wedge.
- b. The failure plane sides of the wedge and their line of intersection must daylight in the slope face.

3. Toppling failure - see Figure 13.3:

- a. The centre of gravity of the block must be outside the base of the block.
- b. The direction of topple must be within

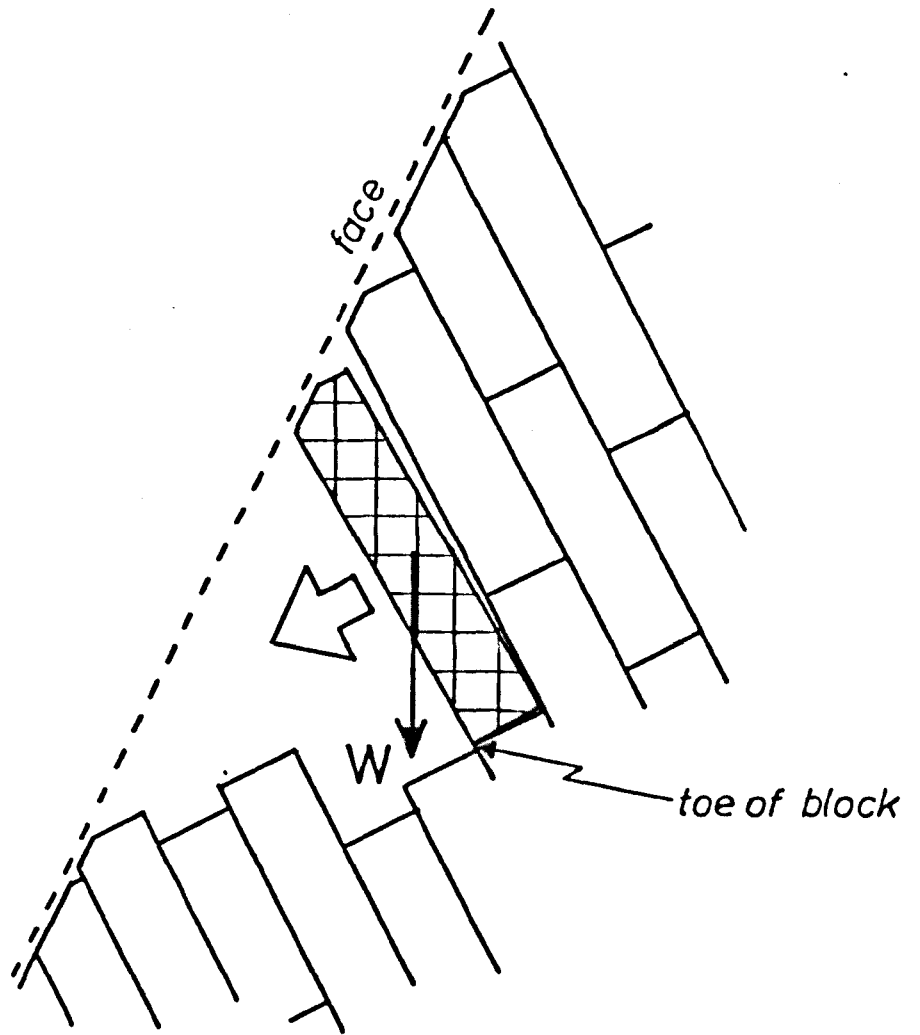


Fig. 13.3.  
*Toppling failure.*

approximately twenty degrees of the dip azimuth of the face.

- c. The toppling block must have a free release surface into the excavation.

### 13.3 DETAILED STABILITY ANALYSIS OF EACH LOCATION

#### 13.3.1 Foreword

Stability analyses should be carried out prior to or during the design stage. However the author was only involved in one such survey at pre-split location number nine, there being no such surveys at locations one to eight inclusive. The bulk of this chapter is therefore a back analysis of what should have been carried out before the commencement of excavation. The widespread occurrence of instability throughout pre-split locations one to eight has further complicated the abstraction of field data on the other geotechnical factors which affect the success of a pre-split face.

Pre-split locations one to nine inclusive occur in metamorphic gneisses of varying grades and intrusions. Due to the relative failure of the application of pre-splitting techniques to these faces at locations one to eight, the general feeling arose amongst senior engineers for both the client, consultant and major contractors that the pre-splitting technique did not work in metamorphic strata.

In a majority of locations it will be shown that major instability was present which was infact the main cause of failure of the face profile. In addition the application of pre-splitting at location number nine on a 'relatively' stable face proved highly successful compared with the results of bulk blasting in a neighbouring box cutting on the same contract.

### 13.3.2 Location Number One. (Figure 13.4)

At locatin number one the discontinuity survey (as shown in Figure 13.4) taken on the south west facing design slope (d.s.) shows three distinct discontinuity concentrations - A, B and C. The friction circle is plotted with the design slope.

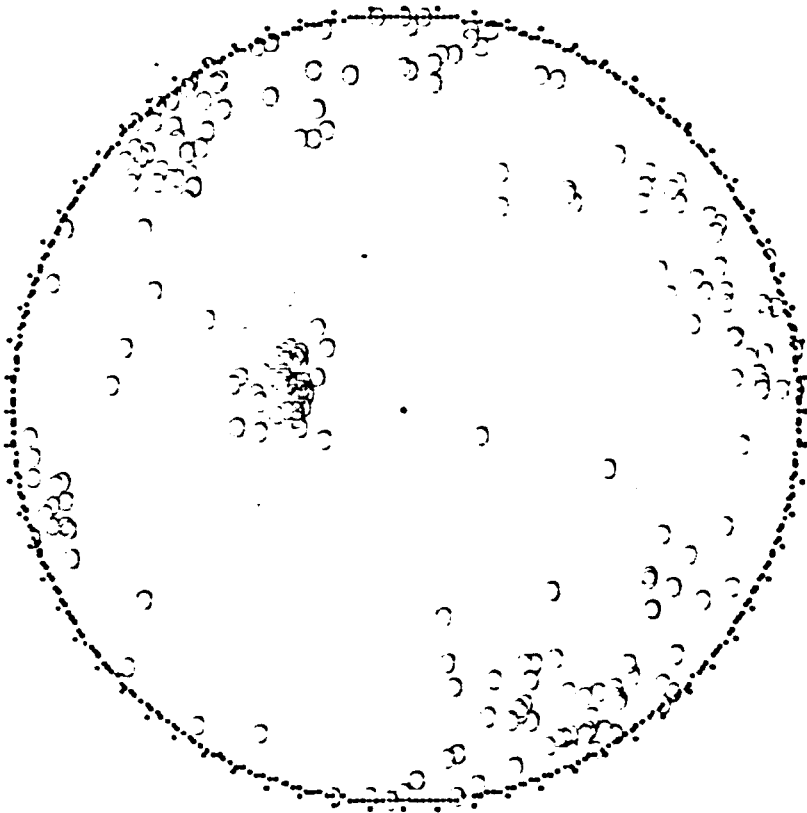
Fig. 13.4  
location number 1.

SCALE = 100MM

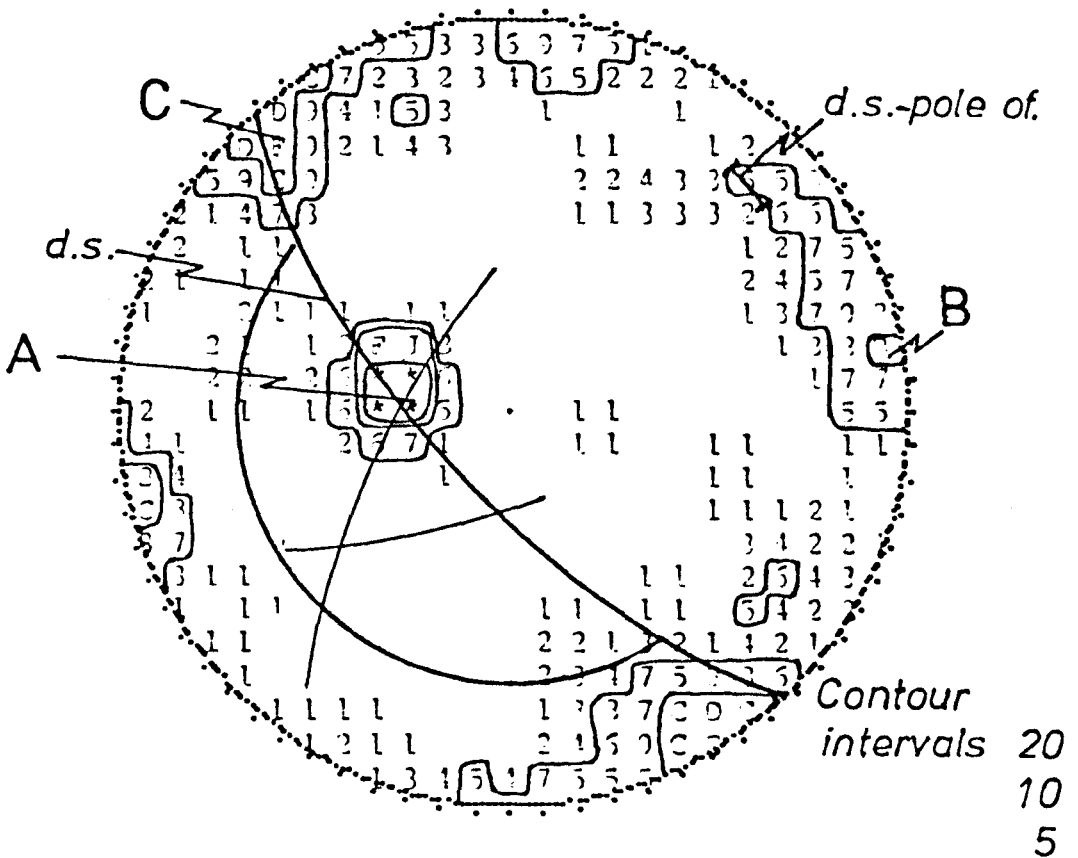
SCHEMATIC

FOLDS

NO. OF POINTS = 232



DENSITY PLOT - SEARCH ELLIPSE = 1.00



It may be seen that minor amounts of plane failure from a minor portion of concentration B may occur and that localised wedge failure may occur along the intersection of two localised minor subset concentrations.

The pole to the design face just lies within the 5% contour of group B. However this set is thought not likely to have any major effect as its major concentration lies approximately forty degrees away.

From site examination there are no major stability problems, failure being localised and of wedge type as described. This locality gave some of the best examples of pre-splitting from the first eight localities.

### 13.3.3 Location Number Two. (Figure 13.5)

At pre-split location number two the discontinuity survey taken from the south west facing face as shown in Figure 13.5 shows the probability of wedge failure along the intersection of discontinuity concentrations A and C, the majority of slippage occurring on set C with set A acting predominantly as release surfaces.

Fig. 13.5.  
location number 2.

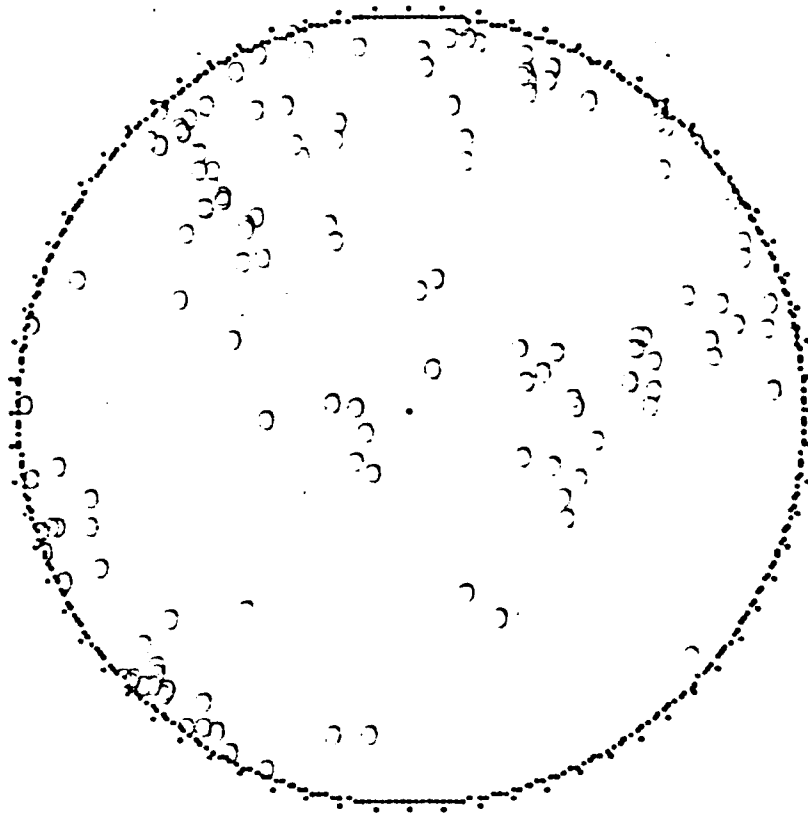
SCALE = 100000

SCHMIDT

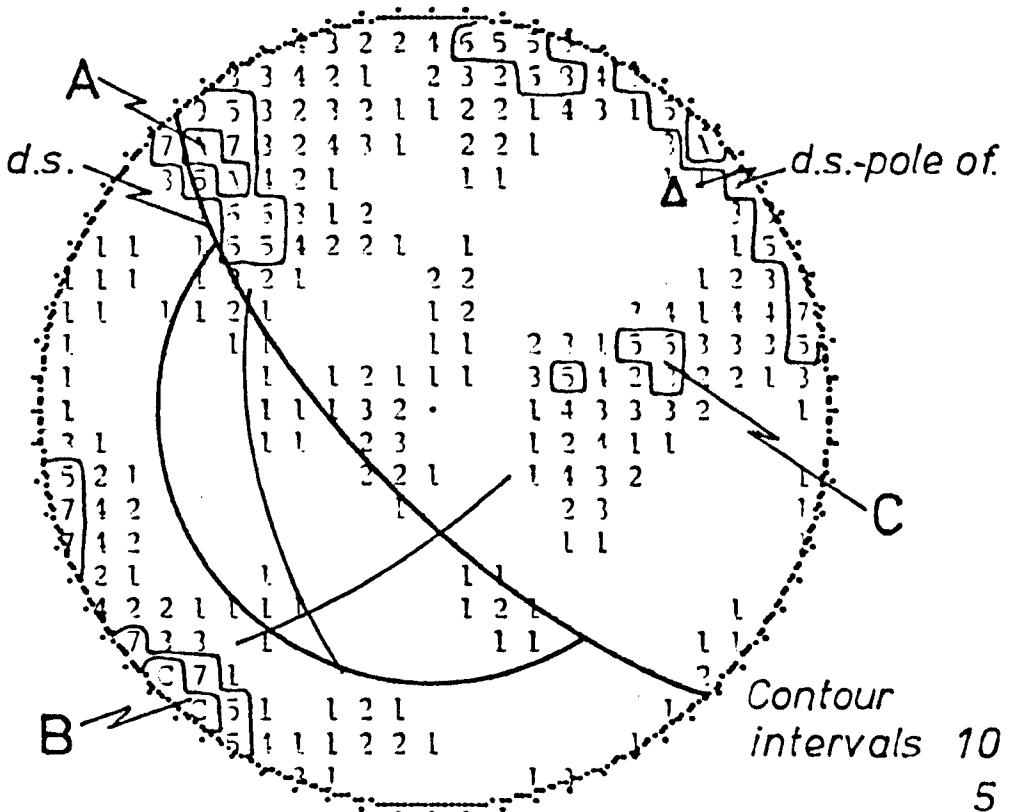
POLES

NO. OF POINTS =

142



DENSITY PLOT - SEARCH ELLIPSE = 1.00 3



Site examination shows that there was some such wedge failure but the rock has a predominantly very broken and heaved appearance. However the total absence of a pre-split and presumably the cause of its failure is not stability but close proximity of a major joint set to the design face. This is well identified from Figure 13.5 where the pole of the design face is shown to be within fifteen degrees of discontinuity pole concentration B.

#### 13.3.4 Location Three. (Figures 13.6 and 13.7)

There are two faces at location number three where pre-splitting was used - a low east facing face and a high west facing face, each face forming the side of a cutting.

A discontinuity stereographic projection for the low face is given in Figure 13.6 which illustrates:

- a. Possible minor plane failure from discontinuity concentration C and
- b. major wedge failure along the intersection of concentrations D and B.

Fig. 13.6.  
location number 3.

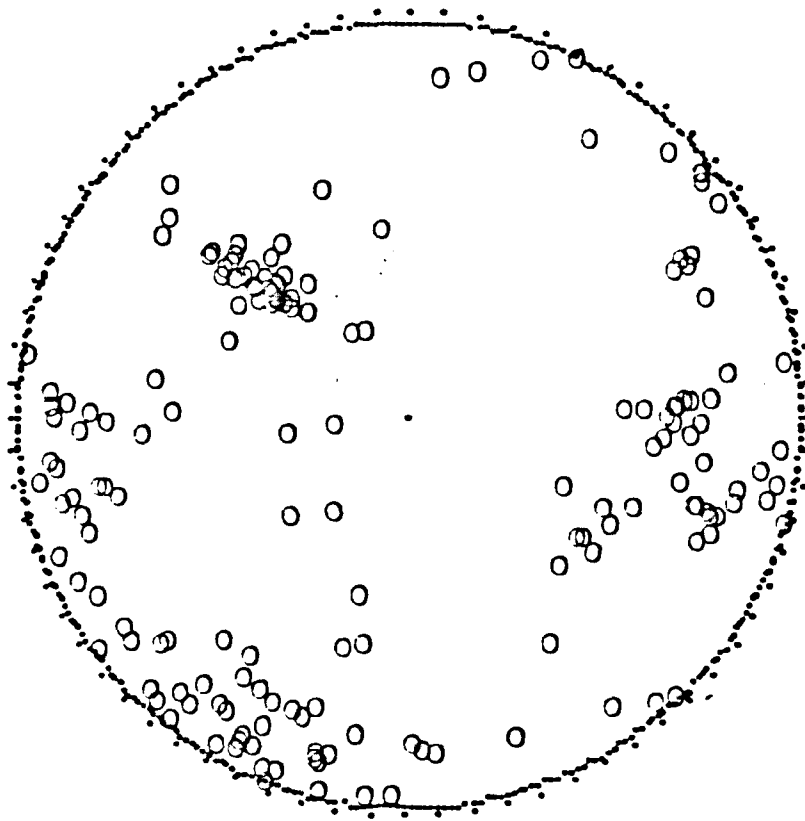
SCALE = 100MM

SCHMIDT

POLES

NO. OF POINTS =

179



DENSITY PLOT - SEARCH ELLIPSE = 1.00 %

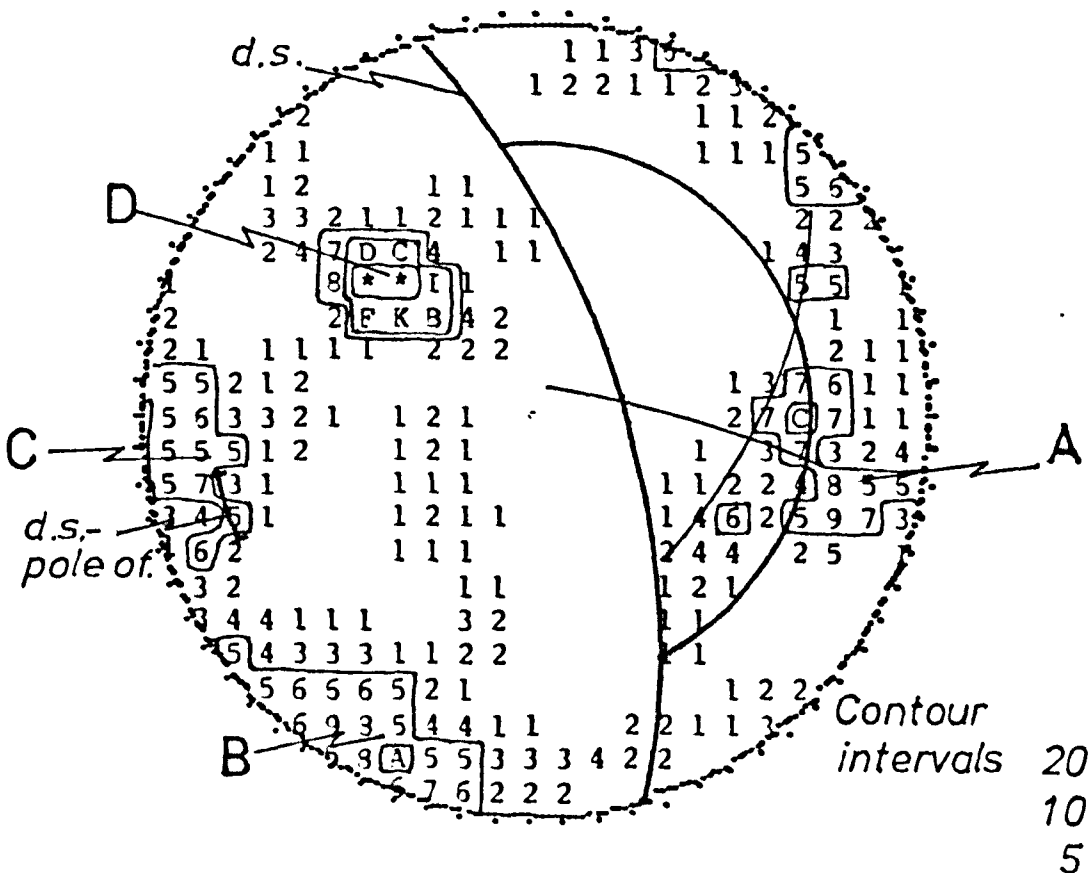


Fig. 13.7.  
location number 3.

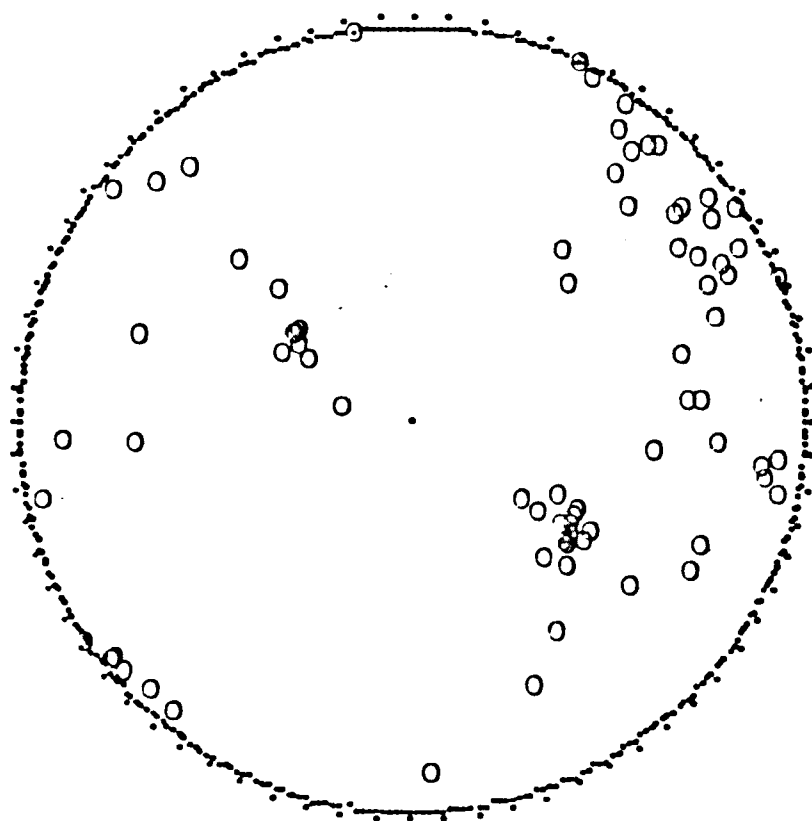
SCALE = 100MM

SCHMIDT

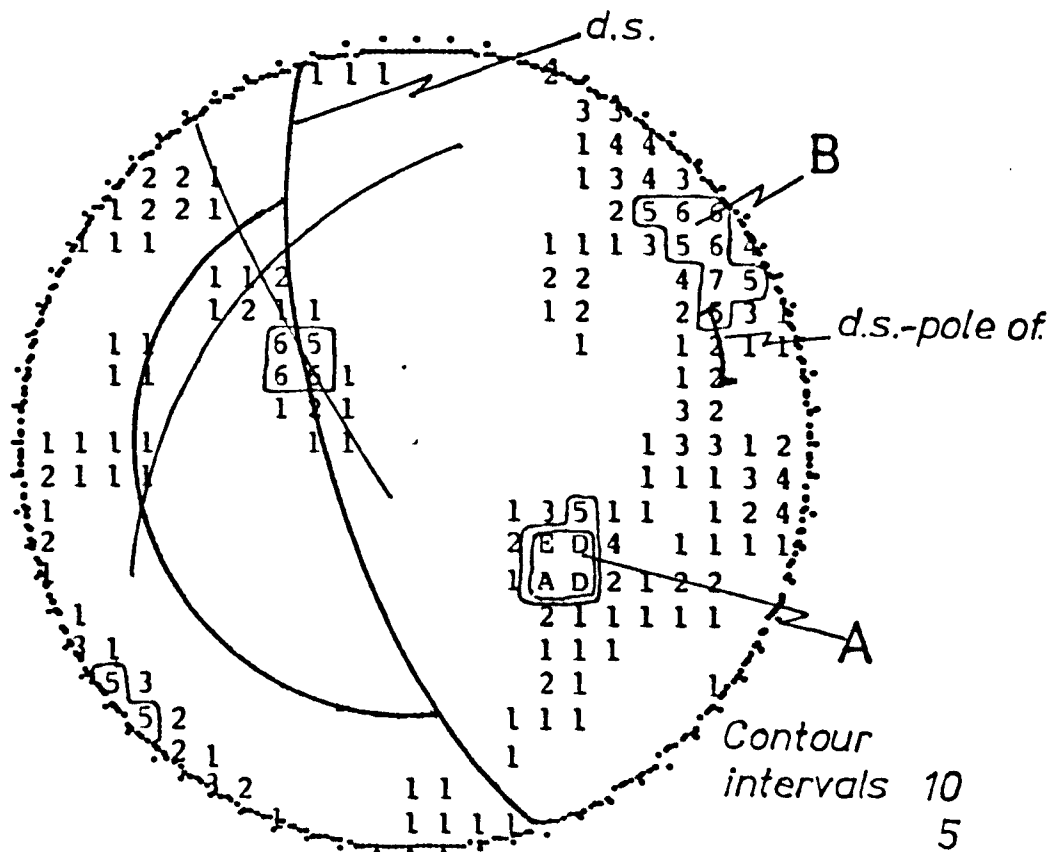
POLES

NO. OF POINTS =

79



DENSITY PLOT - SEARCH ELLIPSE = 1.00



These failures were present in the face which was poorly pre-split, the pole of the design slope being within concentration C as shown by the stereoplot.

A discontinuity stereographic projection for the high face is given in Figure 13.7 which illustrates that major wedge failure will occur on the intersection of concentrations (joint sets) A and B which are the prevalent sets for this face.

Massive failure of this specified type occurred during excavation resulting in huge volumes of excess rock having to be excavated or removed at extra expense in order to stabilize this face. It is important to note that the pole of the design slope also partially lies within discontinuity concentration B.

#### 13.3.5 Location Number Four. (Figures 13.8 and 13.9)

The geometry of this location is somewhat similar to location number three in that it is a cutting with a west facing high face and an opposed low face.

The stability of the low face is displayed by

Figure 13.8 which illustrates the possibility of plane failure from part of discontinuity set A and no significant wedge failure.

Some plane failure was apparent in the face but a very rough finish was obtained with few pre-split half barrels. This is thought to be due mainly to bad blasting.

In contrast the stability of the high west facing pre-split slope is displayed by Figure 13.9 which illustrates the possibility of major plane failure along discontinuity set A dipping directly into the carriageway at approximately forty five degrees and possible wedge failure along the intersection of sets A and B dependent on the angle of friction of the discontinuity sets.

In the field plane failure is predominant at the south end of the face and in the rest is present in the top portions of the face. This was one of the more successful pre-split faces although having an overall splitting index of under 30%.

SCALE = 100MM

SCHMIDT

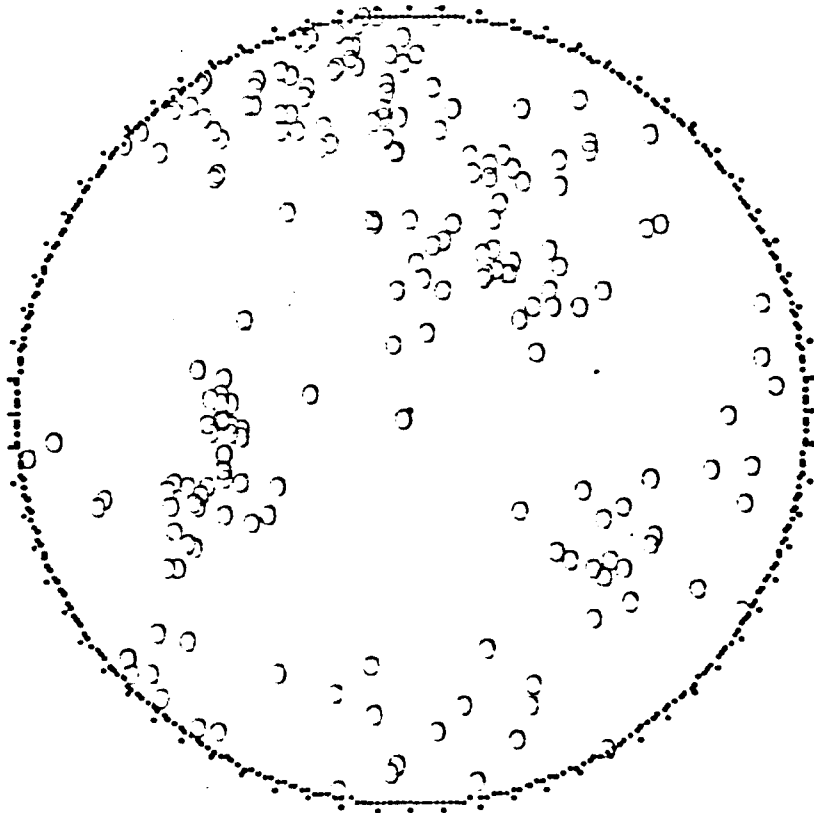
POLES

NO. OF POINTS =

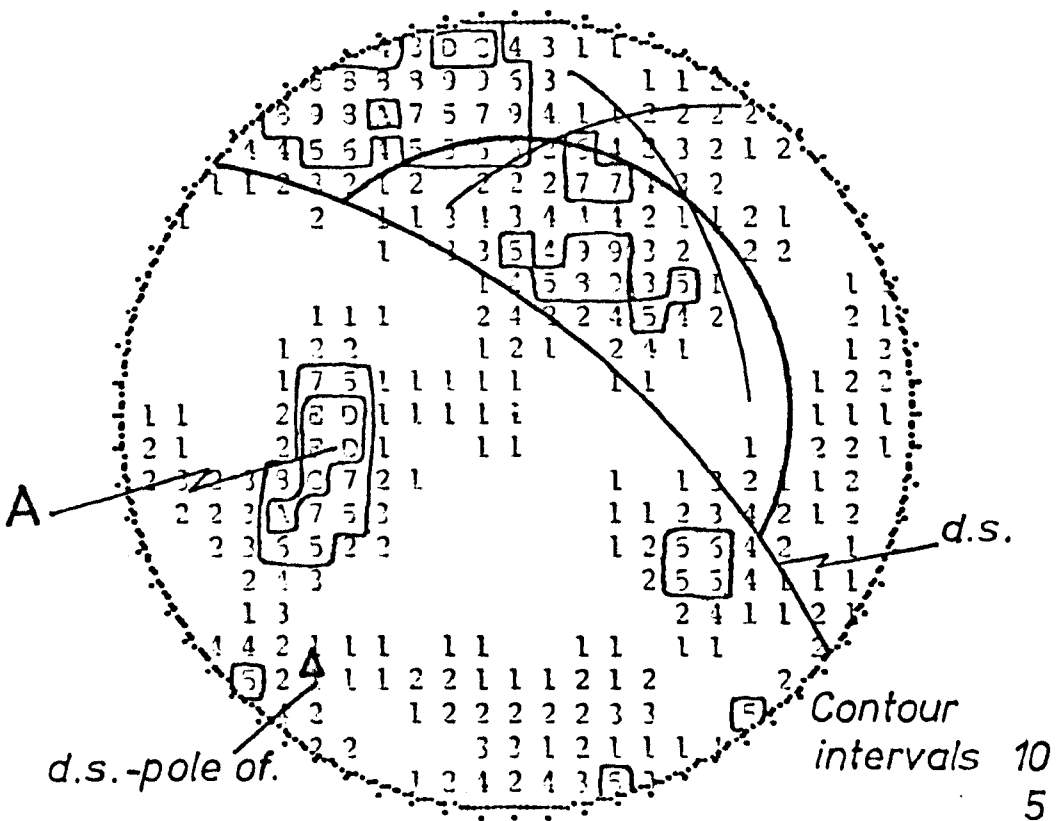
200

Fig. 13.8.

location number 4.  
low face.



DENSITY PLOT - SEARCH ELLIPSE = 1.00 3



SCALE = 10MM

SCHEMATIC

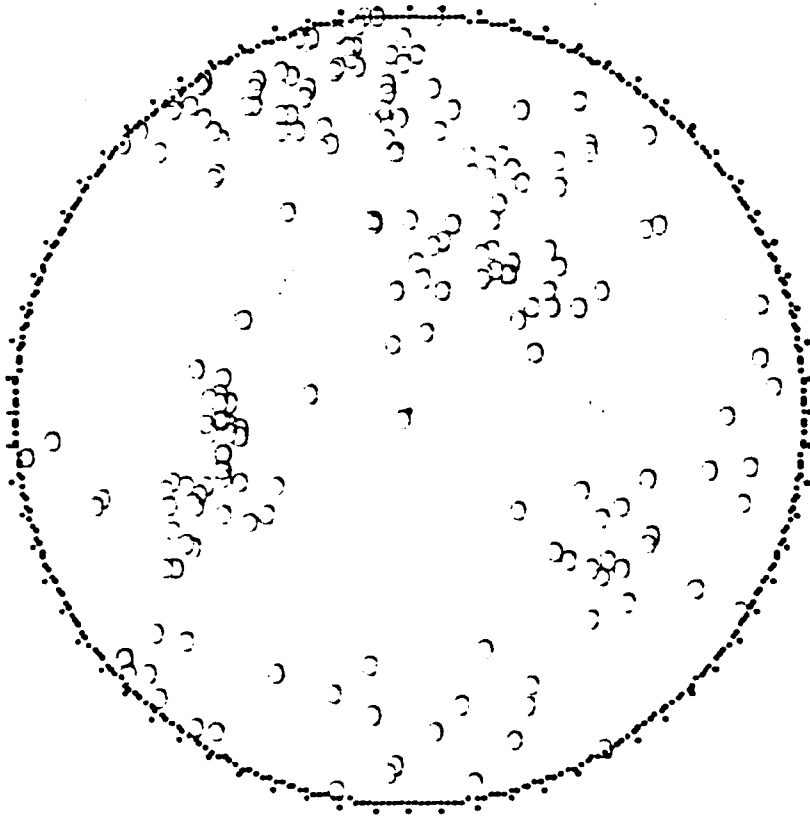
POLES

NO. OF POINTS =

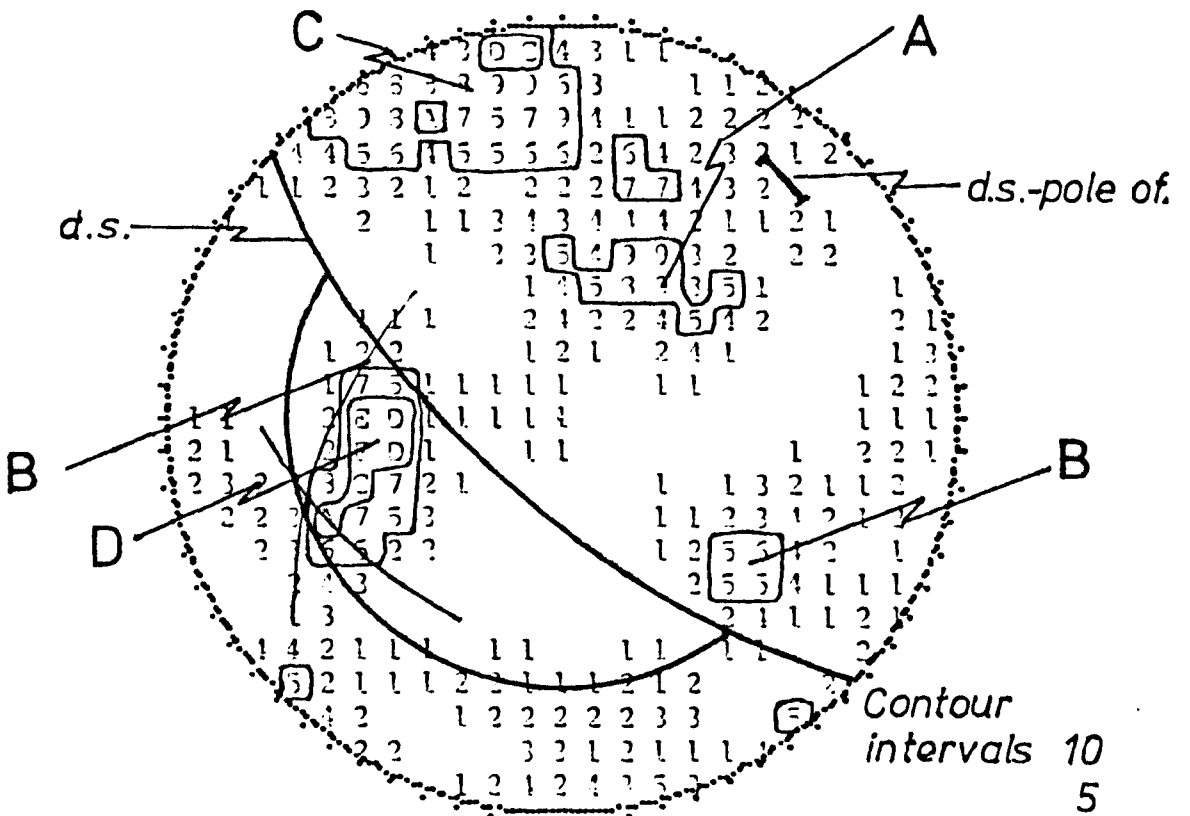
200

Fig. 13.9.

location number 4.  
high face.



DENSITY PLOT - SEARCH ELLIPSE = 1.00



13.3.6 Location Number Five. (Figure 13.10)

Figure 13.10 illustrates the distribution of discontinuities at location number five. It can be readily seen that there are no real major stability problems involved apart from minor instability from the intersection of two joint sets B and D. Also some steep plane failure is possible.

This was the second best pre-split face from locations one to eight, wedge and some plane failure mainly occurring in the top portions of the face. Minor problems were present within the face due to the close proximity of joint sets E and C, but where major discontinuities have occurred the deviating boreholes have tended to follow these. Some areas of the face show few pre-split half barrels and in these areas this jointing is more predominant.

13.3.7 Location Number Six. (Figure 13.11)

The pre-splitting at location number six was not very successful. The lack of success in obtaining the designed profile is attributable firstly and predominantly to stability problems and secondly to

Fig. 13.10.  
location number 5.

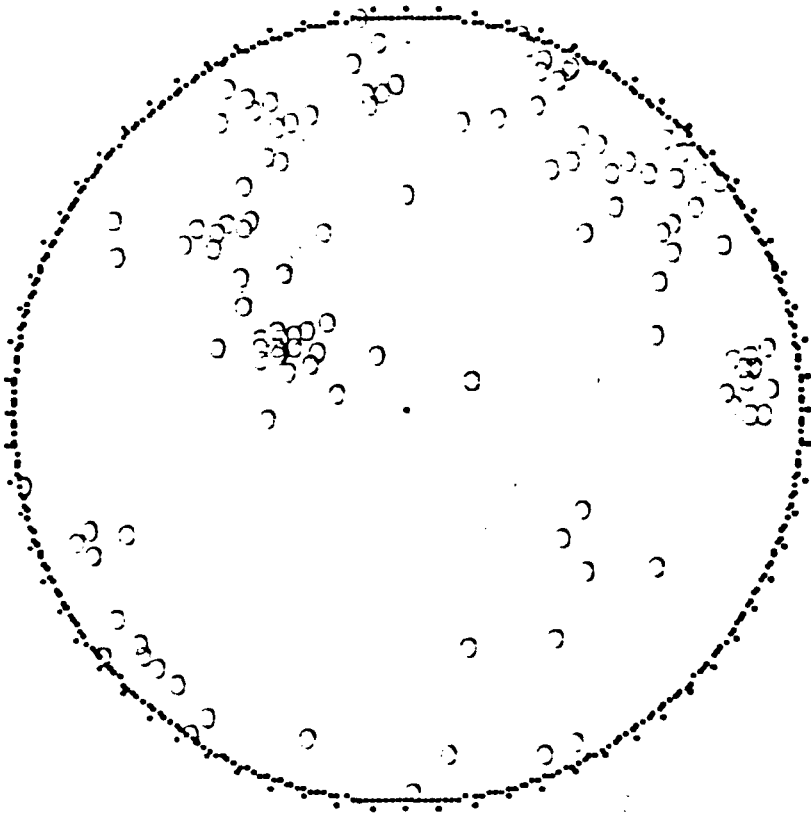
SCALE = 100MM

SCHMIDT

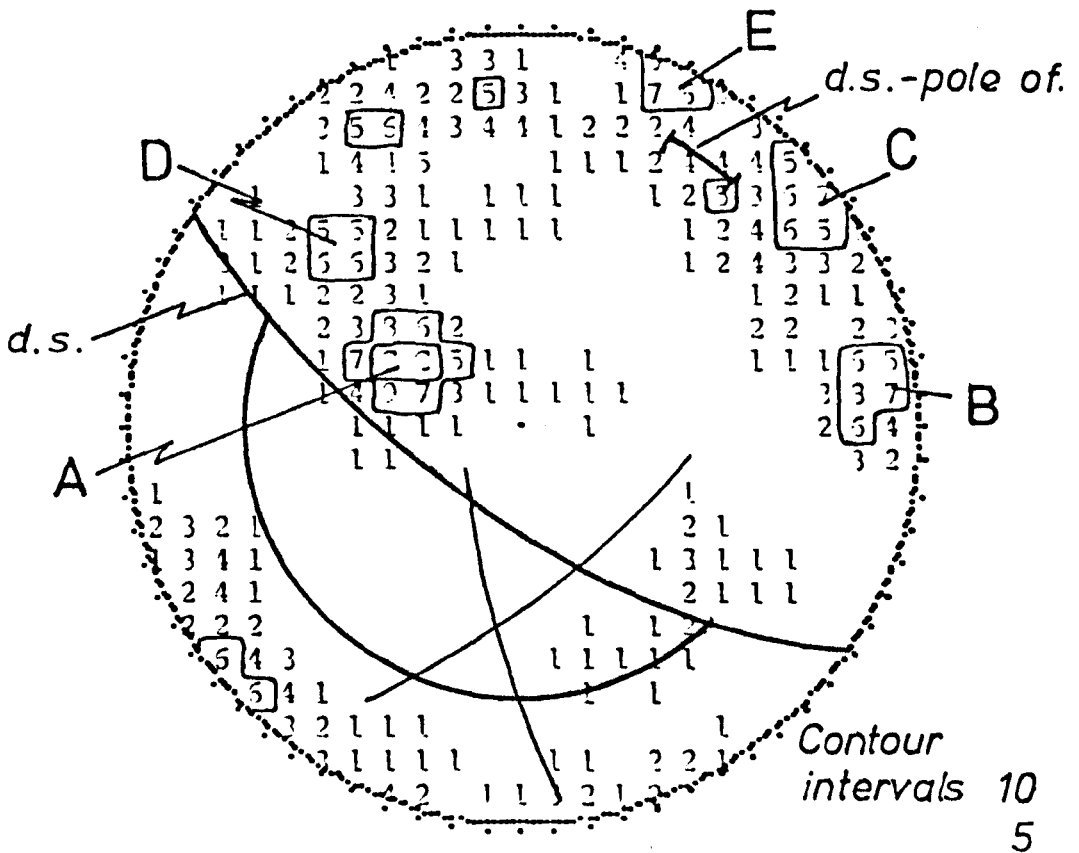
POLES

NO. OF POINTS =

120



DENSITY PLOT - SEARCH ELLIPSE = 1.00 3



the presence of three closely grouped discontinuity sets within twenty degrees of the design face.

Figure 13.11 clearly shows minor plane failure from discontinuity subset C and major wedge failure on the intersection of discontinuity sets A and C. This intersection is represented as a zone in the diagram due to the extent of the major discontinuity set A.

#### 13.3.8 Location Number Seven. (Figure 13.12)

There was significant failure of the pre-split face at location number seven due to instability of the rock mass, in fact so much so that the face was trimmed back to a more stable angle of 63.4 degrees (2:1). The reasons for this failure are illustrated in Figure 13.12.

It can be seen that due to the spread of poles that some plane failure, especially from the edges of discontinuity concentrations A and B is possible. Major wedge failure can occur along the intersection of discontinuity sets A and B with further wedge failure possible along the intersection of sets A and C.

Fig. 13.11.

location number 6.

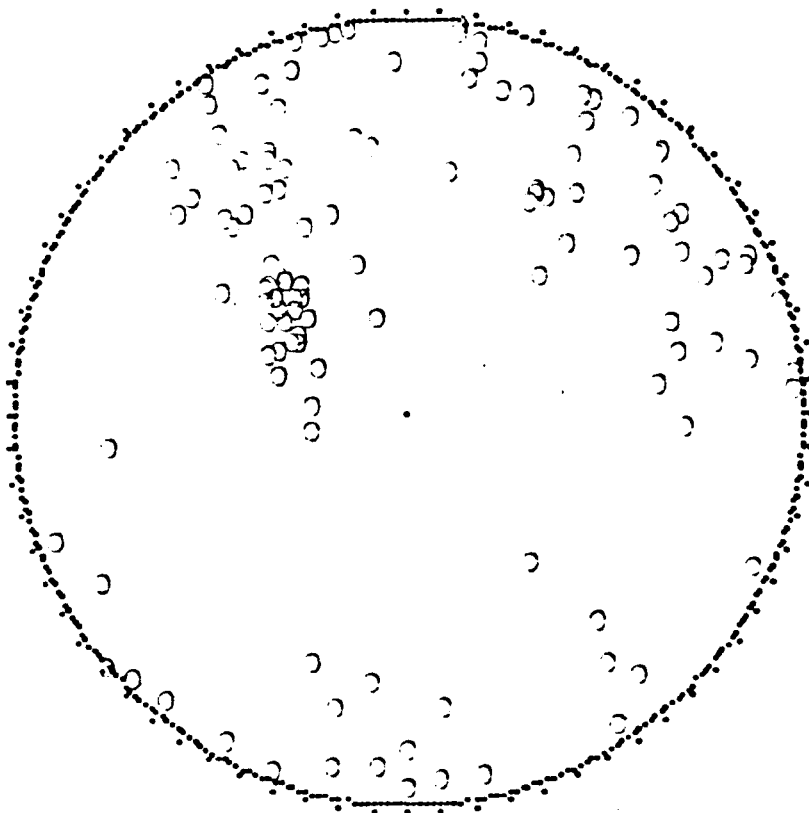
SCALE = 100:1

SCHMIDT

POLES

NO. OF POINTS =

120



DENSITY PLOT - SEARCH ELLIPSE = 1.00 3

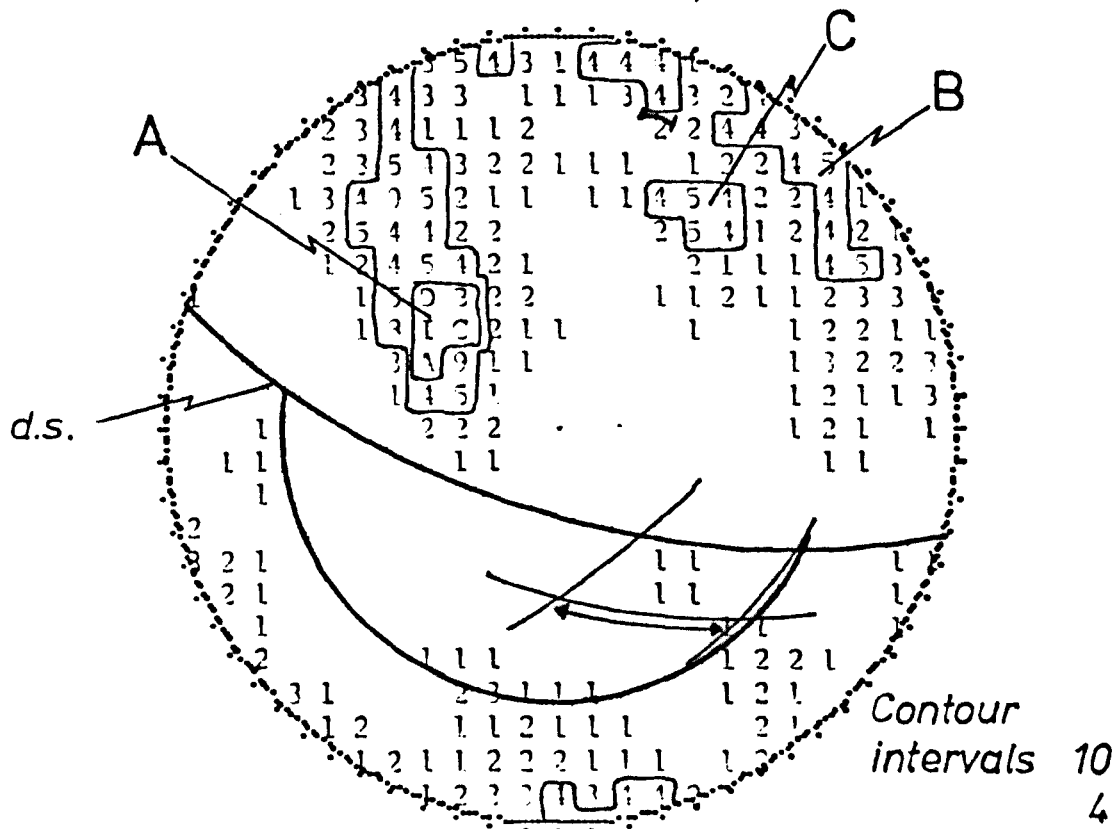


Fig. 13.12.

location number 7.

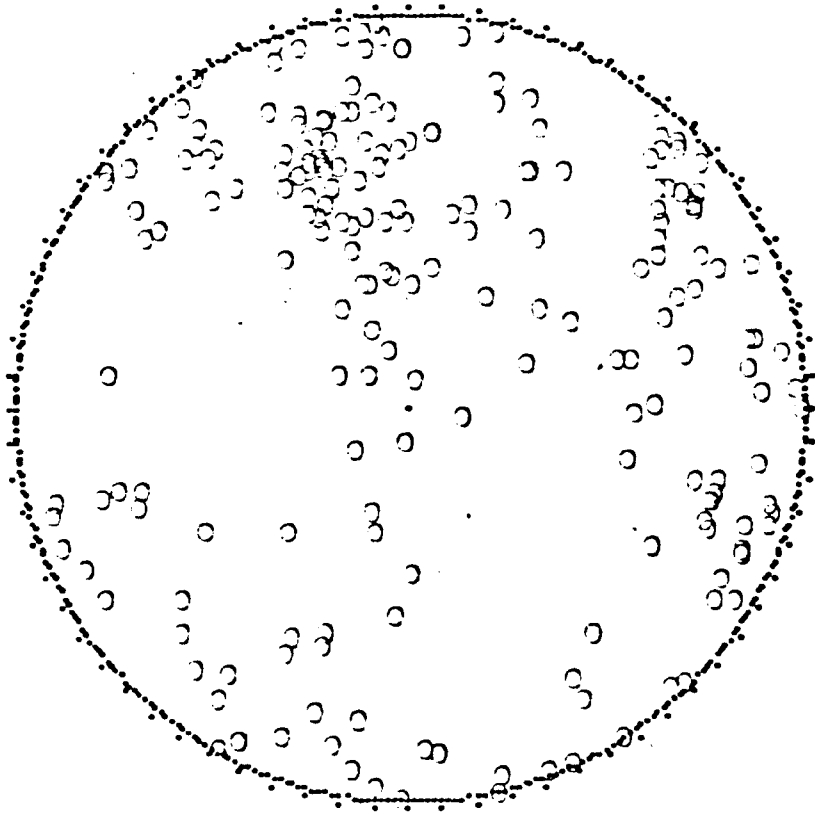
SCALE = 10000

SEARCH

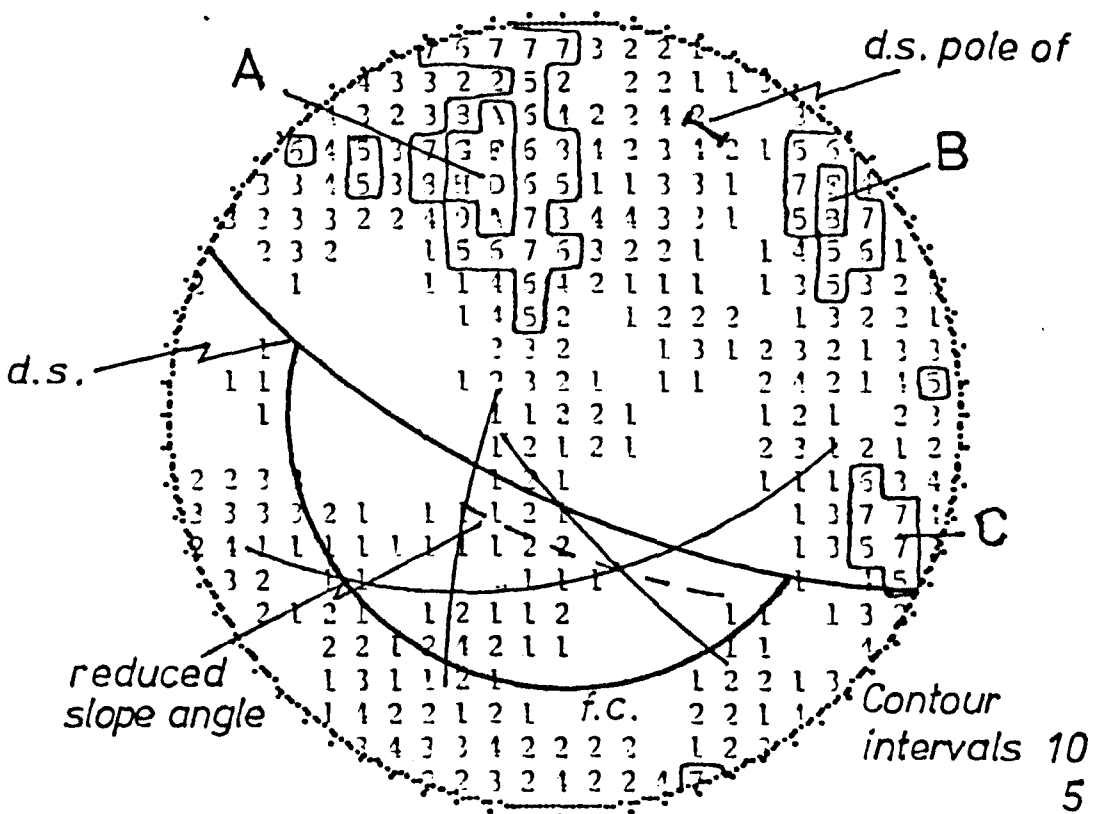
POLES

NO. OF POINTS =

210



DENSITY PLOT - SEARCH ELLIPSE = 1.00 3



It is obvious that the reduced slope angle by trim blasting negates the possibility of wedge failure between sets A and B. However the latter failure between sets A and C is still visible throughout the face, (the half barrels belonging to smooth wall blasts).

#### 13.3.9 Location Number Eight. (Figure 13.13)

The only real stability problem (from Figure 13.13) at pre-split location number eight is localised plane failure inclined at approximately forty degrees to the face. This plane failure is encircled on the diagram. Relatively few readings were taken at this face due to its relatively low height and extent compared with localities one to seven.

#### 13.3.10 Location Number Nine. (Figure 13.14)

The author (as already intimated) was closely involved with pre-splitting at location number nine and was also involved in preliminary site investigation. The stability of the final face is illustrated by figure 13.14 which shows three possible

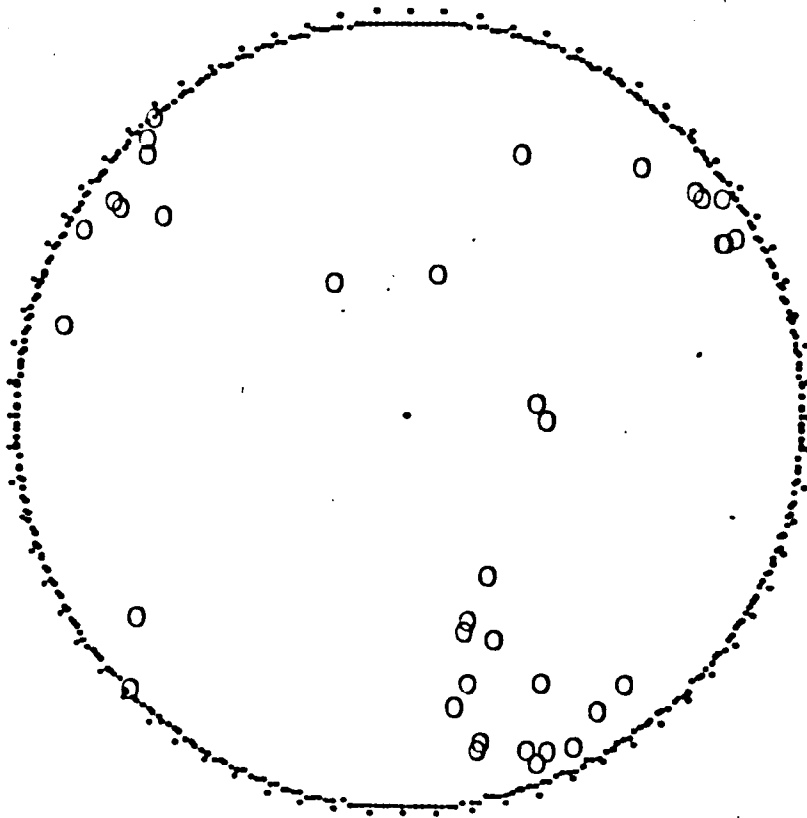
Fig. 13.13.  
location number 8.

SCALE = 100MM

SCHMIDT

POLES

NO. OF POINTS = 37



DENSITY PLOT - SEARCH ELLIPSE = 1.00

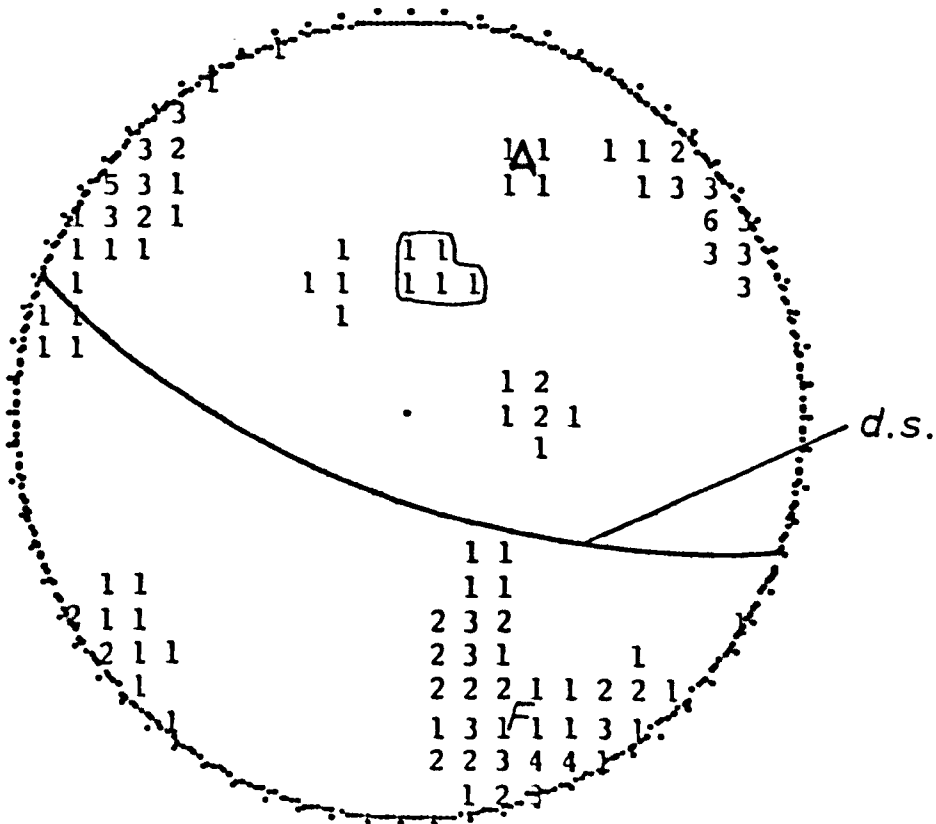


Fig. 13.14.  
location number 9.

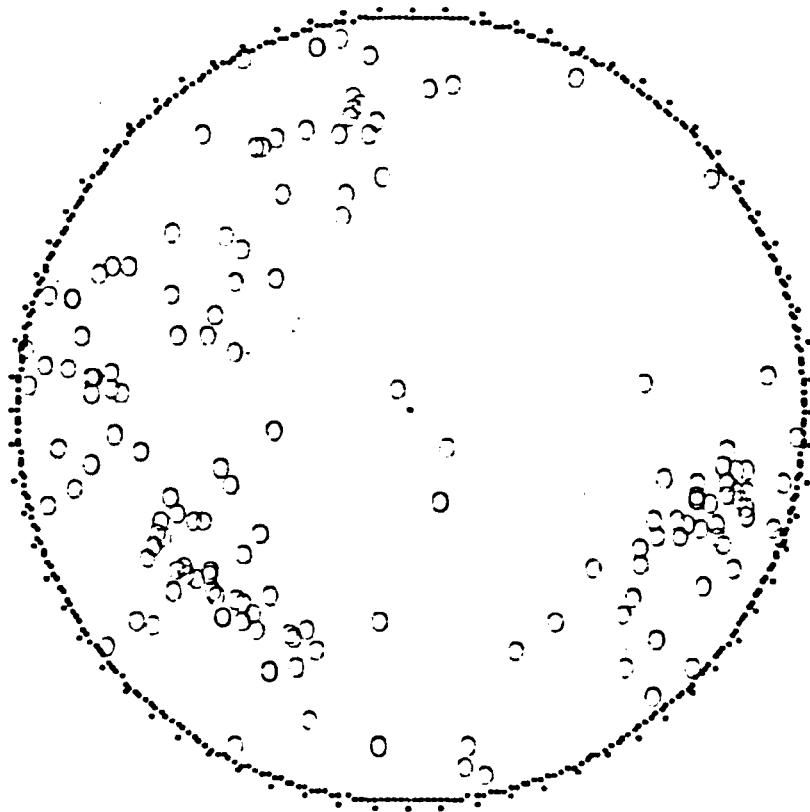
SCALE = 10041

SCHMIDT

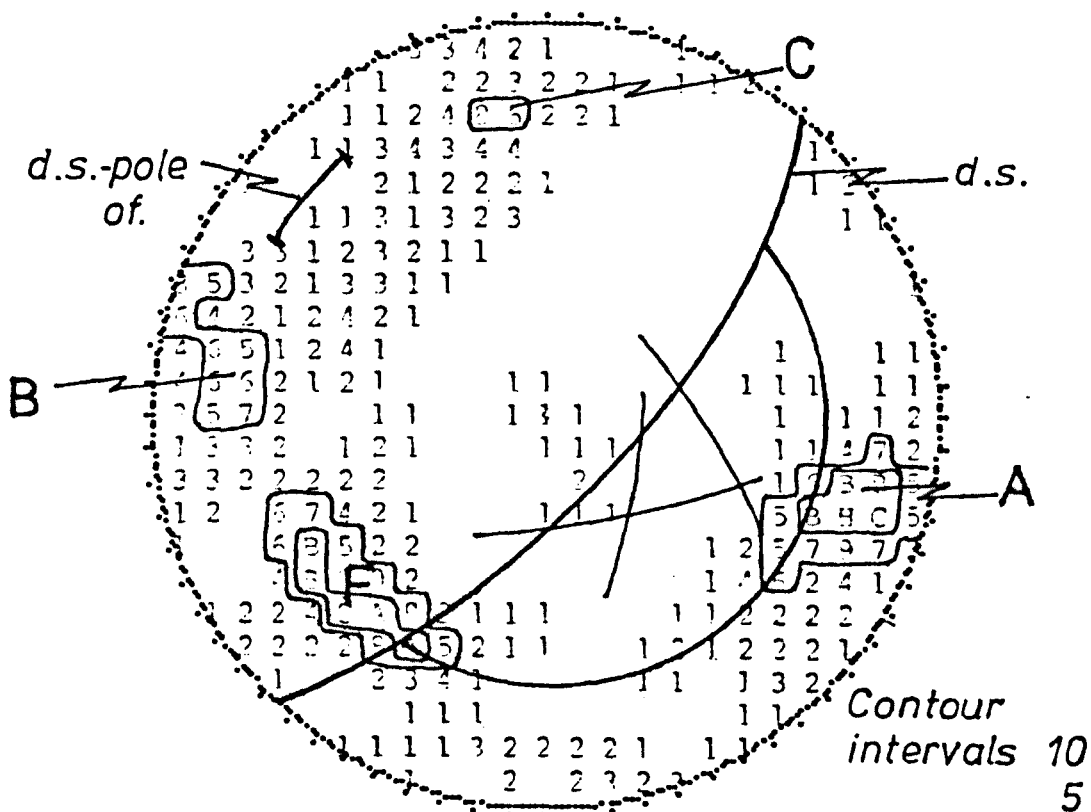
POLES

NO. OF POINTS =

155



DENSITY PLOT - SEARCH ELLIPSE = 1.00 3



modes of failure. The first is by minor amounts of plane failure from disseminated joint planes of sixty five degrees dip, these accounting for very minor amounts of rock failure. Secondly and more importantly by wedge failure through the combination of the Foliation (F) and discontinuity concentration C. However due to the geometry involved, slippage would predominantly occur along plane C, the foliation being orientated approximately perpendicular to the face. Thirdly by wedge failure along the intersection of the two small discontinuity concentrations B and C.

Due to the extremely dominant foliation however, this has generally limited the size of unstable blocks in the face and although instability was present, the volumes of rock involved were extremely low. A highly successful pre-split face was obtained.

### 13.3.11 Location Number Ten. (Figure 13.15)

It is obvious from the major concentrations of poles displayed in Figure 13.15 that there are no sizeable stability problems to be encountered. The pre-splitting is highly successful and failures in the face are limited to the outcrop on benches of a couple

Fig. 13.15.

location number 10.

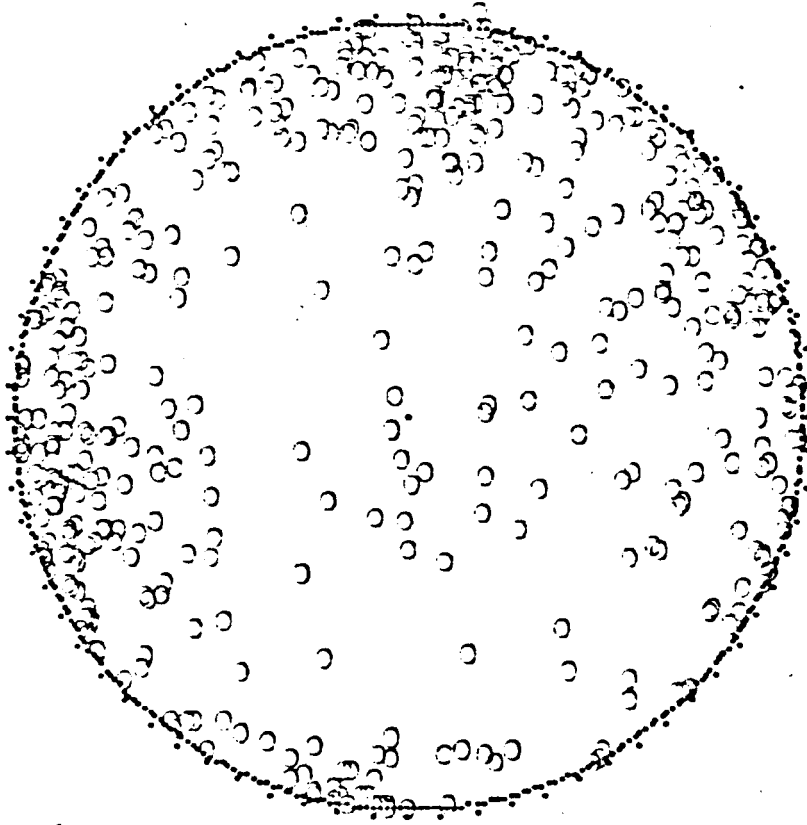
SCALE = 10000

SECTION

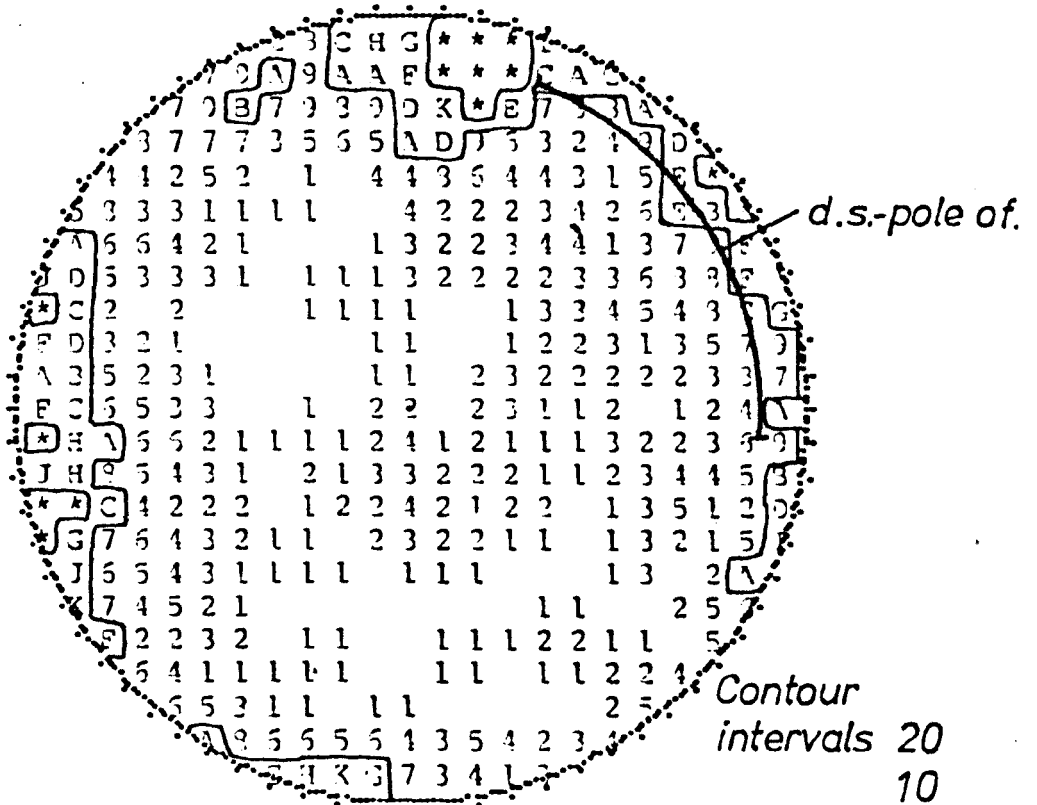
90655

NO. OF POINTS =

476



DENSITY PLOT - SEARCH ELLIPSE = 1.00 3



of shear planes passing through the lava complex, with an extremely low relative volume of material absent mainly due to preventive measures.

The high curvature of this face is represented by the line of the poles to the face at different points, the majority of the face being within the bottom twenty degrees of this line. It is worthwhile to note in passing that the portion of the face which failed to pre-split was the most southerly facing and whose pole lies within five degrees of the major discontinuity concentration.

#### 13.3.12 Location Number Eleven. (Figure 13.16)

Location number eleven is the Associated Portland Cement Quarry at Dunbar (Oldest Production Quarry) which has two main faces both of which are pre-split. One face is a protected haul road and the other the main production face, as seen from Figure 13.16 these are roughly perpendicular to each other. Figure 13.16 clearly illustrates that there are no serious stability problems on either face and the faces stand extremely well in the quarry.

DUNBAR TOTAL.

SCALE = 100MM

SCHMIDT

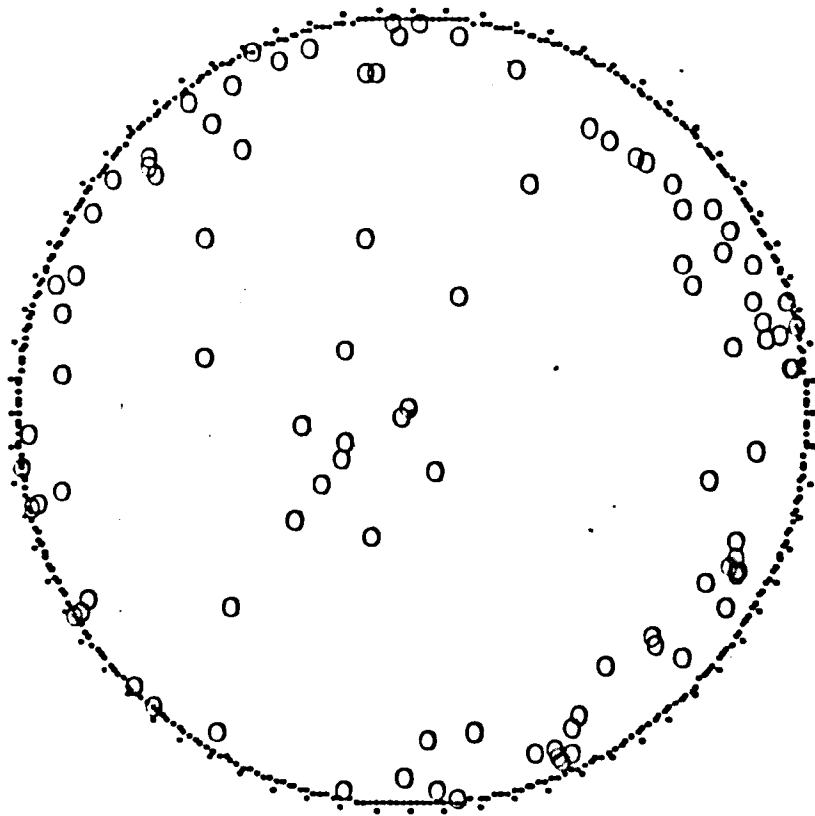
POLES

NO. OF POINTS =

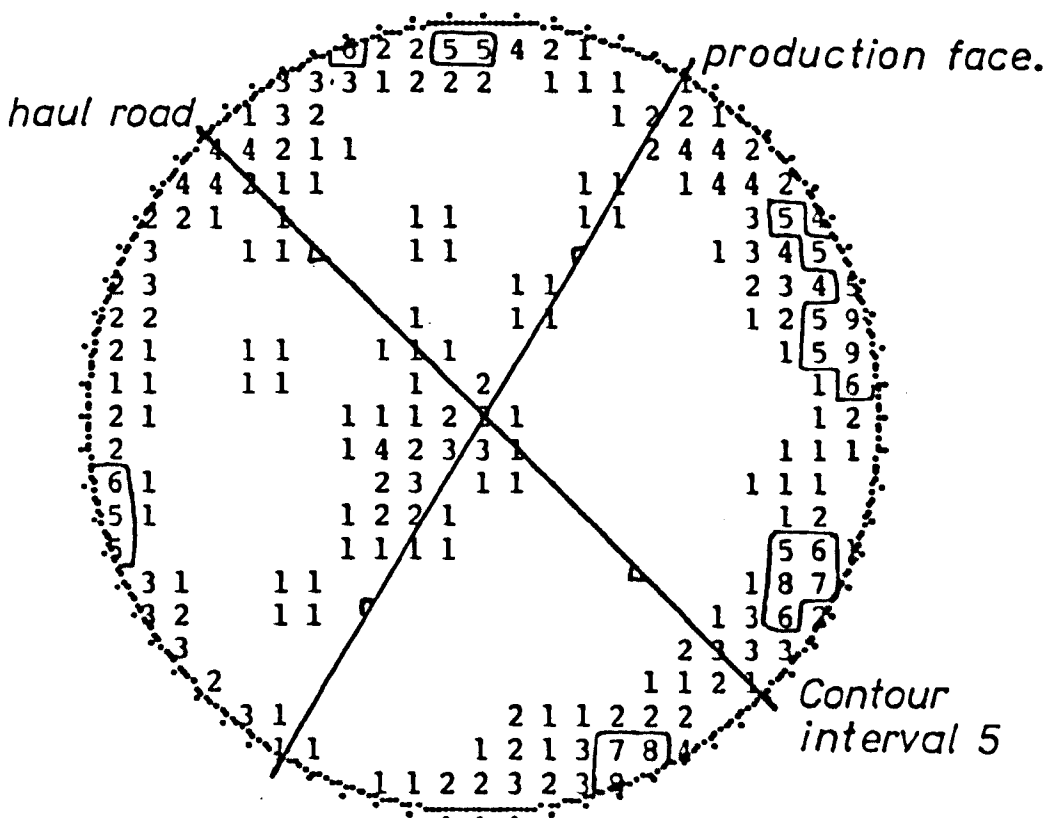
100

Fig. 13.16.

location number 11.



DENSITY PLOT - SEARCH ELLIPSE = 1.00 %



OK,

#### 13.4 DISCUSSION

It may appear unusual to the reader but it is fact that no stability survey whatsoever was made for the whole of locations one to eight inclusive, pre-excavation. The 71.5 degree slope angle was arbitrarily chosen as it is 3:1 which was the common design slope in rock for this area, and for no other logical reason.

From the previous detailed analyses it is obvious that some of these pre-split faces were doomed to failure from the outset due to rock stability problems. In most of these cases relatively expensive pre-splitting should not even have been considered. In other cases, lowering the design slope angle would have remedied the majority or at least a large proportion of the instability in certain cases. A noteworthy example of such a case is location number seven where the face was cut back to 63.4 degrees (2:1) by smoothwall blasting which eliminated the majority of wedge failures.

Although this chapter may state the obvious to geotechnical engineers, by the author's field experience the majority of site engineers whether they

be regional or consulting engineers, have little knowledge of slope stability analysis or blasting, the majority of the cuttings being designed by draughtsmen and surveyors without consulting reality in the field.

### 13.5 CONCLUSIONS

It can be concluded that stability is a decisive factor in the success of any design slope on its excavation, be it bulk blasted or pre-split.

It is therefore imperative that a rigorous discontinuity survey and geotechnical appraisal be made by suitably qualified personnel before the design stage is completed.

The final face angle should be chosen as that which minimises instability within an economically viable level.

If instability is still present in a major form in the final design face then the proposed use of pre-split blasting should be reconsidered.

## 14 GEOSTATIC STRESS FIELDS

### 14.1 FOREWORD

Due predominantly to the fact that in the British Isles there have been no major geostatic stress fields recorded at the surface which are of sufficient magnitude to effect surface pre-splitting, this chapter is included for completeness and academic interest only. However in such countries as the United States and Canada, surface static stress fields of sizeable magnitude have been reported, (Nicholls and Duvall, 1966a etc.) and also in deep hard rock mining operations such as in South Africa the geostatic stress fields created by the great depths are considerably large, (Plewman and Starfield, 1965) and seriously affect sub-surface pre-splitting operations.

### 14.2 PREVIOUS WORK

Work on the effect of static stress fields on the mechanisms of pre-splitting has been carried out by

Kutter (1967) and Nicholls and Duvall (1966a). Nicholls and Durrall concluded that "it is much easier to pre-split in the direction of the maximum insitu compressive strength than at any angle to this direction" and also "that the tensile stress generated (by the pre-splitting effect between the pre-split boreholes) must exceed, at every point between holes to be pre-split, the sum of the insitu compressive stress at right angles to the pre-split line and the dynamic tensile strength of the rock".

The conclusions of other authors' work roughly coincide with those of Nicholls and Duvall. However the author disagrees on slight technicalities with Nicholls and Duvall, such that in the author's view "the sum of the insitu compressive stress at right angles to the pre-split line" should read "the sum of the insitu compressive stress in the propagating fracture tip at right angles to the pre-split line" as the process is predominantly caused by quasi-static rather than dynamic effects and is therefore related to fracture extension rather than the dynamic breakage of intact rock, as is agreed within their work.

### 14.3 THEORY

As the initial zone of fracturing around a borehole is created by the tangential tensile hoop stresses of the dynamic compressive pulse, the effect of a geostatic stress field on this will be dealt with first.

Using the analogy for a single hole of a hole in an infinite plate with an internal pressure ( $P_i$ ) of zero (the transit of the dynamic shock wave through the borehole wall precedes the pressure build up of the gases of detonation) the tangential stress at the surface of the hole created by the geostatic stress field with principal stresses ( $\sigma_1$  and  $\sigma_2$  ( $\sigma_1 > \sigma_2$ )) from Kirsch's solution is:-

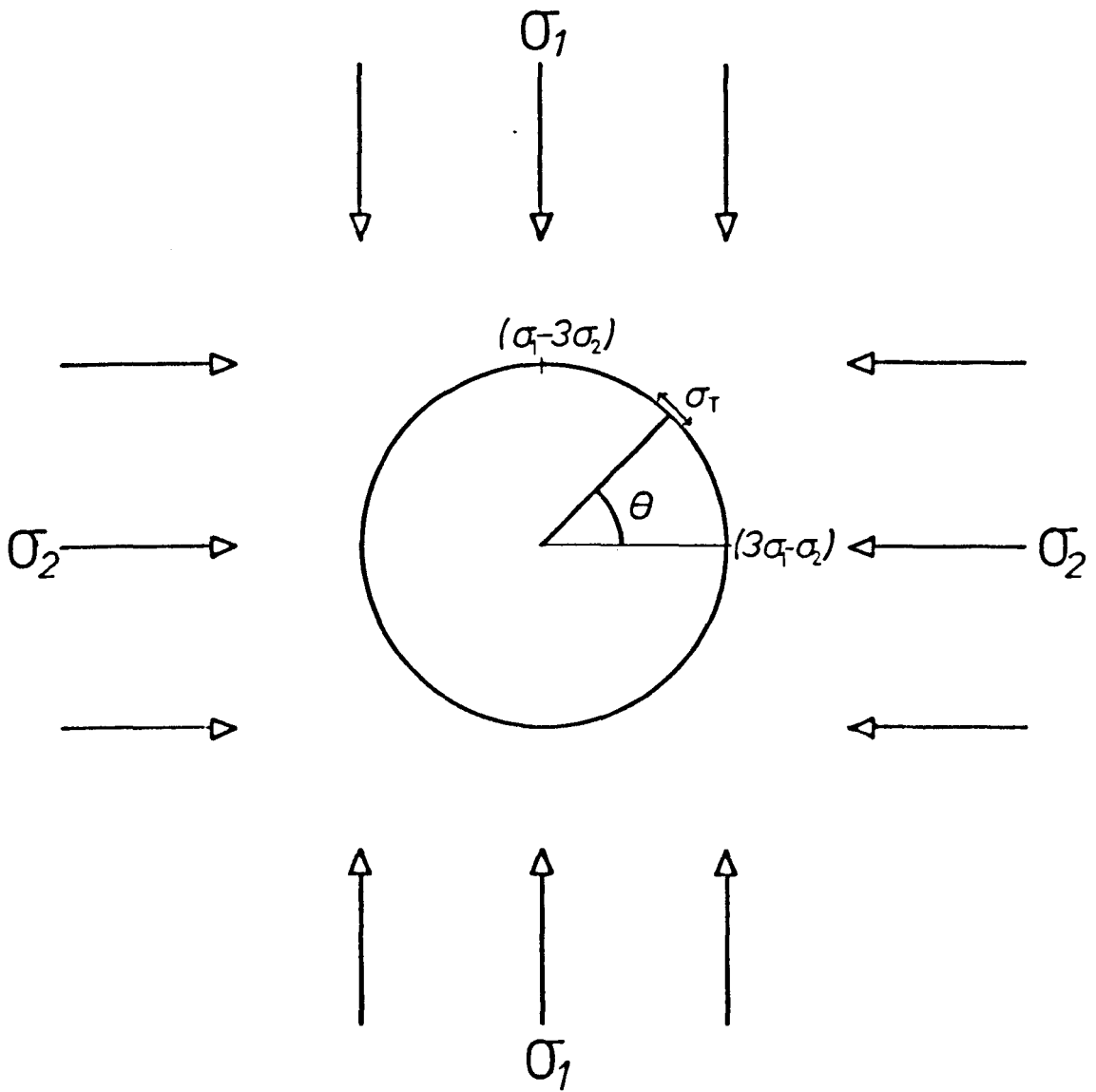
$$\sigma_T = \sigma_1 + \sigma_2 + 2(\sigma_1 - \sigma_2)\cos 2\theta \quad \text{see Figure 14.1.}$$

where  $\theta$  is the angle between the point on the circumference of the hole at which the tangential stress is measured, the centre of the borehole and axis of the second principal stress.

From this equation it can be seen that maximum tangential stress;

$$\sigma_T^{\text{MAX}} = 3\sigma_1 - \sigma_2$$

occurs when  $\theta=0$  and  $\pi$  i.e. parallel to the first



$$\sigma_\tau = \sigma_1 + \sigma_2 + 2(\sigma_1 - \sigma_2)\cos 2\theta$$

Fig. 14.1.

*Tangential stresses at the surface of a circular opening subject to a planar external stress field.*

principal stress whereas minimum tangential stress;

$$\sigma_T^{\text{MIN}} = 3\sigma_2 - \sigma_1$$

occurs when  $\theta = \pi/2$  and  $3\pi/2$  i.e. parallel to the second principal stress.

The radial stress, due to zero internal pressure is:

$$\sigma_R = 0$$

The longitudinal stress;

$$\sigma_L = \sigma_3 + V(\sigma_1 - \sigma_3)$$

where  $V$  is the Poisson's Ratio of the medium and  $\sigma_3$  is parallel to the borehole.

As the minimum tangential stress occurs perpendicular to the first principal stress then fracturing is most likely to occur first at these two points, extending radially outwards from the borehole and parallel to .

If the maximum peak tangential stress component within the tensile tail of the dynamic compressive wave =  $Pd$  (approximating the point of fracture initiation to the surface of the borehole) and the dynamic tensile strength of the medium =  $Td$ , three separate cases exist mathematically, (see Figure 14.2).

$$(1) \quad -Pd < 3\sigma_2 - \sigma_1 + Td$$

i.e.  $-Pd$  is less than the sum of the minimum

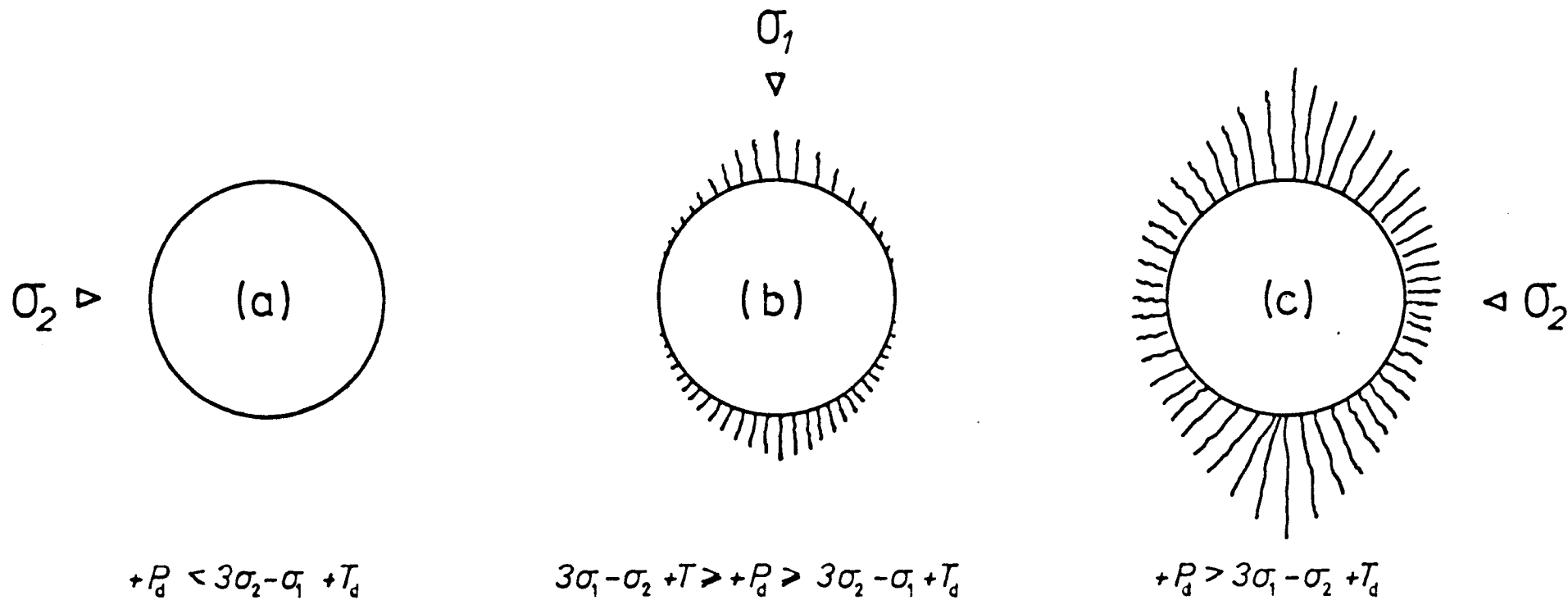


Fig. 14.2.

Conditions for fracture initiation at the surface of a borehole in a biaxial stress field

(a) no fracture initiation. (b) no fracture initiation parallel to  $\sigma_2$ .

(c) fracturing throughout borehole circumference illustrating preferential fracture growth parallel to  $\sigma_1$ .

tangential static stress and the dynamic tensile strength of the rock, and therefore no fracturing of the borehole wall can occur.

$$(2) \quad 3\sigma_1 - \sigma_2 + T_d > -Pd > 3\sigma_2 - \sigma_1 + T_d$$

as  $-Pd > 3\sigma_2 - \sigma_1 + T_d$  fracturing will occur parallel to the direction of  $\sigma_1$  at  $\theta = \pi/2$  and  $3\pi/2$  as  $3\sigma_1 - \sigma_2 + T_d > -Pd$  the peak tangential dynamic tensile stress is not sufficient to overcome the sum of the maximum tangential static stress and tensile strength of the rock and therefore no radial fracturing will occur perpendicular to the direction of  $\sigma_1$  at  $\theta=0$  and  $\pi$  (Figure 14.2b).

$$(3) \quad -Pd > 3\sigma_1 - \sigma_2 + T_d$$

as the peak dynamic tangential tensile radial stress exceeds the sum of both the maximum static tangential stress and the dynamic tensile strength, the radial fracturing will occur throughout the circumference of the borehole but persist longer in the direction parallel to  $\sigma_1$  due to the more favourable stress conditions, (Figure 14.2c).

The worst orientation of the maximum principal stress to a pre-split line for the initiation of fracturing around the pre-split boreholes is with the maximum principal stress aligned at right angles to the pre-split line. In cases (1) and (2) there would

be no initial fracturing around the boreholes in the plane of pre-split available for extension by the explosion gases to form the pre-split.

If the geostatic stress field is greater at any point than the quasi-static stress field from neighbouring boreholes, all fracturing (case (2)) will tend to deflect away from the pre-split line and no direct pre-split will be formed. For case (3) the longest fractures will be preferentially elongated by the explosion gases at the expense of the shortest fractures which are orientated along the pre-split line. This process will effectively increase damage zone extent into the rock and reduce the maximum successful pre-split borehole separation.

Conversely the most favourable stress field orientation to pre-splitting is with the maximum principal stress aligned parallel to the pre-split line and with the minimum principal stress ( $\sigma_3$ ) parallel to the boreholes. Due to the preferential formation of fractures by the dynamic component parallel to the maximum principal stress in both cases (2) and (3), the extent of the damage zone into the rock surrounding the pre-split line is reduced and providing that the deviatoric stress ( $\sigma_1 - \sigma_2$ ) is

sufficiently high, the maximum successful pre-split borehole separation will increase.

The effect of the geostatic stress field on the quasi-static propagation of the initial fracturing is as follows:

Assuming that explosion gases are driven into the fractures induced by the dynamic component around a blast hole and that they fill the fracture concerned (as indicated by results in Chapter Eleven) then whilst the pressure within the borehole and thus the crack remains sufficient, the propagation of that fracture will continue.

Using the original Griffith energy balance (Griffith, 1921) then during stable fracture propagation:

$$\frac{dW_e}{dC_0} = \frac{dW_s}{dC_0}$$

where:  $W_e$  is the elastic strain energy

$W_s$  the surface energy in the free faces of the pre-existing (Griffith) crack

$C_0$  the half length of the pre-existing (Griffith) crack

i.e. the change in elastic energy is equal to the

change in surface energy by the creation of new cracks. However in this case we are driving the fracture by internal pressure and not by external forces and the elastic strain energy at the tip of the crack will remain constant during propagation as the pressure remains constant (due to the large reservoir of the borehole, (see Chapter Three)). Therefore neglecting the relatively small amount of reversible strain energy 'absorbed' by the increase in length of the crack:

$$dW_g = dW_s$$

where:  $W_g$  is the energy of the explosion gases

As the crack is small in volume compared with the borehole then an extreme degree of propagation is theoretically possible. However, in practice due to the high number of fractures produced and their relatively high total volume, coupled with the rapid venting of explosive gases through the borehole collar, the driving pressure within the borehole and thus the fractures concerned is quickly sufficiently reduced to inhibit fracture extension. As soon as the force exerted by the gas pressure drops below that of the geostatic stresses the fracture will close, terminating propagation.

Due to the complexity and 'state of the art' at present no further reference will be made to the measurement of surface energy as it is considered a field of research in itself!

Hoek (1965) observed that if an angled fracture is submitted to an external stress field, (see Figure 14.3), then the minimum tangential stress on the surface of the fracture occurs parallel to the line of the fracture at a point approximately ninety degrees radially away from the original crack tip towards the direction of maximum principal stress, (Figure 14.3). The new fracture formed extends in a direction approximately perpendicular to the original fracture and slowly aligns itself with the maximum principal stress. Although Hoek gave adequate proof and description of this phenomenon he was never able to mathematically explain the processes involved.

In the process of hydrofracture however the crack is internally pressurized which, with zero geostatic stress field conditions produces a tangential stress bulb extending from the crack tip with maximum surface tangential tensile stress at the apex of the crack and orientated perpendicular to the crack. Providing that the fracture is not aligned with  $\sigma_2$  then the

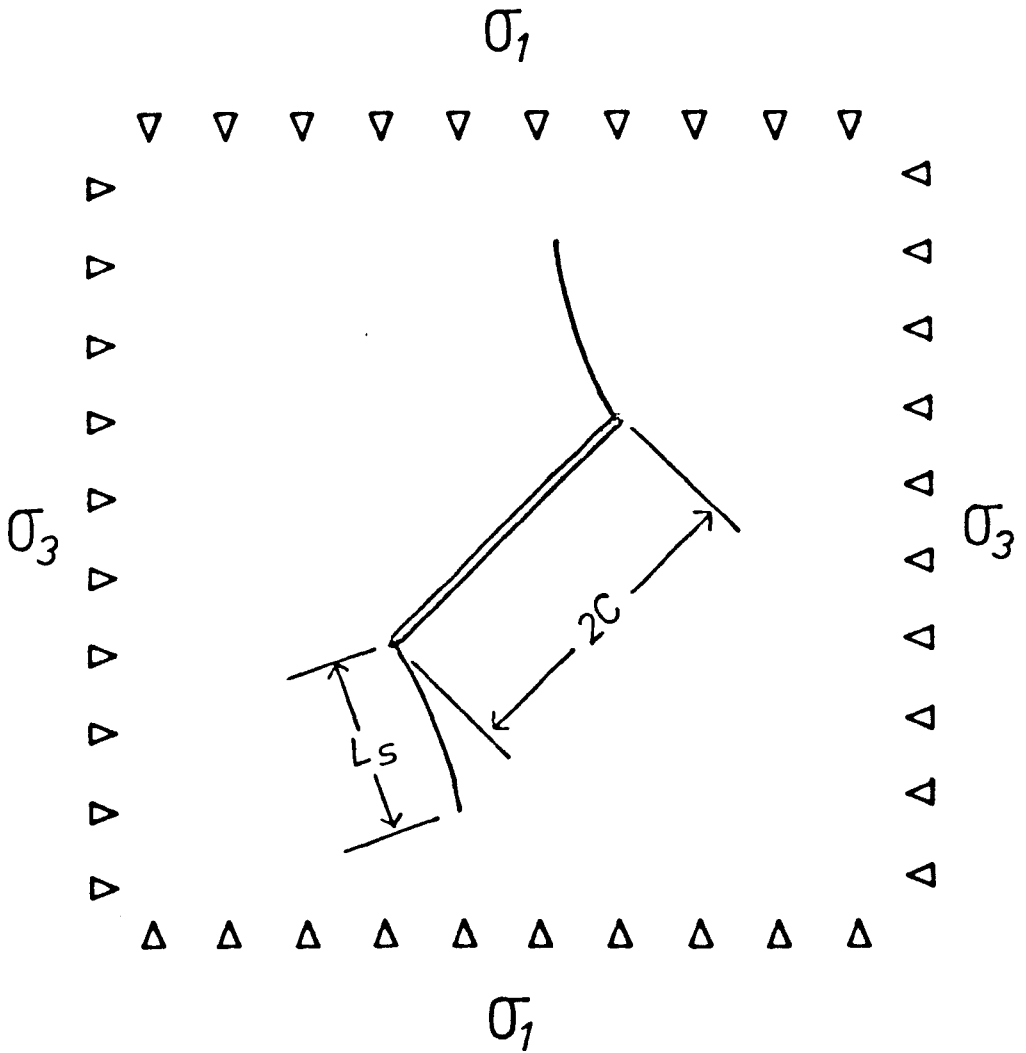


Fig. 14.3.

*Propogation of a fracture in rock subject to an external stress field after Hoek (1965.)*

*Illustrating fracture extension approximately parallel to the principal stress.*

additional stresses exerted on the fracture periphery by the geostatic stress field will move the point of maximum tangential tensile stress by an increment; dependant on the relative sizes of the geostatic field and its relative orientation and the internal pressure of the fracture towards the maximum principal stress. If we take the propagation of the fracture in increments of  $dL$  (where  $L$  is the length of the fracture) a change of orientation towards the maximum principal stress of  $d\theta$  will occur, resulting in the 'constant' curving of the fracture in that direction, the radius of curvature being dependent on the ratio of the resultant tangential stress components and the orientation of the geostatic stress field to the fracture.

As before, the most detrimental geostatic stress field orientation for quasi-static fracture extension is with the maximum principal stress orientated perpendicular to the pre-split line and the most beneficial with the maximum principal stress parallel to the pre-split line.

15 SUMMARY OF CONCLUSIONS

The predominant mechanism in the formation of a pre-split fracture is the effect and interaction of the quasi-static components of energy release from neighbouring boreholes within a pre-split panel. However, the dynamic component of energy release is responsible for the initiation of fracturing around each borehole.

In the pre-splitting process, fracturing is initiated at or near the borehole wall by the dynamic component in each individual pre-split hole. This initial fracturing is then considerably extended by the quasi-static component. For normal field pre-split borehole separations, no fracturing is initiated midway between boreholes by the superposition of dynamic shock waves.

A pre-split fracture may be formed solely by the dynamic component of energy release. However the maximum dynamic pre-split borehole separation is less than one sixth of normal maximum pre-split borehole separation incorporating the quasi-static component.

The role of the superposition of quasi-static

stress fields has been over estimated in the past, pre-split fractures being primarily formed by the overlapping of fracture zones from neighbouring boreholes.

From observations in the field, the most important non-geotechnical factor affecting the success of pre-split blasting is drilling accuracy. For guaranteed successful pre-splitting in non-adverse conditions borehole wander should not exceed 25% of the design borehole separation at any point.

The orientation and geometry (extent) of any major discontinuity or discontinuity set have been found to be the most important geotechnical factors affecting the success of pre-split blasting, both in the laboratory and in the field.

Discontinuities orientated perpendicular to the design line of a pre-split have little effect on its success. However as the intersection angle between the design face and the discontinuity decreases, overbreak of the face increases with the associated loss of pre-split half barrels and integrity. For intersection angles less than twenty degrees, total failure of the pre-split occurs with excessive

overbreak.

The worst discontinuity conditions possible for the application of pre-split blasting are where large scale continuous, or medium scale interconnected discontinuities strike within twenty degrees to the final design face.

The effect of discontinuities on the success of pre-splitting decreases with decreasing angle of dip. The dominant fractures from blast holes are roughly perpendicular to the discontinuity planes involved, this being a function of geometry alone.

The occurrence of multiple discontinuities of a single set between pre-split boreholes has no deleterious effect on the success of the pre-split in excess of that created by single discontinuities of the same orientation other than a slight increase in overbreak to the final face, i.e. discontinuity set orientation and extent is far more important than discontinuity frequency.

For fixed charging and borehole diameter, the maximum successful pre-split borehole separation is inversely proportional to the 'static' tensile rock

strength. This relationship holds true up to a critical rock strength where the dynamic component of energy release is no longer sufficient to initiate a significant radial fracture zone for extension by the quasi-static gas component and the maximum successful pre-split borehole separation accordingly drops significantly.

The effect of weathering is to weaken and loosen the rock mass near to the surface and therefore the upper portions of design faces. If consideration of this fact is not taken into account during the loading of pre-split holes and a reduction in charge density not made for these horizons, then excessive damage will occur, resulting in reduced success and increased instability problems.

The effect of water in a borehole is primarily to effectively couple the explosive to the rock, negating the effect of any decoupling present. Correspondingly, a larger zone of blast damage will be created due to the excessive confining of the charge.

From experimentation with dye, it was concluded that fluid does enter the radial fracture zone around the borehole and that the effect of the quasi-static

component of energy release can be therefore likened to hydrofracture. However as the radial fractures propagate, the rate of injection of fluid falls behind the rate of fracture extension.

It can be concluded that stability is a decisive factor in the success of any design slope on its excavation, irrespective of excavation technique. However any failure of a pre-split face due to intrinsic instability of the rock mass is a failure of the rock mass and not the pre-split!

Sizeable geostatic stress fields may affect the effectiveness and maximum successful borehole separation of pre-splitting, depending on their mutual orientations. However as there are no sizeable surface geostatic stress fields in the British Isles, this geotechnical factor can be considered of minimal importance with respect to highway cuttings.

## 16 ACKNOWLEDGEMENTS

I wish to express my gratitude and thanks to the following people, firms and authorities without whose help, funding, permission and constructive criticism this project would not have been brought to fruition.

Dr. Ian Farmer, Reader in Mining Engineering at Newcastle University and my Supervisor, for arranging my contract and giving me his sound advice and guidance, the Science Research Council and the Transport and Road Research Laboratory for the joint funding of the research and my Industrial Supervisor, Dr. George Matheson of T.R.R.L. for arranging site access and giving constructive criticism.

In addition I would like to thank the following for allowing site and quarry access:

Scottish Development Department

Highland Region Roads Department

Tayside Region Roads Department

Associated Portland Cement - Dunbar

Foster Yeomans

and the following firms for Explosives information:

Explosives and Chemical Products Ltd.

Nobel Explosives (especially Jon Jones

of Technical Services)

For assistance in the laboratories, manufacture of constraints, moulds and explosives store - John Moore, Colin Dixon and Tom Shepardon.

For rock cutting and machining of strength testing specimens Bill Clasper and John and Lindsay Moore for their help casting concrete blocks whilst I was invalided with a broken leg, without all of whom the completion of this study on schedule would not have been feasible.

Further thanks are given to Mr. A. Szaki and Mr. N. Tomlin, departmental lecturers, who have given assistance with certain minor technical matters.

Finally I acknowledge the help of my wife, Mrs. G. M. Worsey for the word processing of this text and assistance in its compilation.

17 REFERENCES

- Asklof, C.A. and A. Nylander 1968. **Cylindrical and Spherical Wave Expansion Processes in Rock Materials.** Swedish Research Institute of National Defence, Report FOA 2C2286-44.
- Aso, K. 1966. **Phenomena Involved in Pre-splitting by Blasting.** Stanford University: Unpublished Ph.d. Thesis.
- Atchison, T.C., W.I. Duvall and J.M. Pugliese 1964. **Effect of Decoupling on Explosion Generated Strain Pulses in Rock.** U.S. Bureau of Mines, R.I. 6333.
- Atchison, T.C., and J.M. Pugliese 1964a. **Comparative Studies of Explosives in Limestone.** U.S. Bureau of Mines, R.I. 6395.
- Atchison, T.C. and J.M. Pugliese 1964b. **Comparative Studies of Explosives in Granite - Second Series of Tests.** U.S. Bureau of Mines, R.I. 6434.
- Atchison, T.C. and J. Roth 1961. **Comparative**

Studies of Explosives in Marble. U.S. Bureau of Mines, R.I.5797.

Austin, C.F., L.N. Cosner and J.K. Pringle 1966. Shock Wave Attenuation in Elastic and Anelastic Rock Media. Society of Mining Engineering Transactions, March 1966, 16-30.

Baker, W. 1972. New Techniques in Resolitting. Proceedings of the 1st. Conference on Drilling and Blasting, Phoenix Arizona.

Barenblatt, G.I. 1962. The Mathematical Theory of Equilibrium Cracks in Brittle Fracture. Advances in Applied Mechanics, 7, 55-129.

Barker, D.B., N.L. Fournery and D.C. Holloway 1979. Photoelastic Investigation of Elaw Initiated Cracks and Their Contribution to the Mechanisms of Fragmentation. Proceedings of the 20th. U.S. Symposium on Rock Mechanics, Austin Texas, 119-126.

Barron, K. 1971. Brittle Fracture Initiation in and Ultimate Failure of Rocks. International Journal of Rock Mechanics, 8, 541-551.

- Bergmann, O.R., F.C. Wu and J.W. Edl 1974. Model Rock Blasting Measures, Effect of Delays and Hole Pat- terns on Rock Fragmentation. Engineering and Mining Journal, 175 (6), 124-127.
- Berzal, J.L. 1976. Blasting Vibration Levels Transmitted Across Fracture Planes. Mining Magazine, 135 (4), 361-363.
- Bjorn, J.I. 1969. Improving Limestone Pillars by Pre- splitting. Proceedings of the International Symposium, International Society of Rock Mechanics, 143-146.
- Brost, F.B. 1970. A Study of Blasting Phenomena and Problems of Blasting Under High Stress. University of Witwatersrand: Unpublished M.Sc. Dissertation.
- Brown, A.N. 1968. Notes on an Investigation Into the Basic Fracture Mechanisms Encountered in Controlled Blasting. Journal of the South African Institute of Mining and Metallurgy, 69 (3), 146-149.

Brown, C. and J. Brigando 1972. Pre-splitting and Smooth-wall Blasting in La Canonea Pit. *Minina Engineering*, 24 (9), 50-52.

Bur, T.R., W.C. Lyle, H.R. Nicholls and T.E. Slykhouse 1967. Comparison of Two Methods For Studying Relative Performance of Explosives in Rock. U.S. Bureau of Mines, R.I. 6888.

Calder, P. 1977. Perimeter Blasting. In *Pit Slope Manual*. Canada Centre for Mineral and Energy Technology Report, 77-14, 1-82.

Carrasco, L.G. and L.W. Saperstein 1977. Surface Morphology of Pre-split Fractures in Plexiglas Models. *International Journal of Rock Mechanics*, 14, 261-275.

Dally, J.W., W.L. Fourney and D.C. Holloway 1975. Influence of Containment of the Borehole Pressures on Explosive Induced Fracture. *International Journal of Rock Mechanics*, 12, 5-12.

Dally, J.W. and W.L. Fourney 1977. Fracture Control in Construction Blasting. Proceedings of the

18th. U.S. Symposium on Rock Mechanics,  
2A6,1-7.

Devine, J.F., R.H. Beck, V.C. Meyer and W.I. Duvall  
1965. Vibration Levels Transmitted Across a  
Pre-split Fracture Plane. U.S. Bureau of  
Mines, R.I. 6695.

Dick, R.A. 1968. Factors in Selecting and Applying  
Commercial Explosives and Blasting Agents.  
U.S. Bureau of Mines Information Circular,  
8405.

Edgeston, H.E. and F.E. Barstow 1941. Further  
Studies of Glass Fracture with High-Speed  
Photography. Journal of the American Ceramic  
Society, 24, 131-137.

Edwards, J.C. and R.F. Cheiken 1974. Detonation  
Calculations With a Percus-Yevick Equation  
of State. U.S. Bureau of Mines, R.I. 7905.

Fennel, M.H., R.P. Plewman and A.N. Brown 1966.  
Smooth Blasting and Pre-splitting.  
Association of Mine Managers of South Africa.  
Papers and Discussions, 1966-1967, 811-863.

Fogelson, D.E., D.V.D'Andrea and R.L.Fischer 1965.  
Effects of Decoupling and Type of Stemming on  
Explosion-Generated Pulses in Mortar: A  
Laboratory Study. U.S. Bureau of Mines,  
R.I.6679.

Fogelson, D.E., M.I.Duvall and T.C.Atchison 1959.  
Strain Energy in Explosion-Generated Strain  
Pulses. U.S. Bureau of Mines, R.I.5514.

Forsthoft, W. 1973. The Protection of Slopes in a  
Limestone Quarry by Blasting Using the  
Pre-splitting Method. Nobel Hafta, 4,151-156.

Fourney, W.L., J.W.Dally and D.C.Holloway 1974.  
Stress Wave Propagation from Inclined Line  
Charges Near a Bench Face. International  
Journal of Rock Mechanics, 11,393-401.

Fries, I.F. 19 . Profile Accuracy in Blasting.  
Lucerne: Swiss Explosives Industries, p.1-6.

Griffin, G.L. 1973. Mathematical Theory to  
Pre-splitting Blasting. Proceedings of the  
11th. Engineering Geology and Soils  
Engineering Symposium, Pocatello Idaho,

217-225.

Haas, C.J. and J.S. Rinehart 1962. Some Aspects of Coupling Between Explosives and Rock. U.S. Naval Ordnance Test Station/Colorado School of Mines.

Hoek, E. 1965. Rock Fracture Under Static Stress Conditions. WNNR/CSIR, Ref., ME/MR/4263, Report MEG383.

Hoek, E. and J.W. Bray 1977. Pre-split Blasting. In Rock Slope Engineering. London: Institute of Mining and Metallurgy (3rd. Edition), p.302-304.

Holman, R.C. 1967. Pre-splitting in Tunnels. Colliery Engineering, July 1967.

Hoover, T. et.al. 1972. Pre-splitting Interim Report Number Two. Sacramento: California State Division of Highways, Materials and Research Department. CA HWY MR 632955(2) 72 21.

Johansson, C.H. and P.A. Persson 1970. Detonics of

**High Explosives.** London: Academic Press.

Johston, S.G. 1973. **Blasting Advances at Hammersley Iron.** *Mining Magazine*, 129 (2), 120-121.

Jones, J.P. 1978. **Factors Affecting a Successful Pre-split.** University of Newcastle-upon-Tyne: Unpublished M.Sc. Dissertation.

Jones, J.P. 1980. **Personal Communications.**

Katsuyama, K., K.Sassa and I.Ito 1973. **Computer Calculations of the Effects of Pre-split on Blasting in Close Proximity to It.** *Journal of the Mining and Metallurgy Institute of Japan*, 89 (1024), 357-362.

Kisslinger, C. and I.N.Giupta 1963. **Studies of Explosion Generated Dilational Waves in Two-Dimensional Models.** *Journal of Geophysical Research*, 68 (18), 5197-5206.

Kutter, H.K. 1967. **The Interaction Between Stress Wave and Gas Pressure in the Eruptive Process of an Underground Explosion in Rock.** With

Particular Application to Pre-splitting.  
University of Minnesota: Unpublished Ph.d.  
Thesis.

Kutter, H.K. and C. Fairhurst 1968. The Roles of  
Stress Wave and Gas Pressure in Pre-splitting.  
Proceedings of the 9th. Symposium of  
Practical Rock Mechanics, A.I.M.E., 265-284.

Kutter, H.K. and C. Fairhurst 1971. On the Fracture  
Process in Blasting. International Journal of  
Rock Mechanics, 8, 181-202.

Langefors, U. and B. Kihlstrom 1978. In The Modern  
Technique of Rock Blasting. Stockholm:  
Almqvist and Wiksell.

Laroque, G.E. and D.F. Coates 1972. Comparative  
Ground- Shock Measurements for Evaluating  
Pre-splitting. Western Miner, 45 (12), 33-38.

Lutton, R.J. 1977. Probability of Specified Ground  
Vibrations from Blasting. Proceedings of  
the 18th. U.S. Symposium on Rock Mechanics,  
3C2, 1-7.

- Matheson, G.D. 1979a. The Splitting Index.  
Transport and Road Research Laboratory, LF889.
- Matheson, G.D. 1979b. Measurement of Drill Rod and  
Drill Hole Attitudes in Prec-split Blasting.  
Transport and Road Research Laboratory, LF889.
- Matheson, G.D. 1980. Personal Communications.
- Matheson, G.D. 1981. Instability Assessment,  
Preliminary Investigations. Transport and  
Road Research Laboratory, LR in press.
- Matheson, G.D. and C. Swindells 1981. Seismic  
Detection and Measurement of Blast  
Disturbance. Transport and Road Research  
Laboratory, LF928.
- McCormick, J. 1972. Geology and Blasting.  
Proceedings of the 1st. Conference on  
Drilling and Blasting, Phoenix Arizona.
- Mellor, M. 1976. Controlled Perimeter Blasting in  
Cold Regions. Hanover, N.H.: Cold Regions  
Research and Engineering Laboratory,  
CRREL-TR-267.

Mellor, M., A. Kovacs and J. Hnotiuk 1977.  
Destruction of Ice Islands With Explosives.  
P.O.A.C. 77, Proceedings of the Fourth  
International Conference, St. Johns  
Newfoundland, 753-763.

Nicholls, H.R. and W.I. Duvall 1966a. Pre-splitting  
Rock in the Presence of a Static Stress Field.  
U.S. Bureau of Mines, R.I. 6843.

Nicholls, H.R. and W.I. Duvall 1966b. Effect of  
Charge Diameter on Explosive Performance.  
U.S. Bureau of Mines, R.I. 6806.

Nicholls, H.R. and V.E. Hooker 1962. Comparative  
Studies of Explosives in Salt. U.S. Bureau  
of Mines, R.I. 6041.

Paine, S.R., D.K. Holmes and E. Clark 1961.  
Pre-split Blasting at the Niagara Power  
Project. Explosives Engineer, June  
1961, 71-93.

Pearson, C.M. 1980. Permeability Enhancement by Ex-  
plosive Initiation in the South-West Granites.  
With Particular Reference to Hot Dry Rock

Energy Systems. Cambourne School of Mines:  
Unpublished Ph.d. Thesis.

Perkins, T.K. and W.W.Krech 1968. The Energy  
Balance Concept of Hydraulic Fracturing.  
Journal of the Society of Petroleum Engineers,  
8, 1-12.

Plewman, R.P. and A.M.Starfield 1965. The Effects  
of Finite Velocities of Detonation and  
Propagation on the Strain Pulses Induced in  
Rock by Linear Charges. Journal of the South  
African Institute of Mining and Metallurgy, 66  
(3), 77-96.

Pritchard-Davies, E.W.P. 1970. The Future of  
Direction Control in Diamond Drilling. Quarry  
Mine and Pit, 1970, 2-8.

Porter, D.D. and C.Fairhurst 1971. A Study of  
Crack Propagation Produced by the Sustained  
Borehole Pressure in Blasting. Proceedings of  
the 12th. U.S. Symposium on Rock Mechanics,  
497-513.

Raton, S. and B.B.Dhar 1976. Controlled Blasting

in Rock Excavation Projects - A Review.  
Mining Magazine, January 1976,25-32.

Reichmuth,D.R. 1967. Point Load Testing of  
Brittle Materials to Determine Tensile  
Strength & Relative Brittleness. Proceedings  
of the 9th. U.S. Symposium on Rock  
Mechanics, Golden Colorado.

Schultz,T.C. 1972. Investigation into Splitting  
Effects in Explosively Loaded Small Diameter  
Holes with Stress Raisers. University of  
Johannesburg: Unpublished Ph.d. Thesis.

Selberg,H.L. 1951. Transient Compression Waves  
From Spherical and Cylindrical Cavities.  
Arkiv for Eksik, Band5,Nr.7.

Short,N.M. 1961. Fracturing of Rock Salt by a  
Contained High Explosive. Colorado School of  
Mines Quarterly, 56 (1),221-258.

Smith,A.K. and R.Barnett 1965. Theoretical  
Consideration and Practical Applications of  
Smooth-wall Blasting. Proceedings of the 7th.  
U.S. Symposium on Rock Mechanics, 68-89.

Sneddon, I.N. 1946. The Distribution of Stress in the Neighbourhood of a Crack in an Elastic Solid. Proceedings of the Royal Society, 187, 229.

Stenhouse, D. 1967. Some Applications of the Pre-splitting Technique in Rock Blasting. Mining and Minerals Engineering, December 1967.

Swindells, C. 1981. Seismic Inspection of Excavated Rock Slopes. University of Dundee: Unpublished Thesis.

Talbot, C. 1977. A2 Realignment Calvina to Inverness County Boundary Reasons for the Variable Degree of Success in Pre-splitting the Rock Face. University of Dundee: Centre for Industrial Research and Consultancy Report.

Teller, A.E. 1972a. Mean What You Say or Say What You Mean. Proceedings of the 1st Conference on Drilling and Blasting, Phoenix Arizona.

Teller, A.E. 1972b. Pre-splitting Bonuses Optimize Blasting. Rock Products, 75 (8), 58-92.

- Teller, A.E.' 1972c. Rules of Thumb for Blasting. Proceedings of the 1st. Conference on Drilling and Blasting, Phoenix Arizona.
- Trudinger, J.P. 1973. An Approach to the Practice of Pre-splitting in Anisotropic Rock Masses. Bulletin of the Association of Engineering Geologists, 10 (3), 161-171.
- Wiebols, G.A. and N.G.W. Cook 1965. An Elementary Analysis of the Displacements Generated in Rock by a Linear Explosive Charge. Journal of the South African Institute of Mining and Metallurgy, 66 (3), 97-108.
- Wilbur, I., W.I. Duvall and J.M. Pugliese 1965. Comparison Between End and Axial Methods of Detonating an Explosive in Granite. U.S. Bureau of Mines, R.I. 6900.
- Worsey, P.N., I.W. Farmer and G.D. Matheson 1981. Mechanics of Pre-splitting in Discontinuous Rock. Proceedings of the 22nd. U.S. Symposium on Rock Mechanics, M.I.T., Cambridge Massachusetts.

Unknown Author, 1964. Dunbar Cement. Mining and Minerals Engineering, December 1964, 130-136.

Unknown Author, 1977. Pre-splitting Adopted for Shaft sinking Project in Lancashire. Mining and Quarrying, March 1977.

Appendix A

METHOD OF CASTING

A-1 PROBLEMS ENCOUNTERED AND TECHNIQUE ADOPTED

Unfortunately it was soon discovered that Polyester resin has a maximum casting volume above which the setting rate is uncontrollable. The direct effects of this can be described as follows:

During the setting process the catalyst (hardner) causes the resin to change its chemistry and solidify and associated with this process is the liberation of a fairly sizeable quantity of heat. Generally speaking the higher the temperature, the higher the rate of reaction and thus a higher rate of heat liberation is experienced. The effect thus snowballs very rapidly above a critical mass.<sup>12</sup>

The resultant effect is that whilst the outer edge

-----  
<sup>12</sup> It was found that the magnitude of the critical mass was dependent on the surface area of the mass and thus its shape. E.g. the critical mass of a plate would be higher than for that of a cube, as a plate has a higher surface area per unit volume.

is shrinking due to normal setting the central 'MASS' is contracting relative to the outer limits, due to its increased temperature and thus setting at a faster rate. This uneven contraction causes high tensile forces to be set up within the block which if sufficient result in failure.

Thus resin blocks had to be cast in layers. By slowing down the setting rate using just over the minimum amount of catalyst recommended (5 ml/kilo), it was found that castings of just over 25 mm in depth were possible. However this was using fresh resin and during the casting of early blocks using resin which had been stored for over three months in unfavourable conditions a cast was lost due to exothermic failure.

#### A-2 HOMOGENEITY

Polyester resin in itself is isotropic being a liquid and it also has this property when it is a solid. However when cast in layers some doubt is raised. Let us consider a single layer:

As the material is isotropic then a single layer will show isotropic characteristics. Add other such

layers and we then have an isotropic block except at discontinuities - which are represented by the layering. Thus a layered block is isotropic in both axes along the layering but anisotropic perpendicular to the layering.

The layering surfaces themselves present the major weaknesses if any in the blocks. To find whether there was any in-homogeneity in the blocks, they were sonically tested at Dundee University by Chris Swindells, who found that the seismic velocities in all three axes were identical to all intents and purpose. However, if the junctions between layers represent any difference in strength, as they are minutely thin compared with the layers themselves then any noticeable difference in seismic velocity should not be detected.

As was suspected, weaknesses along the junctions between layers were found in model blasting and the layers were seen to separate at isolated points on certain junctions, but only in a minority of cases.

The individual blocks were subject to Photoelastic analysis which showed that only minimal residual stresses were present compared with the strengths of

each block and that the majority of these stresses occurred at the edge of each block and between successive layers.

### A-3 CURING

As the different layers cast were subject to differential shrinking, time to allow the 'plastic' resin to dissipate any residual stresses was necessary. Also the blocks needed time to harden and to reach a point at which their strength parameters were uniform and no longer dependent on time. In general a minimum of one month was allotted for this, from time of extraction of the blocks from the moulds to machining. During this time the blocks were subject to moderate heating (40 degrees centigrade) to assist and also increase the rate of curing.

### A-4 MOULDS

Initially a purpose built six inch cube mould was used, but for convenience a 150 mm cube, and then twenty eight inch moulds were used, mainly for speed. At first blocks were cast individually, but this was

considered too painstaking and up to six 6 inch moulds were then used at one time. During the latter part of the first phase of model blasting twenty eight inch moulds were used for both convenience and larger blocks, blocks being sawn to the appropriate lengths.

Appendix B

WAVE TRAPS

Before the theory of wave traps can be explained, a basic knowledge of the process of wave reflection at a free face and its resultant affect on the material through which it is travelling is required.

B-1 THEORY OF SLABBING

When a wave in compression passing through a body encounters a free face, it is reflected from the free face as a tensile wave. This has been shown by a number of authors in practice and theory (Wilbur, Duval and Atchinson (1965) etc.).

Firstly consider the reflection of a plane triangular longitudinal pulse travelling normally to a plane free face as shown in Figure B .1 (taken from Wilbur, Duval and Atchinson (1965) ). Figures B.1 a,b,c,d,e and f show the resulting pulse at equal increments of time after initial contact with the free face. The dotted lines below the X axis represent the compressive pulse incident at the free face, the

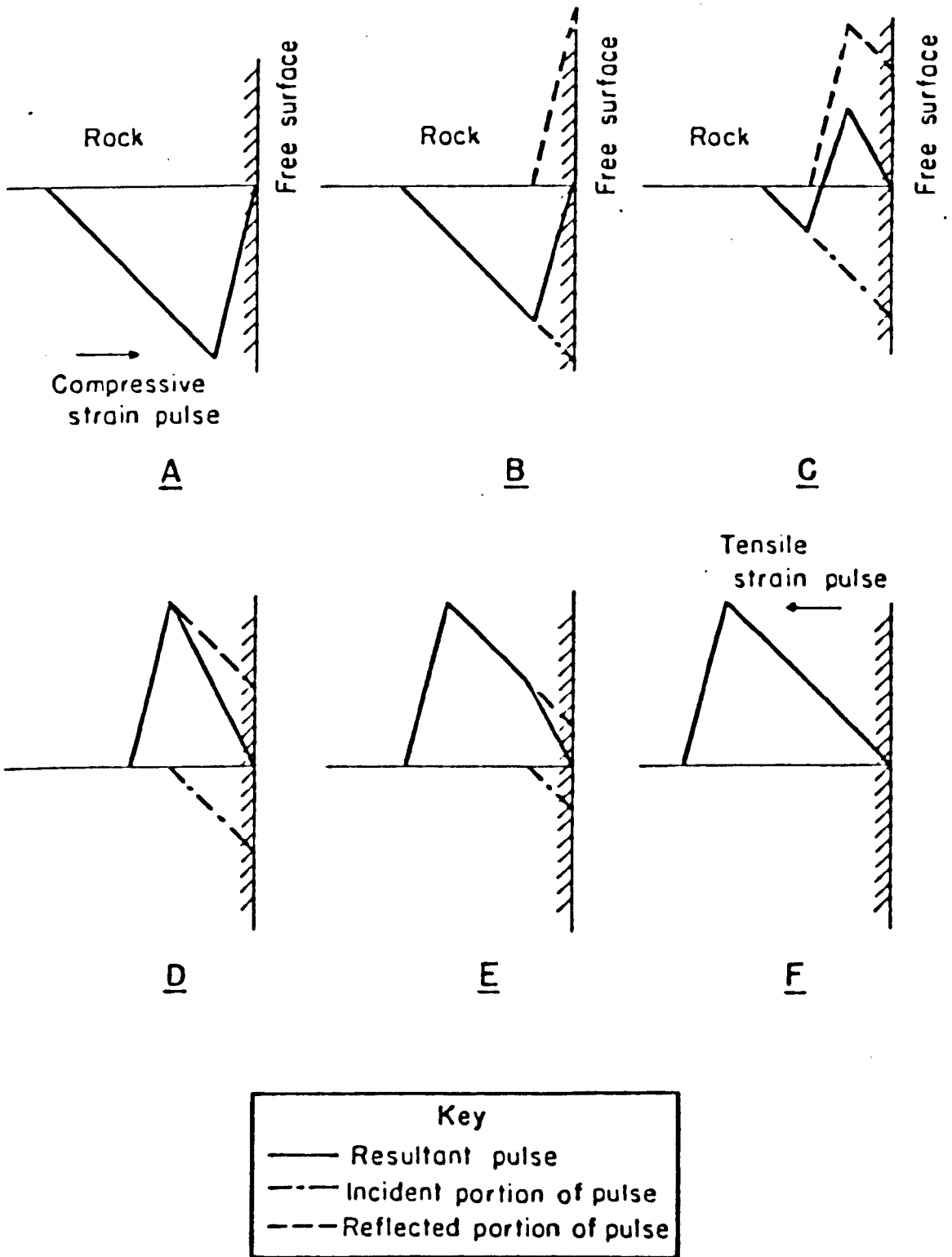


Fig. B.1. Reflection of a triangular compressive strain pulse.

dotted lines above represent the reflected tensile pulse and the solid line represents the actual (resulting) strain pulse that the rock experiences.

As can be seen from Figure B.1 the compressive strain pulse is steadily converted into a tensile pulse moving in an opposing direction from the free face. When the tail of the compressive pulse has reached the face then it will have been converted to a tensile pulse in its entirety. However, until the tail of the compressive pulse has done so then both parts of the reflected tensile pulse and compressive pulse occupy the same space, this resulting in the addition of the two giving a resultant which will be either a reduced compressive or reduced tensile pulse or they may even cancel each other out at a given point in time and space along the X axis, as shown in Figure B.1c.

The above is valid providing the magnitude of the resultant pulse remains below the tensile strength of the rock. If these conditions are exceeded then tensile failure of the material will occur, resulting in scabbing parallel to the free face from where the resultant pulse exceeds the tensile strength of the material. This process is known as slabbing and is

shown in Figure B.2.

Consider the point where the resultant pulse exceeds the tensile strength of the medium (Fig. B.2b), as stated above tensile failure occurs, producing a free slab of the outer surface. This effectively moves in the free surface with a fresh one being created. The part of the pulse which was inbetween the new and old free surface is now trapped within the free slab which moves away from the new, free surface. Remaining now in the material is the 'tail' of the pulse which on moving forward, is reflected in the tensile phase as before. If the magnitude of the resultant pulse again exceeds the tensile strength of the material then the process will be repeated.

Note: because of this effect the peak of the resulting tensile reflection of an incident compressive pulse at a free surface will never exceed the tensile strength of that material.

Considering a normal block with a point explosive source, then if the outgoing compressive wave were of sufficient strength then minor slabbing would occur, the peak of the resulting tensile reflected wave being

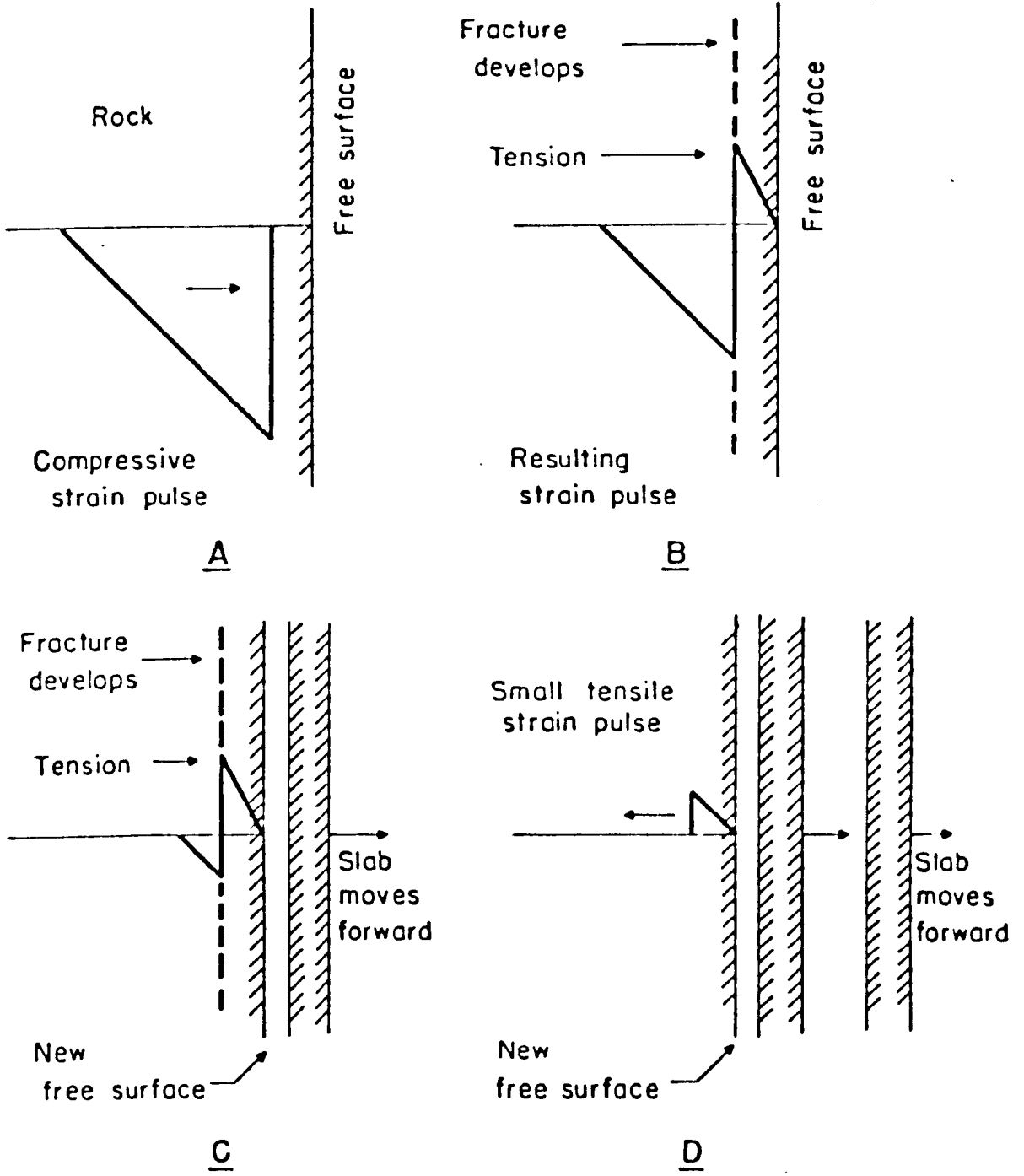


Fig. B. 2. Tensile fracture by reflection of a compressive strain pulse.

reduced to below the tensile strength of the material. Thus the reflecting dynamic waves within the block would be reduced considerably. However, it is possible that although reduced, they may still exist in damaging magnitude, thus the need for wave traps.

## B-2 THEORY OF WAVE TRAPS

Wave traps are virtually an extension of the block such that there is a parallel fracture to the side of the block on every side, see Figure B.3 The wave traps are restrained against the block with clamps, giving a nominal pressure to keep the unit from coming apart.

On impact, the incident pulse being of compressive phase, further strengthens the block-wave trap interface and as the block and wave traps are of identical material, the interface becomes 'invisible' and the compressive pulse passes through unaffected. When the compressive pulse reaches the free face of the wave trap it is then reflected, the process having already been described. However, when the tensile phase reaches the block/wave trap interface, it is reflected back as tensile pulses cannot be transmitted across a break. The pulse being reflected in

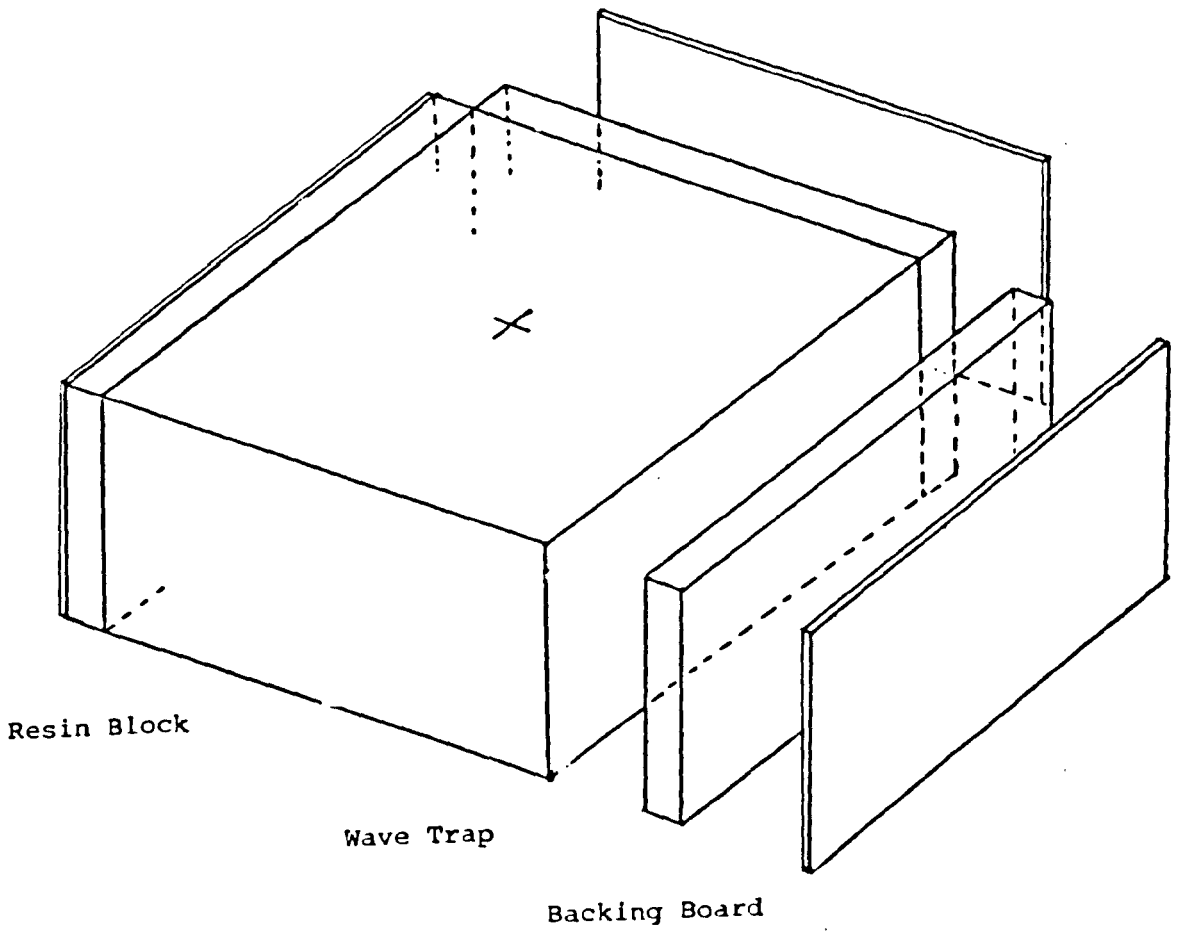


Fig. B.3. Resin Block with Wave Traps.

compression (see Figure B.4). Thus the block is protected from any reflected dynamic waves.

### B-3 WAVE TRAP DESIGN

The most important factor that should be considered when designing a wave trap is the pulse width of the compressive pulse. For instance, if the tensile reflected pulse is sinusoidal in shape and the wave trap thin, then if the resultant pulse is in compression at that point and time, the interface will remain closed and the tensile reflected component will escape from the wave trap until the resultant pulse becomes tensile. This effect may also occur with secondary waves following up a primary pulse (shear waves excluded by their very nature). Although escape in such a case may occur, it will be fairly negligible in magnitude compared with the maximum peak of the resultant reflected tensile pulse.

To eliminate any leakage from the wave traps there are therefore two considerations to be made:

- a. The width of the wave trap should exceed half the incident pulse width (the wave having to

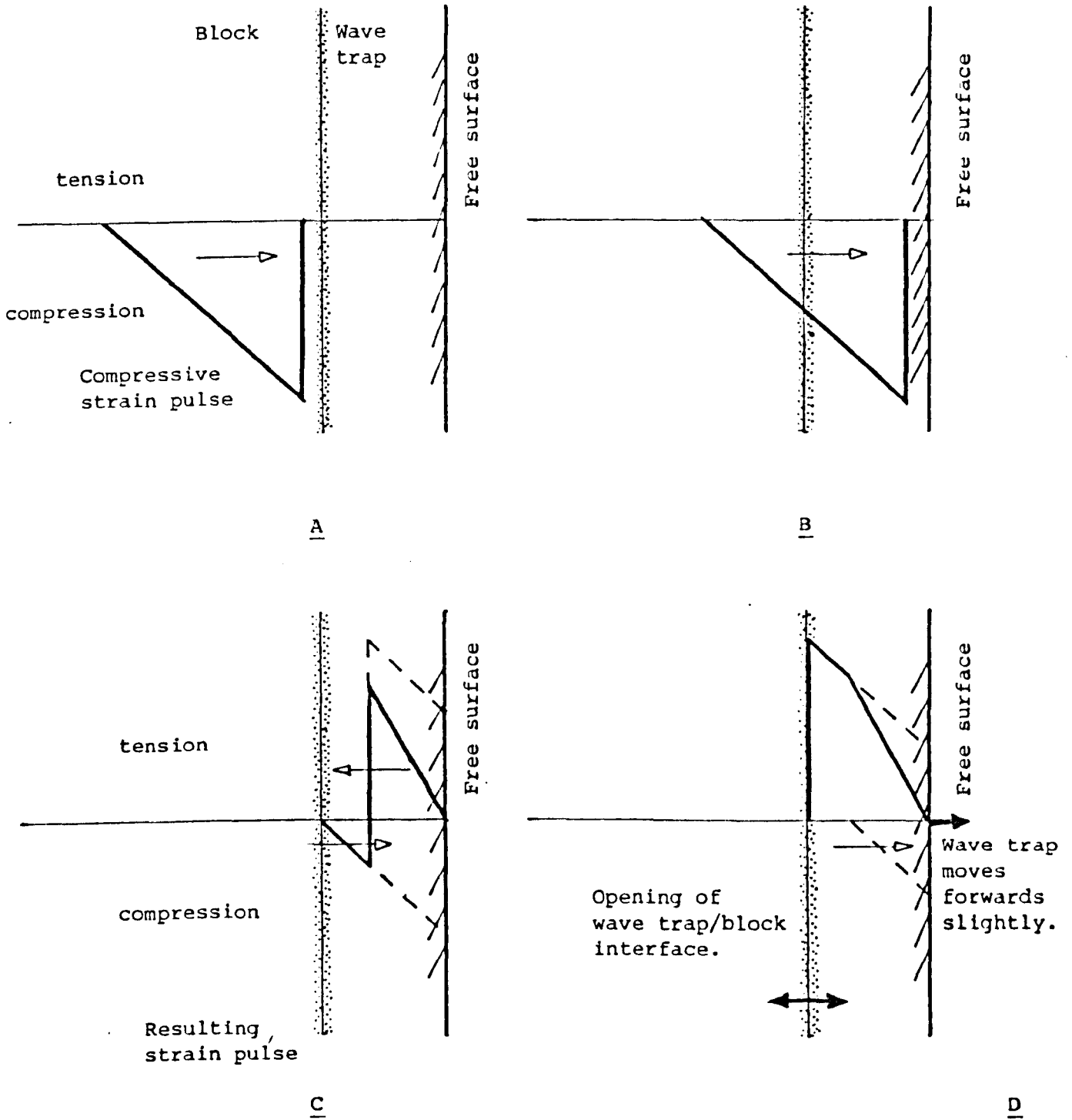


Fig. B.4 . Wave trap in Action (by Author).

pass through and then back through the wave trap).

- b. The constraints should not exert such forces on the block-wave trap interface such that their constraining effect is detrimental to the efficiency of the traps.

#### B-4 DIMENSIONS

With results on compressive pulse width for differing borehole conditions by Dally, Fournay and Holloway (2 and 3) a wave trap width of 12.5 mm was calculated to be generously sufficient. The value was also chosen as it was the minimum size that was easily obtainable with the cutting equipment available, strength (fragility) also being taken into consideration.

The wave traps were cut and machined from 150 mm cubes of Polyester resin and machined flat to 12.5 mm width, the original traps were 150 mm square but later ones 150 x 75 mm.

Appendix C

DELAY EXPERIMENT, IESI 15

C-1 THEORY

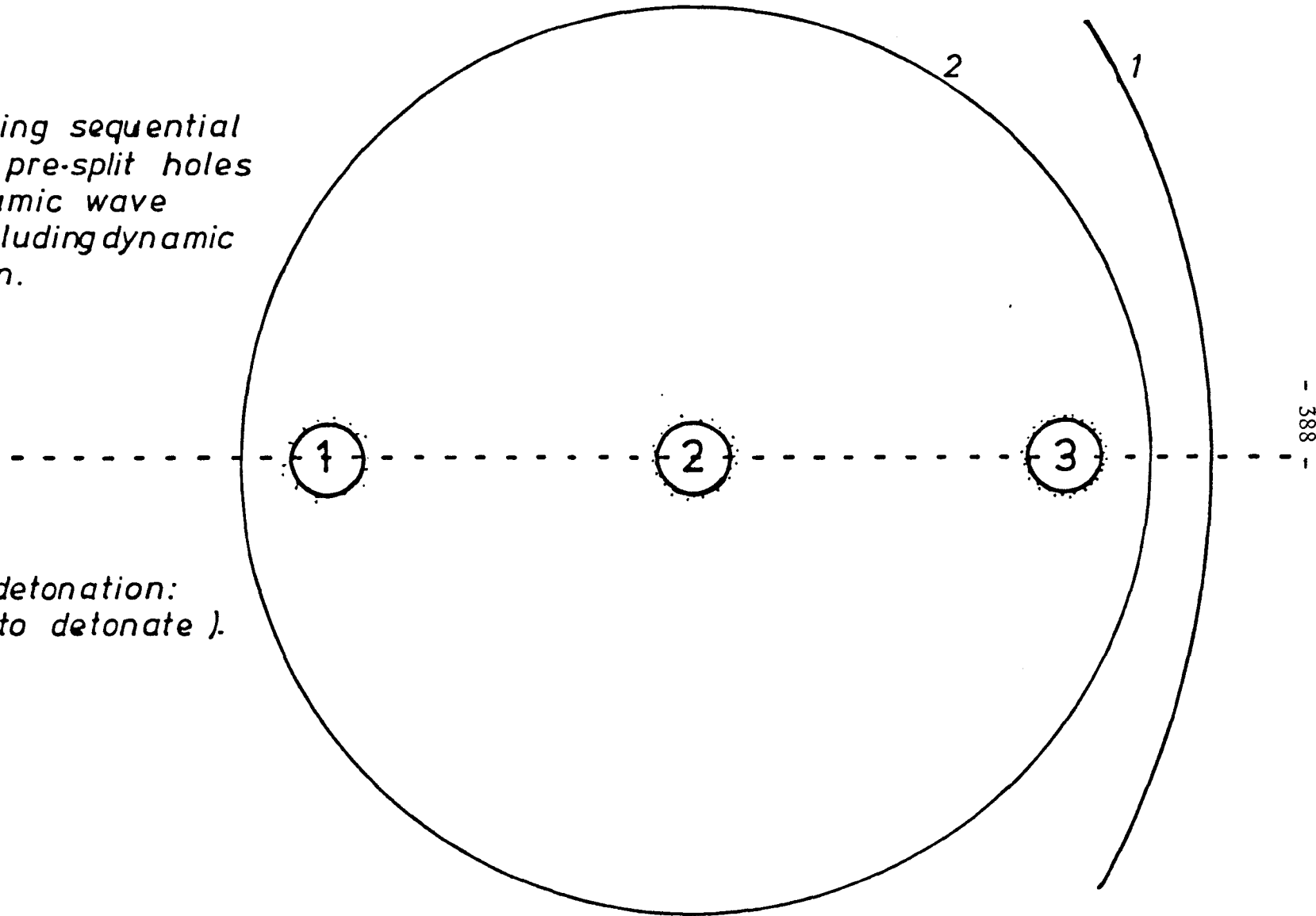
As a seismic wave expands spherically from a point source at constant velocity, if the firing of successive holes in a pre-split panel are delayed such that the dynamic wave from the first hole has passed the second hole before it is detonated (and so on), then no interaction of dynamic components will occur (see Figure C.1).

However in pre-split blasting, the explosive charges are not point charges but linear. Therefore for end detonation, the time taken for the explosive column to detonate must be taken into account.

Therefore for a test comprised of 3 x 9.525 mm diameter holes, 70 mm deep and spaced at 38.1 mm centres in 2.5 km/s seismic velocity resin using 7 km/s detonating cord, the required delay element per hole is:

Fig. C.1.

*Figure illustrating sequential detonation of pre-split holes including dynamic wave fronts for excluding dynamic wave interaction.*



*Sequence of detonation:  
1 ,2 ,3 (about to detonate ).*

$$0.070/7000 + 0.038/2500 = 25.2 \text{ us}$$

Therefore using 7 km/s detonating cord, incremental lengths per hole in excess of:

$$7000 \times 0.0000252 = 17.64 \text{ cm are required.}$$

In test 15, incremental delays of 27 us were obtained using incremental lengths of 19 cm of P.E.T.N. detonating cord per hole.

Appendix D

EXPERIMENTATION TEST NUMBER LISTINGS

Series (a) Experimentation in Resin.

Test Nos: 7,8,9,10,11,21,22,23,24,25,26,27

Series (b) Experimentation in Resin.

Test Nos: 33,36,37,45,46,47

Series (c) Experimentation in Resin.

Test Nos: 3,4,6,12,13,14,16,17,18,

19,20,28,29,30,31,32,35,39,40,41,42

Series (d) Experimentation in Resin.

Test Nos: 34,38,44

Series (e) Experimentation in Resin.

Test No: 15

Single Discontinuity Testing in Resin.

Test Nos: 43,48,49,54,55,56,57

Single Discontinuity Testing in Sandstone.

Test Nos: 53,58,59,60,61,62,65,66

Single Discontinuity Testing in Concrete.

Test Nos: 75,76,77,78,81,82

Multiple Discontinuity Testing in Sandstone.

Test Nos: 63,64,67,68,69,70

Strength - Maximum p.s. Separation  
Experimentation.

Test Nos:

Springwell Sandstone - 50,51

Concrete - 71,72,73,74

Limestone - 92,93,95

Dolomitic Limestone - 90,91,94

Granite - 87,88,89

Dolomite - 79,80,83

Water Coupling Experimentation.

Test Nos: 84,85,86

Appendix E

MODEL TESTING SHOT FIRING DATA

TEST NO.	1	DATE:	13/6/80	PHASE:	1
BRIEF DESCRIPTION: Single hole in 6" <sup>3</sup> block to test suitability of detonating cord.					

PARAMETER	inches	mm	OTHER
Block Type			Resin
Block length	6	152.	
Block width	6	152	
Block height	6	152	
No. of Boreholes			1
Borehole diameter	$\frac{1}{8}$	3.175	
Borehole depth	$4\frac{1}{2}$	114	
Borehole spacing	—		Centers
No. of Detonators			1
Delay			—
Cord used per hole	9	229	12 Grain
Discontinuities	None		
Photographs	1		

Results: Block shattered but remained in situ. Heavy radial cracking with little concentric cracking. Block in many pieces but held together in wave traps and constraints.

Comments: Too much radial cracking - cord probably too strong. Absence of spalling at edge of block shows wave traps are effective.

TEST NO.	2	DATE:	14/6/80	PHASE:	1
----------	---	-------	---------	--------	---

BRIEF DESCRIPTION: Two holes in block to estimate whether presplitting can be performed using the cord available.

PARAMETER	inches	mm	OTHER
Block Type			Resin
Block length	6	152	
Block width	6	152	
Block height	6	152	
No. of Boreholes			2
Borehole diameter	$\frac{1}{4}$	3.175	
Borehole depth	$4\frac{1}{2}$	114	
Borehole spacing	$1\frac{1}{2}$	31.75	Centers
No. of Detonators			9
Delay			—
Cord used per hole	9		12 grain per ft.
Discontinuities	None		
Photographs	4 photographs + 2 slides (colour)		

Results: Wrecking of top half of blocks and wave traps.  
But on examination of bottom of block, a strong pre-split was found.

Comments: Split plane V chared by explosives, smallscale morphological crack features present but not clearly visible. Block fractured on either side of split but split walls fairly strong with little spalling.

TEST NO.	3	DATE:	9/10/79	PHASE:	1
----------	---	-------	---------	--------	---

BRIEF DESCRIPTION: First attempt to gain a pre-split using the new 4 grain per foot cord obtained from Canada via I.C.I. (Nobel Explosives).

PARAMETER	inches	mm	OTHER
Block Type			Resin
Block length		150	
Block width		150	
Block height		150	
No. of Boreholes			3
Borehole diameter	$\frac{1}{8}$	3.175	
Borehole depth	$4\frac{1}{2}$	114	
Borehole spacing	$1\frac{1}{2}$	31.75	Centers
No. of Detonators			1
Delay			—
Cord used per hole	9	229	4 grain per ft.
Discontinuities	None		
Photographs	5		

Results: Block remained in-situ but quite alot of radial fractures present. Presplit plane vissible, on removal block separated to show pre-split plane with reasonable features.

Comments: One wave trap broken due to no backing will be re-moded in future. Good pre-split with bottom blasted out of block (wedge shape with bottoms of boreholes preserved), but also shattering of block causing slow dissintegration after photography due to shifting and vibration.

TEST NO.	4	DATE:	10/10/79	PHASE:	1
BRIEF DESCRIPTION: Now using half blocks in an attempts to conserve stocks. Attempt to cause pre-split but with less shattering by increasing decoupling and spacing.					

PARAMETER	inches	mm	OTHER
Block Type			Resin
Block length		150	
Block width		150	
Block height		75	
No. of Boreholes			2
Borehole diameter	3/16	4.763	
Borehole depth		75	
Borehole spacing	1 1/2	47.63	Centers
No. of Detonators			1
Delay			—
Cord used per hole	9	229	4 grain per foot
Discontinuities	None		
Photographs	2		

Results: Less shattering caused but still 4 cracks making edge, block intact though. Good pre-split formed, radial fracture cylinders around boreholes did not overlap.

Comments: Interesting to note that no radial fractures were elongated 'between' the boreholes except the pre-split, also the split continues away from the left hand side borehole in both directions

TEST NO. 5	DATE: 11/10/79	PHASE: 1
BRIEF DESCRIPTION: Attempt to obtain a split using $\frac{1}{4}$ " boreholes, investigate effect of decoupling at same time.		

PARAMETER	inches	mm	OTHER
Block Type			Resin
Block length	6	152	
Block width	6	152	
Block height	3	76	
No. of Boreholes			2
Borehole diameter	$\frac{1}{4}$	6.35	
Borehole depth	3	76	
Borehole spacing	$1\frac{1}{4}$	47.63	Centers
No. of Detonators			1
Delay			—
Cord used per hole	6	152	4 grain per foot
Discontinuities	None		
Photographs	1		

Results: No presplit fracture, but encouraging fractures at bottom, and LH. borehole. Fractures on mid-line but not long enough. Still fracture zone around B/hole at 10mm from edge of hole.

Comments: Borholes too far apart to be pres-plit. Block also one of first batch, may be stronger.

TEST NO.	6	DATE:	11/10/79	PHASE:	1
----------	---	-------	----------	--------	---

BRIEF DESCRIPTION: Higher decoupling than in 5 for same result and reasons. Investigate effect of decoupling on blast damage and pre-split.

PARAMETER	inches	mm	OTHER
Block Type			Resin
Block length	6	152	
Block width	6	152	
Block height	3	76	
No. of Boreholes			3
Borehole diameter	5/16	7.938	
Borehole depth	3	76	
Borehole spacing	15/16	23.8	Centers
No. of Detonators			1
Delay			—
Cord used per hole	6	152	4 grain per foot
Discontinuities	None		
Photographs	1		

Results: As block was drilled for 2 holes with block 5, and after experiencing failure to pre-split of 5, an extra hole was drilled midway and loaded respectively. 3 holes less damage than in 5 but pre-split plane formed.

Comments: Blast damage reduced to 7mm. Half block from earliest casted block, the other half was used in blast 5.

TEST NO.	7	DATE:	18/10/79	PHASE:	1
BRIEF DESCRIPTION: To measure effect of decoupling on blast damage for single borehole, right through block.					

PARAMETER	inches	mm	OTHER
Block Type			Resin
Block length		150	
Block width		150	
Block height		75	
No. of Boreholes			1
Borehole diameter	3/16	4.763	
Borehole depth		75	
Borehole spacing	—	—	Centers
No. of Detonators			1
Delay			—
Cord used per hole	6	76	4 grain per foot
Discontinuities	None		
Photographs	1		

Results: Good breakage but not to edge. Apparently more damage at bottom of hole?

Comments: Seems more damage than for 2 holes but could be resin tho as of different batch to unsuccessful pre-split trial 5.

TEST NO. 8	DATE: 18/10/79	PHASE: 1
BRIEF DESCRIPTION: Aim: To measure effect of different decoupling ratios on blast damage for single borehole, right through block.		

PARAMETER	inches	mm	OTHER
Block Type			Resin
Block length		150	
Block width		150	
Block height		75	
No. of Boreholes			1
Borehole diameter	$\frac{1}{4}$	6.35	
Borehole depth		75	
Borehole spacing	—	—	Centers
No. of Detonators			1
Delay			—
Cord used per hole	6	152	4 grains per foot
Discontinuities	None		
Photographs	1		

Results: As in test No. 7 but less damage to block, again dense radial fracture zone with a few extended fractures.

Comments: Apparent split along one of the casting levels within the block, probable weakness plane - extended by blasts 9 and 10.

TEST NO. 9	DATE: 19/10/79	PHASE: 1
BRIEF DESCRIPTION: Single $5/16$ " Hole 4 grain cord. Aim: to measure effect of different decoupling ratios on blast damage for single borehole, right through block.		

PARAMETER	inches	mm	OTHER
Block Type			Resin
Block length		150	
Block width		150	
Block height		75	
No. of Boreholes			1
Borehole diameter	$5/16$	7.938	
Borehole depth		75	
Borehole spacing	—	—	Centers
No. of Detonators			1
Delay			—
Cord used per hole	6	152	4 grain per foot
Discontinuities	None		
Photographs	1		

Results: Nice small , dense radial fracture zone, no other visible effects.

Comments: Hole near corner of block but no bad effects occurring due to high decoupling.

TEST NO.	10	DATE:	19/10/79	PHASE:	1
----------	----	-------	----------	--------	---

BRIEF DESCRIPTION: Single  $5/16$ " hole 4 grain cord.  
 Aim: to measure effect of different decoupling ratios on blast damage for single boreholes, right through block.

PARAMETER	inches	mm	OTHER
Block Type			Resin
Block length		150	
Block width		150	
Block height		75	
No. of Boreholes			1
Borehole diameter	$11/32$	8.731	
Borehole depth		75	
Borehole spacing	—	—	Centers
No. of Detonators			1
Delay			—
Cord used per hole	6	152	4 grain per foot
Discontinuities	None		
Photographs	1		

Results: Nice small, dense radial fracture zone, no other visible effects.

Comments: Hole near corner of block but no bad effects due to high decoupling.

TEST NO.	11	DATE:	19/10/79	PHASE:	1
----------	----	-------	----------	--------	---

**BRIEF DESCRIPTION:** Single  $\frac{1}{8}$ " hole. 4 Grain Cord.  
**Aim:** To measure effect of different decoupling ratios on blast damage for single borehole, right through block.  
 (Decoupling trials - single hole).

PARAMETER	inches	mm	OTHER
Block Type			Resin
Block length		150	
Block width		150	
Block height		75	
No. of Boreholes			1
Borehole diameter	$\frac{1}{8}$	3.175	
Borehole depth		75	
Borehole spacing	—	—	Centers
No. of Detonators			1
Delay			—
Cord used per hole	6	152	4 grain per foot
Discontinuities	None		
Photographs	1		

**Results:** Fairly wide dense radial fracture zone with several longer fractures. A fracture from B/H splitting the block into 2 roughly equal pieces.

**Comments:** Very good morphological surface features on fractures cutting block will look good in thesis to compare with test No. 3 photographs.

TEST NO. 12	DATE: 1/11/79	PHASE: 1
BRIEF DESCRIPTION: Attempt to presplit resin block with 3 holes. Part of experiment to find max. pre-split separation dependency on decoupling		

PARAMETER	inches	mm	OTHER
Block Type			Resin
Block length		150	
Block width		150	
Block height		75	
No. of Boreholes			3
Borehole diameter		8	
Borehole depth		75	
Borehole spacing	1 1/4	28.6	Centers
No. of Detonators			1
Delay			—
Cord used per hole	6	152	4 grain per foot
Discontinuities	None		
Photographs	1		

**Results:** Hole No. misfired hole 2 and 3 OK. Pre-split between all holes and edge of block! Even through missfired hole. Good damaged zones around 2 and 3, 1 has none.

**Comments:** Must investigate any pre-split occurred across No. 1 hole to edge. Both by model testing and theory.

TEST NO. 13	DATE: 7/11/79	PHASE: 1
<b>BRIEF DESCRIPTION:</b> Attempt to pre-split resin block with 3 holes - part of experiment to find max. pre-split separation + dependency on decoupling.		

PARAMETER	inches	mm	OTHER
Block Type			Resin
Block length		150	
Block width		150	
Block height		75	
No. of Boreholes			3
Borehole diameter	5/16	7.938	
Borehole depth		75	
Borehole spacing	1½	38.1	Centers
No. of Detonators			1
Delay			-
Cord used per hole	8	203	4 grains per foot
Discontinuities	None		
Photographs	1		

**Results:** Good presplit obtained, breakage to sides of block giving 2 pieces, shattering around holes some damage seen in rest of block parallel to presplit plane.

**Comments:**  
Fracture zones from blast holes do not overlap

TEST NO. 14	DATE: 7/11/79	PHASE: 1
<b>BRIEF DESCRIPTION:</b> Attempt to pre-split resin block with 3 holes, part of experiment to find max. pre-split separation + dependency on decoupling.		

PARAMETER	inches	mm	OTHER
Block Type			Resin
Block length		150	
Block width		150	
Block height		75	
No. of Boreholes			3
Borehole diameter	$\frac{1}{2}$	6.35	
Borehole depth		75	
Borehole spacing	$1\frac{1}{2}$	38.1	Centers
No. of Detonators			1
Delay			-
Cord used per hole	8	203	4 grains per foot
Discontinuities	None		
Photographs			1

<b>Results:</b> Good pre-split formed better than in test 13, good fracture around boreholes, breakage of block in two by pre-split plane, no other damage seen in block.
--

<b>Comments:</b> Fracture zones from blast holes do not overlap
--

TEST NO. 15	DATE: 9/11/79	PHASE: 1
----------------	------------------	-------------

**BRIEF DESCRIPTION:**

Attempt to ascertain whether the detonation waves from boreholes have any interrelated effect on each other - delay experiment.

PARAMETER	inches	mm	OTHER
Block Type			Resin
Block length		150	
Block width		150	
Block height		75	
No. of Boreholes			3
Borehole diameter	5/16	7.938	
Borehole depth		75	
Borehole spacing	1½	38.1	Centers
No. of Detonators			1
Delay		190 per hole	27 µs
Cord used per hole	8, 13, 18	203/330/457	4 grain per foot
Discontinuities	None		
Photographs			1

**Results:**

Pre-split obtained - very good breakage along P/S line but seems to have more damage per individual borehole than when simultaneously detonated.

**Comments:**

This extra damage could just be a one off.

TEST NO. 16	DATE: 9/11/79	PHASE: 1
BRIEF DESCRIPTION: Attempt to attain pre-split failure in resin block using 3 holes - part of experiment to find max. pre-split separation and dependency on decoupling.		

PARAMETER	inches	mm	OTHER
Block Type			Resin
Block length		150	
Block width		150	
Block height		75	
No. of Boreholes			3
Borehole diameter	5/16	7.938	
Borehole depth		75	
Borehole spacing	1 3/4 c		Centers
No. of Detonators			1
Delay			-
Cord used per hole	8	203	4 grain per foot
Discontinuities	None		
Photographs			1

**Results:**  
Good pre-split obtained, less damage around each hole than in delay experiment No.15.

**Comments:**  
Less damage - especially concerning longer individual fractures.  
  
We still do not seem to be near the limit of pre-splitting for 5/16" holes.

TEST NO. 17	DATE: 16/11/79	PHASE: 1
<p>BRIEF DESCRIPTION:          4 gpf and in <math>\frac{5}{16}</math> " Attempt to find limit of pre-split for          holes using 3 boreholes drilled          diagonally across block.</p>		

PARAMETER	inches	mm	OTHER
Block Type			Resin
Block length		150	
Block width		150	
Block height		75	
No. of Boreholes			3
Borehole diameter	$\frac{5}{16}$	7.938	
Borehole depth		75	
Borehole spacing	2	50.8	Centers
No. of Detonators			1
Delay			-
Cord used per hole	8	203	4 grain per foot
Discontinuities	None		
Photographs			1

<p>Results:          A good pre-split with more than usual damage around          boreholes especially for longest cracks.</p>
--

<p>Comments:          Only pre-split between holes and holes cracked          to side of block.</p>
---

TEST NO. 18	DATE: 16/11/79	PHASE: 1
BRIEF DESCRIPTION: Attempt to find limit of pre-split for 4 gpf cord in $\frac{1}{2}$ " holes using 3 boreholes drilled diagonally across block.		

PARAMETER	inches	mm	OTHER
Block Type			Resin
Block length		150	
Block width		150	
Block height		75	
No. of Boreholes			3
Borehole diameter	$\frac{1}{2}$	6.35	
Borehole depth		75	
Borehole spacing	2	50.8	Centers
No. of Detonators			1
Delay			-
Cord used per hole	8	203	4 grain per foot
Discontinuities	None		
Photographs			1

Results:

A good pre-split obtained with more than usual damage i.e. compared with closer spacings, around boreholes especially for longer cracks.

Comments:

Pre-split better, more distinct and not only confined to between boreholes but still cracking to side of constrained block i.e. 45° to P/S time for end holes.

TEST NO. 19	DATE: 19/11/79	PHASE: 1
-------------	----------------	----------

BRIEF DESCRIPTION:  
 „Attempt to find max. presplit b/h separation for 5/16 holes using 4 gpf cord. 3 holes set in a line diagonally across block

PARAMETER	inches	mm	OTHER
Block Type			Resin
Block length		150	
Block width		150	
Block height		75	
No. of Boreholes			3
Borehole diameter	5/16	7.938	
Borehole depth		75	
Borehole spacing	2½	63.5	Centers
No. of Detonators			1
Delay			-
Cord used per hole	8	203	4 grain per foot
Discontinuities	None		
Photographs			2

Results:  
 A complete pre-split was not obtained but only just not! Fractures overlapping from successive b/hs with no p/s breakage further down block. - Some bad damage in top of block for some reason.

Comments:  
 Fractures longer in top of block than bottom. As boreholes get further apart there seems to be more damage laterally from boreholes to pre-split line.

TEST NO. 20	DATE: 19/11/79	PHASE: 1
BRIEF DESCRIPTION: Attempt to find max. presplit b/h separation for $\frac{1}{4}$ " holes using 4 gpf cord. 3 holes set in a line diagonally across block.		

PARAMETER	inches	mm	OTHER
Block Type			Resin
Block length		150	
Block width		150	
Block height		75	
No. of Boreholes			3
Borehole diameter	$\frac{1}{4}$	6.35	
Borehole depth		75	
Borehole spacing	$2\frac{1}{2}$	63.5	Centers
No. of Detonators			1
Delay			-
Cord used per hole	8	203	4 grain per foot
Discontinuities	None		
Photographs			1

**Results:**  
Pre-split obtained but net very strong, some doubt as to whether there is a distinct plane. Fractures from boreholes only overlapping by approximately 1cm.

**Comments:**  
Would be O.K. for rock but in this homogeneous material the block is still intact (i.e. doesn't fall apart), end cracks off at approx.  $35^{\circ}$  to pre-split plane cracking to edge of block. Cracks long in rough split direction, but much shorter perpendicular to split.

TEST NO. 21	DATE: 30/11/79	PHASE: 1
BRIEF DESCRIPTION: Single shot used in experiments for determination of blast damage relationship to decoupling and decoupling ratio of 1:1		

PARAMETER	inches	mm	OTHER
Block Type			Resin
Block length		150	
Block width		150	
Block height		70	
No. of Boreholes			1
Borehole diameter	$1/10$	2.54	
Borehole depth		70	
Borehole spacing			Centers
No. of Detonators			1
Delay			-
Cord used per hole	6"	152	4 grain p.f.
Discontinuities	None		
Photographs			1

Results: High breakage, dense fracturing, block held together in/by restraints over 10 weeks to edge of block.

Comments: used to fill holes in intial graph. 1:1 decoupling with 4 grains/ft cord.  
 N.B. Hole was first drilled using a smaller diam. drill and then drilled from either side with a short  $1/10$ " drill using the inital smaller hole as a guide.

TEST NO. 22	DATE: 30/11/79	PHASE: 1
BRIEF DESCRIPTION: Single shot part of experiment to determine the blast damage to decoupling relationship.		

PARAMETER	inches	mm	OTHER
Block Type			Resin
Block length		150	
Block width		150	
Block height		65	
No. of Boreholes			1
Borehole diameter	5/32	3.969	
Borehole depth		65	
Borehole spacing	-	-	Centers
No. of Detonators			1
Delay	-	-	-
Cord used per hole	6"	152	4 grain per foot
Discontinuities	None		
Photographs			1

Results: Good fracturing but not as far as edge of block, good dense radial fracture zone.

Comments: Main cracks perpendicular to constraints, but constraints only tightened to 5 ft lbs. for each bolt so only a very marginal stress field. Also other long cracks straight in other directions.

TEST NO. 23	DATE: 6/12/79	PHASE: 1
BRIEF DESCRIPTION: Single shot-part of the experiment to determine the relationship between blast damage and decoupling.		

PARAMETER	inches	mm	OTHER
Block Type			Resin
Block length		150	
Block width		150	
Block height		70	
No. of Boreholes			1
Borehole diameter	$\frac{1}{2}$	12.7	
Borehole depth		70	
Borehole spacing	-	-	Centers
No. of Detonators			1
Delay			-
Cord used per hole	6"	152	4 grain per foot
Discontinuities	None		
Photographs			1

Results: Well formed limited circular blast damage zone
---

Comments:
-----------

TEST NO. 24	DATE: 6/12/79	PHASE: 1
BRIEF DESCRIPTION: Single shot - part of the experiment to determine the relationship between blast damage and decoupling.		

PARAMETER	inches	mm	OTHER
Block Type			Resin
Block length		150	
Block width		150	
Block height		70	
No. of Boreholes			1
Borehole diameter	7/16	11.113	
Borehole depth		70	
Borehole spacing	-	-	Centers
No. of Detonators			1
Delay			-
Cord used per hole	6"	152	4 Grain per foot
Discontinuities	None		
Photographs			1

Results: Well formed limited circular blast damage zone

Comments:

TEST NO. 25	DATE: 14/12/79	PHASE: 1
BRIEF DESCRIPTION: Single shot-part of the experiment to determine the relationship between blast damage and decoupling.		

PARAMETER	inches	mm	OTHER
Block Type			Resin
Block length		150	
Block width		150	
Block height		70	
No. of Boreholes			1
Borehole diameter	5/8	15.875	
Borehole depth		70	
Borehole spacing	-	-	Centers
No. of Detonators			1
Delay			-
Cord used per hole	6	152	4 grain per foot
Discontinuities	None		
Photographs			1

Results: Well formed limited circular blast damage zone.

Comments: Slight splitting around one of casting layers. Nothing else out of usual.

TEST NO. 26	DATE: 14/12/79	PHASE: 1
BRIEF DESCRIPTION: Single shot-part of the experiment to determine the relationship between blast damage and decoupling.		

PARAMETER	inches	mm	OTHER
Block Type			Resin
Block length		150	
Block width		150	
Block height		70	
No. of Boreholes			1
Borehole diameter	3/4	19.05	
Borehole depth		70	
Borehole spacing	-	-	Centers
No. of Detonators			1
Delay			-
Cord used per hole	6	152	4 grain per foot
Discontinuities	None		
Photographs			1

Results:  
Well formed very limited damage zone.

Comments:

TEST NO. 27	DATE: 14/12/79	PHASE: 1
BRIEF DESCRIPTION: Single shot-part of experiment to determine the relationship between blast damage and decoupling.		

PARAMETER	inches	mm	OTHER
Block Type			Resin
Block length		150	
Block width		150	
Block height		70	
No. of Boreholes			1
Borehole diameter	1"	25.4	
Borehole depth		70	
Borehole spacing	-	-	Centers
No. of Detonators			1
Delay			-
Cord used per hole	6	152	4 grain per foot
Discontinuities	None		
Photographs			1

Results: Only slight cracking around hole.

Comments:

TEST NO. 28	DATE: 11/1/80	PHASE: 1
BRIEF DESCRIPTION: Triple ½" hole shot-part of experiment to determine dependency of hole separation on decoupling 8" hole		

PARAMETER	inches	mm	OTHER
Block Type			Resin
Block length	8	203	
Block width	6	152	
Block height		70	
No. of Boreholes			3
Borehole diameter	½	6.35	
Borehole depth		70	
Borehole spacing	2½	63.5	Centers
No. of Detonators			1
Delay			-
Cord used per hole	8	203	4 grain per foot
Discontinuities	None		
Photographs	1		

Results: One hole mis-fire, other two O.K.  
Split between 2 fixed holes for top half of block, assumed better split if no misfire

Comments: Bottom layer badly damaged due to presence of bubbles. This was caused during casting as it was the bottom layer.  
Also presence of cracks towards the constraints - possibly due to over tightening of constraints.

TEST NO. 29	DATE: 15/1/80	PHASE: 1
BRIEF DESCRIPTION: Triple ½" hole short-part of experiment to determine dependency of hole separation on decoupling 10" block.		

PARAMETER	inches	mm	OTHER
Block Type			Resin
Block length	10	254	
Block width	6	152	
Block height		70	
No. of Boreholes			3
Borehole diameter	½	6.35	
Borehole depth		70	
Borehole spacing	3	76.2	Centers
No. of Detonators			1
Delay			—
Cord used per hole	10	254	4 grain per foot
Discontinuities	None		
Photographs	1		

Results: Pre-split definitely not obtained, good shatter zones around boreholes with fractures from different boreholes only craking in two places. Splay fractures at ends.

Comments: This block for some reason displays numerous side fractures orientated perpendicular to the main restrained sides. An effect which has not been noticed before.

TEST NO. 30	DATE: 16/1/80	PHASE: 1
BRIEF DESCRIPTION: Attempt to find borehole spacing of $3/16$ " holes for a successful pre-split using 4 grain per foot cord.		

PARAMETER	inches	mm	OTHER
Block Type			Resin
Block length	10	254	
Block width	6	152	
Block height		70	
No. of Boreholes			3
Borehole diameter	$3/16$	4.763	
Borehole depth			
Borehole spacing	3	76.2	Centers
No. of Detonators			1
Delay			-
Cord used per hole	10"	254	4 grain per foot
Discontinuities	None		
Photographs	1		

Results: Good pre-split obtained between 3 holes, double split between two. Good damage zones around boreholes. Splay Fracture at either end of line.

Comments: Relatively good results but bottom layer of block seems to be of different composition, with minor parting at its interface with the next layer up.

TEST NO. 31	DATE: 18/1/80	PHASE: 1
BRIEF DESCRIPTION: Attempt to find new borehole spacing of $3/16$ " holes for a successful pre-split using 4 grain/ft. cord.		

PARAMETER	inches	mm	OTHER
Block Type			Resin
Block length	10	254	
Block width	6	152	
Block height		70	
No. of Boreholes			3
Borehole diameter	$3/16$ "	4.763	
Borehole depth			
Borehole spacing	$3\frac{1}{2}$	88.9	Centers
No. of Detonators			1
Delay			—
Cord used per hole	10"	254	4 grain/ft.
Discontinuities	NONE		
Photographs	1		

Results: Good pre-split obtained again but single split throughout, good damage zones with splaying of centre borehole also this time.

Comments: Good results again but some parting effect is present at top of bottom layer as in previous test.

TEST NO. 32	DATE: 23/1/80	PHASE: 1
BRIEF DESCRIPTION: Attempt to find max presplit separation for $3/16$ " holes using 4 grain per foot cord.		

PARAMETER	inches	mm	OTHER
Block Type			Resin
Block length	10	254	
Block width	6	152	
Block height		68	
No. of Boreholes			3
Borehole diameter	$3/16$ "	4.763	
Borehole depth			
Borehole spacing	4	101.6	Centers
No. of Detonators			1
Delay			—
Cord used per hole	10"	254	4 grain/ft.
Discontinuities	NONE		
Photographs	1		

Results: Good pre-split formed but very concave in one direction also other long length fractures. Good damage zones.

Comments: Damage zones seem to have increased in size with far more cracks having being ('grossly' elongated), pre-split plane very uneven.

TEST NO. 33	DATE: 23/1/80	PHASE: 1
BRIEF DESCRIPTION: A single $\frac{1}{2}$ hole on the edge of a half block. Experiment to find out how much damage the detonation wave alone causes.		

PARAMETER	inches	mm	OTHER
Block Type			Resin
Block length		75	
Block width		153	
Block height		71	
No. of Boreholes			1
Borehole diameter	$\frac{1}{2}$	3.175	
Borehole depth		71	
Borehole spacing		—	Centers
No. of Detonators			1
Delay			—
Cord used per hole	6"	152	4 grain/ft.
Discontinuities	NONE		
Photographs	Top and Side		

Results: Small damage zone increasing slowly in width with depth.

Comments: Better shown on side than top view.

TEST NO. 34	DATE: 25/1/80	PHASE: 1
BRIEF DESCRIPTION: Twin hole test to obtain max tve pre-split separation for two (half) holes, providing the dynamic component of blast only.		

PARAMETER	inches	mm	OTHER
Block Type			Resin
Block length		150	
Block width		51	
Block height		71	
No. of Boreholes			2
Borehole diameter	$\frac{1}{8}$	3.175	
Borehole depth		71	
Borehole spacing		50	Centers
No. of Detonators			1
Delay			—
Cord used per hole	6"	152	4 grain/ft.
Discontinuities	NONE		
Photographs	2		

Results: Shattering around holes as before for  $\frac{1}{8}$ " holes some resemblance of p/s. but block fairly intact - concluded: No definite p/s.

Comments: Alot of damage to block due to the absence of wave traps. Inverted Christmas tree affect of damage down the line of detonation as usually found in most tests.

TEST NO. 35	DATE: 31/1/80	PHASE: 1
BRIEF DESCRIPTION: Attempt to find max pr-split separation for $\frac{3}{16}$ " holes using 4 grain per foot cord.		

PARAMETER	inches	mm	OTHER
Block Type			Resin
Block length	14	355.6	
Block width	6	153	
Block height		72	
No. of Boreholes			3
Borehole diameter	$\frac{3}{16}$ "	4.763	
Borehole depth		72	
Borehole spacing	5"		Centers
No. of Detonators			1
Delay			—
Cord used per hole	12"	305	4 grain/ft <sup>-1</sup>
Discontinuities	NONE		
Photographs	2		

Results: Gross failure to obtain a pre-split although some cracks elongated a little way along pre-split line.

Comments: Good damage zones as per. usual.

TEST NO. 36	DATE: 1/2/80	PHASE: 1
BRIEF DESCRIPTION: Attempt to find effect of dynamic component only using $\frac{1}{2}$ borehole ( $\frac{3}{16}$ " ) in slice of perspex block.		

PARAMETER	inches	mm	OTHER
Block Type			Resin
Block length		147	
Block width		40	
Block height		70	
No. of Boreholes			1
Borehole diameter	$\frac{3}{16}$	4.7625	
Borehole depth		70	
Borehole spacing	—	—	Centers
No. of Detonators			1 ( $\frac{1}{2}$ )
Delay			—
Cord used per hole	7"	178	4 grain/ft <sup>-1</sup>
Discontinuities	NONE		
Photographs	2		

Results: Shallow fracture zone approx. 9mm radiating out from edge of borehole. Few longer radiating fractures.

Comments: Again damage in block higher than usual but most stopped by wave traps.

TEST NO. 37	DATE: 1/2/80	PHASE: 1
BRIEF DESCRIPTION: Attempt to find effect of dynamic component only using $\frac{1}{2}$ borehole ( $\frac{5}{16}$ " ) in slice of perspex block. Part of series of experiments to determine dynamic damage.		

PARAMETER	inches	mm	OTHER
Block Type			Resin
Block length		153	
Block width		36	
Block height		70	
No. of Boreholes			1
Borehole diameter	$\frac{5}{16}$	7.9375	
Borehole depth		70	
Borehole spacing	—	—	Centers
No. of Detonators			1 (0.5)
Delay			—
Cord used per hole	7"	178	4 grain/ft <sup>-1</sup>
Discontinuities	NONE		
Photographs	4		

Results: V small fractured zone around edge of borehole. No inverted christmas tree effect this time.

Comments: Again no extended fractures extending outwards from damage zone.

TEST NO. 38	DATE: 31/1/80	PHASE: 1
BRIEF DESCRIPTION: Attempt to find max. dynamic pre-split separation for $\frac{1}{2}$ " holes (using half holes on the edges of a sliced block).		

PARAMETER	inches	mm	OTHER
Block Type			Resin
Block length		149	
Block width		42	
Block height		72	
No. of Boreholes			2
Borehole diameter	$\frac{1}{2}$	3.175	
Borehole depth		72	
Borehole spacing		40	Centers
No. of Detonators			1
Delay			—
Cord used per hole	6"	152	4 grain/ft <sup>-1</sup>
Discontinuities	NONE		
Photographs	3		

Results: Apparent cracking between boreholes but block remains intact, therefore no p/s has occurred.  
High damage in block due to no wave traps.

Comments: Inverted christmas tree damage effect present for both boreholes. This is seen very well from the side.

TEST NO.	39	DATE:	6/1/80	PHASE:	1
BRIEF DESCRIPTION: Attempt to find max. pre-split separation for $\frac{1}{8}$ " holes using standard cord.					

PARAMETER	inches	mm	OTHER
Block Type			Resin
Block length	14		
Block width	6	153	
Block height		68	
No. of Boreholes			3
Borehole diameter	$\frac{1}{8}$	3.175	
Borehole depth		68	
Borehole spacing	5		Centers
No. of Detonators			1
Delay			—
Cord used per hole	12		4 grain/ft
Discontinuities	NONE		
Photographs	1		

Results: Good, fairly straight, pre-split, good damage zones around boreholes.

Comments: Pre-split fractures largest fractures, no extraneous damage or layer separation at casting horizons.

TEST NO.	40	DATE:	13/1/80	PHASE:	1
BRIEF DESCRIPTION: Attempt to find max. pre-split separation for $\frac{1}{8}$ " holes using standard cord.					

PARAMETER	inches	mm	OTHER
Block Type			Resin
Block length	18		
Block width	6	152	
Block height			
No. of Boreholes			3
Borehole diameter	$\frac{1}{8}$	3.175	
Borehole depth			
Borehole spacing	6		Centers
No. of Detonators			1
Delay			—
Cord used per hole	14		4 grain/ft
Discontinuities	NONE		
Photographs	1		

Results: Pre-split formed, good damage zones around boreholes, many other major fractures.

Comments: Pre-split double between holes, also pre-split plane starting to curve and become concave. More damage around holes than in last test.

TEST NO.	41	DATE:	20/1/80	PHASE:	1
BRIEF DESCRIPTION: Attempt to find max. pre-split separation for $\frac{1}{8}$ " hole.					

PARAMETER	inches	mm	OTHER
Block Type			Resin
Block length	18	450	
Block width	26	150	
Block height		72	
No. of Boreholes			3
Borehole diameter	$\frac{1}{8}$	3.175	
Borehole depth		72	
Borehole spacing	7		Centers
No. of Detonators			1
Delay			—
Cord used per hole	14		4 grain/ft.
Discontinuities	NONE		
Photographs	1		

Results: Good pre-split between inner and top borehole, but just failed with outer borehole - outer borehole crack making 95% of ground. Good damage zones around boreholes.

Comments: Relatively same amount of damage as in 40. Pre-split fracture is not vertical throughout but is spirally twisted.

TEST NO. 42	DATE: 20/1/80	PHASE: 1
BRIEF DESCRIPTION: Attempt to find max pre-split separation for $\frac{3}{8}$ " holes.		

PARAMETER	inches	mm	OTHER
Block Type			Resin
Block length	6		
Block width	6		
Block height		72.5	
No. of Boreholes			3
Borehole diameter	$\frac{3}{8}$	9.525	
Borehole depth		72.5	
Borehole spacing		50	Centers
No. of Detonators			1
Delay			—
Cord used per hole	8"		4 grain/ft
Discontinuities	NONE		
Photographs	1		

Results: Good fairly straight pre-split formed between all holes, continuing to one edge of block in str. line. Well formed small damage zones around all boreholes.

Comments: Some vertical cracking in bottom of block which represents tacky top surface of original moulded beam.  
\*Note : All cracks at right angles to pre-split line.

TEST NO. 43	DATE: 27/2/80	PHASE: 2
BRIEF DESCRIPTION: Attempt to find affect of introducing single fractures at 45° to, on the presplit plane		

PARAMETER	inches	mm	OTHER
Block Type			RESIN
Block length	10		
Block width	6		
Block height		70	
No. of Boreholes			3
Borehole diameter	3/16"	4.763	
Borehole depth		70	
Borehole spacing	3		Centers
No. of Detonators			1
Delay			N/A
Cord used per hole	10		4 grains/ft
Discontinuities	Middistance Single 45° to p/s		
Photographs	2 top view		

**Results:** Irregular preslit formed, splitting/fracturing tending to find the shortest route from the borehole to the fracture plane.

**Comments:** Also quite a few fractures bending towards the fracture planes (important!) and a fracture initiated from the top edge of the block towards and perpendicular to the 'line' of presplit.

TEST NO. 44	DATE: 27/2/80	PHASE: 1
-------------	---------------	----------

**BRIEF DESCRIPTION:** Attempt to find max. dynamics pre-split separation using rested boreholes (half) with 1/8" diameter boreholes.

PARAMETER	inches	mm	OTHER
Block Type			RESIN
Block length		153	
Block width		30	
Block height		70	
No. of Boreholes			2
Borehole diameter	1/8"	3.175	
Borehole depth		70	
Borehole spacing		30	Centers
No. of Detonators			1
Delay			N/A
Cord used per hole	6		4 grain/ft
Discontinuities	NONE		
Photographs	2 (top + side)		

**Results:** High shattering around hole, block not in two pieces but cracks seen in backs of boreholes and block flexes around middle. Will only take slight pressure to break. Therefore not split just.

**Comments:** Top of block smashed badly due to no metal top plate. 1/2" piece of wood was used and detonator punched straight through it.

TEST NO. 45	DATE: 1/5/80	PHASE: 1
<p><b>BRIEF DESCRIPTION:</b> Attempt to determine the damage the seismic component makes as part of half borehole series using 1/10" <math>\frac{1}{2}</math> hole.</p>		

PARAMETER	inches	mm	OTHER
Block Type			RESIN
Block length		41	
Block width		150	
Block height		70	
No. of Boreholes			1
Borehole diameter	1/10"	2.54	
Borehole depth		70	
Borehole spacing		N/A	Centers
No. of Detonators			1
Delay			-
Cord used per hole	6		4 grain/ft
Discontinuities			
Photographs	NONE		

**Results:** Medium small damage zone around borehole with numerous cracks emanating out from the borehole.

**Comments:** Reverse christmas tree effect very distinct showing build up of wave damage.

TEST NO.	46	DATE:	27/2/80	PHASE:	1
BRIEF DESCRIPTION: Attempt to determine the damage the seismic component makes as part of the series of experiments to determine the relationship between shock wave damage and decoupling.					

PARAMETER	inches	mm	OTHER
Block Type			RESIN
Block length		153	
Block width		42	
Block height		70	
No. of Boreholes			1
Borehole diameter	3/8"	9.525	
Borehole depth		70	
Borehole spacing		N/A	Centers
No. of Detonators			1 shared with 47
Delay			-
Cord used per hole	6		4 grains/ft
Discontinuities			
Photographs	2 (top + side)		

**Results:** Very small damage zone around boreholes with numerous cracks emanating out from borehole approx. 13mm long.

**Comments:** The reverse christmas tree effect on this one might be due to cord being further into borehole i.e. nearer borehole wall at top.

TEST NO.	47	DATE:	27.2.80	PHASE:	1
----------	----	-------	---------	--------	---

**BRIEF DESCRIPTION:** Attempt to determine the damage the seismic component makes as part of the experimental series to determine the relationship between sockwave damage and decoupling.

PARAMETER	inches	mm	OTHER
Block Type			RESIN
Block length		153	
Block width		40	
Block height		69	
No. of Boreholes			1
Borehole diameter	1/2"	12.7	
Borehole depth		69	
Borehole spacing		N/A	Centers
No. of Detonators			1 shared with 46
Delay	-	-	-
Cord used per hole	6		4 grains/ft
Discontinuities			
Photographs	1 (top + side)		

**Results:** Very minute amount of damage around borehole very elongated fractures.

**Comments:** Same as in 46, a reversed christmas tree effect but not much damage. Probably just addition of shock wave damage back up the borehole.

TEST NO.	48	DATE:	6/3/80	PHASE:	2
----------	----	-------	--------	--------	---

**BRIEF DESCRIPTION:** Attempt to find affect of introducing single fractures at 30° on the presplit plane.

PARAMETER	inches	mm	OTHER
Block Type			RESIN
Block length	10		
Block width	6		
Block height		70	
No. of Boreholes			3
Borehole diameter	3/16"	4.763	
Borehole depth		70	
Borehole spacing	3		Centers
No. of Detonators			1
Delay			N/A
Cord used per hole	10		4 grain/ft
Discontinuities	Middistance single 30° to p/s		
Photographs	1 top view		

**Results:** Very irregular presplit, multiple cracking around plane, would result in loss of midd hole. Initial cracking to joint planes at 90° and also cracks from other boreholes merge to cracks from centre borehole.

**Comments:** Would result in overbreak causing loss of half barrels certainly for use of midborehole. If not would leave a weakened presplit plane, without a very strong presplit.

TEST NO. 49	DATE: 6/3/80	PHASE: 2
BRIEF DESCRIPTION: Attempt to find affect of introducing single fractures at 60°, on the pre-split plane..		

PARAMETER	inches	mm	OTHER
Block Type			RESIN
Block length	10		
Block width	6		
Block height		70	
No. of Boreholes			3
Borehole diameter	3/16"	4.763	
Borehole depth		70	
Borehole spacing	3		Centers
No. of Detonators			1
Delay			N/A
Cord used per hole	10		4 grains/ft
Discontinuities	Middistance single 60° to p/s		
Photographs	1 top view		

**Results:** Pre-split formed but mainly by cracking straight to joint planes . Therefore p/s very jagged. Also some fractures from other boreholes curving to these points.

**Comments:** Would not result in much overbreak if any with under-break in places. There should be no loss of half barrels.

TEST NO.	50	DATE: 3.4.80	PHASE: 2
<b>BRIEF DESCRIPTION:</b> Assessment of amount of explosive required to presplit sandstone with 3/8" holes at various B/H seps..			

PARAMETER	inches	mm	OTHER
Block Type			Sandstone
Block length	12	305	
Block width	8	203	Connected to 51 & 52
Block height	5½	140	
No. of Boreholes			4
Borehole diameter	3/8	9.525	
Borehole depth	5.1/2	140	
Borehole spacing	3	76	Centers
No. of Detonators			1
Delay			N/A
Cord used per hole			Single 11 gr/ft
Discontinuities	NONE		
Photographs	Above + presplit surface		

**Results:**  
 Successful presplit, fairly straight

**Comments:**  
 No spaying at ends. Presplit slightly uneven and does not connect centres of boreholes for inner 2 holes.

TEST NO. 51	DATE: 3/4/80	PHASE: 2
<b>BRIEF DESCRIPTION:</b> Assessment of amount of explosive required to presplit sandstone with 3/8" holes at various B/H seps.		

PARAMETER	inches	mm	OTHER
Block Type			Sandstone
Block length	12	305	
Block width	8	203	Connected to 50 + 52
Block height	5½	140	
No. of Boreholes			3
Borehole diameter	3/8"	9.525	
Borehole depth	5½	140	
Borehole spacing	3½	89	Centers
No. of Detonators			1
Delay			N/A
Cord used per hole			Single 11 gr/ft
Discontinuities	NONE		
Photographs	1 top view		

<b>Results:</b> Failure to presplit
--

<b>Comments:</b> No open or closed fractures observed with naked eye.
--

TEST NO. 52	DATE: 3/4/80	PHASE: 2
<b>BRIEF DESCRIPTION:</b> Assessment of amount of explosive required to presplit sandstone with 3/8" holes at various B/H seps.		

PARAMETER	inches	mm	OTHER
Block Type			SANDSTONE
Block length	12	305	
Block width	8	203	
Block height	5½	140	
No. of Boreholes			3
Borehole diameter	3/8"	9.525	
Borehole depth	5½	140	
Borehole spacing	4	102	Centers
No. of Detonators			1
Delay			N/A
Cord used per hole			Double 11 gr/ft
Discontinuities	NONE		
Photographs	Above + presplit surface.		

**Results:**  
 Good presplit obtained, splaying at edges of block from outer holes and also presplit not as straight as in test 50.

**Comments:**  
 Surface of presplit is visibly looser than in test 50 with more material scabbing from the presplit surface, indicating a higher number of new fractures and higher amounts of disturbed rock along the presplit.

TEST NO. 53	DATE: 16/4/80	PHASE: 2
<b>BRIEF DESCRIPTION:</b> Presplit in sawn block of rock with jointing mid-distance between boreholes vertical and at 30° to hole line		

PARAMETER	inches	mm	OTHER
Block Type			SANDSTONE
Block length	24	610	
Block width	12	305	
Block height	5½	140	
No. of Boreholes			5
Borehole diameter	3/8"	9.525	
Borehole depth	5½	140	
Borehole spacing	4	102	Centers
No. of Detonators			1
Delay			N/A
Cord used per hole	24	610	Doubled 11 gr/ft
Discontinuities	Mid-distance, single, vertical 30° top/s		
Photographs	3 from above		

**Results:**  
 Good split occurred in majority of holes, but is influenced by immediate breakages to discontinuities.

**Comments:**  
 Apart from presplit there is immediate breakage to jointing (shown best at ends) but this fracturing is also 'bent' by Quasistatic Stress field superposition quite markedly

TEST NO.	54	DATE: 1/5/80	PHASE: 2
BRIEF DESCRIPTION: Pre-split in Resin with angled jointing middistance between boreholes at 15° to hole line.			

PARAMETER	inches	mm	OTHER
Block Type			RESIN
Block length	10		
Block width	6		
Block height		70	
No. of Boreholes			3
Borehole diameter	3/16"	4.763	
Borehole depth		70	
Borehole spacing			Centers
No. of Detonators			1
Delay			N/A
Cord used per hole	8		4 grains/ft
Discontinuities	Middistance single 15° to p/s		
Photographs	1 top view.		

**Results:** Splitting between boreholes but no obvious straight pre-split. Fracturing occurs mainly towards discontinuities i.e. shortest path and then along the discontinuity.

**Comments:** The second fracturing which affects overbreak is that of fractures bending round to cut into the discontinuity plane opposite the former fracturing.

TEST NO.	55	DATE:	1/5/80	PHASE:	2
BRIEF DESCRIPTION: Pre-split in resin with angled jointing middistance between boreholes at 75° to hole line.					

PARAMETER	inches	mm	OTHER
Block Type			RESIN
Block length	10		
Block width	6		
Block height		70	
No. of Boreholes			3
Borehole diameter	3/16	4.763	
Borehole depth		70	
Borehole spacing	3		Centers
No. of Detonators			1
Delay			N/A
Cord used per hole	8		4 grain/ft
Discontinuities	Middistance single 75° to p/s		
Photographs	1 top view		

Results: No obvious distinct pre-split plane but fracturing along shortest route to discontinuities giving a stepped face. i.e. breakage between all holes.

Comments: The presence of the discontinuities seems to be slightly suppressing a (perfect) pre-split.

TEST NO. 56	DATE: 1/5/80	PHASE: 2
BRIEF DESCRIPTION: Pre-split in Resin with angled discontinuities middistance between boreholes at 90° to hole line.		

PARAMETER	inches	mm	OTHER
Block Type			RESIN
Block length	10		
Block width	6		
Block height		70	
No. of Boreholes			3
Borehole diameter	3/16"	4.763	
Borehole depth		70	
Borehole spacing	3		Centers
No. of Detonators			1
Delay			N/A
Cord used per hole	8		4 grains/ft
Discontinuities	Single 90° to line of boreholes		
Photographs	1 top view		

Results: Pre-split slightly more obvious than in No. 55 but multiple fractures reaching perpendicular discontinuities.

Comments: Few fractures show signs of bending towards the line of the boreholes.

TEST NO. 57	DATE: 1/5/80	PHASE: 2
BRIEF DESCRIPTION: Pre-split in Resin with angled discontinuities middistance between boreholes at 0° to hole line.		

PARAMETER	inches	mm	OTHER
Block Type			RESIN
Block length	10		
Block width	6		
Block height		70	
No. of Boreholes			3
Borehole diameter	3/16"	4.763	
Borehole depth		70	
Borehole spacing	3		Centers
No. of Detonators			1
Delay			N/A
Cord used per hole	8		4 grain/ft
Discontinuities	Single 0° to line of boreholes.		
Photographs	1 top view		

**Results:** Definite pre-split between holes as well as perpendicular breakage to discontinuities.

**Comments:** Pre-split was not expected to be so obvious as was obtained due to the very close proximity of the 'top' discontinuity.

TEST NO. 58	DATE: 6/6/80	PHASE: 2
<b>BRIEF DESCRIPTION:</b> Presplit in sawn block of rock with jointing mid-distance between boreholes vertical and at 30° to hole line.		

PARAMETER	inches	mm	OTHER
Block Type			SANDSTONE
Block length	24	610	
Block width	12	305	
Block height	5½	140	
No. of Boreholes			5
Borehole diameter	3/8"	9.525	
Borehole depth	5½	140	
Borehole spacing	4	102	Centers
No. of Detonators			1
Delay			N/A
Cord used per hole	24	610	Doubled 11gr/ft
Discontinuities	Mid-distance, single, vertical, 30° to p/s		
Photographs	1 view from above		

**Results:**  
 Presplit obtained between boreholes which was observed to be influenced by perpendicular cracking to discontinuities

**Comments:**  
 Main cracking to discontinuities was not perfectly perpendicular and was up to 15° off in some cases towards the line of the presplit.

TEST NO.	59	DATE: 20.6.80	PHASE: 2
<b>BRIEF DESCRIPTION:</b> Presplit in sawn block of rock with jointing middistance between boreholes at 60° to hole line.			

PARAMETER	inches	mm	OTHER
Block Type			Rock/sst
Block length	24	610	
Block width	7½	191	
Block height	6	152	
No. of Boreholes			5
Borehole diameter	3/8"	9.525	
Borehole depth	6	152	
Borehole spacing	4	102	Centers
No. of Detonators			1
Delay			N/A
Cord used per hole	24	610	2 x 11 gr/ft
Discontinuities	Single, middistance, vertical at 60° to P/S		
Photographs	2 from above.		

**Results:**  
 Strong presplit between all holes, but presplit is a zone rather than a single fracture. Splaying at either end appart from presplit extension.

**Comments:**  
 Main breakage to jointing is subperpendicular by up to 20° for some boreholes.  
 Black blot shaped marks due to oil spillage by unknown person or persons.

TEST NO. 60	DATE: 20/6/80	PHASE: 2
<b>BRIEF DESCRIPTION:</b> Presplit in sawn block of rock with jointing middistance between boreholes at 50° to hole line.		

PARAMETER	inches	mm	OTHER
Block Type			rock/sst
Block length	24	610	
Block width	7½	191	
Block height	6	152	
No. of Boreholes			5
Borehole diameter	3/8"	9.525	
Borehole depth	6	152	
Borehole spacing	4	102	Centers
No. of Detonators			1
Delay			N/A
Cord used per hole	24	610	2 x 11 gr/ft
Discontinuities	Single, middistance, vertical at 50° to p/s		
Photographs	2 from above		

**Results:**  
 Connection of fracturing between all holes subperpendicular fracturing to jointing dominant with secondary curving fractures from adjacent holes connecting to these.

**Comments:**  
 Main fracturing subperpendicular, by up to 15° towards presplit line.  
 Oil staining post blasting is present on the top surface of the block.

TEST NO. 61	DATE: 27.6.80	PHASE: 2
<b>BRIEF DESCRIPTION:</b> Presplit in sawn block of rock with jointing middistance between boreholes at 40° to hole line		

PARAMETER	inches	mm	OTHER
Block Type			rock/sst
Block length	24	610	
Block width	7½	191	
Block height	6	152	
No. of Boreholes			5
Borehole diameter	3/8"	9.525	
Borehole depth	6	152	
Borehole spacing	4	102	Centers
No. of Detonators			1
Delay			N/A
Cord used per hole	24	610	2 x 11 gr/ft
Discontinuities	2 single, middistance, vertical at 40° to p/s		
Photographs	1 from above		

**Results:**  
 Connection of fracturing between all holes, presplit present as a wide zone fracturing. Main fracturing subperpendicular to jointing with secondary curving fractures connecting from adjacent holes.

**Comments:**  
 Main fracturing subperpendicular by up to 12° towards presplit line.

TEST NO. 62	DATE: 27.6.80	PHASE: 2
<b>BRIEF DESCRIPTION:</b> Presplit in sawn block of rock with jointing middistance between boreholes at 10° to hole line		

PARAMETER	inches	mm	OTHER
Block Type			rock/sst
Block length	24	610	
Block width	7½	191	
Block height	6	152	
No. of Boreholes			5
Borehole diameter	3/8"	9.525	
Borehole depth	6	152	
Borehole spacing	4	102	Centers
No. of Detonators			1
Delay			N/A
Cord used per hole	24	610	2 x 11 gr/ft
Discontinuities	Single, vertical, middistance at 10° to p/s		
Photographs	1 from above		

**Results:**  
 Connection of fracturing between all holes where jointing is present, poor presplit obtained which is again a zone..  
 Fracturing to joints from 2 holes away.

**Comments:**  
 Dominant fracturing again perpendicular to jointing, highly curved secondary fracturing seen (curving by up to 65° toward primary fracturing.)

TEST NO. 63	DATE: 15/8/80	PHASE: 2
<b>BRIEF DESCRIPTION:</b> Presplit in sandstone block with (twin) multiple discontinuities at 60° to the hole line and placed at 1/3 distances between holes.		

PARAMETER	inches	mm	OTHER
Block Type			rock/sst
Block length	24	610	
Block width	7½	191	
Block height	5½	133	
No. of Boreholes			5
Borehole diameter	3/8"	9.525	
Borehole depth	5.1/4"	133	
Borehole spacing	4	102	Centers
No. of Detonators			1
Delay			n/A
Cord used per hole	24	610	2 x 11 gr/ft
Discontinuities	Multiple (2) at 60° to p/s, 1/3 borehole sep..		
Photographs	1 from above		

**Results:**

An irregular continuous break between boreholes is achieved but is dominated by the jointing. The dominant fracturing from the boreholes is perpendicular to the jointing.

**Comments:**

The only fracturing to 'cross' joints is perpendicular to the joints. There are normally 2 fractures within mid slabs one emanating from each bordering borehole, some of these fractures bifurcate.

TEST NO. 64	DATE: 15/8/80	PHASE: 2
<b>BRIEF DESCRIPTION:</b> Presplit in sandstone block with (twin) multiple discontinuities at 60° to hole line and equidistantly separated.		

PARAMETER	inches	mm	OTHER
Block Type			Rock/sst
Block length	24	610	
Block width	7½	191	
Block height	5½	133	
No. of Boreholes			5
Borehole diameter	3./8"	9.525	
Borehole depth	5½	133	
Borehole spacing	4	102	Centers
No. of Detonators			1
Delay			N/a
Cord used per hole	24	610	2 x 11 gr/ft
Discontinuities	Equidistant multiple (2) at 60° to p/s		
Photographs	1 from above		

**Results:**  
 An irregular continuous break between boreholes is achieved but is dominated by the jointing. The dominant fracturing from the boreholes is perpendicular to the jointing. Some secondary fracturing curving to primary fracturing is occasionally seen.

**Comments:**  
 Again only perpendicular fracturing across jointing is observed. 2 of which are present within mid slabs, with the occasional tendency for bifurcation.

TEST NO. 65	DATE: 1/10/80	PHASE: 2
<b>BRIEF DESCRIPTION:</b> Presplit in sandstone block with jointing middistance between boreholes at 80° to the hole line.		

PARAMETER	inches	mm	OTHER
Block Type			rock/sst
Block length	22.1/2	572	
Block width	7.1/2	191	
Block height	5½	133	
No. of Boreholes			5
Borehole diameter	3/8"	9.525	
Borehole depth	5½	133	
Borehole spacing			Centers
No. of Detonators			1
Delay			N/A
Cord used per hole	24	610	2 x 11 gr/ft
Discontinuities	Single, vertical, middistance at 80° to p/s		
Photographs	2 from above		

**Results:**  
 Good presplit between holes, main fracturing subperpendicular to jointing by max. 5° towards presplit line.

**Comments:**  
 Secondary fracturing is observed but has now become a minor feature of the experiment. The slightly undulose shape of the presplit is most likely due to the influence of flaws within the rock.

TEST NO. 66	DATE: 1/10/80	PHASE: 2
-------------	---------------	----------

**BRIEF DESCRIPTION:**  
 Presplit in sandstone block with jointing middistance between boreholes at 90° to the hole line.

PARAMETER	inches	mm	OTHER
Block Type			Rock/sst
Block length	23½	597	
Block width	7½	191	
Block height	5½	133	
No. of Boreholes			5
Borehole diameter	3/8"	9.525	
Borehole depth	5½	133	
Borehole spacing			Centers
No. of Detonators			1
Delay			N/A
Cord used per hole	24	610	2 x 11 gr/ft
Discontinuities	Single, vertical, middistance at 90° to p/s		
Photographs	2 from above		

**Results:**  
 Good presplit between holes. Presplit is generally straight, with some minor parallel sympathetic fracturing on either side.

**Comments:**  
 Sub "horizontal" discontinuity at base of block below bottom left corner has been opened up by blasting.

TEST NO. 67	DATE: 6/10/80	PHASE: 2
-------------	---------------	----------

**BRIEF DESCRIPTION:**  
 Presplit in sandstone block with multi jointing (twin) 2/3" from boreholes on either side at 60° to hole line

PARAMETER	inches	mm	OTHER
Block Type			Rock/sst
Block length	22½	578	
Block width	9½	241	
Block height	6	152	
No. of Boreholes			5
Borehole diameter	3/8"	9.525	
Borehole depth	6	152	
Borehole spacing	4	102	Centers
No. of Detonators			1
Delay			N/A
Cord used per hole	24	610	2x11 gr/ft
Discontinuities	Multiple (2) At 2/3" from borehole centres, at 60°		
Photographs	2 from above		

**Results:**  
 The dominant fracturing from the boreholes is perpendicular to the jointing, however considerable splaying is present. Connection between boreholes is achieved however a poor pre-split is obtained.

**Comments:**  
 Again only perpendicular fracturing is observed crossing jointing, 2 of which are present within mid slabs (one from each neighbouring borehole)  
 No bifurcation of these fractures are observed.

TEST NO. 68	DATE: 6/10/80	PHASE: 2
<b>BRIEF DESCRIPTION:</b> Presplit in sandstone block with equidistant multiple (triple) jointing at 60° to hole line.		

PARAMETER	inches	mm	OTHER
Block Type			Rock/sst
Block length	22	559	
Block width	9½	241	
Block height	6	152	
No. of Boreholes			5
Borehole diameter	3/8"	9.525	
Borehole depth	6	152	
Borehole spacing	4	102	Centers
No. of Detonators			1
Delay			N/A
Cord used per hole	24	610	2 x11 gr/ft
Discontinuities	1" equidistant at 60°, holes in between		
Photographs	2 from above		

**Results:**  
 The dominant fracturing from the boreholes is perpendicular to the jointing. Considerable splaying is again present. Although connection between boreholes is achieved a poor presplit is obtained.

**Comments:**  
 The perpendicular fracturing across successive mid slabs of rock between boreholes is not always directly connected, there being a slight displacement along jointing which is uniform in direction (dextral).

TEST NO. 69	DATE: 14/10/80	PHASE: 2
<b>BRIEF DESCRIPTION:</b> Presplit test in block of sandstone with sawn discontinuities orientated at 60° to the hole line and spaced at 1/5" boreholes.		

PARAMETER	inches	mm	OTHER
Block Type			Rock/sst
Block length	20.8	526	
Block width	9.5	240	
Block height	6	152	
No. of Boreholes			5
Borehole diameter	3/8"	9.525	
Borehole depth	6	152	
Borehole spacing	4	102	Centers
No. of Detonators			1
Delay			N/A
Cord used per hole	24	610	2x11 gr/ft
Discontinuities	Multiple (x4) at 60° to p/s, 1" separation		
Photographs	1 from above		

**Results:**  
 Breakage between holes achieved but a poor ill defined pre-split is obtained. The only fracturing to cross the jointing is orientated perpendicular to it.

**Comments:**  
 Generally a single fracture from each hole cuts across successive jointing up to the joint before the adjacent hole.  
 Some of the jointing bifurcates generally, at the extremes.

TEST NO. 70	DATE: 14/10/80	PHASE: 2
-------------	----------------	----------

**BRIEF DESCRIPTION:**

Presplit test in block of sandstone testing the effect of  
(a) closed discontinuities passing through boreholes and  
(b)

PARAMETER	inches	mm	OTHER
Block Type			Rock/sst
Block length	23.14	585	
Block width	9.5	240	
Block height	6	152	
No. of Boreholes			5
Borehole diameter	3/8"	9.525	
Borehole depth	6	152	
Borehole spacing	4	102	Centers
No. of Detonators			1
Delay			N/A
Cord used per hole	24	510	2 x 11 gr/ft
Discontinuities	2 at 60° thru holes, 2 at 75° near holes		
Photographs	1 from above		

**Results:**

Single discontinuities through holes at 60° to presplit seem to have little to no effect on the propagation of the presplit. However the 2 opposed 75° (to hole line) discontinuities have caused a failure to split.

**Comments:**

Although there is a good presplit for the former there is evidence that fracturing from the intersected boreholes is reduced. This tallies with field evidence for closed joints cutting boreholes.

In the case of the 75° joints it is felt that for fracturing between boreholes to occur fractures must bisect at an angle of 30° therefore mutually detrimental.

TEST NO.	71	DATE:	13/1/81	PHASE:	2
BRIEF DESCRIPTION: Attempt to find maximum presplit borehole separation with single 11 grain cord and $\frac{3}{8}$ inch holes in concrete (4 to 1 mix).					

PARAMETER	inches	mm	OTHER
Block Type			Concrete
Block length	24	610	
Block width	9	229	
Block height	6	152	
No. of Boreholes			3
Borehole diameter	$\frac{3}{8}$ "	9.525	
Borehole depth	6	152	
Borehole spacing	3	76	Centers
No. of Detonators			1
Delay			N/A
Cord used per hole	18	457	Single 11 gr/ft.
Discontinuities	None		
Photographs	1 above		

Results: Successfull presplit with splaying at ends.

Comments:

TEST NO.	72	DATE:	13/1/81	PHASE:	2
BRIEF DESCRIPTION: Attempt to find maximum presplit borehole separation with single 11 grain cord and $\frac{3}{8}$ " holes in concrete (4 to 1 mix).					

PARAMETER	inches	mm	OTHER
Block Type			Concrete
Block length	24	610	
Block width	9	229	
Block height	6	152	
No. of Boreholes			4
Borehole diameter	$\frac{3}{8}$ "	9.525	
Borehole depth	6	152	
Borehole spacing	$3\frac{1}{2}$	89	Centers
No. of Detonators			1
Delay			N/A
Cord used per hole	24	457	Single 11 gr/ft.
Discontinuities	None		
Photographs	1 above		

Results: Successful presplit with twin fracturing between boreholes

Comments:

TEST NO.	73	DATE:	14/1/81	PHASE:	2
BRIEF DESCRIPTION: Test to find maximum presplit borehole separation for 4:1 concrete.					

PARAMETER	inches	mm	OTHER
Block Type			Concrete
Block length	24	610	
Block width	9	229	
Block height	6	152	
No. of Boreholes			3
Borehole diameter	¾"	9.525	
Borehole depth	6	152	
Borehole spacing	4	102	Centers
No. of Detonators			1
Delay			N/A
Cord used per hole	18"	457	Single 11 gr/ft.
Discontinuities	None		
Photographs	1 above		

Results: Good presplit fairly undulose but amplitude less than borehole diameter. No splaying at end.

Comments: Fracture single, no multiple presplit.

TEST NO.	74	DATE:	14/1/81	PHASE:	2
BRIEF DESCRIPTION: Test to find maximum presplit borehole separation for 4:1 concrete.					

PARAMETER	inches	mm	OTHER
Block Type			Concrete
Block length	24	610	
Block width	9	229	
Block height	6	152	
No. of Boreholes			3
Borehole diameter	$\frac{3}{8}$ "	9.525	
Borehole depth	6	152	
Borehole spacing	$4\frac{1}{2}$	114	Centers
No. of Detonators			1
Delay			N/A
Cord used per hole	18	457	Single 11 gr/ft.
Discontinuities	None		
Photographs	1 above		

Results: Just failure to presplit between 2 of the 3 holes highly undulose split between other holes.

Comments: Marginally over maximum presplit borehole separation.

TEST NO. 75	DATE: 19.1.81	PHASE: 2
<b>BRIEF DESCRIPTION:</b> Presplit in 4:1 mix concrete block with discontinuities dipping at 30°, striking at 45° to the hole line		

PARAMETER	inches	mm	OTHER
Block Type			CONCRETE
Block length	24	610	
Block width	9	229	
Block height	6	152	
No. of Boreholes			6
Borehole diameter	3/8"	9.525	
Borehole depth	6	152	
Borehole spacing	4	102	Centers
No. of Detonators			1
Delay			N/A
Cord used per hole	24	610	Single 11 gr/ft
Discontinuities	3 @ 30 dip 45° to p/s 2½" sep.		
Photographs	1 above		

**Results:**  
 Failure to split between 2 holes splitting generally between holes except when in the presence of joints where fracturing roughly perpendicular to the jointing has occurred. Fair amount of overbreak

**Comments:**  
 Fracturing perpendicular to the jointing tends to be slightly sub-perpendicular by up to 10-15° max. towards the pre-split line.  
 Normal pre-split where jointing is not present except for 1 failure. Thus the presence of jointing may reduce the max. borehole separation

TEST NO.	76	DATE:	19.1.81	PHASE:	2
BRIEF DESCRIPTION: Pre-split in 4:1 mix concrete block with discontinuities dipping at 45°, striking 45° to the hole line.					

PARAMETER	inches	mm	OTHER
Block Type			CONCRETE
Block length	24	610	
Block width	9	229	
Block height	6	152	
No. of Boreholes			6
Borehole diameter	3/8"	9.525	
Borehole depth	6	152	
Borehole spacing	4	102	Centers
No. of Detonators			1
Delay			N/A
Cord used per hole	24	610	Single 11 gr/ft
Discontinuities	4 @ 45° dip 45° to p/s 2½" sep		
Photographs	1 above		

Results:  
Fairly strong pre-split though some fracturing perpendicular to the jointing is seen but on the whole dominant. Less overbreak than previous test.

Comments:  
Again fracturing to jointing is sub-perpendicular by 10° or so towards the pre-split line. Presplit fracture failure irregular in nature.

TEST NO.	77	DATE:	20.1.81	PHASE:	2
BRIEF DESCRIPTION: Pre-split in 4:1 mix concrete block with discontinuities perpendicular to the hole line and dipping at 30°					

PARAMETER	inches	mm	OTHER
Block Type			CONCRETE
Block length	24	610	
Block width	9	229	
Block height	6	152	
No. of Boreholes			6
Borehole diameter	3/8"	9.525	
Borehole depth	6	152	
Borehole spacing	4	102	Centers
No. of Detonators			1
Delay			N/A
Cord used per hole	24	610	Single 11 gr/ft
Discontinuities	5 @ 30 dip, 90° to p/s, 2½" sep.		
Photographs	2 above		

**Results:**  
Failure to split 2 boreholes on top 1 on bottom surface pre-split fairly straight fracturing perpendicular to the jointing.

**Comments:**  
Slight tendency of failure to presplit may signify that the presence of 30° jointing may reduce the maximum borehole separation for presplit success.

TEST NO. 78	DATE: 20.1.81	PHASE: 2
BRIEF DESCRIPTION: Presplit in 4:1 mix concrete block with discontinuities perpendicular to the hole line and dipping at 45°.		

PARAMETER	inches	mm	OTHER
Block Type			CONCRETE
Block length	24	610	
Block width	9	229	
Block height	6	152	
No. of Boreholes			6
Borehole diameter	3/8"	9.525	
Borehole depth	6	152	
Borehole spacing	4	102	Centers
No. of Detonators			1
Delay			N/A
Cord used per hole	24	610	Single 11 gr/ft
Discontinuities	6 @ 45° dip, 90° to p/s, 2½" sep.		
Photographs	2 above		

**Results:**  
 A much better defined presplit was obtained than in test 77 but slightly irregular in shape. Fracturing perpendicular to jointing

**Comments:**  
 A very slight tendency for incomplete presplit suggesting the same as in test 77.

TEST NO.	79	DATE:	20.1.81	PHASE:	2
<p>BRIEF DESCRIPTION:</p> <p>Attempt to find maximum borehole separation with 3/8" holes for successful presplit in Whinstone.</p>					

PARAMETER	inches	mm	OTHER
Block Type			DOLERITE
Block length	27	686	
Block width	12	305	
Block height	7	178	
No. of Boreholes			4
Borehole diameter	3/8"	9.525	
Borehole depth	7	178	
Borehole spacing	3	76'	Centers
No. of Detonators			1
Delay			N/A
Cord used per hole	18	457	Single 11 gr/ft
Discontinuities	NONE		
Photographs	1 above		

<p>Results:</p> <p>Failure to presplit</p>
--

<p>Comments:</p> <p>No cracking around boreholes seen</p>
---

TEST NO. 80	DATE: 20/1/81	PHASE: 2
-------------	---------------	----------

BRIEF DESCRIPTION:  
 Attempt to find maximum borehole separation with 3/8" holes for successful presplit in Whinstone.

PARAMETER	inches	mm	OTHER
Block Type			DOLERITE
Block length	27	686	
Block width	12	305	
Block height	7	178	
No. of Boreholes			5
Borehole diameter	3/8"	9.525	
Borehole depth	7	178	
Borehole spacing	2	51	Centers
No. of Detonators			1
Delay			N/A
Cord used per hole	18	457	Single 11fr/ft
Discontinuities	NONE		
Photographs	1 above		

Results:  
 Failure to presplit.

Comments:  
 only slight cracking seen around some boreholes.

TEST NO.	81.	DATE:	22.1.81	PHASE:	2
BRIEF DESCRIPTION: Presplit in 4 ; 1 mix concrete block with multiple jointing dipping at 45°, striking parallel to the hole line					

PARAMETER	inches	mm	OTHER
Block Type			CONCRETE
Block length	24	610	
Block width	9	229	
Block height	6	152	
No. of Boreholes			6
Borehole diameter	3/8"	9.525	
Borehole depth	6	152	
Borehole spacing	4	102	Centers
No. of Detonators			1
Delay			N/A
Cord used per hole	24	610	Single 11 gr/ft
Discontinuities	2 dipping 45°, strike // to p/s		
Photographs	1 above		

Results:  
Successful presplit of block. Flyrock from top part of block

Comments:  
No breakage perpendicular to discontinuities

TEST NO.	82	DATE:	22.1.81,	PHASE:	2
BRIEF DESCRIPTION:					
Presplit in 4:1 mix concrete block with multiple jointing dipping at 30°, striking parallel to the hole line					

PARAMETER	inches	mm	OTHER
Block Type			CONCRETE
Block length	24	610	
Block width	9	229	
Block height	6	152	
No. of Boreholes			6
Borehole diameter	3/8"	9.525	
Borehole depth	6	152	
Borehole spacing	4	102	Centers
No. of Detonators			1
Delay			N/A
Cord used per hole	24		Single 11 gr/ft
Discontinuities	2 dipping 30°, strike // to p/s		
Photographs	1 above		

Results:  
 Successful presplit of block.  
 Flyrock from thin part of top layer of block.

Comments:  
 Badly broken corner due to accident during assembly.  
 No breakage perpendicular to discontinuities

TEST NO.	83	DATE:	22.1.81	PHASE:	2
BRIEF DESCRIPTION: Attempt to find max presplit borehole separation in Dolerite using 3/8" holes and single 11 grain cord.					

PARAMETER	inches	mm	OTHER
Block Type			DOLERITE
Block length	27	686	
Block width	12	305	
Block height	7	178	
No. of Boreholes			7
Borehole diameter	3/8"	9.525	
Borehole depth	7	178	
Borehole spacing	1½	38	Centers
No. of Detonators			1
Delay			N/A
Cord used per hole	18	457	Single 11gr/ft
Discontinuities	NA		
Photographs			

Results: Successful presplit obtained.
---

Comments: Slight irregularity in shape.
--

TEST NO.	84	DATE: 23.1.81	PHASE: 2
----------	----	---------------	----------

BRIEF DESCRIPTION:  
Water coupled test in resin.

PARAMETER	inches	mm	OTHER
Block Type			RESIN
Block length	6	152	
Block width	5	127	
Block height	3	76	
No. of Boreholes			1
Borehole diameter	1/4"	6.35	
Borehole depth	3	76	
Borehole spacing	-	-	Centers
No. of Detonators			1
Delay			N/A
Cord used per hole	9	229	4 grain/ft
Discontinuities	NONE		
Photographs			

Results:  
Heavy damage with extensive cracking around borehole, fracturing reaches edge of block.

Comments:  
Damage far in excess of that obtained for the same test without water coupling.

TEST NO. 85	DATE: 23.1.81	PHASE: 2
BRIEF DESCRIPTION: Water coupled test in resin		

PARAMETER	inches	mm	OTHER
Block Type			RESIN
Block length	6	152	
Block width	5	127	
Block height	3	76	
No. of Boreholes			1
Borehole diameter	3/16	4.7625	
Borehole depth	3	76	
Borehole spacing	-	-	Centers
No. of Detonators			1/
Delay			N/A
Cord used per hole	9	229	4 grain/ft
Discontinuities	NONE		
Photographs			

**Results:**  
Heavy damage with extensive cracking around borehole, fracturing reaches edge of block.

**Comments:**  
Damage far in excess of that obtained for the same test without water coupling. Roughly the same amount of damage is obtained as in test 84, which is approximately equal to that obtained for a fully coupled hole.

TEST NO. 86	DATE: 19.2.81	PHASE: 2
-------------	---------------	----------

**BRIEF DESCRIPTION:**

Attempt to find the penetration of fluid into the fracutres created around a shot hole on detonation.

PARAMETER	inches	mm	OTHER
Block Type			RESIN
Block length	6	155	
Block width	5 1/4	133	
Block height	1	73	
No. of Boreholes			1
Borehole diameter	3/16	4.763	
Borehole depth		133	
Borehole spacing		N/A	Centers
No. of Detonators			1
Delay			N/A
Cord used per hole	6	150	
Discontinuities	NONE		
Photographs			

**Results:**

Same degree of fracturing as in test 85 (and 84). Dye penetrated up 28mm just less than half of the damage zone extent.

**Comments:**

Surface tension of the dye used was measured at 0.475 poise.

TEST NO. 87	DATE: 26.2.81	PHASE: 2
-------------	---------------	----------

**BRIEF DESCRIPTION:**  
 Attempt to find maximum borehole separation for successful presplit in granite.

PARAMETER	inches	mm	OTHER
Block Type			GRANITE
Block length	a13		
Block width	a18		
Block height	a6		
No. of Boreholes			5
Borehole diameter	3/8	9.525	
Borehole depth	a6		
Borehole spacing	2	51	Centers
No. of Detonators			1
Delay			N/A
Cord used per hole	20	508	single 11 gr/ft
Discontinuities	NONE		
Photographs	NONE		

**Results:** SUCCESSFUL PRESPLIT

**Comments:**

TEST NO.	88	DATE:	26/2/81	PHASE:	2
----------	----	-------	---------	--------	---

**BRIEF DESCRIPTION:**  
 Attempt to find maximum borehole separation for successful presplit in granite

PARAMETER	inches	mm	OTHER
Block Type			GRANITE
Block length	a 13		
Block width	a 18		
Block height	a 6		
No. of Boreholes			4
Borehole diameter	3/8	9.525	
Borehole depth	a 6		
Borehole spacing	2½	64	Centers
No. of Detonators			1
Delay			N/A
Cord used per hole	20	508	Single 11 gr/ft
Discontinuities	NONE		
Photographs	NONE		

**Results:** SUCCESSFUL PRESPLIT

**Comments:**

TEST NO. 89	DATE: 2/3/81	PHASE: 2
-------------	--------------	----------

**BRIEF DESCRIPTION:**  
 Attempt to find maximum borehole separation for successful presplit in Granite

PARAMETER	inches	mm	OTHER
Block Type			GRANITE
Block length	a 19		
Block width	a 9		
Block height	a 6		
No. of Boreholes			6
Borehole diameter	3/8	9.525	
Borehole depth	a 6		
Borehole spacing	3	76	Centers
No. of Detonators			1
Delay			N/A
Cord used per hole	20	508	Single 11 graint
Discontinuities	NONE		
Photographs	NONE		

**Results:** FAILURE TO SPLIT

**Comments:**

TEST NO. 90	DATE: 6.4.81	PHASE: 2
-------------	--------------	----------

**BRIEF DESCRIPTION:**  
 Attempt to find maximum borehole separation for successful pre-split in Dolomitic Limestone.

PARAMETER	inches	mm	OTHER
Block Type			Dolomitic Limestone
Block length	a 13		
Block width	a 18		
Block height	a 6		
No. of Boreholes			4
Borehole diameter	3/8	9.525	
Borehole depth	a 6		
Borehole spacing	3	76	Centers
No. of Detonators			1
Delay			N/A
Cord used per hole	20	508	
Discontinuities	NONE		
Photographs			

**Results:**  
 FAILURE TO PRE-SPLIT

**Comments:**

TEST NO. 91	DATE: 15.4.81	PHASE: 2
-------------	---------------	----------

**BRIEF DESCRIPTION:**  
 Attempt to find maximum borehole separation for successful pre-split in Dolomitic Limestone

PARAMETER	inches	mm	OTHER
Block Type			Dolomitic Limestone
Block length	a 23		
Block width	a 17		
Block height	a 6		
No. of Boreholes			7
Borehole diameter	3/8	9.525	
Borehole depth	a 6		
Borehole spacing	2	51	Centers
No. of Detonators			1
Delay			N/A
Cord used per hole	20	508	Single 11 grain
Discontinuities	NONE		
Photographs	NONE		

**Results:**  
 SUCCESSFUL PRE-SPLIT

**Comments:**

TEST NO. 92	DATE: 15.4.81	PHASE: 2
<b>BRIEF DESCRIPTION:</b> Attempt to find maximum borehole separation for successful pre-split in Limestone		

PARAMETER	inches	mm	OTHER
Block Type			Limestone
Block length	a 21½		
Block width	a 14½		
Block height	a 5		
No. of Boreholes			5
Borehole diameter	3/8	9.525	
Borehole depth	a 5		
Borehole spacing	4	102	Centers
No. of Detonators			1
Delay			N/A
Cord used per hole	20	508	Single 11 grain
Discontinuities	NONE		
Photographs	NONE		

<b>Results:</b> FAILURE TO PRESPLIT
--

<b>Comments:</b>
------------------

TEST NO. 93	DATE: 15.4.81	PHASE: 2
-------------	---------------	----------

**BRIEF DESCRIPTION:**  
 Attempt to find maximum borehole separation for successful presplit in Limestone

PARAMETER	inches	mm	OTHER
Block Type			LIMESTONE
Block length	a 21		
Block width	a 12		
Block height	a 6		
No. of Boreholes			5
Borehole diameter	3/8	9.525	
Borehole depth	a 6		
Borehole spacing	3	76	Centers
No. of Detonators			1
Delay			N/A
Cord used per hole	20	508	Single 11 grain
Discontinuities	NONE		
Photographs	NONE		

**Results:**  
 -  
 Poor pre-split failure to connect between all holes.

**Comments:**

TEST NO. 94	DATE: 16.4.81	PHASE: 2
<b>BRIEF DESCRIPTION:</b> Attempt to find maximum borehole separation for successful pre-split in Dolomitic Limestone		

PARAMETER	inches	mm	OTHER
Block Type			Dolomitic Limestone
Block length	a 24		
Block width	a 23		
Block height	a 5½		
No. of Boreholes			9
Borehole diameter	3/8	9.525	
Borehole depth	a 5½		
Borehole spacing	2½	64	Centers
No. of Detonators			1
Delay			N/A
Cord used per hole	22	559	Single 11 grain
Discontinuities	NONE		
Photographs	NONE		

<b>Results:</b>  GOOD STRAIGHT PRE-SPLIT
--

<b>Comments:</b>  
--------------------------

TEST NO.	95	DATE:	16.4.81	PHASE:	2
----------	----	-------	---------	--------	---

**BRIEF DESCRIPTION:**  
 Attempt to find maximum borehole separation for successful pre-split in Limestone.

PARAMETER	inches	mm	OTHER
Block Type			LIMESTONE
Block length	a 19		
Block width	a 17		
Block height	a 7		
No. of Boreholes			6
Borehole diameter	3/8	9.525	
Borehole depth	2½	64	
Borehole spacing			Centers
No. of Detonators			1
Delay			N/A
Cord used per hole	20	508	Single 11 grain
Discontinuities			
Photographs			

**Results:**  
 GOOD PRE-SPLIT BUT ROCK ALSO BROKEN.

**Comments:**

Appendix E

PRE-SPLII SITE COMPOSITE PHOTOGRAPHS

# Fig. F.1.

Pre-split location No.1

(North to South).

Geology: Isoclinaly folded metamorphic psammities with some pelites - described as undifferentiated Moine Schists.

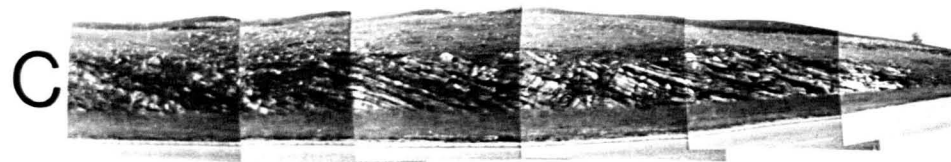
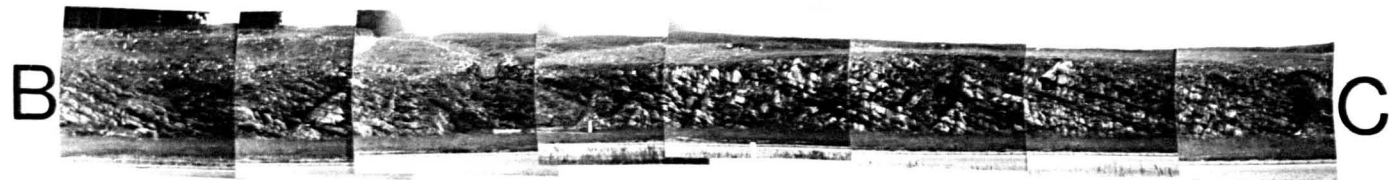
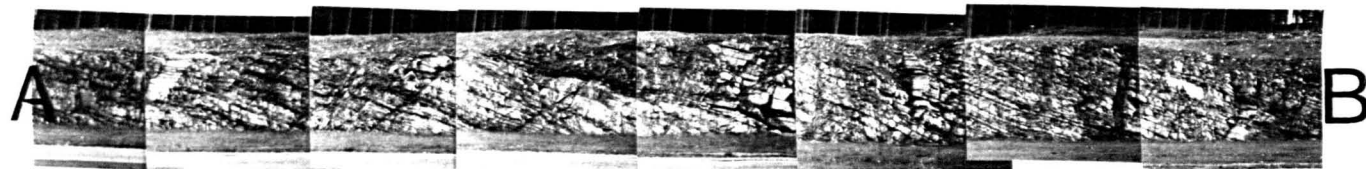
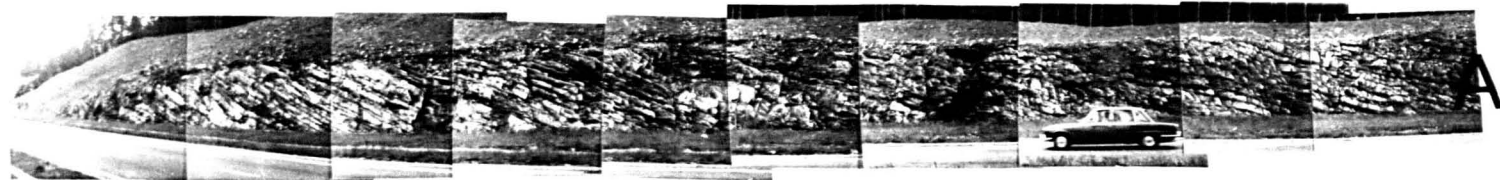


# Fig.F.2.

Pre-split location No. 2  
(South end of east face).

Geology: Isoclinaly folded  
metamorphic psammites with  
occasional pelitic bands -  
described as undifferentiated  
Moine Schists.

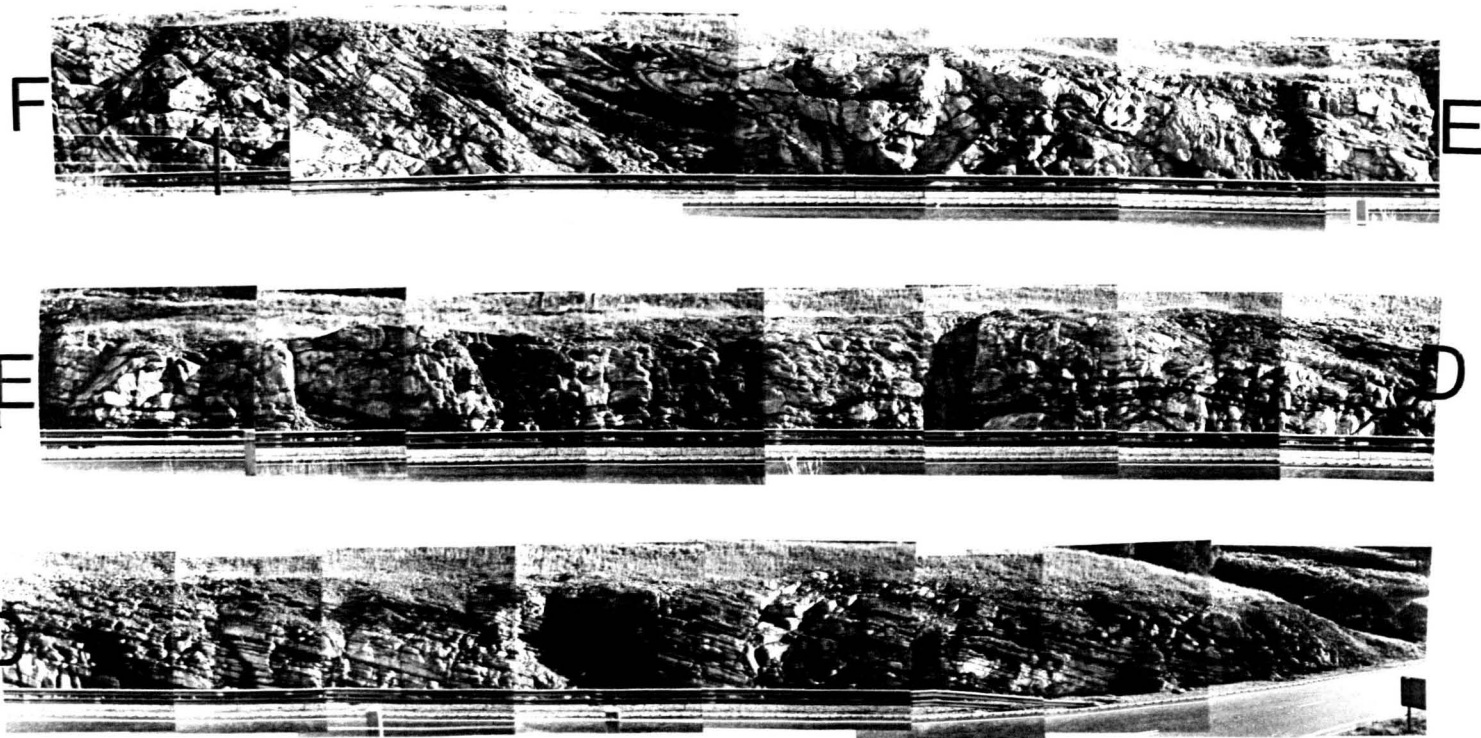


# Fig.F.3.

Pre-split location No. 3

(east face)

Geology: Isoclinaly

folded metamorphic

psammites with faulted

felsite 'sill' at south

end.

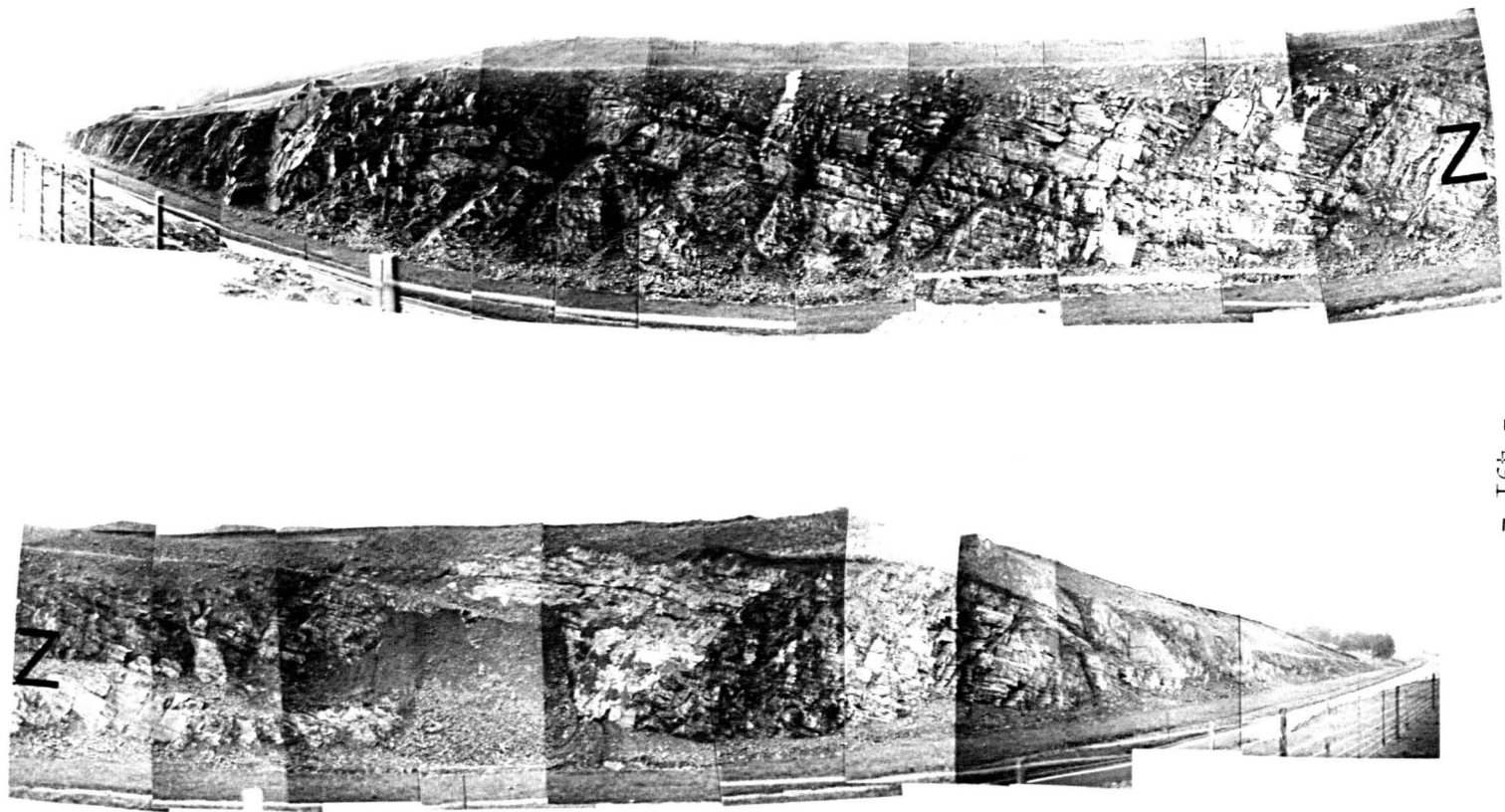


# Fig. F.4 .

Pre-split location No. 3

(west face)

Geology: Isoclinaly folded

metamorphic psammites -

described as undifferentiated

Moine Schists

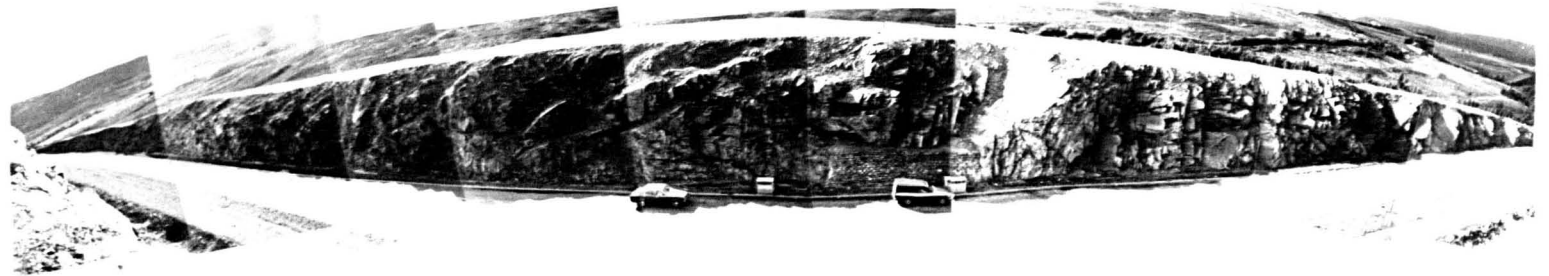


# Fig. F.5.

Pres-split Location No. 4

(east face)

Geology: Isoclinaly

folded metamorphic

psammites with pelitic

bands - described as

undifferentiated Moine

Schist.

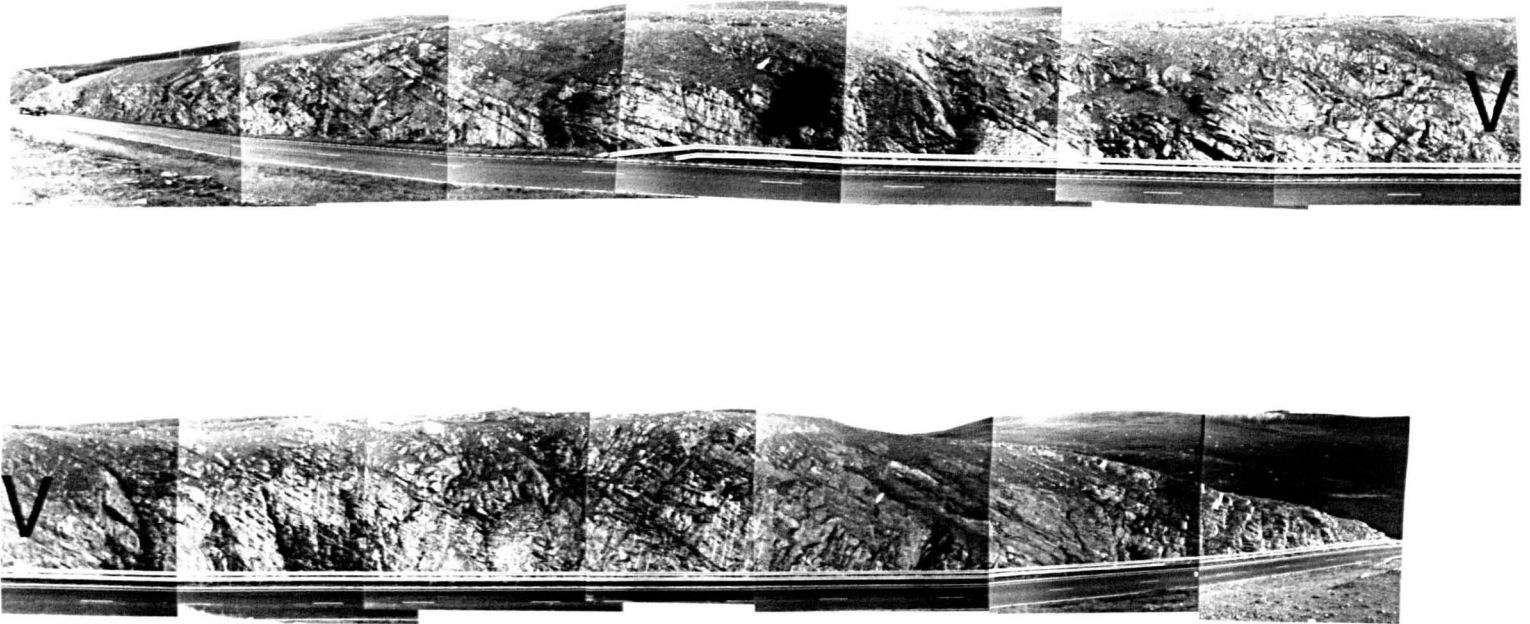


# Fig. F.5.

Pres-split Location No. 4

(east face)

Geology: Isoclinaly

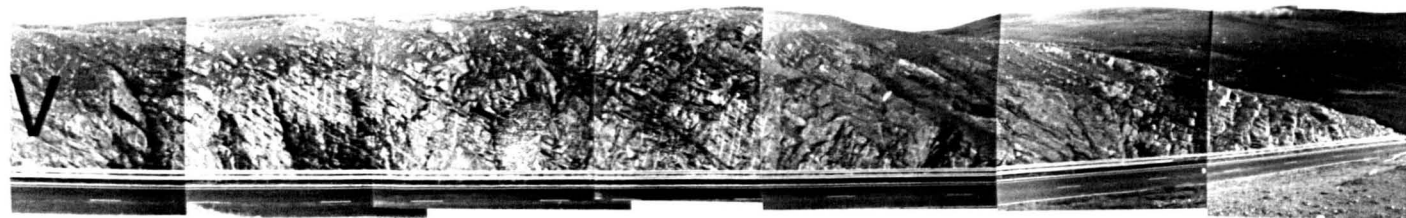
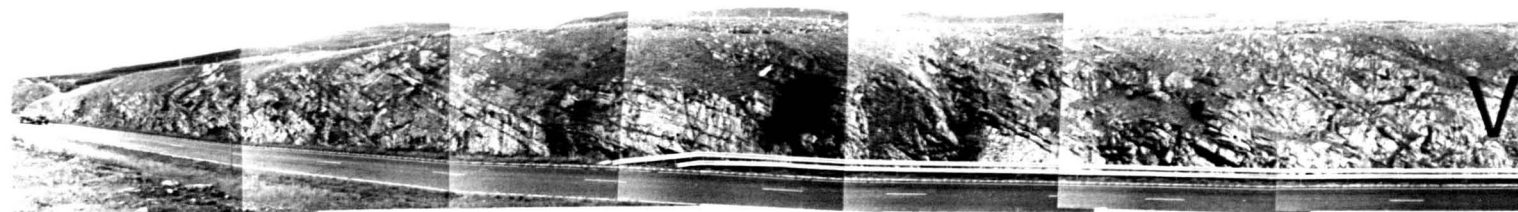
folded metamorphic

psammites with pelitic

bands - described as

undifferentiated Moine

Schist.



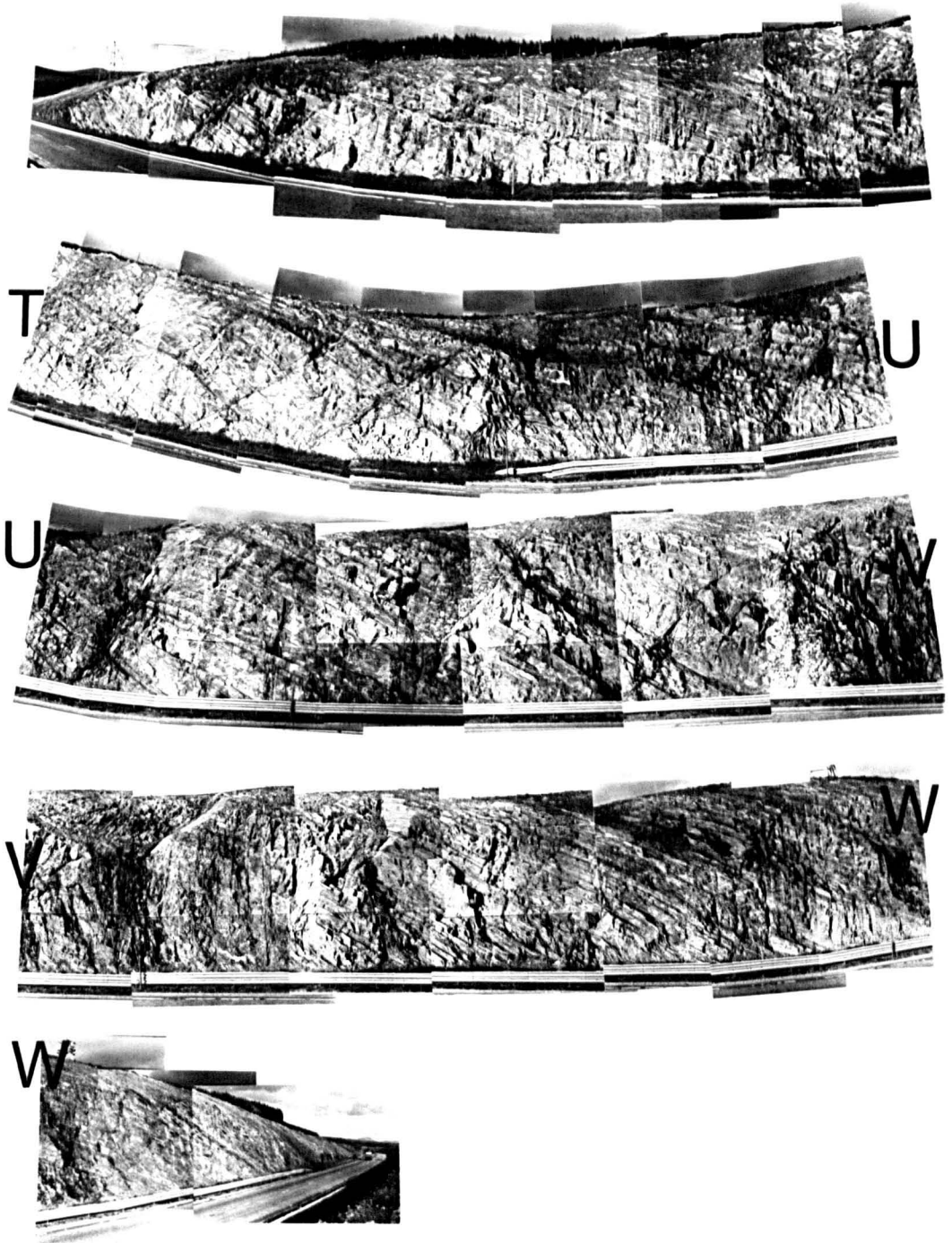


Fig.F.6.

Pre-split location 5. (East face)

Geology: Isoclinally folded metamorphic psammities with occasional pelitic bands - described as undifferentiated Moine Schist.

Fig. F.7.

Pre-split location 6. (North to South - right to left)

Geology: Isoclinaly folded metamorphic psammities with occasional thin pelitic bands -  
described as undifferentiated Moine Schist.

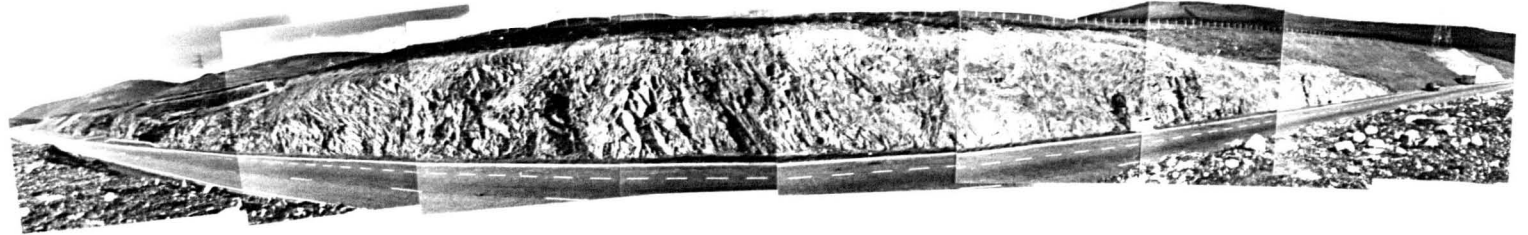


Fig. F.8.

Pre-split location 7 (North to South - right to left)

Geology: Isoclinaly folded metamorphic psammities with occasional thin pelitic bands, fold noses present in face.

- described as undifferentiated Moine Schist.

Comment: The final face is smooth blasted back to a slope of 2:1.

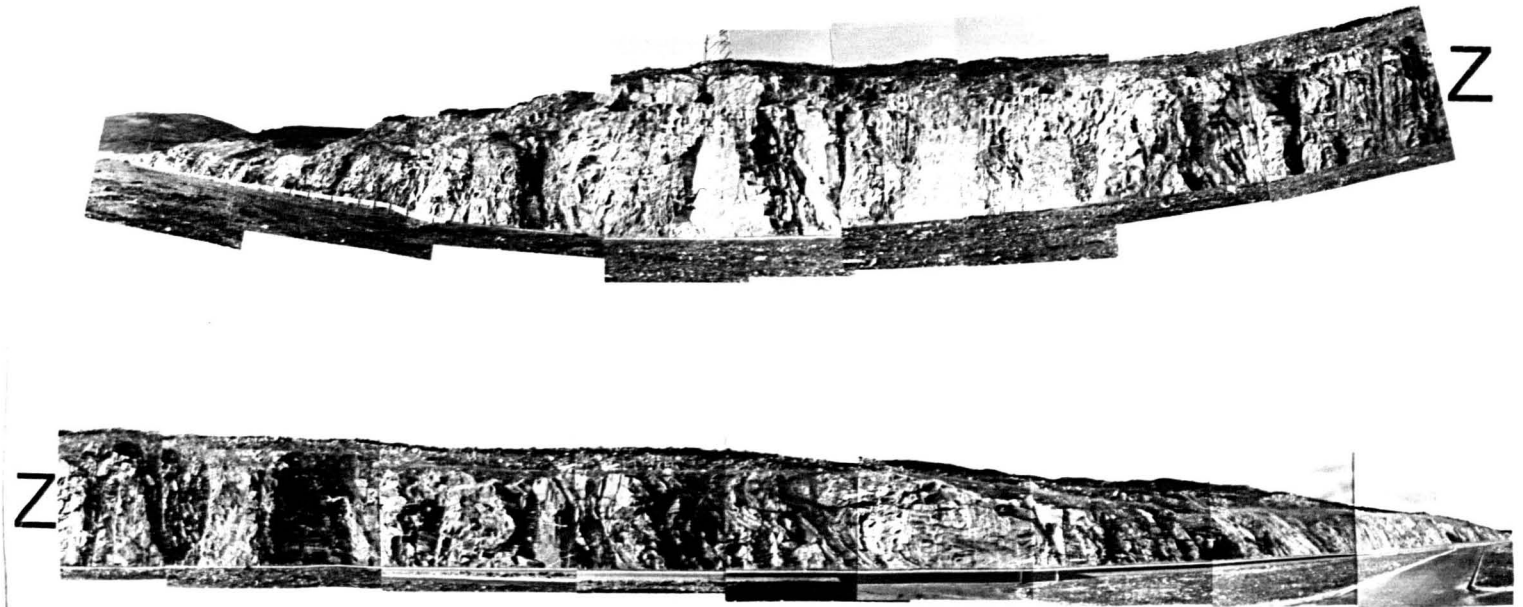
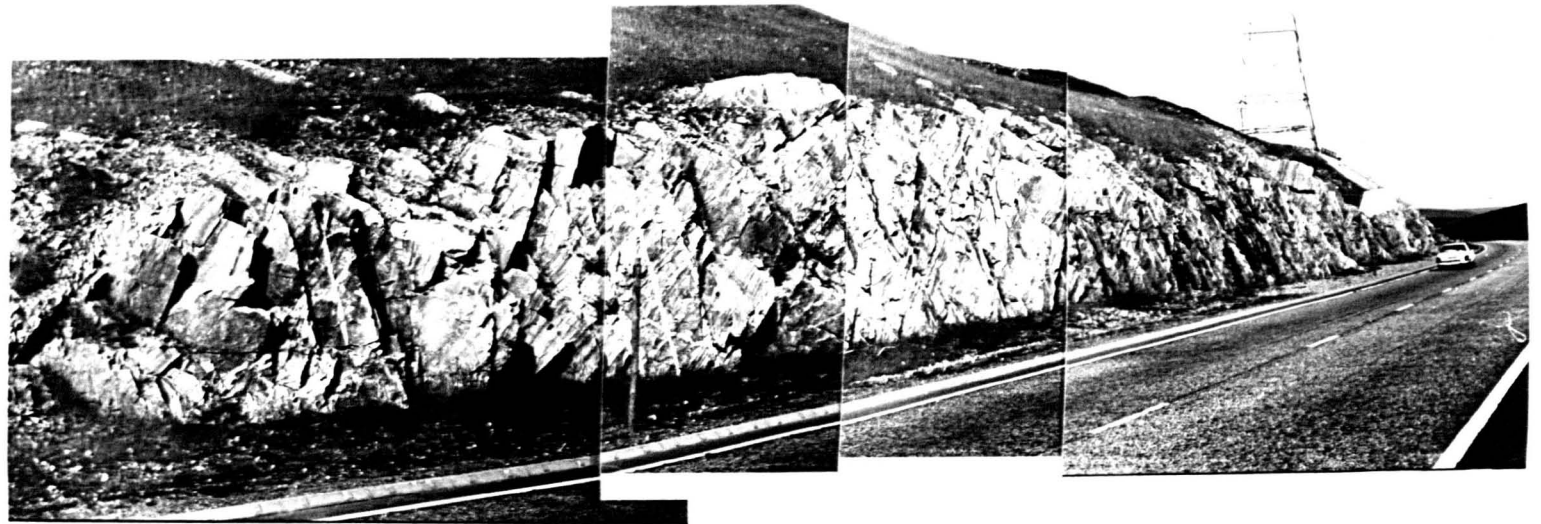


Fig.F.9.

Pre-split location 8.

Geology: Isoclinaly folded metamorphic banded psammities - described as undifferentiated Moine Schist.



## Fig. F.10.

Pre-split location 9.

Geology: Steeply dipping metamorphic psammities with some pelitic bands, two metamorphosed quartzite bands or quartz sills and metamorphosed quartz porphyry dykes.

Foliation parallel to bedding.

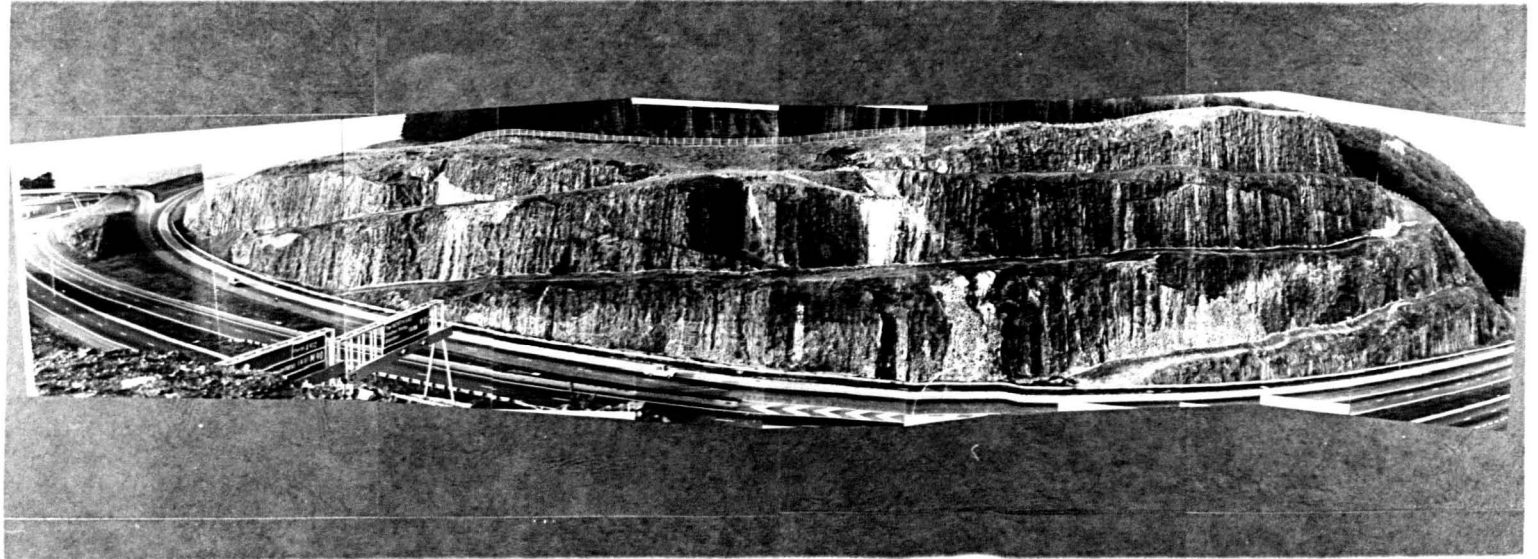
- described as Quartzose feldspathic schistose flags (Moine).



## Fig. F.11.

Pre-split location 10.

Geology: Gently dipping  
rhyolitic? lava flows;  
upper lavas fine grained  
and lower amygdaloidal  
with chlorite, calcite  
and quartz (vars)  
infillings.



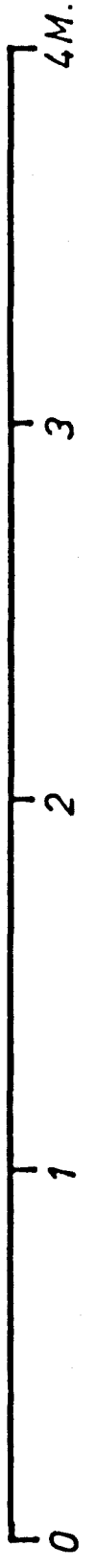
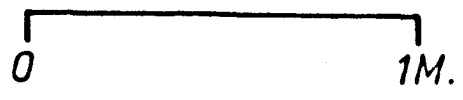
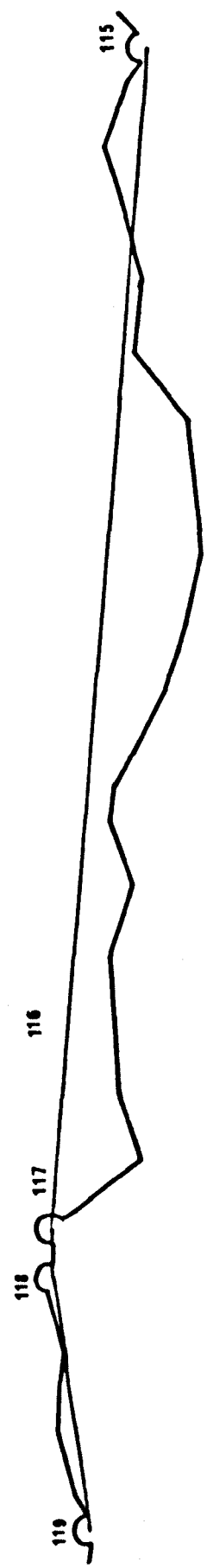
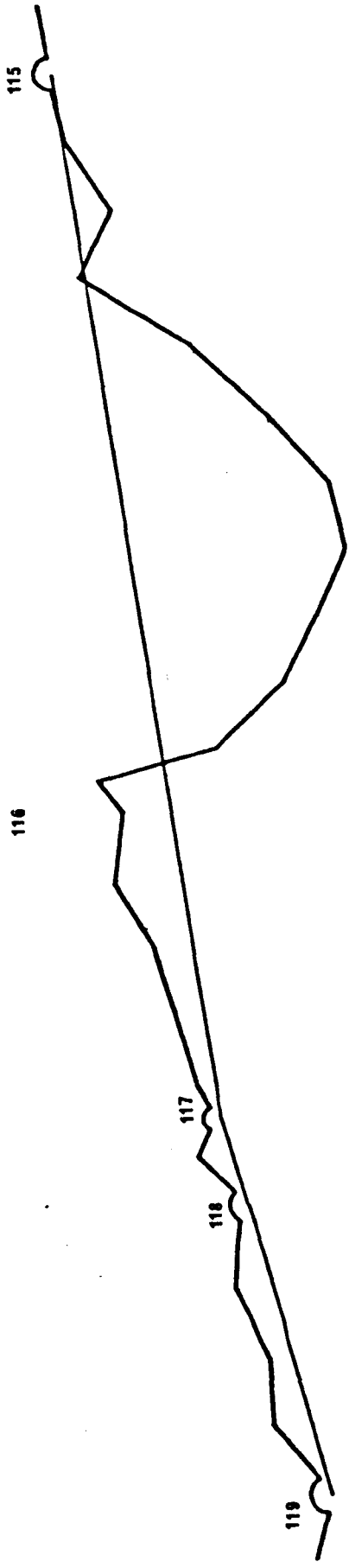
Appendix G

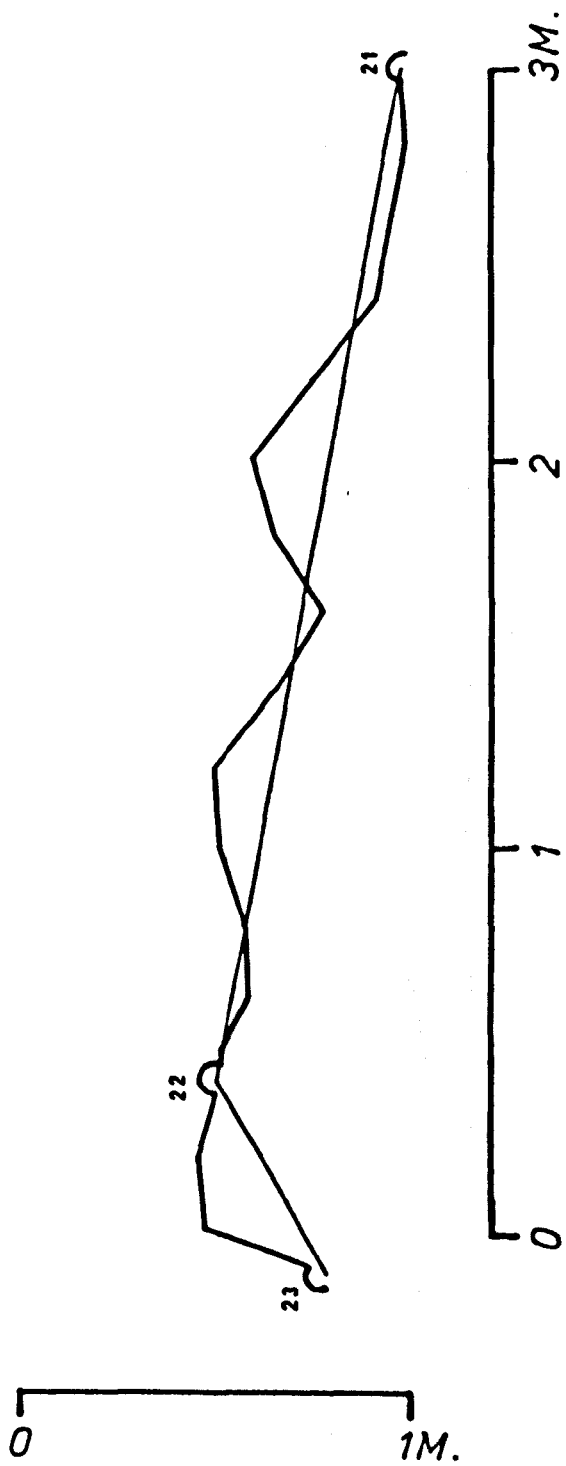
SCALED OVERBREAK DRAWINGS - LOCATION NINE

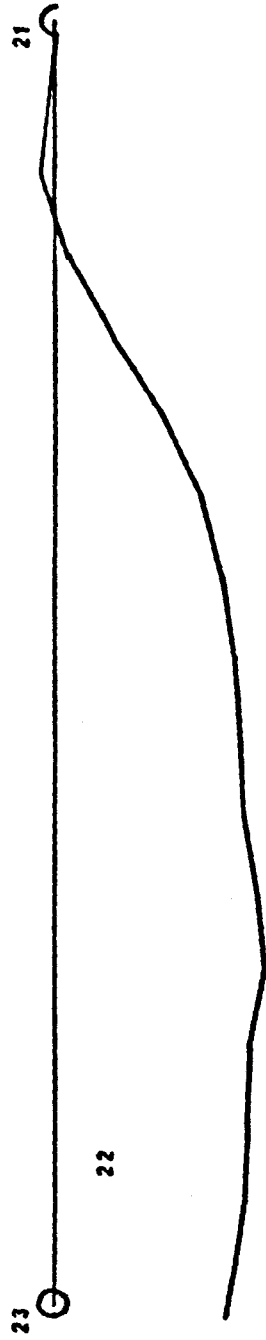
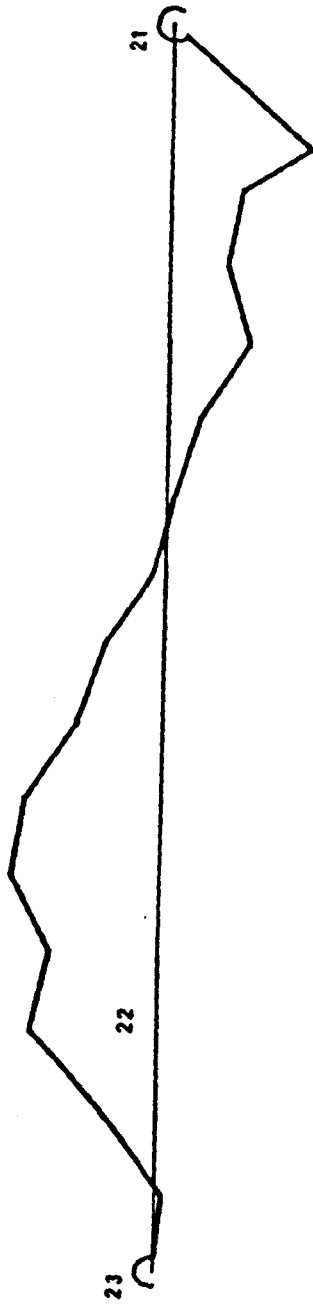
Notes:

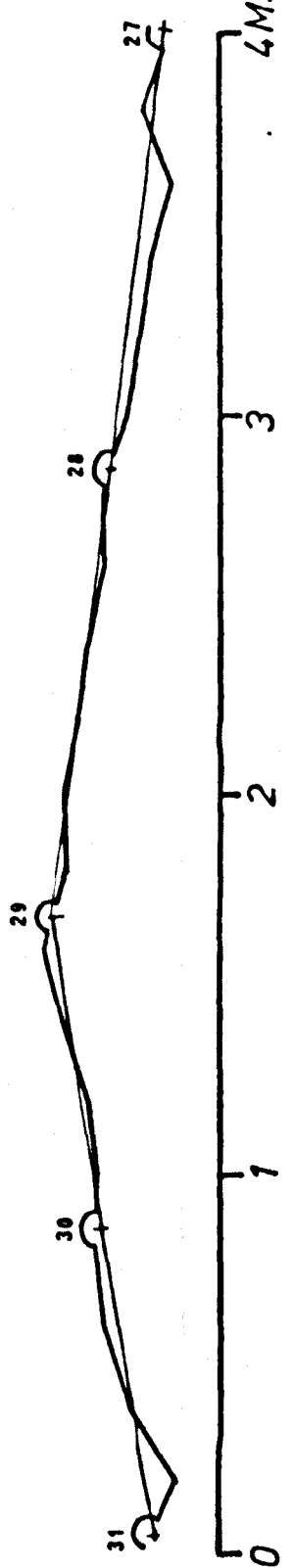
Each pre-split borehole is indicated by its number of occurrence in the final face at pre-split location number nine, numbering from north to south.

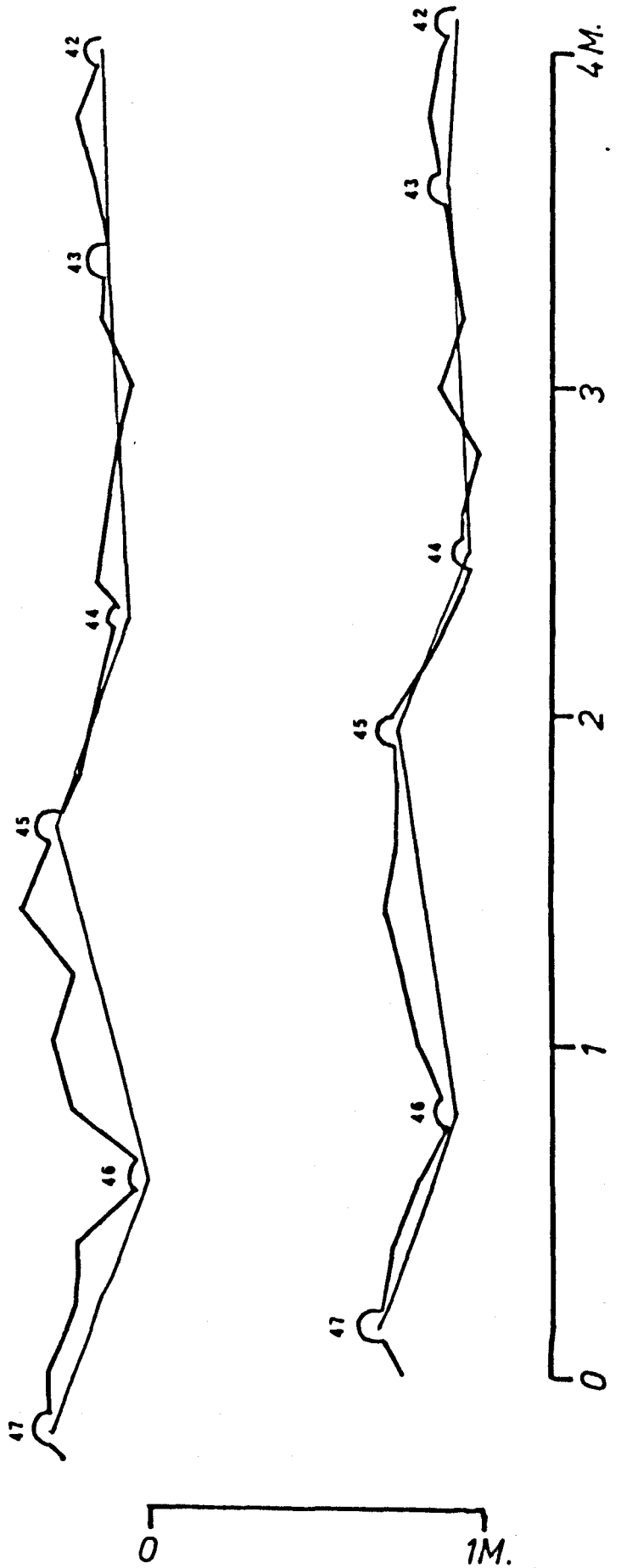
The line drawn between boreholes indicated the base line used for measurement of overbreak and underbreak, i.e. breakage is measured from the line directly connecting boreholes and not from the design face line.

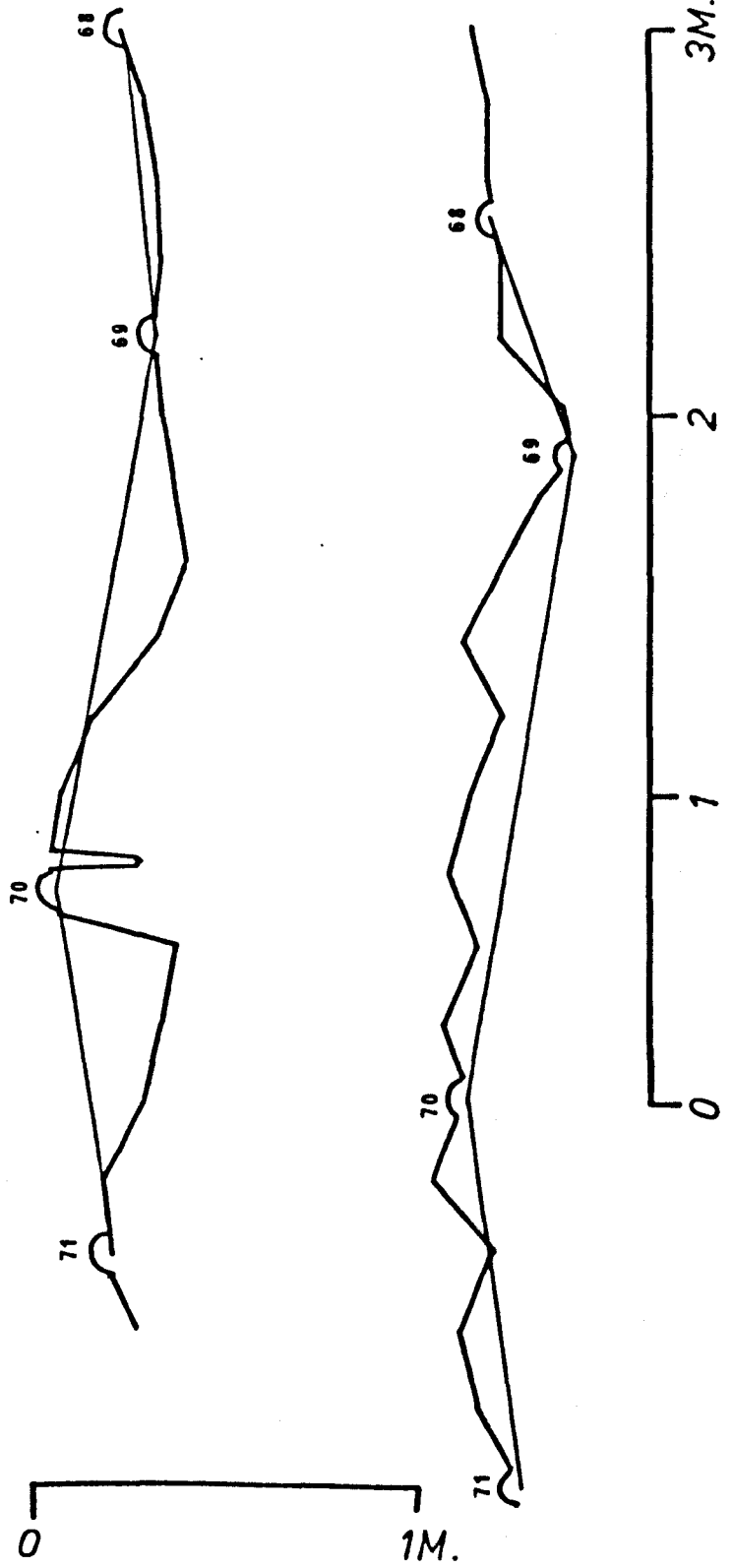


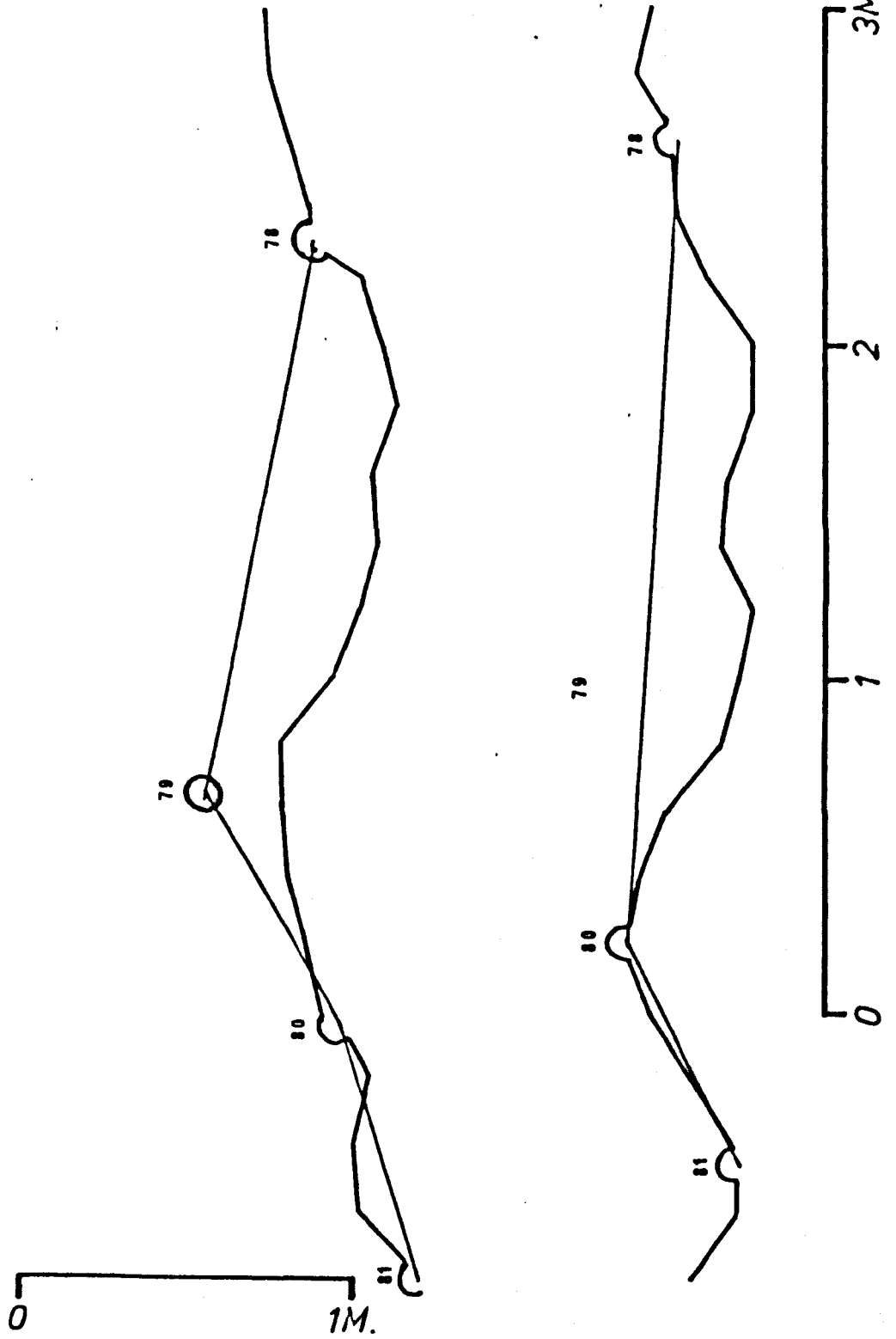


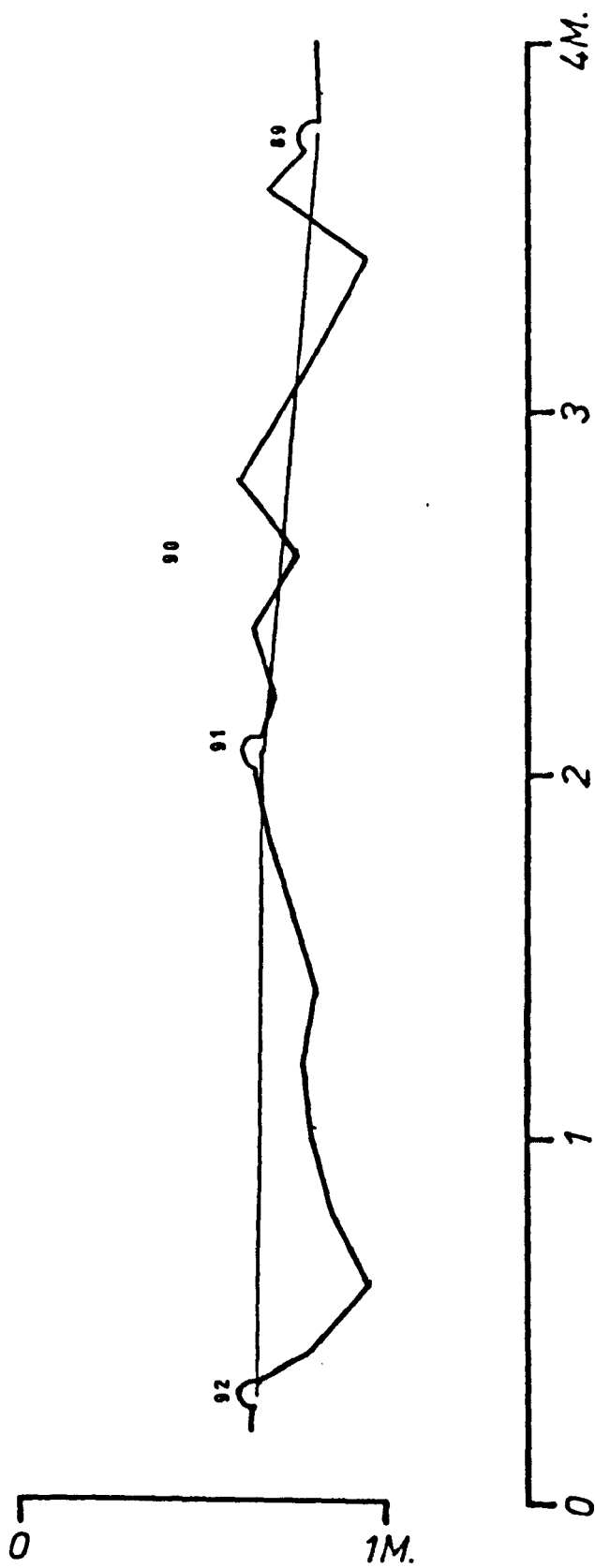


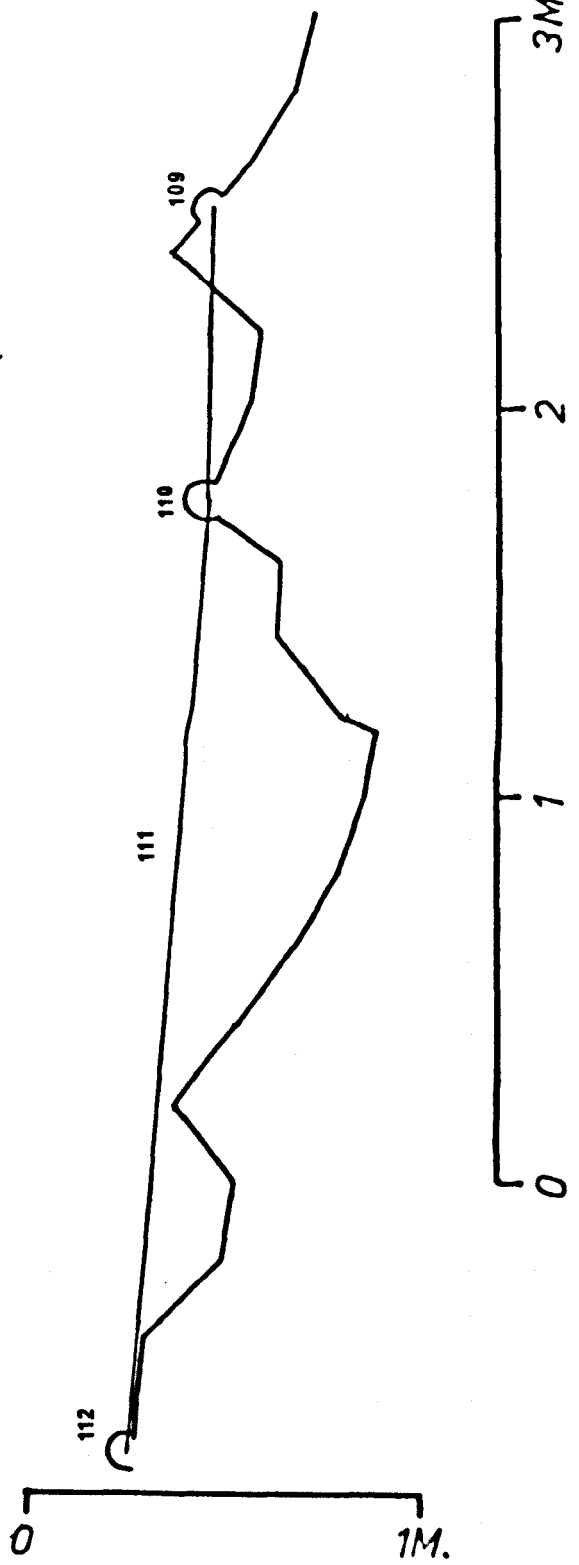
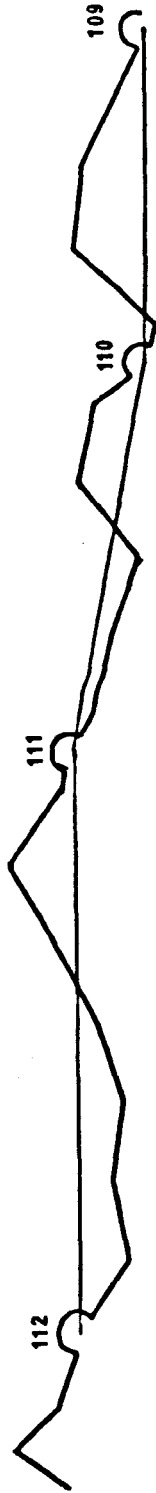


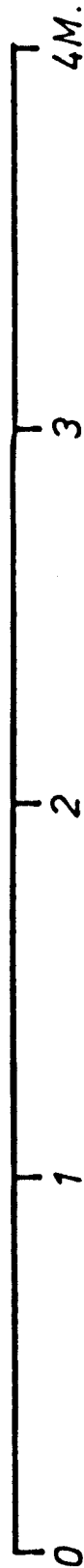
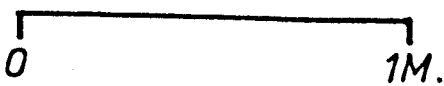
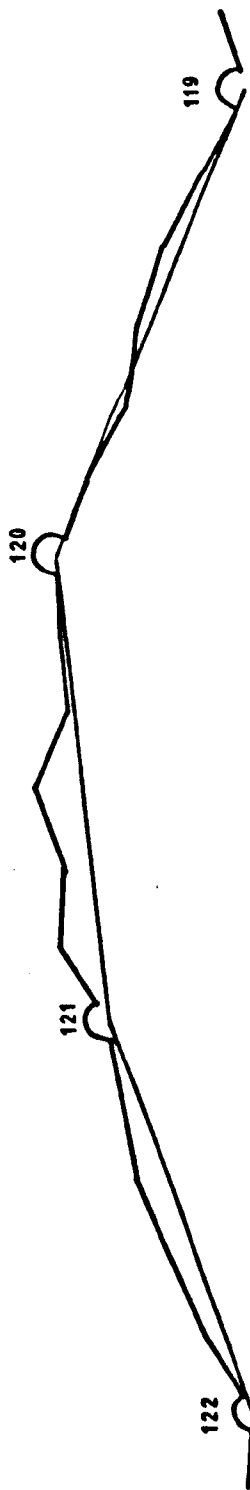


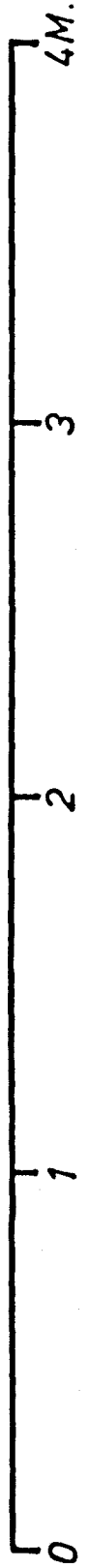
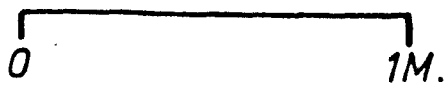












Appendix H

LABORATORY STRENGTH TESTING RESULTS

H-1 TESTING SPECIFICATIONS

Both compressive and tensile strength testing was undertaken using Newcastle standard compressive and tensile strength test specimen sizes, which are:

Compressive: (axial load test)

cylinders of 2:1 height to width ratio

height = 84 mm

width = 42 mm

Tensile: (brazilian disc test)

cylindrical specimens

diameter = 42 mm

thickness = 21 mm

H-2 SPRINGWELL SANDSTONE

Medium grained homogenous Carboniferous Sandstone.

Source: Springwell Quarries, Tyne and Wear

Tests: 5 compressive; 49.26, 49.26, 49.15, 49.23, 47.21

MPa

Av. 48.82 MPa

10 tensile;

3.89, 3.94, 3.77, 3.71, 3.95, 3.59, 3.69, 4.03, 3.55, 3.85 MPa

Av. 3.80 MPa

H-3 CONCRETE

4:1 ratio building sand to portland cement mix concrete.

Tests: 6 compressive;

13.75, 14.63, 18.01, 16.17, 17.79, 7.94 MPa

Av. 14.71 MPa

11 tensile;

1.44, 1.79, 2.29, 2.05, 1.57, 1.31, 1.62, 2.26, 1.34, 1.26, 0.85

MPa

Av. 1.62 MPa

H-4 RAISBY LIMESTONE

Muddy fossiliferous crystalline bedded limestone.  
(Magnesian Limestone - Permian.)

Source: Raisby Quarries, County Durham

Tests: 4 compressive; 49.08, 52.11, 45.83, 156.62 MPa

Av. 75.91 MPa

8 tensile; 8.59, 4.65, 9.49, 3.97, 3.83, 2.38, 9.38, 6.06 MPa

Av. 6.04 MPa

H-5 RAISBY DOLOMITIC LIMESTONE

Hard banded dolomitic limestone with sparse vugs.  
(Magnesian Limestone - Permian.)

Source: Raisby Quarries, County Durham

Tests: 5 compressive; 156.3, 172.5, 169.6, 187.7, 135.7  
MPa

Av. 164.4 MPa

10 tensile;

6.46, 8.80, 10.61, 10.54, 8.41, 9.63, 12.12, 8.23, 8.93, 7.76  
MPa

Av. 9.15 MPa

H-6 CREETOWN GRANITE

Coarse grained white granodiorite.

Source: Creetown Granite Quarries, via T.R.R.L.

Tests: 5 compressive; 178.9, 176.6, 169.7, 171.7, 160.0  
MPa

Av. 171.38 MPa

10 tensile;

10.93, 10.19, 10.33, 10.35, 11.13, 8.50, 11.44, 11.12, 9.92,

10.92 MPa

Av. 10.48 MPa

H-7 WHINSDONE

Coarse grained dolerite.

Source: redundant kerb stones ex. whin sill

Tests: 5 compressive; 167.5, 171.4, 170.3, 168.2, 170.7

MPa

Av. 169.6 MPa

10 tensile;

11.11, 12.99, 11.98, 11.69, 13.50, 12.20, 12.99, 12.92, 13.21,

13.50 MPa

Av. 12.61 MPa